Norwegian University
of Life Sciences

Master's Thesis 2020 30 Credits
Faculty of Science and Technology

Mechanical assessment of a steel dissipating system for RC buildings retrofitting with CLT panels

Magnus Rød Hatletveit
Structural Engineering and Architecture

Abstract

Lack of seismic capacity is a common problem for older low-rise, reinforced concrete frame structures. To tackle this problem, a new friction energy dissipating system meant for retrofitting, is proposed. The system consists of externally mounted CLT-elements connected with steel profiles to the beams of reinforced concrete (RC) buildings. Each of the steel profiles consists of two separate plates, linked through a friction connection consisting of preloaded bolts sliding in elongated holes.

As the project is in its early stages, the author has been tasked with determining the capacity of three proposed profile designs, as well as creating improved profile designs. To do this, a combination of hand calculations and FEM modeling in Ansys® *Academic Research Workbench, Release 19.2* has been performed.

To determine the slip force of the friction connection, a separate simulation was devised to test the equations derived for the hand calculations. From this test, the results showed strong correlation with the equation derived from the hand calculations, and suggested two effective friction surfaces per preloaded bolt for the single lap jointed friction connection.

For the profile simulations, the supports were modeled as two elements consisting of the steel plate and a combined element, consisting of the CLT/concrete and the connectors. The external profile loading was derived from an approach based on the moment distribution of the CLT element resulting from the applied seismic shear forces.

In total, six different profiles were examined in this thesis. The base profile applied a simple design, where the plate connected to the front of the CLT-element and bent around the element towards the RC-beam. From the modeling, it was determined that all these designs with front mounted CLT-steel connections would induce large eccentricities, resulting in unfavorable moment stresses acting in the plates and connections.

For the rear mounted CLT-steel connection profile designs, it was observed that these eccentric moments were greatly reduced. As a result, a new profile design, attempting to reduce the system eccentricity was tested. With exception of the friction connection, this new design greatly improved the profile stresses. In addition, a new proposal for the concrete connection was designed for the profile, increasing the center distances and diameter of the concrete anchors. This resulted in greatly improved concrete capacity.

The rear mounted design required a new mounting procedure, as the original approach intended to mount the profiles before installing the CLT-elements. As a result, a new simplified mounting procedure, as well as a new profile adjustment concept was proposed for the rear mounted CLT-steel profile.

For the friction connections, large stress concentrations were observed around the preloaded bolts for all the profiles. It was determined that an elastic-plastic analysis would be required for these connections, as EN 1993-1-8:2005 utilized a plastic capacity calculation for bolt connections.

Lastly, the characteristic slip load of the friction dissipating system was compared to an estimated optimal slip load for a representable structure. The results indicated that the system as calculated, would be capable of providing optimal slip load for lower seismic regions, but would likely need an increased slip capacity for higher seismic regions.

Sammendrag

Manglende seismisk kapasitet er et vanlig problem for eldre blokker med rammekonstruksjoner av betong. I denne oppgaven, analyseres en ny type friksjonsdemper. Systemet består av utvendig monterte krysslaminerte elementer, festet til det eksisterende bygget med stålprofiler. Hver av disse profilene består av to separate stålplater, forbundet med forspente skruer, utformet for å skli i avlange under seismiske hendelser.

Ettersom prosjektet er i oppstartsfasen, har forfatteren fått i oppgave å estimere kapasiteten til tre forhåndsbestemte profil design. Basert på disse resultatene, skal forfatteren foreslå nye profil design. For å gjennomføre disse oppgavene, har forfatteren benyttet en kombinasjon av hånd beregninger og FEM analyser ved hjelp av Ansys® *Academic Research Workbench, Release 19.2*.

For å bestemme nødvendig forspenning av skruene i friksonsforbindelsen til de forskjellige profilene, ble det utviklet en separat FEM-modell. Fra disse simuleringene ble det funnet en sterk korrelasjon mellom nødvendig forspenning utledet for håndberegningen og simuleringene. I tillegg, indikerte simuleringene to effektive friksjons flater for den enkelt skjøtede forbindelsen.

For modelleringen av de forskjellige profilene, ble opplagerforbindelsene modellert som to elementer, bestående av profilens stålplate og ett kombinert element bestående av CLT/betong elementene og de tilhørende forbinderne. De eksterne kreftene som virket på de forskjellige opplagerne til profilene, ble estimert fra moment fordelingen som resulterte fra CLT-elementene påvirket av seismiske skjærkrefter.

Totalt, ble seks forskjellige profiler testet i denne oppgaven. De originale profilene, hadde et design hvor stål platen var festet på forsiden av CLT-elementene, og deretter ble bøyd mot betong bjelken. Fra simuleringen av disse profilene, ble det observer store spenninger i platene og forbindelsene, som resulterte fra de horisontale eksentrisitetene mellom betong og CLT opplagerne.

For profilene med CLT-forbindelsen på baksiden av elementet, ble det observert en stor reduksjon disse spenningene. Basert på dette, ble det designet en ny profil designet for å redusere disse eksentrisitetene så mye som mulig. Dette resulterte i økt kapasitet for både platene og CLT-stål forbindelsene i profilen, sammenlignet med de originale profilene. I tillegg, ble betong forbindelsen endret ved å øke diameteren og senter avstanden på betong-ankrene.

Den eksisterende fremgangsmåten for montering av systemet krevde at CLT-stål forbindelsen var på forsiden av CLT-elementet. Dette resulterte i et nytt forslag for en justeringsforbindelse for den nye profilen, samt en ny fremgangsmåte for montering.

For alle de testede friksjonsforbindelsene, ble det observert spenninger over den plastiske kapasiteten til profilene. Som et resultat, ble det konkludert med at det var behov for en elastisk-plastisk analyse av forbindelsen, ettersom EN 1993-1-8:2005 benyttet plastiske materialegenskaper ved beregning av bolt forbindelser.

Til slutt, ble antall friksjonsdempere estimert fra en optimal demper kraft for et representativt bygg under forskjellige seismiske forhold. Fra estimeringen, ble det konkludert at systemet som foreslått, ville kunne tilby optimal friksjonskapasitet i områder med lavere seismisk aktivitet. For områder med høyere seismisk aktivitet, indikerte resultatene et behov for økt friksjonskapasitet i hvert element.

Acknowledgement

I would like to thank my supervisor, Roberto Tomasi for providing me with the required knowledge in seismic design, to be able to carry out this thesis. I would also like to thank my co-supervisor Francesco Boggian, for taking the time to guide me through the process of writing this thesis, even as it stretched beyond the original time span. I am also great full, if not slightly frustrated, for all the insight and work that has been provided through regular discussions with both of my supervisors.

Furthermore, I would like to thank Phd student, Carola Tardo and the university of Catania, for providing the designs of the original profiles. I am also great full for their initiation of this project, as it gave me the opportunity to work with such a complex and interesting topic.

Lastly, I would like to extend my deepest gratitude to Tor Grobstok, for helping me with proofreading, and keeping me sane during the coronavirus lockdown.

ÅS, July 2020

Magnus Rød Hatletveit

Table of contents

1 Introduction

The European union has commissioned the development of a new friction dissipating system, for improving seismic behavior of existing buildings. The proposed system consists of CLT-elements connected to the external beams of existing reinforced concrete building using steel profiles as shown in Figure 1-1. Each of the steel profiles consists of two separate plates connected by a friction connection consisting of preloaded bolts in elongated holes. The friction system is intended to be mounted as columns for the entire height of the building at several locations.

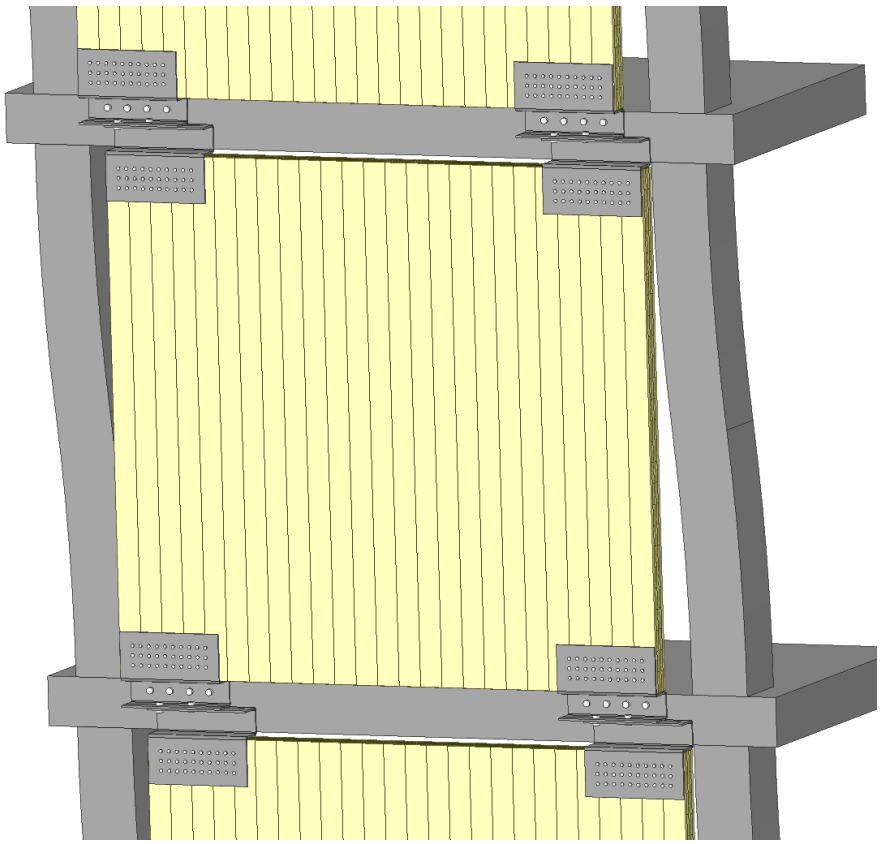

Figure 1-1: Proposed friction energy dissipating system. (Images used courtesy of ANSYS, Inc.)

As the project is in the first year of a four-year program, the design of the steel profiles and the friction dissipating connection is yet to be determined. As a result, the author has been tasked with determining the capacity of three predefined profiles, in addition to estimating the required bolt preloading for the friction connection. To do this, an approach for the external loading of the profiles must be determined, as well as a method for testing the connections and profiles.

Based on the resulting capacities of the original profiles, the author is tasked with developing and testing new profile designs, intended to improve potential weaknesses of the original profiles. Part of this process is to propose a mounting procedure for the best performing profiles.

Lastly, the feasibility of the friction system should be studied for a representative structure. To do this, the estimated characteristic friction capacity should be used to determine if the system will be able to provide adequate damping for a representative structure.

To conduct these tasks, the author has opted to use Ansys® *Academic Research Workbench, Release 19.2* to simulate the profiles of the thesis. These simulations in combination with hand calculations will be used as the basis for the thesis results and discussion.

1.1 Profiles

The base design of the profiles is seen in Figure 1-2, consist of four connections. Connection B is the concrete connection. This connection is responsible for transferring and resisting the seismic shear forces between the story and the friction damper, as well as resisting the vertical forces from the resulting rotation of the CLT-element.

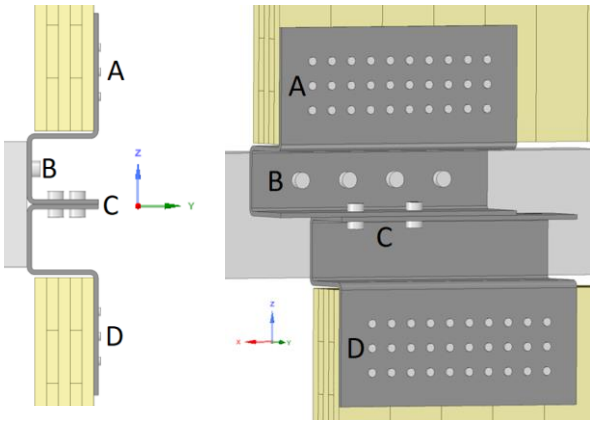

Figure 1-2: Profile connections and coordinate system. (Images used courtesy of ANSYS, Inc.)

Connection C is the friction connection, consisting of two preloaded bolts in elongated holes. This connection will be designed to slide at a certain critical shear load. The resulting shear force will have to be transferred to the bottom of each CLT-element through the CLT-steel connections of connection A and D. The CLT-steel connections will also transfer the vertical forces of the CLT-elements into the profiles. The different profiles are described with the nomenclature of Table 1-1.

Table 1-1: Nomenclature for profiles.

Profile nomenclature			
1° element	Thickness [mm]	8	8 mm
2°element	n° preloaded bolts	2B	2 bolts (CLT thickness 100 mm)
3° element	Variations	R	Reinforcement
		DP	Double plate
		SR	Side reinforcement
		AP	Alternative profile

Original profile designs:

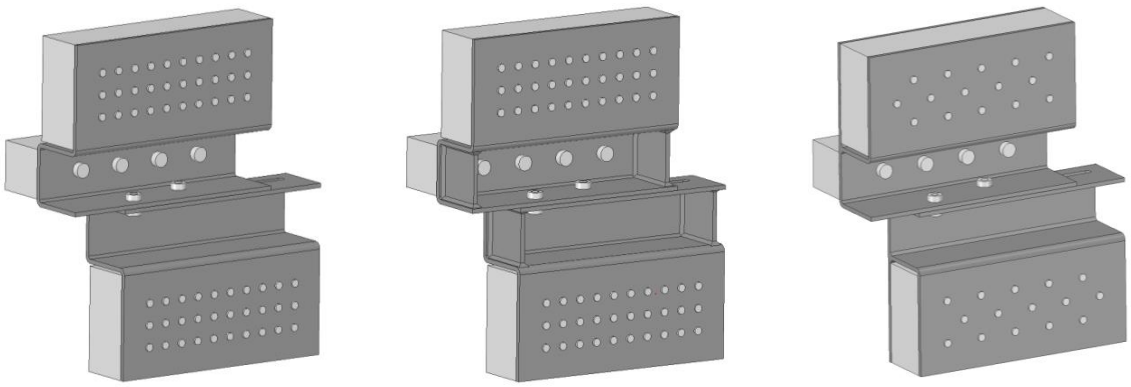

Profile 8-2B *Profile 8-2B-R* *Profile 8-2B-DP*

Figure 1-3: Original profile designs (Images used courtesy of ANSYS, Inc.)

The three original profiles proposed for this thesis are shown in Figure 1-3. Profile 8-2B consist of two 450 mm wide, 8mm thick plates, made of S235 steel. Profile 8-2B-R differ from profile 8-2B, with the introduction of reinforcement at the outer edges of the bent sections. For both the profiles, the CLT-steel connections consist of 30 screws. Profile 8-2B-DP is designed with an extra rear plate for the CLT-connection. As a result, the front and rear CLT-connections each consist of 15 screws. All the original profiles are designed with a concrete connection located in the top plate. These connections consist of four M12 concrete anchors with 90 mm spacing.

The friction connection of the original profiles, consist of two separate elongated holes in the bottom plate, as shown in Figure 1-4. For the top plate, normal holes are located at the center of the elongated holes.

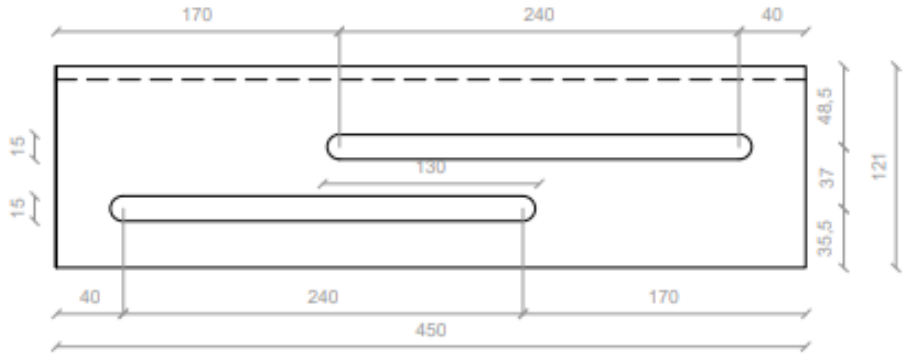

Figure 1-4: Bottom plate of friction connection for profile 8-2B.

New profile designs:

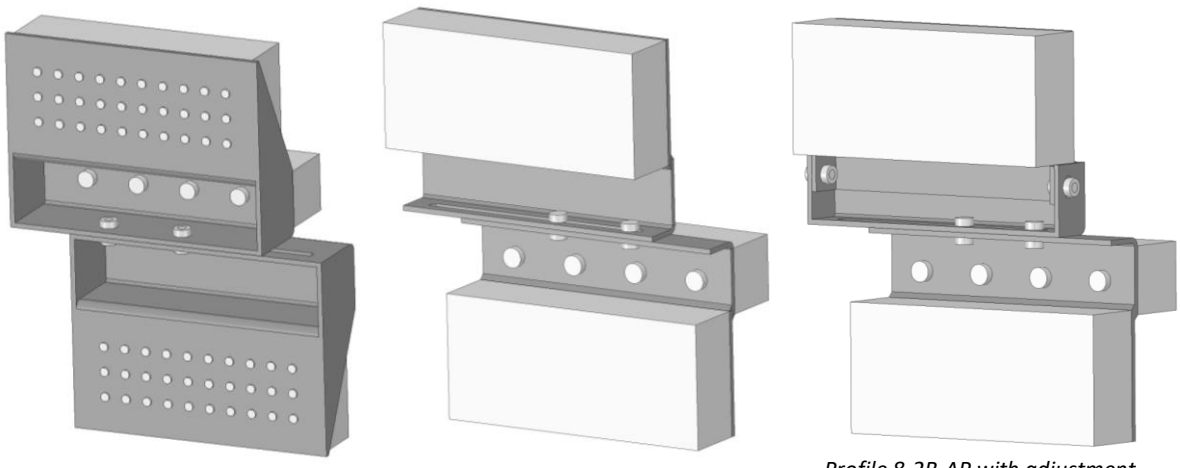

Figure 1-5: New profile designs. (Images used courtesy of ANSYS, Inc.)

The new profile design proposals are shown in Figure 1-5. Profile 8-2B-SR is based on the same design as profile 8-2B, with the same layout for the CLT-steel and concrete connections. Profile 8-2B-SR differs from profile 8-2B, by shrinking the width the profile by 8 mm on each side. It also introduces reinforcement on the edges stretching the entirety of the profile. Lastly, the connection moves the two preloaded bolts to one elongated hole, which is located at the outer edge of the profile, as shown in Figure 1-6.

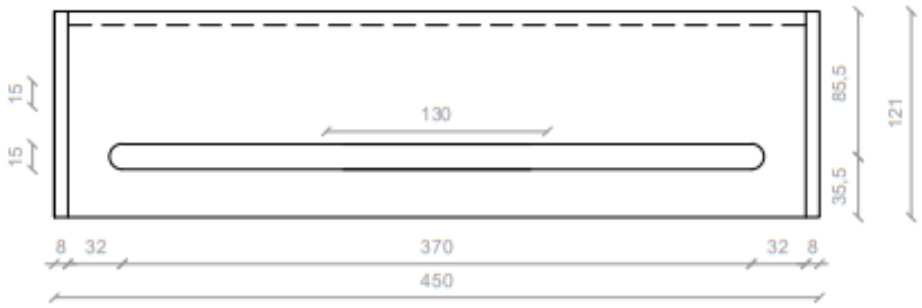

Figure 1-6: Elongated hole for friction connection of profile 8-2B-SR.

Profile 8-2B-AP is designed with a rear mounted CLT-steel connection design, as shown in Figure 1-7. For this design, the upper profile of consisted of two separate plates, welded together. In addition, the preloaded bolts are situated in the same elongated hole, located closer to the vertical edge of the profile. Unlike the other profiles, the elongated hole, is situated in the top profile, while the concrete connection is situated in the bottom profile. In addition, the spacing of the concrete connectors were increased to 110 mm.

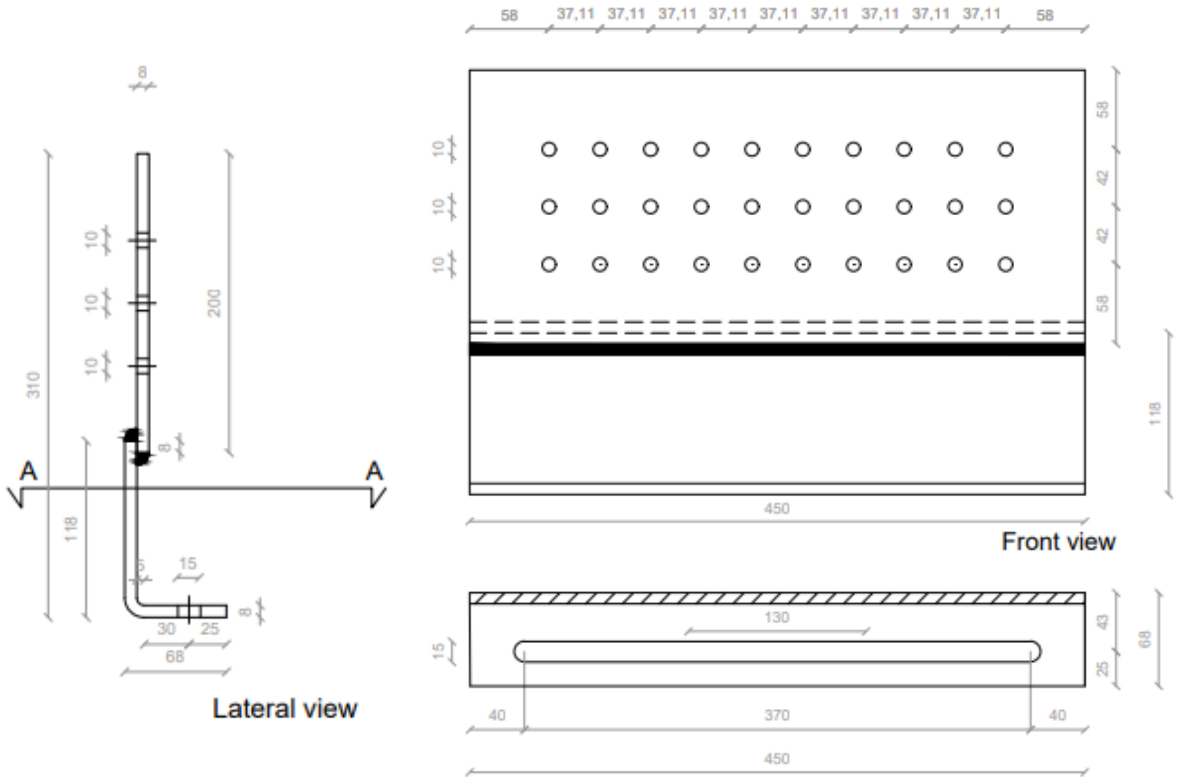

Figure 1-7: Upper plates of 8-2B-AP.

Profile 8-2B-AP with the adjustment connection, is proposed as a concept. As a result, no finalized technical drawing is provided. The adjustment mechanism consists of preloaded bolts located at the outer edges of the upper profile, as a replacement for the welded connection of profile 8-2B-AP, as shown in Figure 1-5.

2 Theory

2.1 Earthquake aftershocks

For many large seismic events it is common for several after shakes to occur. On August 24. 2016, a series of earthquakes upwards of magnitude (M) 6.2 was recorded, killing almost 300 people, and leaving 20 000 people homeless in the Lazio region of Italy, near the Apennine mountain range (L. Chiaraluce, 2017). Within an hour of the first shake, another earthquake of M 5.6 was reported. In total 44 seismic events with M 4.0 and larger were registered over the next two and a half months with two of these earthquakes of M 6.2 and M 6.6 occurring less than 30 km away from the first shake on October 26 (USGS, 2016).

The effect of these after shakes can be severe for constructions designed reliant on plastic absorption of seismic energy. Ruiqiang (2014) investigated the strength degradation effect of earthquakes and their aftershocks on structures. To do this the duration and mean period of a wide range of far field earthquakes of M5 and above were considered using a pushover analysis with a deteriorating cyclic hysteretic model to simulate the plastic hinges.

From the seismic data, a general trend of reduced mean period of the aftershock compared to the main shock was observed. For all the cases the duration of the after shakes had a shorter duration than the main shakes, but there were some exceptions for the mean period. Based on the information on the duration and strength of the aftershock, collapse fragility curves were created for different after shakes as shown in Figure 2-1. Four different initial damage states (DS) were considered. These arranged from DS_0, which represented a single degree of freedom structure with little to no damage from the main earthquake, to DS_3, which represent a severe DS before the aftershock Ruiqiang (2014).

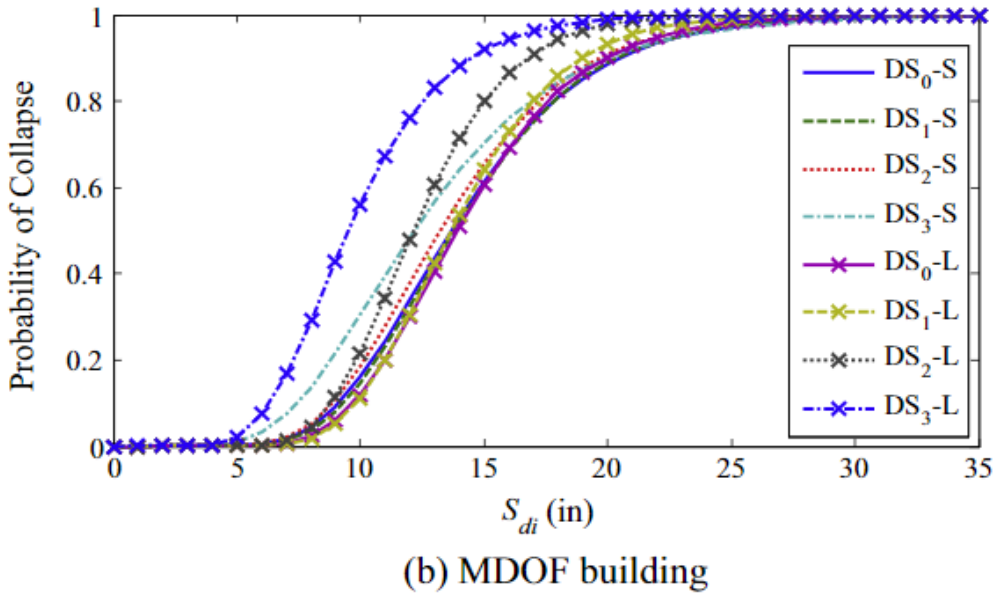

Figure 2-1: Collapse risk of buildings with different levels of initial earthquake damage (DS_{0-3}) exited by aftershocks of short (S) and long (L) duration (Ruiqiang, 2014).

From the analysis of Figure 2-1 It was observed that earthquakes of long duration, were especially vulnerable for aftershocks, when having sustained plastic damage in a previous seismic event. The same was observed for short duration earthquakes, if the building had sustained large plastic deformations in the previous seismic event Ruiqiang (2014).

2.2 Earthquake engineering

All members of the European Committee for Standardization (CEN) are bound to comply with EN 1998-1:2004 *Eurocode 8: Design of structures for earthquake resistance* (CEN, 2004, p.1). The general purpose of EN 1998-1:2004 according to clause 1.1.1(1) is to ensure that human lives are protected, damage is limited and structures for important civil protection remain operational in the event of an earthquake (CEN, 2004, p.15).

To ensure these values the values EN 1998-1:2004 specifies two fundamental requirements. The first of which is the "No-collapse requirement". This requirement states that a structure should be able to withstand a seismic design load defined by EN 1998-1:2004 without global or local collapse. This allows for plastic deformation and a certain reduction of residual load bearing capacity after a design seismic event based on national classifications. The design seismic action is associated with a reference probability of exceedance, P_{NCR}, a reference return period T_{NCR} and an importance factor, γ_I, for different building types. The values of P_{NCR} and T_{NCR} are decided by the separate national annexes of each member country, but EN 1998-1:2004 gives a recommended P_{NCR} of 10% over a T_{NCR} of 475 years (CEN, 2004, pp.29). Figure 2-2 displays a map of peak ground acceleration, PGA, in accordance with the recommended values of P_{NCR} and T_{NCR} (Woessner, 2015).

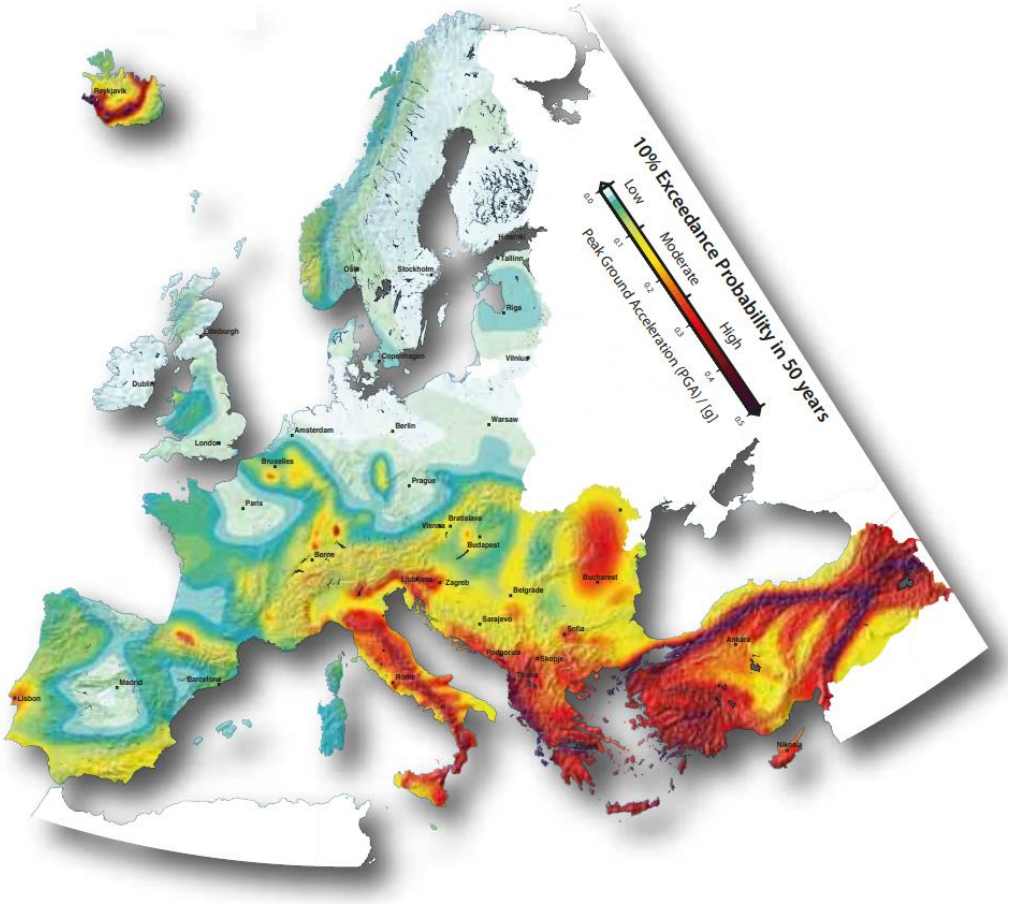

Figure 2-2 Map of PGA expected to be reached or exceeded with a 10% probability in 50 years over a return period of 475 years (Woessner, 2015).

Figure 2-2 shows that the largest European earthquake excitations are concentrated around the Italian and Greek peninsula with a PGA up to 0.5g. In the case of Norway, there are relatively low PGA values with the highest value of approximately 0.1 g found on the west coast as a result of the Mid-Atlantic ridge.

The second fundamental requirement specified by EN 1998-1:2004 is the Damage limitation requirement. This requirement states that a building should be able to withstand a seismic action in accordance with a nations National Annex. The Eurocode recommends using a probability of exceedance equal to 10% and an average return period of 95 years (CEN, 2004). In the case of Norway section NA.2.1 of the Norwegian Annex states that no damage limitation verification has to be performed (CEN, 2014, p.184).

For a shear type frame, each column or shear wall is fixed for rotation, resulting in the following equation for stiffness of each element when shear loads are applied at the supports (P. Larsen 2014, p.29).

$$k = \frac{12\,EI}{H^3}$$

k Element stiffness
E Modulus of elasticity
H Element height
I Area moment of inertia

As the stiffness of a structure is dependent on a reduction factor h^3 with the height, while the increase of mass generally can be considered linear, the period of structures usually increases with its height. EN 1998-1:2004 equation (4.6) gives the following simplified empirical formula for calculation of the first order vibration period of structures below 40 meters:

$$T_1 = C_t\,H^{\frac{3}{4}}$$

T_1 First order period
C_t Construction type factor
H Height of structure

For a five story reinforced concrete frame building with a height of 20 meters this results in a first order period of 0.71 s. Ruiqiang (2014) investigated several moderate to large far field earthquakes and found a medium period of the main and after shakes using Fourier amplitude spectrum as shown in Figure 2-3.

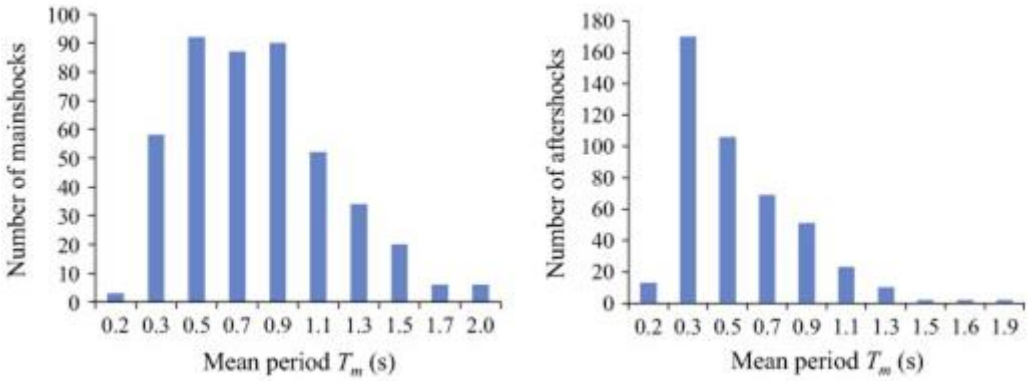

Figure 2-3: Mean periods main- and aftershocks for far field medium to large earthquakes (Ruiqiang, 2014).

From Figure 2-3 it is observed that the mean periods of the earthquakes range from 0.2 to 2.0 s with the majority of the earthquakes having periods around 0.5 to 1.0 s. These periods are similar to the natural frequency of medium sized buildings up to around six floors. This results in an amplification of the structural response as described in the theory of.

Furthermore, the natural period of the local soil conditions of the structure will pose as an additional amplification factor. The natural period of the soil is dependent on the depth, H, and average shear velocity, V of the topsoil levels. EN 1998-1:2004, table 3.1 suggest shear velocity for different ground types with speeds decreasing with lower ground stiffness (CEN, 2004). Sawada (2004) propose a simplified formula for the natural period of a single soil level as shown in the following equation

$$T_g = \frac{4H}{V_s}$$

T_g Natural ground period

The proposed equation for the natural period of the ground gives lower natural ground periods for ground conditions with high stiffness like rocks, and higher periods for softer ground conditions. Figure 2-4 shows the ground acceleration roughly 80 km from the epicenter of the 1999 Kocaeli earthquake for the ground conditions of rock and soft soil (VDC, 1999). For this example, the ground acceleration is more than doubled for the hard ground condition compared to the soft.

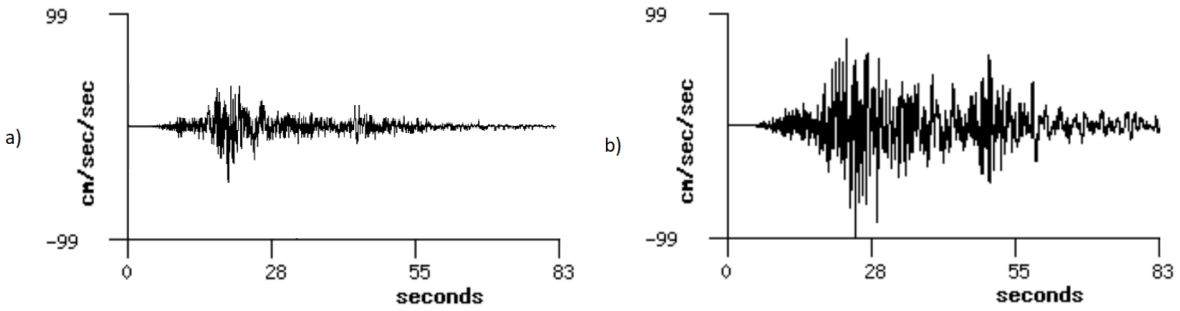

Figure 2-4: Ground acceleration roughly 80 km from epicenter for (a) rock and (b) soft soil (VDC, 1999).

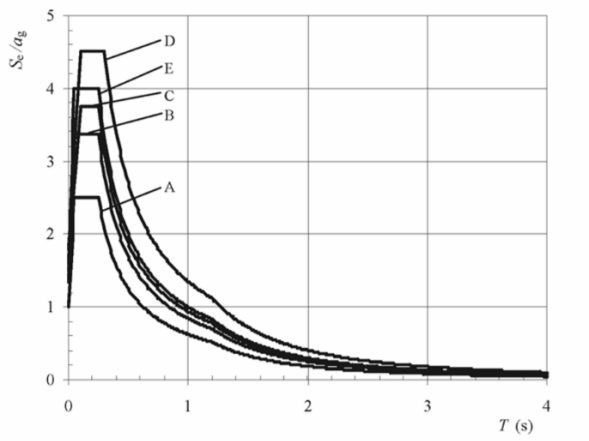

Figure 2-5: Recommended Type 2 elastic response spectra for ground type A to E (5% damping) (CEN, 2004, p.39).

To account for these effects EN 1998-1:2004 has created generalized response spectra, one of which is displayed in Figure 2-5. The spectrum gives recommended amplification factors (S_e) of buildings with first order periods in the range from 0.0 to 4.0 s. The different curves represent the amplified structure response to an earthquake PGA on different soil types. This chart is representative for a building with average viscous damping of 5%. To account for the plastic behavior of different types of buildings in the case of elastic response analysis EN 1998-1:2004 introduce a behavior factor q. This is a factor that reduce the value of the design spectrum (S_d). EN 1998-1:2004 clause 3.2.2.2(8) states that that these design spectra are not sufficient for the design of structures with energy dissipation systems (CEN, 2004).

2.3 Friction damping

A friction damper can be represented as a hysteretic curve consisting of a perfect elastic and perfect plastic behavior where the elastic behavior is a result of the damper bracing stiffness, and the perfect plastic behavior is caused by coulomb damping as shown in Figure 2-6. k_b is defined as damper lateral stiffness when the damper is excited by a force smaller than the slip force F_s.

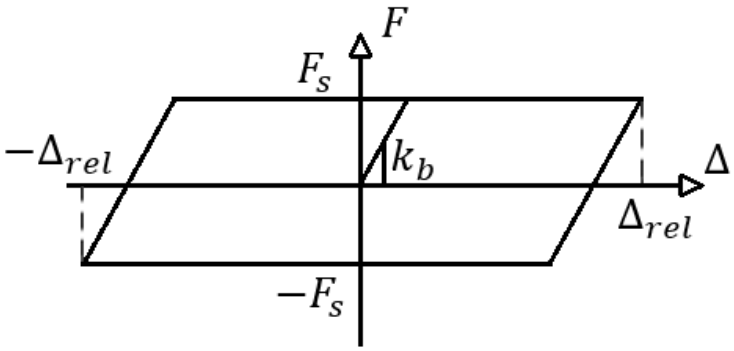

Figure 2-6: Idealized hysteretic behavior of friction damper.

Coulomb damping is the effect of a sliding friction force acting on a system. The friction force of a Coulomb damper always acts in the opposite direction of the system velocity as shown in the SDOF system from Figure 2-7. If displacement to the right is defined as positive, the system will experience a negative slip friction force F_f when moving with $\dot{x} > 0$ as shown in Figure 2-7(b) and a positive force when $\dot{x} < 0$ as shown in Figure 2-7(c). This results in two differential equations of motion for the SDOF system as described in equation (2.1) and (2.2) (Shabana, 2019, p.106).

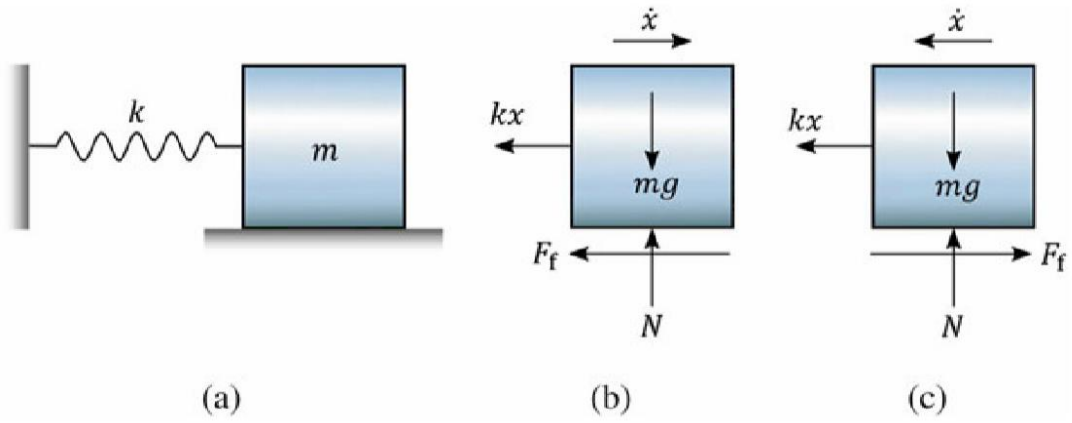

Figure 2-7: Coulomb damping. (Shabana, 2019, p.106)

$$m\ddot{x} = -kx - F_f, \qquad \dot{x} > 0 \tag{2.1}$$

$$m\ddot{x} = -kx + F_f, \qquad \dot{x} < 0 \tag{2.2}$$

These equations can be simplified to one equation as:

$$\ddot{x} + \frac{k}{m}\left(x \pm \frac{F_f}{k}\right) = 0 \tag{2.3}$$

This system can be described further by introducing y as the following:

$$\begin{aligned} y &= x \pm \frac{F_f}{k} \\ \dot{y} &= \dot{x} \\ \ddot{y} &= \ddot{x} \end{aligned} \tag{2.4}$$

This introduction results in a linear, homogenous second-order equation with constant natural frequency defined as $\omega_n = \sqrt{\frac{k}{m}}$. This means that the natural frequency is not affected by the Coulomb damping as it will not attribute to the system stiffness when the friction force is constant (Shabana, 2019, p.106):

$$\ddot{y} + \omega_n y = 0 \tag{2.5}$$

Solving the differential equation for y and then substituting y with equation (2.4), gives the following two equations of motion:

$$x(t) = A_1 \sin(\omega_n t) + A_2 \cos(\omega_n t) - \frac{F_f}{k}, \qquad \dot{x} \geq 0 \tag{2.6}$$

$$x(t) = A_3 \sin(\omega_n t) + A_4 \cos(\omega_n t) + \frac{F_f}{k}, \qquad \dot{x} \leq 0 \tag{2.7}$$

Solving these equations for initial conditions $x(0) = x_0$ and $\dot{x}(0) = \dot{x}_0$ yields the following expressions:

$$x(t) = \frac{\dot{x}_0}{\omega_n} \sin(\omega_n t) + \left(x_0 + \frac{F_f}{k}\right) \cos(\omega_n t) - \frac{F_f}{k}, \qquad \dot{x} \geq 0 \tag{2.8}$$

$$x(t) = \frac{\dot{x}_0}{\omega_n} \sin(\omega_n t) + \left(x_0 - \frac{F_f}{k}\right) \cos(\omega_n t) + \frac{F_f}{k}, \qquad \dot{x} \leq 0 \tag{2.9}$$

To determine the amplitude decrease, a system with initial condition $x(0) = x_0$ and $\dot{x} = 0$ is examined over half a natural system period $T/2 = \pi/\omega_n$ where $\dot{x}_0 \leq 0$:

$$\begin{aligned} x\left(\frac{\pi}{\omega_n}\right) &= (-x_0 + \frac{2F_f}{k}) \\ \dot{x}\left(\frac{\pi}{\omega_n}\right) &= 0 \end{aligned} \tag{2.10}$$

This shows that the amplitude has decreased equal to $2F_f/k$ over half a period. By using the results in equation (2.10) to calculate the next half period an additional amplitude reduction is found. This gives an amplitude reduction of $4F_f/k$ per cycle. Furthermore, the process can be repeated until system is at rest. By doing this it can be verified that the amplitude reduction is linear. It is also important to note that the system is not self-centering (Shabana, 2019, p.108). These results are showcased in Figure 2-8.

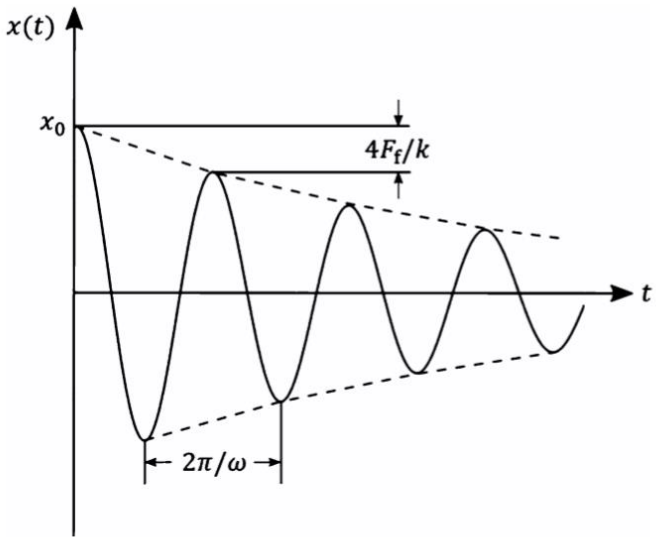

Figure 2-8: Coulomb damped free SDOF vibration (Shabana, 2019, p.108).

(Sang-Hyun Lee, 2008) performed a study, which among other things studied the effect of increased relative slip loads and stiffness for friction dampers based on building seismic shear force distribution. For the study, a numerical analysis was performed using a pseudo-acceleration spectrum with a critical spectral acceleration of 0.225g.

Among other things the study looks at the effects of increasing the system bracing stiffness in relation to the slip force of a SDOF system. The study defines the increased stiffness as a factor $SR = \frac{k_b}{k_f}$, where k_b is the bracing stiffness (of the friction damper) and k_f is the stiffness of the frame without the bracing. The ration of the slip force is determined as the factor $\rho = \frac{f_s}{f_f}$, where f_s is the slip force of the damper and f_f is the critical shear force acting on the original system calculated with a damping ratio of 5% (Sang-Hyun Lee, 2008).

Factor R_d is equal to the critical deformation of the system without the friction damper over the critical displacement with the damper. Factor R_f is the critical seismic shear force acting on the original SDOF system divided by the critical displacement of the friction damped system. R_e is the fraction of the earthquake energy taken by the frame. Figure 2-9 shows the effect of increased ρ and SR for R_d, R_f and R_e (Sang-Hyun Lee, 2008).

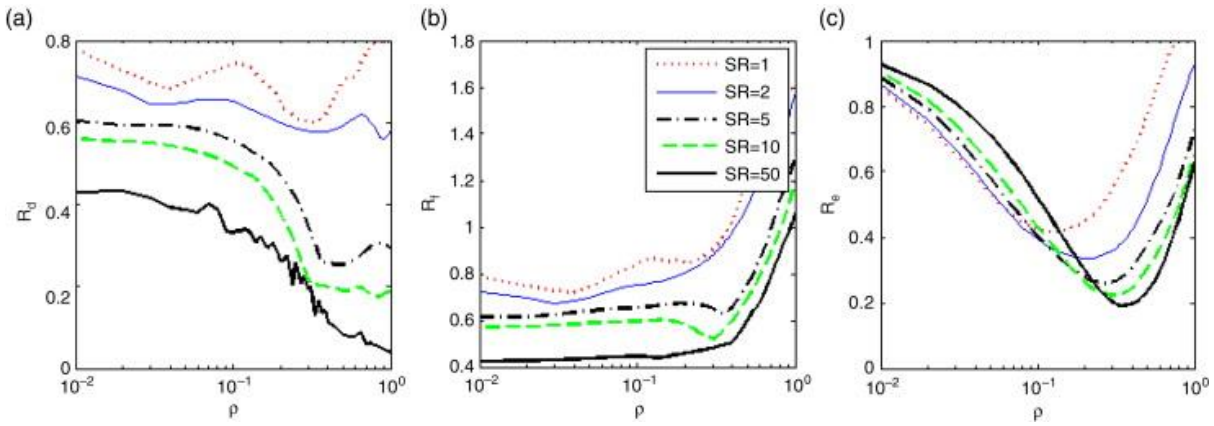

Figure 2-9: Effect of increased ρ and SR for R_d, R_f and R_e of a SDOF system with T_n = 1s (Sang-Hyun Lee, 2008).

From Figure 2-9(a), a large drop in system displacement is observed when ρ approaches 0.2 for the systems with SR over 5. The opposite effect is observed for all the systems of SR with regards to the shear force R_f. As ρ surpass 0.3 a rapid force increase is observed for the system. This is the result of the increased system stiffness transferring more energy as the damper system behave gradually more elastic with its large relative stiffness when ρ increase beyond this value. For the energy absorption of the friction connection, Figure 2-9(c) show how a ρ of around 0.1 to 0.3 provide the largest relative energy absorption for the friction connection.

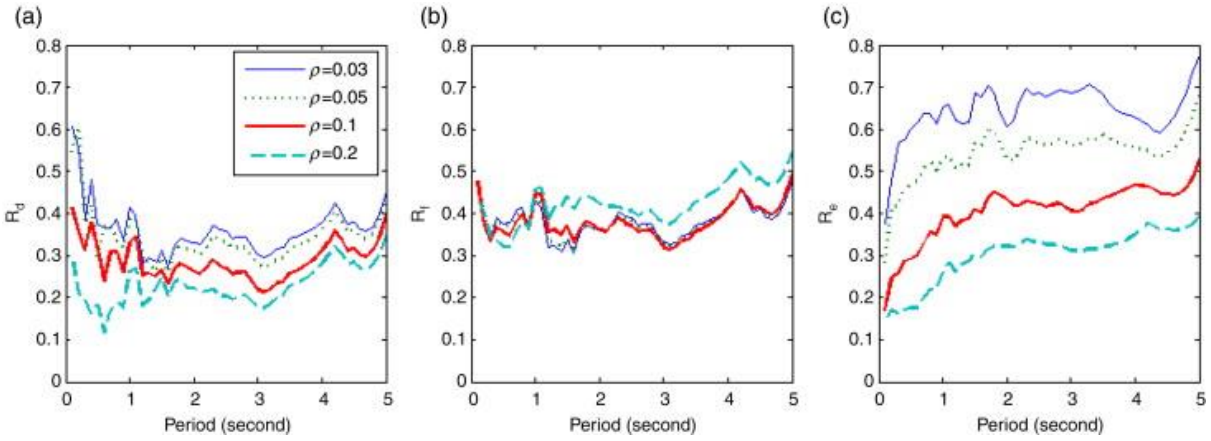

Figure 2-10: Effect of SDOF period on R_d, R_f and R_e for different slip loads (Sang-Hyun Lee, 2008).

Figure 2-10 for the relation of the period and the relative slip force, indicate a slightly beneficial behavior for the lower system periods with a ρ of 0.2. (Sang-Hyun Lee, 2008) goes on to test two different distribution methods of the slip load throughout the stories of the different structures. The total slip load is approximated as the sum of the shear forces acting on the undamped building times ρ. The first distribution method is to evenly distribute the forces among the stories, and the second aims to distribute the forces based on the relative stiffness and inter-story drift for each story using the following equation.

$$f_{si} = F_{total} \frac{k_{fi} S_{dj}}{\sum_{n=1}^{N_f} k_{fn} S_{dn}} \tag{2.11}$$

f_{si}	Slip force for story i
F_{total}	Total system slip force
k_{fi}	Stiffness of floor i
S_{dj}	Inter-story drift of floor i
N_f	Number of floors

(Sang-Hyun Lee, 2008) also experiment with only installing dampeners at some of the stories, as shown in Figure 2-11 for a four-story building where the critical displacement R_{d1} is the result of equation (2.11) and R_{d2} is the resulting critical displacement from the evenly distributed slip load (Sang-Hyun Lee, 2008).

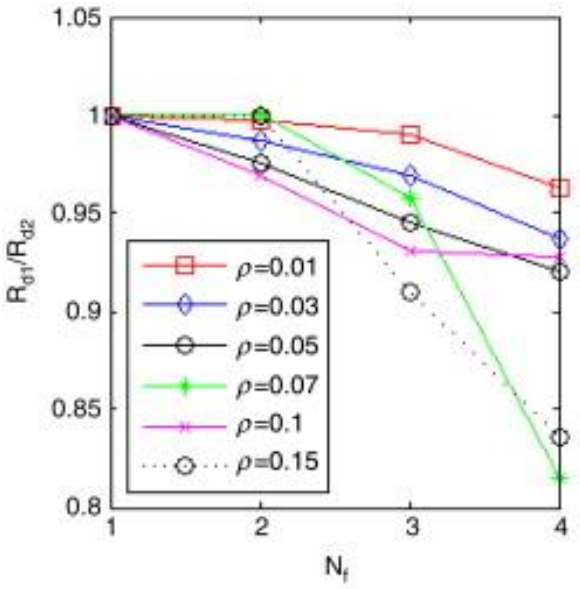

Figure 2-11: Relative displacement of slip force distribution methods of a four-story building (Sang-Hyun Lee, 2008).

With friction dampers installed at each floor, Figure 2-11 shows an approximate 15% improvement for the simulated structure when adjusting the slip force according to equation (Sang-Hyun Lee, 2008).

2.4 Torsion stress

The resulting shear and normal stresses experienced by a cross-section consist of two different torsion effects. The first effect is the St. Venant torsion. The resulting stresses of the cross-section for the St. Venant torsion is dependent on the following equation (Hughes, 2011).

$$\tau = \frac{T_t\, h}{I_T} \tag{2.12}$$

τ Shear stress
T Applied torque
I_T St Venant torsional constant
h Cross-section height

The St Venant torsional constant is equal to the polar moment for circular cross-sections. For all other cross-sections the constant will be a reduced-on account of uneven shear stress distribution (Hughes, 2011). For a rectangular cross-section the constant can be estimated using the following equation (2.13), using the values of Table 2-1 and dimensions from Figure 2-12 (Stibor, 2014).

$$I_T = \alpha\, b\, h^3 \tag{2.13}$$

b Cross-section width
α St Venant parameter for rectangular cross-section

Table 2-1: St Venant torsional constant rectangular parameter (Stibor, 2014).

b/h	1	2	10	∞
α	0.141	0.229	0.312	0.333

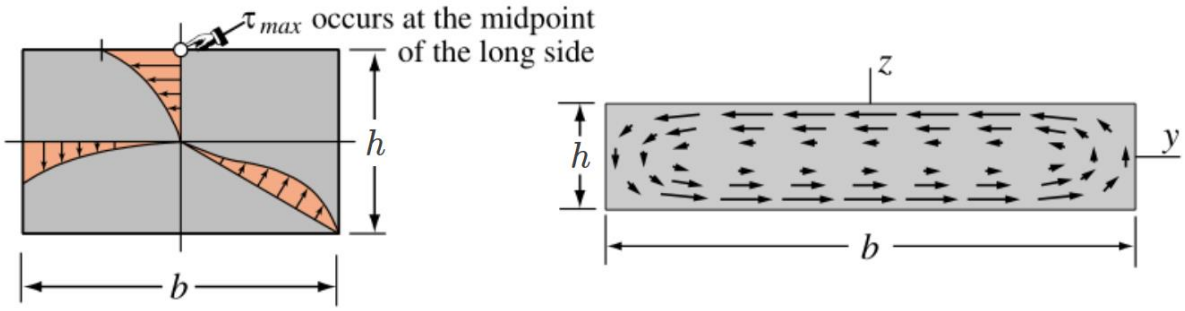

Figure 2-12: Tangential stress distribution for rectangular solid section from torsion (Stibor, 2014).

The St Venant torsional constant for a rectangular cross-section is greatly reduced compared to the equivalent polar moment for the cross-section with increasing b/h relationship. This is because of the shear stress distribution for the critical St Venant shear stress acting at the point closest to the geometry center for the rectangular cross-section as shown in Figure 2-12 (Hughes, 2011).

For any non-circular cross-section, the applied torsion is the sum of the St Venant torsion and an additional warping torsion. The resulting torsion of the combined St Venant and warping torsion can be expressed with the following differential equation (Hughes, 2011).

$$T = G\, I_T\, \varphi' - E\, I_w\, \varphi''' \qquad (2.14)$$

T	Applied system torsion
I_w	Warping constant
φ'	Variation of twisting
φ'''	rate of change of curvature

The warping effect is particularly large for twin flanged sections resulting in a combination of warping moment stresses and shear stresses in the flanges as shown in Figure 2-13 (Hughes, 2011).

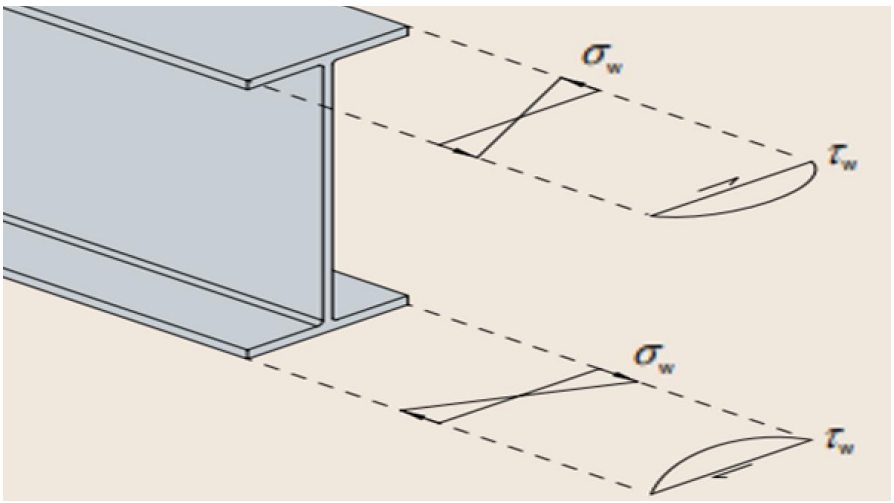

Figure 2-13: Warping normal and shear stress for I-beam (Hughes, 2011).

The resulting distribution of the torsion effects and twisting for a cantilever I-beam can be found solving equation (2.14), with regards for the system distance x (Hughes, 2011).

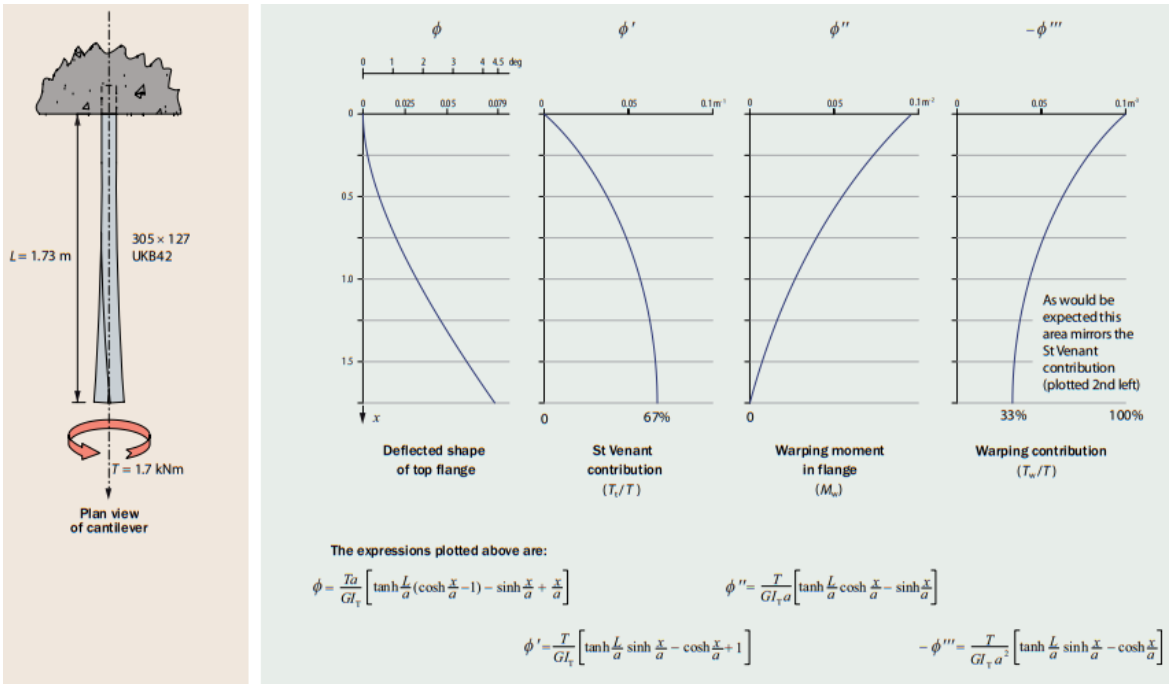

Figure 2-14: General equations for twisting and corresponding plots for I-beam (Hughes, 2011).

From Figure 2-14 the St Venant contribution is zero at x = 0, as the support does not allow for profile warping. The equation for φ'' in Figure 2-14 shows how φ'' depends on the relationship of $tanh\frac{L}{a}$, where L is the length of the cantilever and a is defined as $\sqrt{E\ I_w\ /\ G\ I_T}$. the function of $tanh$ converges towards 1.00 with increasing values of L/a. As a result, warping moment which is linearly dependant on φ'' will increase with increased system length. This holdes true for all cross-sections experiencing warping. Figure 2-14 for φ''' of the I-beam yields a lower contribution of the warping torsion the further the system is from the support (Hughes, 2011).

2.5 Preloaded bolts in tension and shear capacity

A preloaded bolt connection will always be in equilibrium. When an initial preload is induced on the bolt, the heads of the bolt will clamp down on the steel plates resulting in a force distribution as shown in Figure 2-15 (NSC, 2005).

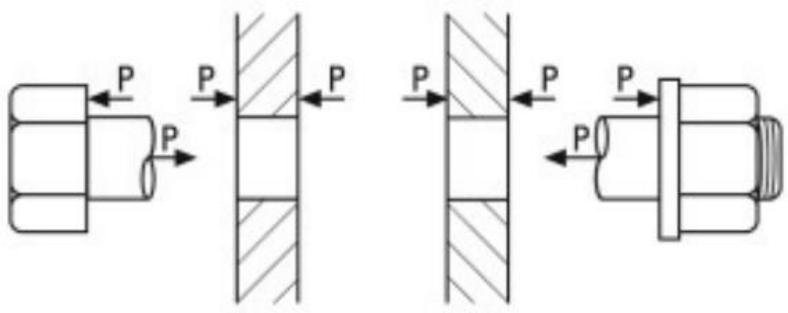

Figure 2-15: System equilibrium for preloaded force (NSC, 2005).

When an external tension force T is applied in the plates, the resulting system of equilibrium must be adjusted to account for the tension force. As the plates are compressed with a preload force P, the external force will reduce the compression force of the plates, while the force between the bolt head and the plate remains the same. The resulting equilibrium system is displayed in Figure 2-16 (NSC, 2005).

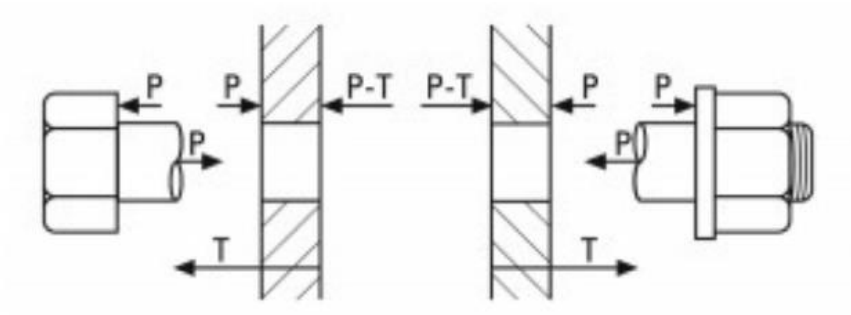

Figure 2-16: Compression forces of preloaded surfaces with applied external tension (NSC, 2005).

Only when the external tension force becomes greater than the bolt preload, the tension of the bolt increase. From this point, the bolt load is equal to the tension load, and the resulting connection will begin to deform as a non-preloaded connection (NSC, 2005).

The shear force acting between two surfaces is dependent on the compression force between the surfaces and the friction constant between the two surface materials p.129 (Tipler, 2008). For the preloaded system described in Figure 2-16, each of the plates will resist sliding through the friction surface between the two plates and the surface between the bolt and plate, resulting in two shear surfaces acting on each plate per bolt. As a result of the tensile force applied of the system, the compression force between the two plates is reduced, resulting in a lower shear capacity between the plates compared to the surface between the bolt and plate. The friction contribution of the surface between the bolt and plate will be dependent on the stiffness of the bolt between the two outer surfaces, as the relative displacement between the two shear surfaces dictates how much each surface will contribute to the shear capacity.

When calculating the friction capacity, the friction constant is multiplied by the tensile force. In addition to this factor, EN 1993-1-8:2005 also require a reduction factor k_s be used when determining the characteristic shear capacity of a system. k_s is a factor determined by the shape holes in the plates. For normal holes following the size requirements of EN 1993-1-8:2005, the factor is equal to 1. For elongated holes with shear forces acting parallel to the hole direction, the Eurocode requires a k_s factor of 0.63 (CEN, 2005).

(Husson, 2008) tested the behavior of M20 preloaded bolt connection in tension with normal and slotted holes. The results of the tension tests are shown in Figure 2-17.

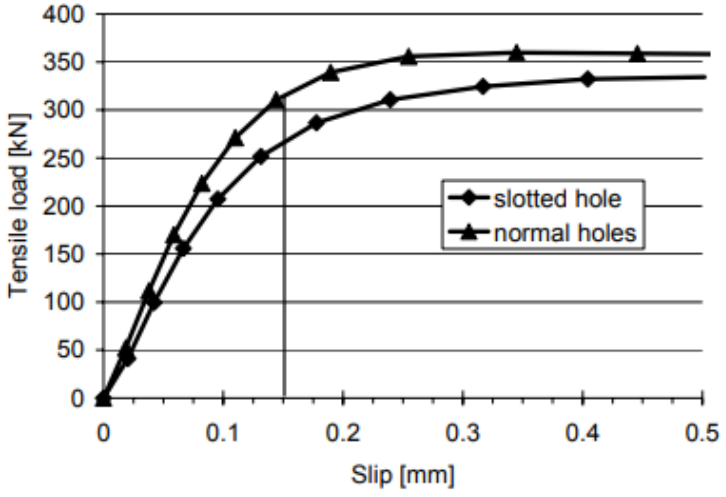

Figure 2-17: Load-slip behavior comparison with normal holes (Husson, 2008).

The maximum capacity reduction for the slotted holes was found to be 15 % compared to the normal holes at a slip deformation of 0.15 mm. For the ultimate capacity estimated to occur at deflection of approximately 0.5 mm with a reduction of 7%. As a result, the study concluded the Eurocode k_s factor appeared to be too conservative (Husson, 2008).

For moments acting on a bolted connection, the resulting moment force couple will compensate for loss in shear capacity from the bolt by compressing the connection. Assuming a constant friction constant, and factor k_s close to 1, the resulting change in connection shear force will be negligible. As a result,

For applied moments, EN 1998-1-8:2004 clause 3.9.2(2) states that no slip resistance reduction is required if the compression counterbalance the tensile force(CEN, 2005). For a connection with constant friction constant over the connection, and factor k_s close to 1, the resulting change in connection shear force will be negligible with the introduction of a moment.

2.6 External force application of profiles

The critical external forces acting on the two profiles acting on a floor can be derived from a critical friction force of the compressed profile $P_{x.c}$. This force is the sum of $P_{xA.c}$ and $P_{xB.c}$ as shown in Figure 2-18. $P_{xA.c}$ is the sum of the horizontal forces transferred from the overlying compression profiles, while $P_{xB.c}$ is the horizontal force transferred from the acting RC floor to the compression profile.

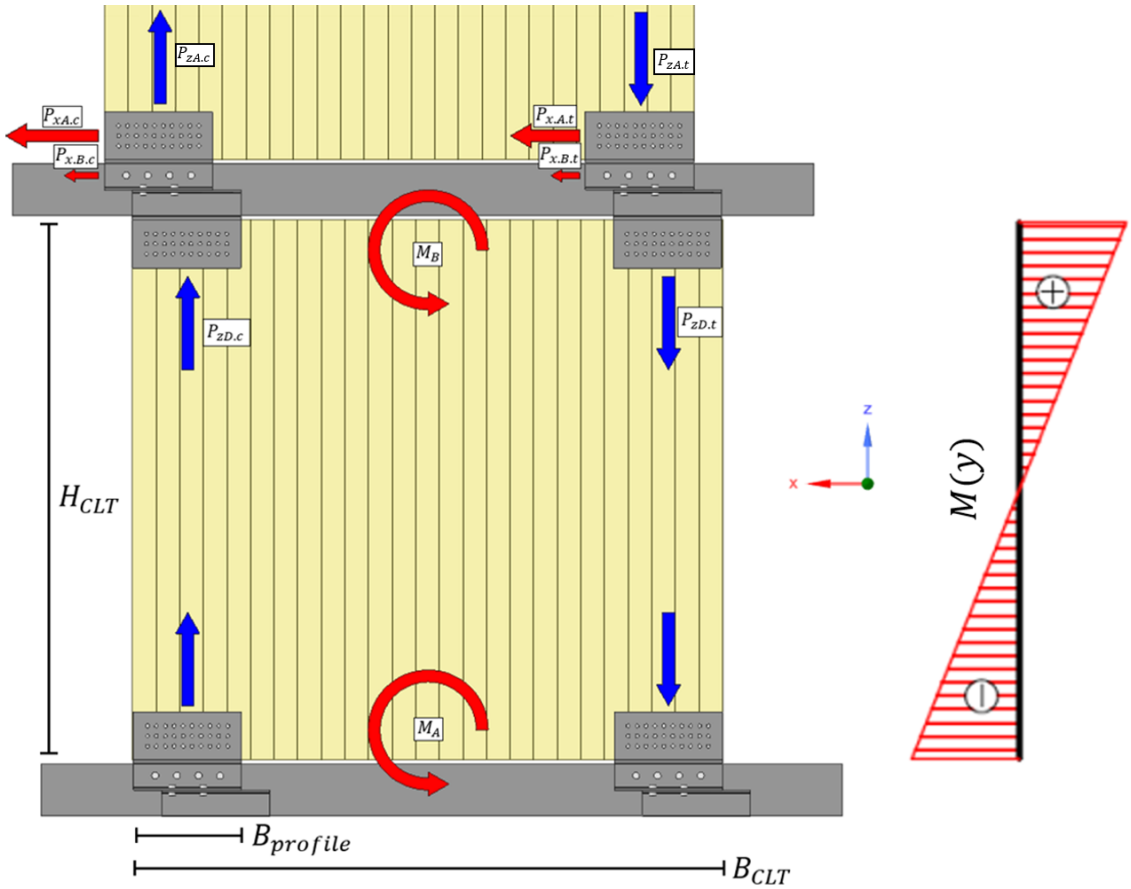

Figure 2-18: Resultant forces from vertical forces in top connection and moment distribution over CLT element. (Images used courtesy of ANSYS, Inc.)

$P_{x.c}$ can be distributed between support A and B as shown in Figure 2-18, using equation (4.11) from EN 1998-1:2004 for the "Lateral Force" method as visualized in Figure 2-19, where connection A transfer the forces from the upper floors and connection B transfer the force from the acting floor.

$$F_i = F_b \frac{z_i \ m_i}{\sum z_j \ m_j}$$ *Eq (4.11), EN 1998-1:2004*

F_i Horizontal force acting on story i;
F_b Seismic base shear;
z_i Height of mass m_i and m_j at applied seismic action
z_j All heights at which a mass m_j act

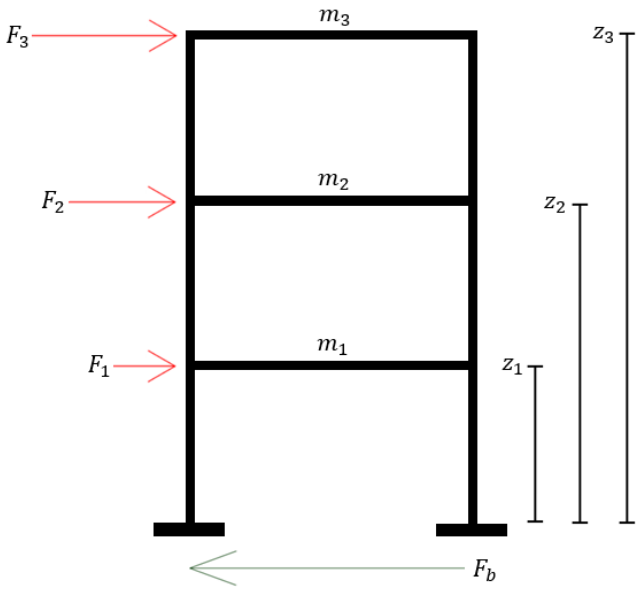

Figure 2-19: Lateral force distribution method.

The vertical forces acting on the system can be calculated considering the CLT wall as a fixed-fixed column with a shear force $2P_{x.avg}$ acting at the top as illustrated in Figure 2-18. The resulting moments at the top and bottom of the CLT plate can then be distributed as force pairs in the top and bottom profiles. $P_{x.avg}$ is the average characteristic friction capacity of the two profiles which are dependent on the resulting compression and tension forces created by the CLT moment. As a result, the average horizontal force for every couple of profiles can be calculated with equation (2.15).

$$P_{x.avg} = \frac{(1+\lambda)\ P_{x.c}}{2} \quad (2.15)$$

λ Friction capacity reduction factor for tension profile

The resulting shear slip force for the overlying CLT friction element must be equal to the sum of $P_{x.A.c}$ and $P_{x.A.t}$. To simplify the horizontal force distribution for the profiles, the same force distribution relation can be assumed for $P_{x.A}$ as $P_{x.D}$, resulting in the following equation for the average force distribution.

$$P_{xA.avg} = \frac{(1+\lambda)\ P_{xA.c}}{2} \quad (2.16)$$

λ Friction capacity reduction factor for tension profile

The force from the weight of the CLT panel and the four corresponding profiles can then be calculated using equation (2.17).

$$P_{CLT.weight} = -g\left(m_{CLT} + 4\,m_{sp}\right) \tag{2.17}$$

m_{CLT} Mass of CLT element
m_{sp} Mass of one steel plate
g Gravitational acceleration

By combining the resulting moment force distribution of Figure 2-18 and the system weight from equation 2.17, the vertical force acting on the compression- and tension- profiles can be calculated using equation (2.18) and (2.19):

$$P_{zD.c} = P_{x.avg}\left(\frac{H_{CLT}}{B_{CLT} - B_{profile}}\right) + \frac{P_{CLT.weight}}{4} \tag{2.18}$$

$$P_{zD.t} = -P_{x.avg}\left(\frac{H_{CLT}}{B_{CLT} - B_{profile}}\right) + \frac{P_{CLT.weight}}{4} \tag{2.19}$$

The resulting vertical forces $P_{zA.c}$ and $P_{zA.t}$ acting on connection A for the tension and compression profile are calculated from equation (2.18) and (2.19), using the average horizontal force calculated in equation (2.16).

Using the theory from *2.5 Preloaded bolts in tension and shear capacity*, the following equation is derived for the friction capacity of the compressed profile assuming factor k_s equal to 1 for the compression area assuming equal shear contribution from all shear surfaces.

$$P_{x.c} = \mu(k_s\, n_{fb}\, n_C\, F_{p.C}\; +\; |P_{z.c}|\,) \tag{2.20}$$

$F_{p.C}$ Bolt preload
k_s Reduction factor for large holes
n_{fb} Number of friction bolts in profile
n_C Friction surfaces per bolt
μ Friction coefficient
$|P_{z.c}|$ Reaction compression force at friction connection

Equation (2.20) is then solved for the bolt preload resulting in equation (2.21).

$$F_{p.C} = \left(\frac{P_{x.c} - |P_{z.c}|\,\mu}{k_s\;\; n_{fb}\, n_C\, \mu}\right) \tag{2.21}$$

Using the preloaded force calculated in equation (2.21) and the vertical force calculated for the tension profile, the friction capacity of the tension profile is calculated in equation (2.22) using the theory of *2.5 Preloaded bolts in tension and shear capacity,* assuming the friction connection acting pinned.

$$P_{x.t} = k_s\, n_{fb}\;\; \mu\left(\; n_C\, F_{p.C} - \left|\frac{P_{zD.t}}{n_{fb}}\right|\right) \tag{2.22}$$

The sum of the resulting friction forces for the compression and tension profiles are then calculated, and λ can be adjusted until the criteria of equation (2.23) is achieved.

$$P_{x.c} + P_{x.t} \approx 2\, P_{x.avg} \tag{2.23}$$

The resulting distribution of horizontal forces in the tension profile between connection A and B can then be approximated assuming linearity between the floors, resulting in equation (2.24) and (2.25).

$$P_{xA.t} = -P_{xA.c}\,\lambda \tag{2.24}$$

$$P_{xD.t} = -P_{xB.c}\,\lambda \tag{2.25}$$

2.7 In plane eccentrically loaded connections

The force distribution of an eccentrically loaded connection will be dependent on the applied shear forces and the resulting moments as shown in Figure 2-20.

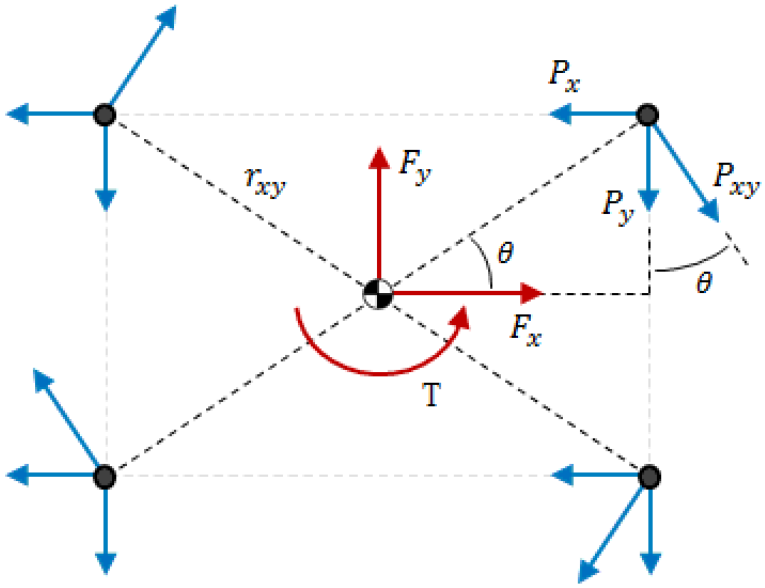

Figure 2-20: Force distribution of in plane moment connection (MechaniCalc).

For a system where the connection plates are considered infinitely stiff, the shear force distribution will only be dependent on the stiffness of the screws. The average shear stress is calculated as the shear force per area as shown in equation (2.26) (Hibbeler, 2013, p.32).

$$\tau_{avg} = \frac{F}{A} \tag{2.26}$$

Hooke's law for shear describes the relationship of shear tress, shear modulus and shear strain (Hibbeler, 2013, p.513).

$$\tau = G\,\gamma \tag{2.27}$$

For a system of connectors affected by a shear force with a rigid connector plate, all the connectors will experience the same amount of strain. If all the connectors are made of the same material, Hooke's law entails that the shear force P_i acting on each connector only depends on the area A_i of each connector as shown in equation (2.28).

$$\frac{F}{\sum A} = G\,\gamma = \frac{-P_i}{A_i} \tag{2.28}$$

For a system consisting of one type of connectors excited by axial forces along a y- and x-axis the force distribution can be simplified to the following equations:

$$P_{i.x} = \frac{F_x}{n} \tag{2.29}$$

$$P_{i.y} = \frac{F_y}{n} \tag{2.30}$$

n Number of connectors

The shear reaction from the applied torsion moment can be calculated from the torsion formula as shown in equation (2.31) (Hibbeler, 2013, p.185) when considering a connection plate much stiffer than the connectors.

$$\tau = \frac{T\, r_{xy}}{J} \tag{2.31}$$

J Polar moment

The polar moment of the connection can be calculated as the sum of the polar moments of the individual fasteners (Hibbeler, 2013, p.791). The polar moment for each connector can be calculated as the sum of moment inertia about the x- and y- axis which can be calculated using the parallel axis theorem for a circular cross section about the geometrical center of the connection resulting in the following equations for each connector.

$$I_x = \frac{1}{4}\,\pi\, R^4 + A\, {r_x}^2 \tag{2.32}$$

$$I_y = \frac{1}{4}\,\pi\, R^4 + A\, {r_y}^2 \tag{2.33}$$

R Radius of connector

Combining equations (2.34) and (2.35) give the following polar moment for a circular cross section:

$$J = A\left(\frac{1}{2}\, R^2 + {r_{xy}}^2\right) \tag{2.34}$$

Combining the equations (2.31) and (2.34) for a system of shear connectors the shear stress can be calculated as:

$$\tau_i = \frac{T\, r_{i.xy}}{\sum A\left(\frac{1}{2}\, R^2 + {r_{xy}}^2\right)} \tag{2.35}$$

The polar moment of the system is dependent on the square values of the connector radius and the distance from the center of rotation. As a result, the effect of the connector radius quickly becomes irrelevant when r_{xy} increases. As a result, the connector radius can be neglected for most systems. Combining this assumption with equation (2.26) and (2.35), results in the following equation for the calculation of shear force in each connector:

$$P_{i.xy} = \frac{T\, r_{i.xy}}{\sum {r_{xy}}^2} \tag{2.36}$$

The components of the resulting formulas can then be calculated using the angle θ in relation to the positive x-axis expressed with the following equations:

$$P_{i.x} = P_{i.xy} \sin\theta \tag{2.37}$$

$$P_{i.y} = -P_{i.xy} \cos\theta \tag{2.38}$$

2.8 Out of plane eccentrically loaded bolt connections

A method for calculation of the moment capacity of a connection is to calculate the connection as a beam in bending, as shown in Figure 2-21. This method assumes Naviers's hypothesis of plane sections of beams in bending remaining plane (Sørensen, 2013, p.27). This assumption allows for the system neutral axis to be determined based on the strain of the compression and tension part of the connection.

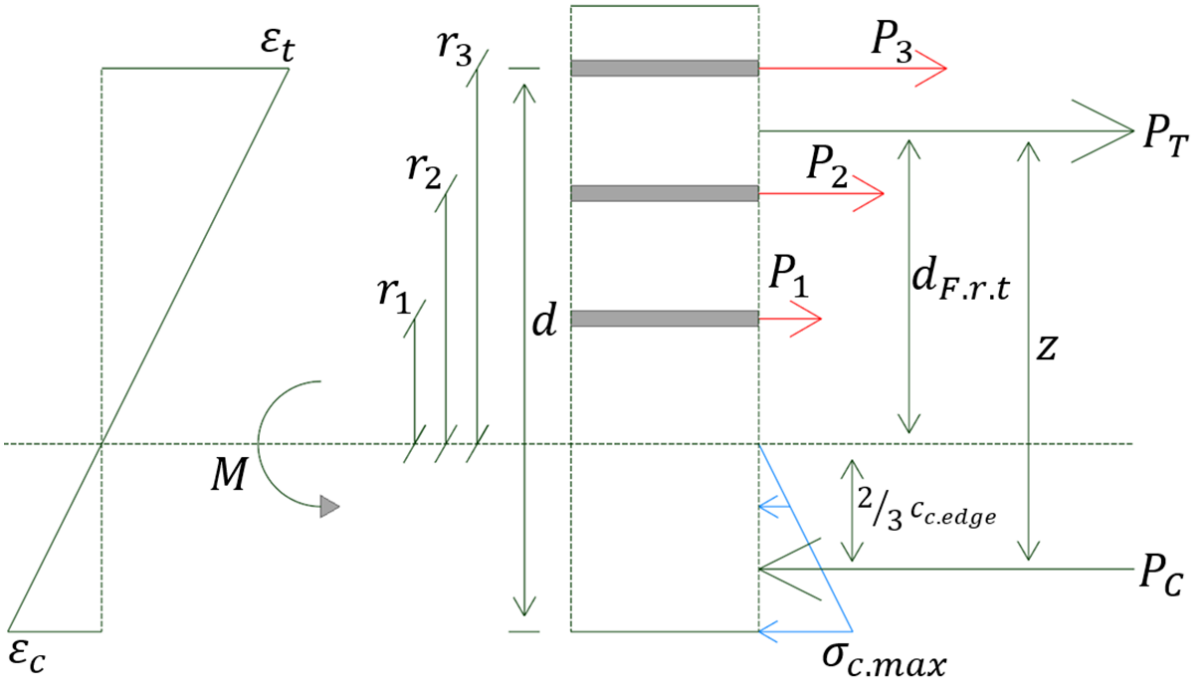

Figure 2-21: Force distribution of out of plane moment connection.

Calculating the neutral axis of the system can be done through an iterative process assuming a distance from the edge of the compression area to the neutral axis for the initial calculation as described in equation (2.39).

$$c_{c.edge} = \lambda\, d \tag{2.39}$$

$c_{c.edge}$	Distance from edge of compressed edge of N.A
d	Active connection height
λ	Iteration factor

For a connection consisting of tension fasteners along the entire connection. only the fasteners on the tension side of the N.A are considered to contribute to the connections tension capacity. For the tension connectors, the reaction moment about N.A can be written with the following equation:

$$M_T = \sum P\, d \tag{2.40}$$

M_T	Reaction moment about N.A for tension connectors
P	Connector force
d	Connector distance to N.A

When using only one type of connectors with a rigid plate, the stress distribution is linearly dependent on the distance from the N.A as shown in equation (2.41) (Hibbeler, 2013):

$$\sigma = \frac{M\, r}{I} \tag{2.41}$$

σ Stress
r Distance from N.A
I Area moment of inertia

As the force of each connector above the N.A, as shown in Figure 2-21 are linearly dependent on the distance from the N.A and the resulting tension force of the connectors has to be the sum of all the connector forces, the force P of each connector can be defined as shown in equation:

$$P_i = P_T \frac{r_i}{\sum r} \tag{2.42}$$

P_T Tension force resultant
r_i Connector distance from N.A

By substituting M_T of equation (2.40) with $P_T\ d_{F.r.t}$ and the P with the relation of equation (2.42), $d_{F.r.t}$ can be calculated using the following equation.

$$d_{F.r.t} = \frac{\sum r^2}{\sum r} \tag{2.43}$$

Considering the compression system to be linearly elastic with a rectangular cross section, the force resultant of the compression cross section will act two thirds of the distance from the neutral axis. The resulting connection lever arm is calculated in equation (2.44):

$$z = d_{F.r.t} + \frac{2}{3}\, c_{c.edge} \tag{2.44}$$

z Connection lever arm

The distribution of the external moment acting on the tension and compression components are then calculated with the following equation:

$$M_t = |M|\ \frac{d_{F.r.t}}{z} \tag{2.45}$$

$$M_c = |M| \frac{2}{3} \frac{c_{c.edge}}{z}$$

M_t Resulting moment taken by tension components
M_c Resulting moment taken by compression components
M External moment acting on connection

The force distribution of the screws can then be calculated using the same approach as equation (2.36), using the formula for distribution of bending normal stress:

$$P_{i.ax} = \frac{M_t \, r_i}{\sum r^2} \tag{2.46}$$

The maximum compression stress in the CLT is calculated using the formula for bending normal stress distribution:

$$\sigma_{c.max} = \frac{M_c \, c_{c.edge}}{I_c} \tag{2.47}$$

$$I_c = \frac{B \, {c_{c.edge}}^3}{3} \tag{2.48}$$

$\sigma_{c.max}$ Maximum compression stress
I_c Moment of inertia for resulting rectangular compression section
B Width of resulting compression section

Using Hooke's law (Hibbeler, 2013, p.880) and linear interpolation the maxim strain of the tension and compression connectors can then be calculated:

$$\varepsilon_c = \frac{\sigma_{c.max}}{f_{yk}} \, \varepsilon_{c.yk} \tag{2.49}$$

$$\varepsilon_t = \frac{P_{ax.max}}{P_{ax.Rk}} \, \varepsilon_{ax.Rk} \tag{2.50}$$

f_{yk} Characteristic yield strength of compression material
ε_c & ε_t Compression and tension strain
$\varepsilon_{c.yk}$ & $\varepsilon_{ax.Rk}$ Characteristic yield strains
$P_{ax.max}$ Largest axial force in tension connector

For Navier's hypothesis to be valid, the rate of change in strain must be equal for the compression and tension components of the connection. The resulting equations are used to iterate λ until the strain rates are equal:

$$\varepsilon'_c = \frac{\varepsilon_c}{c_{c.edge}} \tag{2.51}$$

$$\varepsilon'_t = \frac{\varepsilon_t}{d_{F.r.t}} \tag{2.52}$$

f_{yk} Characteristic yield strength of compression material
ε_c & ε_t Compression and tension strain
$\varepsilon_{c.yk}$ & $\varepsilon_{ax.Rk}$ Characteristic yield strains

For a connection influenced by moments about two axes, the critical axial tension force and compression stress can be calculated as the sum of the critical forces and stresses as the connection is considered to act elastically.

2.9 ETA-11/0030 and EN 1995-1-1:2008

ETA-11/0030 is a European technical assessment for Rothoblaas Self-tapping screws and threaded rods. The assessment outlines an approved method for the calculation of the characteristic and design values of various Rothoblaas screws in different timber materials (ETA-Danmark, 2019).

For CLT connections, the minimum distances of the screws in a connection must satisfy ETA-11/0030 Annex B, for the wide face of CLT members with a minimum thickness of 10 d_1. The minimum distances can be seen in Figure 2-22 and equations of Table 2-2 (ETA-Danmark, 2019).

Table 2-2: Minimum connection distances (ETA-Danmark, 2019, Annex B).

	a_1	$a_{3,t}$	$a_{3,c}$	a_2	$a_{4,t}$	$a_{4,c}$
Plane surface	4 d_1	6 d_1	6 d_1	2.5 d_1	6 d_1	2.5 d_1

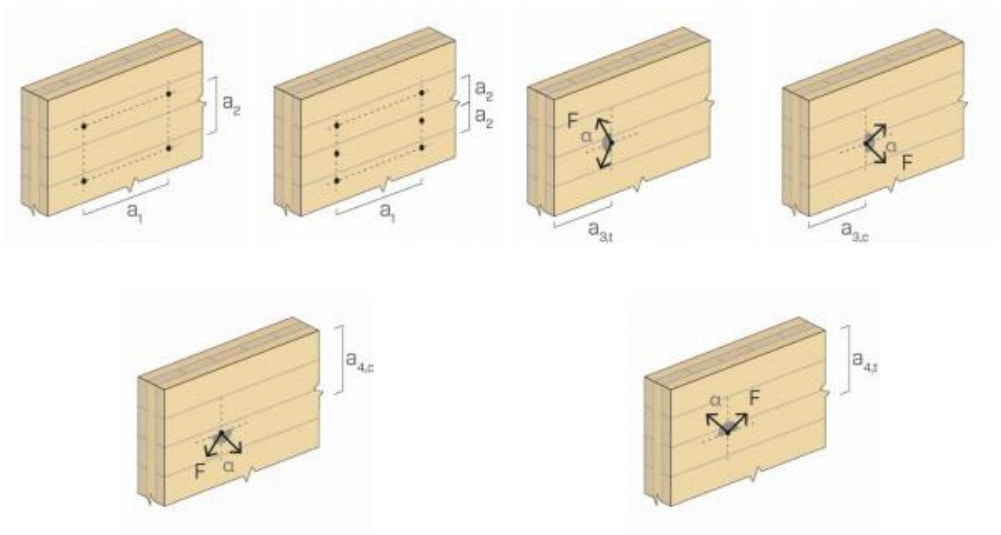

Figure 2-22: Edge distances (ETA-Danmark, 2019, Annex B).

The connection capacities are calculated under clause *3.9 Mechanical resistance and stability* of the ETA-11/0030. The axial withdrawal capacity of a soft wood connection is calculated with the following equation (ETA-Danmark, 2019).

$$F_{ax,Rk} = \frac{n_{ef}\ k_{ax}\ f_{ax,k}\ d_1 * l_{ef}}{k_\beta} \left(\frac{\rho_k}{\rho_a}\right)^{0.8}$$

n_{ef} Effective number of screws in accordance with EN 1995-1-1:2008
l_{ef} Penetration length of threaded part according to EN 1995-1-1:2008
k_{ax} 1.0 for angles to the grain over 45 ˚
k_β 1.0 for timber
d_1 Outer threaded diameter
ρ_k Characteristic timber density
ρ_a Reference density for screw characteristics

In accordance with ETA-11/0030, the efficient number of screws should be calculated in accordance with EN 1995-1-1:2008. For axially loaded screws, EN 1995-1-1:2008 equation (8.41) is used for the

calculation of the efficient number of axially loaded screws, resulting in the following equation (CEN, 2008; ETA-Danmark, 2019)

$$n_{ef} = n^{0.9}$$

n The number of screws in the connection

For the lateral load-carrying capacity, the assessment gives the following formula for the calculation of the embedding strength of predrilled connections in soft wood (ETA-Danmark, 2019).

$$f_{h,k} = \frac{0.082\ \rho_k\ (1 - 0.01\ d_1)}{2.5\ cos^2\alpha + sin^2\alpha}$$

α Angel between the screw and grain direction.

According to ETA-11/0030, the characteristic lateral load carrying capacity shall be calculated according to EN 1995-1-1:2008. For a steel-timber connection consisting of a single section thick steel plate, EN 1995-1-1:2008 equation (8.10) is calculated (CEN, 2008; ETA-Danmark, 2019).

$$F_{v,Rk} = min \begin{cases} f_{h,k}\ t_1\ d_1 \\ f_{h,k}\ t_1\ d_1 \left[\sqrt{2 + \frac{4\ M_{y,Rk}}{f_{h,k}\ d_1\ {t_1}^2}} - 1 \right] + \frac{F_{1ax.Rk}}{4} \\ 2{,}3 \sqrt{M_{y,Rk}\ f_{h,k}\ d_1} \end{cases}$$

$F_{v,Rk}$ Characteristic shear capacity per shear section
t_1 Steel plate thickness
$M_{y,Rk}$ Characteristic yield moment of screw
$\frac{F_{1ax.Rk}}{4}$ Rope effect for Axial withdrawal capacity

EN 1995-1-1:2008 clause 8.2.2(2) states that the contribution of the rope effect for a screw connector can be up to 100% of the characteristic axial withdrawal capacity for a singular connector (CEN, 2008). The two remaining characteristic capacities to be checked are the tensile screw capacity, and the characteristic head pull-through capacity. According to ETA-11/0030, the head pull-through capacity may be disregarded for steel-timber connections, and the tensile capacity is retrieved as a characteristic predetermined value for the specified connector (ETA-Danmark, 2019).

For a connection subjected to a combination of axial and lateral loads, the ETA provides a criterion for the connection design utilization described in equation -. The characteristic capacity can be approximated using the same formula with the characteristic capacities (ETA-Danmark, 2019).

$$\left(\frac{F_{ax,Ed}}{F_{ax,Rd}}\right)^2 + \left(\frac{F_{v,Ed}}{F_{v,Rd}}\right)^2 \leq 1$$

2.10 ETAG 001: Metal anchors for use in concrete

ETAG 001 is the "Guideline for European Technical Approval of Metal Anchors for Use in Concrete." the guideline outlines methods for calculation of critical concrete anchor capacities (EOTA, 2010). ETAG 001 clause 4.2.1 states that the tension loads acting on the anchors due to loads and bending moments should be calculated according to the theory of elasticity following the following assumptions:

- The anchor plate experiences no deformation. This assumption is only valid if anchor plate is sufficiently stiff.
- The stiffness of the anchors is equal and correspond to the elasticity of steel as given by EN 1992-1-1:2008.
- Anchors in the compression zone do not contribute to transmission of normal forces.

For the calculation of the shear distribution clause 4.2.1 describes two different distributions dependent on the mode of failure. For steel failure and concrete pry-out failure, the shear distribution can be calculated as point loads distributed about a center of rotation for moments, and evenly distributed for external shear forces. For a concrete edge failure, only the most unfavorable anchors take up shear loads. This means that the anchors closest to the concrete edge will be the critical connections (EOTA, 2010).

The required tension capacity proofs of ETAG 001 clause 5.2 are summarized in Table 2-3.

Table 2-3: ETAG 001 tension proof criteria (EOTA, 2010).

	Anchor group
Steel failure	$N_{Sd}^{h} \leq N_{Rk,s}/\gamma_{Ms}$
Pull-out failure	$N_{Sd}^{h} \leq N_{Rk,p}/\gamma_{Mp}$
Concrete cone failure	$N_{Sd}^{g} \leq N_{Rk,c}/\gamma_{Mc}$
Splitting failure	$N_{Sd}^{h} \leq N_{Rk,sp}/\gamma_{Msp}$

The characteristic steel failure is calculated using the following equation:

$$N_{Rk,s} = A_s \, f_{uk} \quad [N]$$

f_{uk} Nominal tensile strength [N/mm²]
A_s Threaded cross-section [mm²]

The pull-out resistance $N_{Rk,p}$ is given by relevant anchor ETA. For bonded connections, ETA TR029 clause 5.2.2.3 gives the following approach for the calculation of $N_{Rk,p}$ (EOTA, 2007):

$$N_{Rk,p} = N_{Rk,c}^{0} \frac{A_{p,N}}{A_{p,N}^{0}} \, \psi_{s,Np} \, \psi_{g,Np} \, \psi_{ec,Np} \, \psi_{re,Np} \quad [N]$$

The ideal characteristic capacity is calculated with the following equation:

$$N_{Rk,p}^{0} = \pi \, d \, h_{helix} \, \tau_{Rk} \quad [N]$$

τ_{Rk} Bond resistance retrieved from ETA [N/mm²]
h_{helix} depth of helix element from ETA

Areas $A^0_{p,N}$ and $A_{p,N}$ are calculated in the same way as $A^0_{c,N}$ and $A_{c,N}$ in Figure 2-23 and Figure 2-24, replacing $s_{cr,N}$ and $c_{cr,N}$ with $s_{cr,Np}$ and $c_{cr,Np}$ as calculated in the following equations (EOTA, 2007).

$$s_{cr,Np} = 20\ d\ \left(\frac{\tau_{Rk,ucr}}{7.5}\right)^{0.5} \quad [mm]$$

$$c_{cr,Np} = 0.5\ s_{cr,Np} \quad [mm]$$

$\tau_{Rk,ucr}$ Bond resistance retrieved from ETA [N/mm^2]
h_{helix} Depth of helix element from ETA [mm]

The edge distance factor $\psi_{s,Np}$ is calculated with the following equation (EOTA, 2007):

$$\psi_{s,Np} = 0.7 + 0.3\frac{c}{c_{cr,Np}} \leq 1$$

The failure surface factor $\psi_{g,Np}$ is then calculated (EOTA, 2007):

$$\psi_{g,Np} = \psi^0_{g,Np} - \left(\frac{s}{s_{cr,Np}}\right)^{0.5}\left(\psi^0_{g,Np} - 1\right) \geq 1$$

$$\psi^0_{g,Np} = \sqrt{n} - \left(\sqrt{n} - 1\right)\left(\frac{d\ \tau_{Rk}}{k\sqrt{h_{ef}\ f_{ck,cube}}}\right)^{1.5} \geq 1$$

s Anchor spacing [mm]
n Number of anchors in group
k 3.3 for non-cracked concrete and 2.3 for cracked

Next the factor for eccentrically loaded anchor groups were calculated using the same eccentricity as described in Figure 2-25 (EOTA, 2007; EOTA, 2010).

$$\psi_{ec,Np} = \frac{1}{1 + 2e_N/s_{cr,Np}} \leq 1$$

The last effect calculated is the shell spalling factor $\psi_{re,Np}$. This factor is equal to the shell spalling factor $\psi_{ec,N}$ calculated for the cone failure (EOTA, 2007; EOTA, 2010).The next tension failure mode is the concrete cone failure calculated with the following equation (EOTA, 2010):

$$N_{Rk,c} = N^0_{Rk,c}\frac{A_{c,N}}{A^0_{c,N}}\ \psi_{s,N}\ \psi_{re,N}\ \psi_{ec,N} \quad [N]$$

First the ideal concrete cone capacity is calculated (EOTA, 2010):

$$N^0_{Rk,c} = k_1\sqrt{f_{ck,cube}}\ h_{ef} \quad [N]$$

k_1 7.2 for cracked concrete or 10.2 for non-cracked
h_{ef} Effective embedment depth [mm]

The idealized cone area of the concrete is then calculated as shown in Figure 2-23, while the total cone area for a connection consisting of a singular line of anchors is calculated as shown in Figure 2-24 (EOTA, 2010).

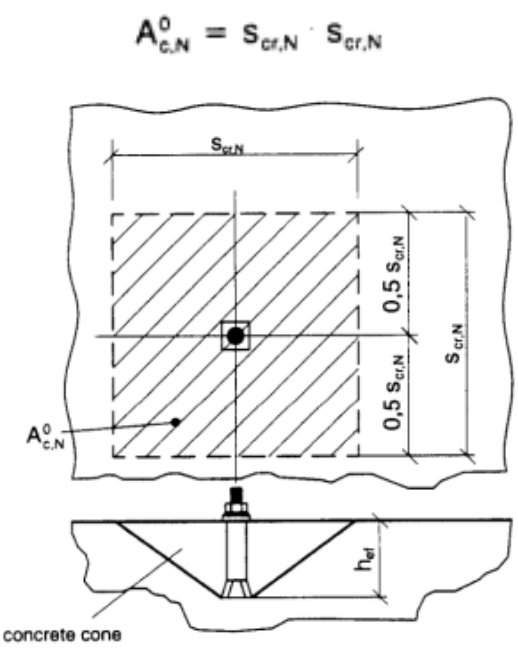

Figure 2-23: Idealized cone area (EOTA, 2010).

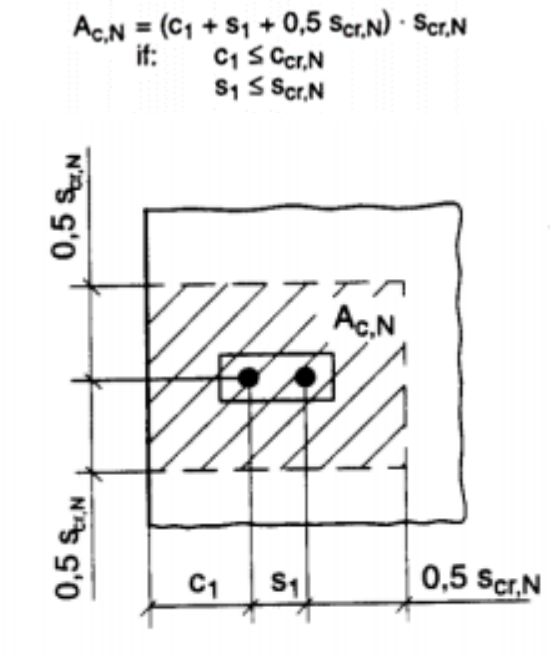

Figure 2-24: Connection cone area (EOTA, 2010).

Next, the edge factor $\psi_{s,N}$ is calculated (EOTA, 2010):

$$\psi_{s,N} = 0.7 + 0.3\frac{c}{c_{cr,N}} \le 1$$

$c_{cr,N}$ Critical edge distance for cone failure [mm]

After this the shell spalling factor $\psi_{re,N}$ is calculated as an effect of reinforcement in the cone area. The reduction factor can be disregarded if the reinforcement spacing is ≥ 150 mm or has diameter ≤ 10 mm with a spacing ≥ 100 mm, otherwise the following equation for the reduction factor is used (EOTA, 2010):

$$\psi_{re,N} = 0.5 + \frac{h_{ef}}{200} \le 1$$

The last reduction factor of the cone failure is the reduction factor for eccentric loading of the connection with an eccentricity calculated according to Figure 2-25. The factor is calculated with the following equation (EOTA, 2010):

$$\psi_{ec,N} = \frac{1}{1 + 2e_N/s_{cr,N}} \le 1$$

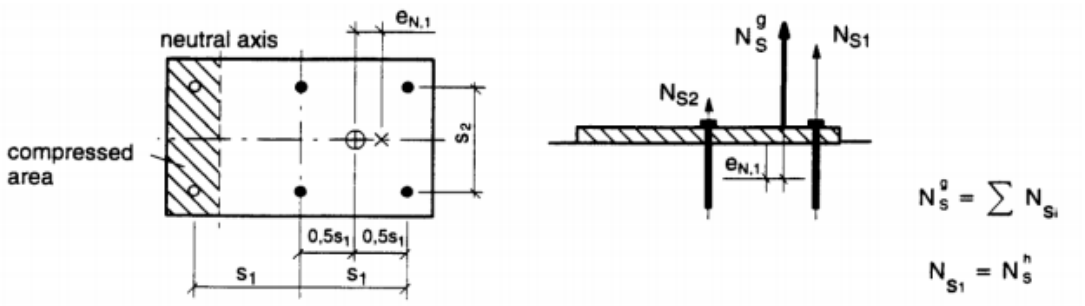

Figure 2-25: eccentricity of tension anchors (EOTA, 2010).

Next the splitting failure is calculated. ETAG 001 clause 5.2.2.6(a) and (b) states that the failure will not occur for uncracked concrete if $c \geq c_{cr,sp}$ and the member depth is greater than h_{ef}. For cracked concrete calculation can be omitted if the concrete cracking is limited to $\sim 3\ mm$ and the characteristic resistance is calculated for cracked concrete. Otherwise the factors calculated above for $N_{Rk,c}$ should be calculated using $c_{cr,sp}$ and $s_{cr,sp}$ instead of $c_{cr,N}$ and $s_{cr,N}$. $\psi_{ec,N}$. In addition, a factor for member depth $\psi_{h,sp}$ should be added resulting in the following equations (EOTA, 2010):

$$N_{Rk,c} = N^0_{Rk,c} \frac{A_{c,N}}{A^0_{c,N}}\ \psi_{s,N}\ \ \psi_{re,N}\ \ \psi_{ec,N}\ \ \psi_{h,sp}$$

$$\psi_{h,sp} = \left(\frac{h}{h_{min}}\right)^{\frac{2}{3}} \leq 1.5$$

h Concrete depth [mm]

h_{min} Concrete height according to minimum edge distance or $c_{cr,sp}$ [mm]

For the connection shear loads ETAG 001 require the proofs shown in Table 2-4 (EOTA, 2010).

Table 2-4: ETAG 001 required shear proofs.

	Anchor group
Steel failure	$V^h_{Sd} \leq V_{Rk,s}/\gamma_{Ms}$
Concrete pry-out failure	$V^g_{Sd} \leq V_{Rk,cp}/\gamma_{Mc}$
Concrete edge failure	$V^g_{Sd} \leq V_{Rk,c}/\gamma_{Mc}$

The characteristic shear resistance of the steel is calculated using the following equation (EOTA, 2010):

$$V_{Rk,s} = 0.5\ A_s * f_{uk}$$

The concrete pry-out failure of an anchor is then calculated (EOTA, 2010):

$$V_{Rk,cp} = k * N_{Rk,c}$$

$k = 2$ Conservative value for $h_{ef} \geq 60\ mm$

According to ETAG 001 clause 5.2.3.3 a connection affected by varying horizontal and vertical shear forces over the connection, the most unfavorable anchor should be calculated for the concrete pry

out failure, resulting in the calculation $N_{Rk,c}$ for the critical anchor using of $A_{c,N}$ as shown in Figure 2-26 (EOTA, 2010):

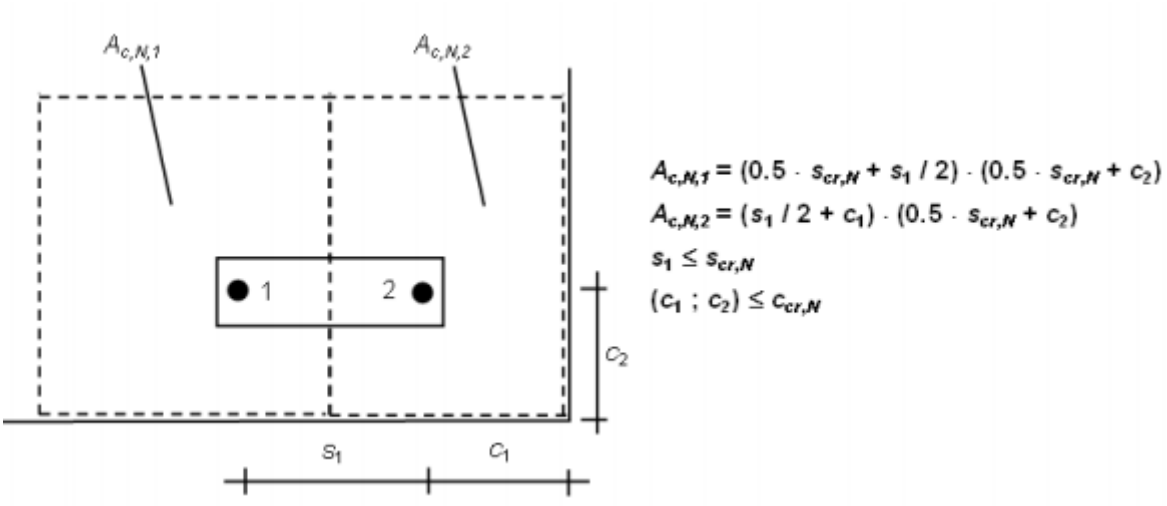

Figure 2-26: Critical anchor cone area (EOTA, 2010).

The next calculation is the concrete edge failure calculated with the following equation (EOTA, 2010):

$$V_{Rk,c} = V^0_{Rk,c} \frac{A_{c,V}}{A^0_{c,V}} \psi_{s,V} \ \psi_{h,V} \ \psi_{\alpha,V} \psi_{ec,V} \psi_{re,V}$$

The initial value of the concrete edge failure is calculated with the following equations (EOTA, 2010):

$$V^0_{Rk,c} = k_1 \, d^{\alpha} \, {h_{ef}}^{\beta} \sqrt{f_{ck,cube}} \, c_1^{1.5}$$

$$\alpha = 0.1 \left(\frac{l_f}{c_1}\right)^{0.5}$$

$$\beta = 0.1 \left(\frac{d_{nom}}{c_1}\right)^{0.2}$$

k_1	1.7 for cracked concrete and 2.4 for non-cracked
l_f	Equal to h_{ef} for low profile connections [mm]
d_{nom}	Equal to d for solid anchors [mm]

The idealized cone edge area of the concrete is then calculated as shown in Figure 2-27, while the total cone area for a connection consisting of a singular line of anchors is calculated as shown in Figure 2-28 (EOTA, 2010):

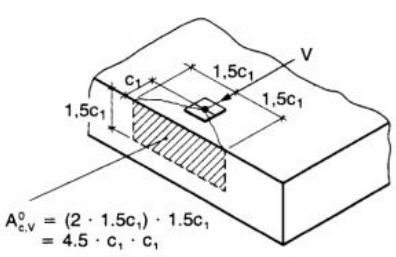

Figure 2-27: Idealized cone edge area (EOTA, 2010).

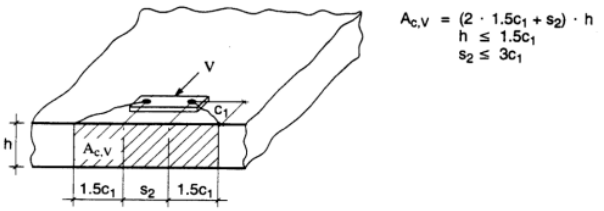

Figure 2-28: Connection cone edge area (EOTA, 2010).

The factor $\psi_{s,V}$ is then calculated as a reduction factor for a corner connection, but the factor can be neglected for a connection with one edge (EOTA, 2010).

The next factor $\psi_{h,V}$ takes in to account the disproportionate decrease of shear resistance due to the member thickness (EOTA, 2010).

$$\psi_{h,V} = \left(\frac{1.5\ c_1}{h}\right)^{\frac{1}{2}} \geq 1$$

Factor $\psi_{\alpha,V}$ is calculated from the angel between the resulting shear force of an anchor group and the direction perpendicular to the concrete edge as shown in Figure 2-29 for a connection affected by a combination of moments and shear forces (EOTA, 2010).

$$\psi_{\alpha,V} = \sqrt{\frac{1}{(\cos \alpha_v)^2 + \left(\frac{\sin \alpha_V}{2.5}\right)^2}} \geq 1$$

α_V Angel between applied force and direction perpendicular to the edge

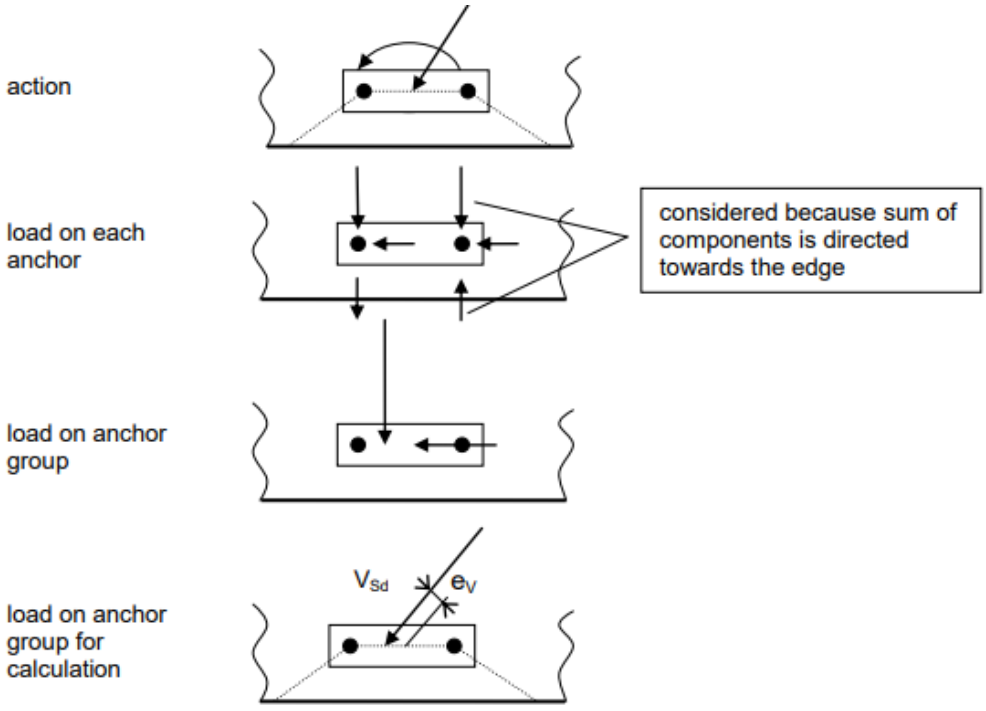

Figure 2-29: Resulting shear edge force and eccentricity (EOTA, 2010).

Factor $\psi_{ec,V}$ is then calculated for the group effect of different shear loads acting on individual anchors of a group using the following equation (EOTA, 2010).

$$\psi_{ec,V} = \sqrt{\frac{1}{1 + \frac{2\ e_V}{3\ c_1}}} \leq 1$$

α_V Angel between applied force and direction perpendicular to the edge

The last factor calculated is $\psi_{re,V}$ which takes in to account the effect of reinforcement of cracked concrete. For un-cracked of cracked concrete without edge reinforcement the factor is set equal to 1. For cracked concrete with straight edge reinforcement with ≥Ø12, a factor of 1.2 can be used. If, in addition to the edge reinforcement, there is shear reinforcement with center distance closer than 100 mm, the factor can be increased to 1.4 (EOTA, 2010).

For the combined effect of shear and tension, ETAG 001 equation (5.9) gives a design criterion:

$$(\beta_N)^\alpha + (\beta_V)^\alpha \leq 1$$

β_N & β_V Critical ratio between design resistance and loading
α 2 for steel failure, 1.5 for all other failure modes

2.11 Ansys® *Academic Research Mechanical, Release 19.2*

Ansys® *Academic Research Mechanical, Release 19.2* is an advanced final element software (FEM), allowing for simulation of complex mechanical models.

FEM calculations are based on partial differential equations. As the number of differential equations grow with the complexity of the model, the vast number of models are not possible, or too complex to be solved using traditional analytical models.

A FEM program is used to calculate approximate numerical equations, resulting in approximate models of the real problem. The differential equations are usually approximated using combinations of linear base functions. These base functions are simulated using grid meshing in Ansys® *Academic Research Mechanical, Release 19.2.* as the numerical method increases with increased sub steps, the refinement of the mesh dictates the precision of the calculations.

Ansys® *Academic Research Workbench, Release 19.2* offers an array of simulation methods, among which are the *Static structural* analysis system for traditional static load systems as well as modal analysis which can be used for dynamic earthquake design. The workbench is a graphical interface allowing for easy modeling and creation of complex 3D models.

For the *Static structural* analysis, Ansys® *Academic Research Workbench, Release 19.2* offers the ability to define material properties relevant to specific simulations. The program allows for the calculations both elastic and elastic-plastic simulations. It also allows for the simulation of orthotropic materials. Supports and forces can be designated to surfaces or elements with rigid or deformable behavior. The function for pre-loading of materials can also allow for the simulation of pre-loaded bolts.

3 Material and method

3.1 Torsion test

The torsion test system consisted of two perpendicular 8mm thick plates with an area of 60x450 mm each connected by a bent section with an internal radius of 5 mm. Automatic hex dominant meshing was used for the model. A deformable moment of 3 kNm was applied about the y-axis on the upper edge, while a fixed support was applied to the bottom edge as shown in Figure 3-1. Relevant resulting stresses were then retrieved from the model.

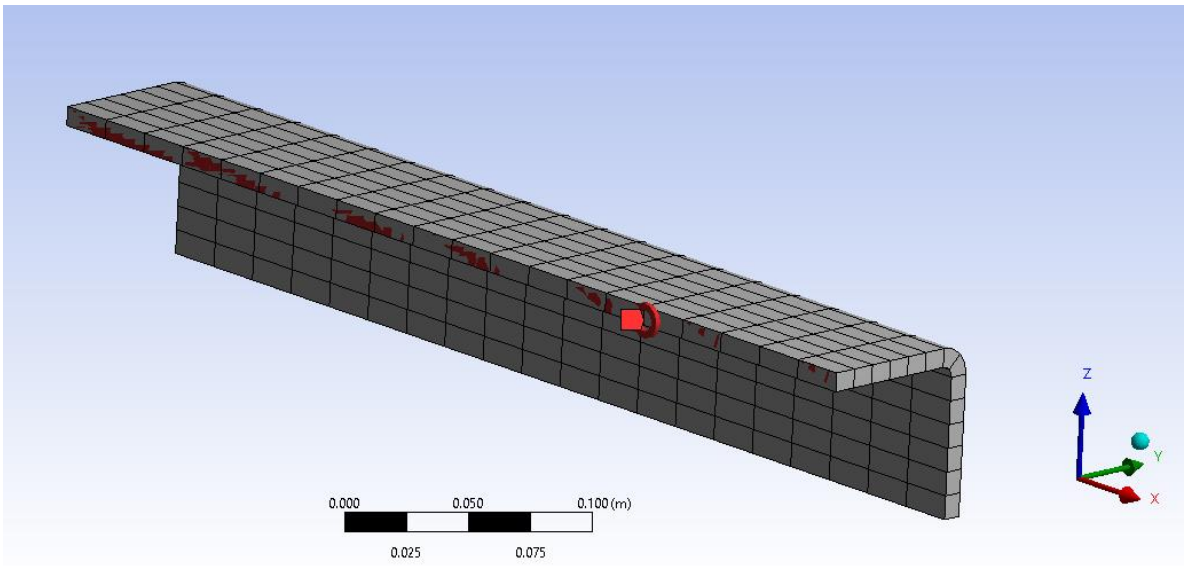

Figure 3-1: Torsion bending test. (Images used courtesy of ANSYS, Inc.)

3.2 Preloaded bolt test

The friction test was performed on a system consisting of two plates connected by a preloaded bolt. The bottom plate consisted of a singular centered hole. The top plate was placed flush with the bottom plate and had a 40 mm tall vertical plate mounted on the inner edge with a 5 mm wide welded edge. The plates were 8 mm thick and had an area of 80x300 mm^2. The holes had a diameter of 15 mm, and the elongated hole had a center length of 240 mm. The preloaded bolts also had a shank diameter of 15 mm with 12 mm thick round nuts using an outer diameter of 28 mm as shown in Figure 3-2.

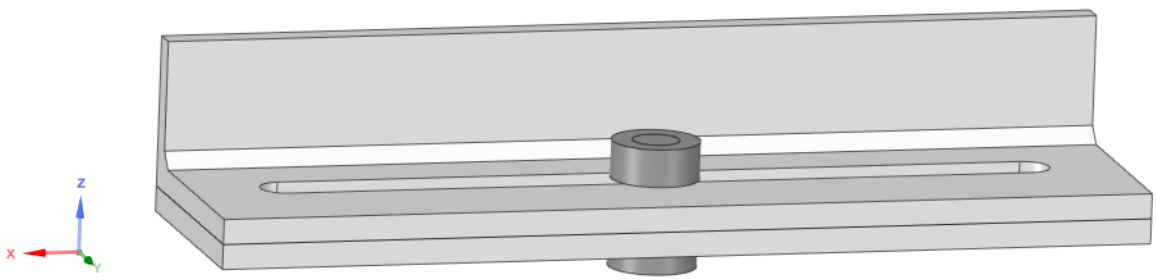

Figure 3-2: Ansys model for friction test. (Images used courtesy of ANSYS, Inc.)

An automatic hex dominant meshing method was used for the preloaded bolt and bottom plate of the model as shown in Figure 3-3. For the top plate, an automatic mesh of tetrahedrons were used, with a level one refinement applied to the surface of the hole.

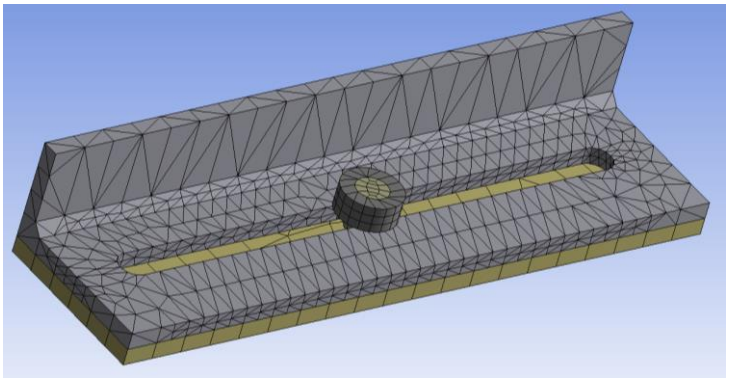

Figure 3-3: Meshing of preloaded test model. (Images used courtesy of ANSYS, Inc.)

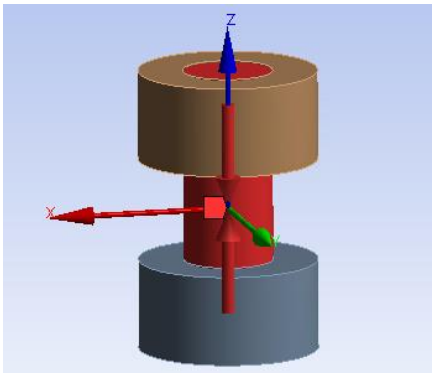

Figure 3-4: Application of bolt preloading (Images used courtesy of ANSYS, Inc.)

The elements of the model were all assigned a perfectly elastic material with a modulus of elasticity of 210 GPa and Poisson's ratio of 0.3. A friction constant (μ) of 0.3 was used for the surfaces. A fixed support was applied to the bottom face of the lower plate, as well as a remote displacement prohibiting rotation about the z-axis. The preloaded force was applied using the preload function with a local coordinate system located in the center of the bolt as shown in Figure 3-4.

The shear force on the system was applied on the left edge of the top plate acting in the positive x-direction. The tension force and moments were applied at the top of the vertical plate.

For each of the tests the shear capacity was calculated assuming a critical capacity for the system when the top plate reached a deformation of 0.5 mm. The shear forces achieved for this relative plate deformation were then compared with the preloaded forces calculated according to *2.5 Preloaded bolts in tension and shear capacity.* The different load combinations calculated for the friction tests were summarized in Table 3-1.

Table 3-1: Shear test cases

Load case	Loading
A	22 kN preloading
B	22 kN preloading + 10 kN tensile force
C	22 kN preloading + 1 kNm M_y
D	22 kN preloading + 10 kN tensile force + 1 kNm M_y

Resulting equivalent stresses were also retrieved from each test. In addition, stress simulations for load case B as well as the design shear resistance of an M14 bolt according to EN 1993-1-8:2005 in normal were ran for Figure 3-2 with normal sized holes. The design resistance of the M14 bolt was calculated according to EN 1993-1-8:2005, as shown in Appendix B. S235 were assumed for the

plates with slip factor A (μ = 0.5) for a singular friction plane. Bolt class 10.9 was assumed for the pretension bolt. Load case A was also run with a reduced μ of 0.01 for the bolt-plate shear plane, as shown in Figure 3-5, while μ remained 0.3 for the shear plane of the plates.

Definition	
Type	Frictional
Friction Coefficient	1.e-002

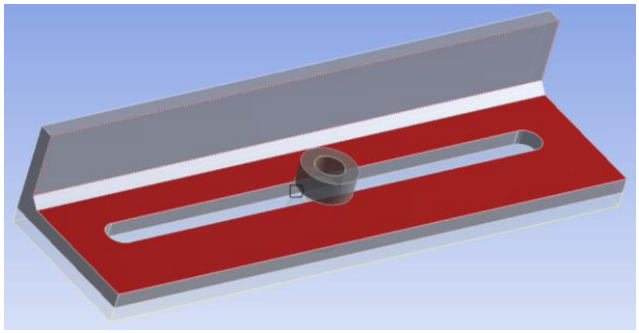

Figure 3-5: Reduced friction coefficient for Bolt-plate surface. (Images used courtesy of ANSYS, Inc.)

3.3 Profile capacity calculations

The six profiles shown in Figure 3-6 were tested in this thesis. The technical drawings for the different profiles summarized in Appendix A, were used for the hand calculations and FEM modeling. Technical drawings for profile 8-28-AP with the adjustment connection was not provided, as it was a proposed concept. All the profiles consisted of four connections, from the top CLT-steel connection A to the bottom connection D.

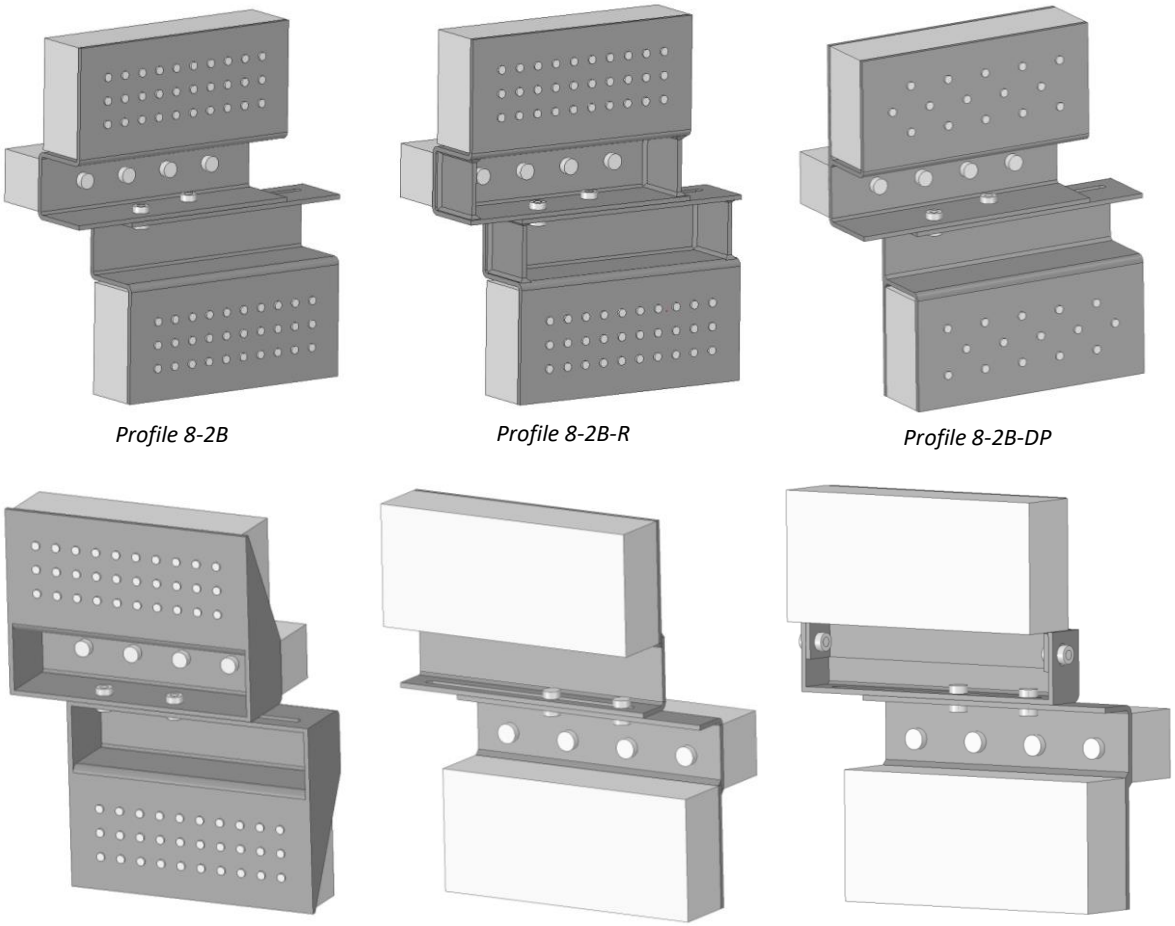

Profile 8-2B *Profile 8-2B-R* *Profile 8-2B-DP*

Profile 8-2B-SR *Profile 8-2B-AP* *Profile 8-2B-AP with adjustment connection*

Figure 3-6: Tested profiles. (Images used courtesy of ANSYS, Inc.)

External forces:

The critical external loads applied on the system were calculated using a shear load P_x of 30 kN on the compression profile using the approach described in *2.6 External force application of profiles,* assuming the friction connection acting pinned. The forces were calculated with a CLT element three meters tall, and four meters wide.

As the friction connection was situated above the concrete connection for profile 8-2B-AP, the resulting external vertical force acting downwards in connection A compressed the profile, differing for the remaining profiles where the vertical force acting upwards in support D compressed the profiles.

Ansys® *Academic Research Mechanical, Release 19.2* simulations:

The material chosen for the profile and preloaded bolts was defined as perfectly elastic with a modulus of elasticity of 210 GPa and Poisson's ratio of 0.3. No material density was assigned to the material as the system weights were considered for the external forces applied.

The two CLT-steel connections were simplified as one element consisting of the CLT element and all the screws. Each of the CLT elements was calculated with an area equal to the steel plate and a thickness of 100 mm. The screws of the connection were calculated as solid un-hinged cylinders with the same diameter as the holes. As the screws and CLT had different elastic modulus, an approach for calculating approximated elastic system modulus was created. For the approach, Hooke's law was considered for the CLT compression parallel to the grain $E_{0.g.mean}$ and perpendicular to the grain:

$$\epsilon_{c.o.k} = \frac{E_{0.g.mean}}{f_{c.0.k}} \tag{3.1}$$

$$\epsilon_{c.90.k} = \frac{E_{90.g.mean}}{f_{c.90.k}} \tag{3.2}$$

$\epsilon_{c.o.k}$	Characteristic strain parallel with grain
$\epsilon_{c.90.k}$	Characteristic strain perpendicular to grain
$E_{0.g.mean}$	Elastic modulus parallel with grain
$E_{90.g.mean}$	Elastic modulus perpendicular to grain
$f_{c.0.k}$	Compressive strength parallel with grain
$f_{c.90.k}$	Compressive strength perpendicular to grain

For the Rothoblaas connectors, the strain for the characteristic axial screw capacity was assumed equal to the characteristic compressive CLT strain, while the characteristic shear capacity was assumed to yield the same strain as the CLT parallel to the grain. These strains were assumed to appear between the cylindrical element surfaces and the main element as shown in Figure 3-7.

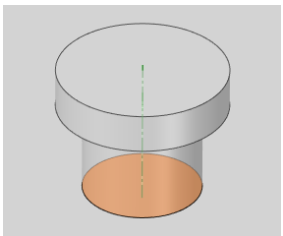

Figure 3-7: Assumed CLT-Rothoblaas element strain surface marked in orange. (Images used courtesy of ANSYS, Inc.)

The average elastic modulus was derived from these strains, and was found using the following equations:

$$E_v = \frac{F_{v,Ek}\ \ E_{0.g.mean}}{A_s\ \ f_{c.0.k}} \tag{3.3}$$

$$E_{ax} = \frac{F_{ax,Ek}\ \ E_{90.g.mean}}{A_s\ \ f_{c.90.k}} \tag{3.4}$$

$$E_{avg} = \frac{E_v + E_{ax}}{2} \tag{3.5}$$

E_v Approximated connector elastic modulus from shear capacity of Rothoblaas
E_{ax} Approximated connector elastic modulus from axial capacity of Rothoblaas
E_{avg} Average elastic modulus

The concrete connection was also calculated as one element with the concrete area equal to that of the adjacent steel plate and a depth of 100 mm. The anchors were calculated with shank diameters of 15 mm and nut diameters of 28 mm and heights of 12 mm. A modulus of elasticity of 200 GPa was used for the concrete-anchor connection element, as suggested from the ETAG 001 clause 4.2.1.

The following support conditions of Table 3-2 were applied to the support elements for both the moment and stress calculations, using rigid remote displacement supports for the CLT connections, and displacement supports for the concrete connection.

Table 3-2: Support conditions for Ansys supports.

Reactions	Supports		
	A	B	D
Δx	Free	Free	Fixed
Δy	Free	Fixed	Free
Δz	Free	Fixed	Free
ϕx	Fixed	Fixed	Fixed
ϕy	Fixed	Fixed	Fixed
ϕz	Fixed	Fixed	Fixed

Two different simulations with different support, force and meshing were performed for each profile. The first simulation type was performed to determine support reactions and the minimum required bolt preload. To determine the moment reaction using the Ansys® *Academic Research Mechanical, Release 19.2* probe moment/force-reaction function, the applied forces and supports had to be situated at the surface of the support elements as shown in Figure 3-8 to avoid eccentricity interfering with the moment reactions. All the supports were defined as rigid, prohibiting twisting and deformation.

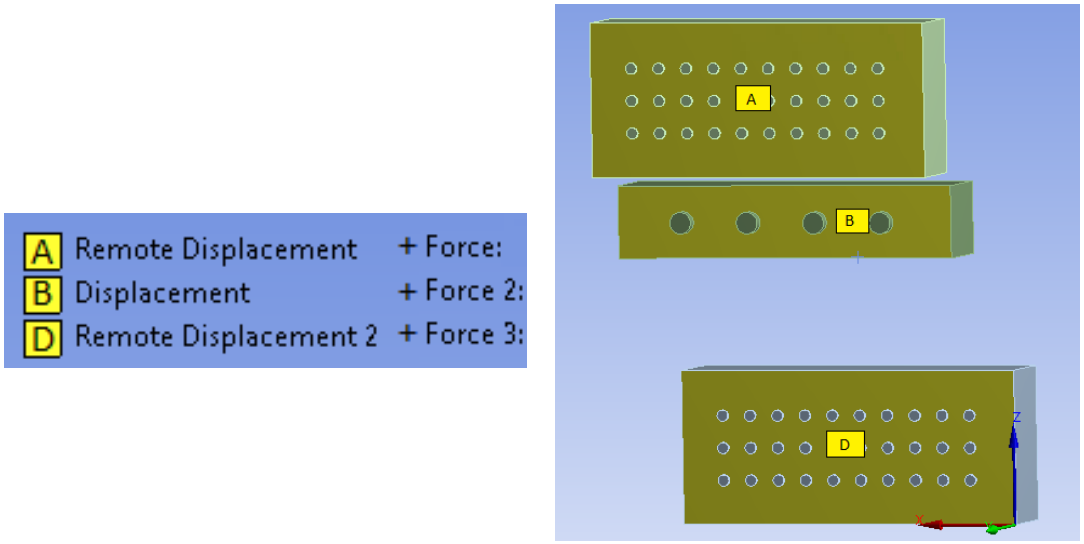

Figure 3-8: Support and force surfaces for moment reaction simulation. (Images used courtesy of ANSYS, Inc.)

The moment simulation was performed as an iterative process with increments of 100 N for the bolt preload, until the relative deformation difference was less than 0.5 mm between the plates of the friction connection. This test was performed for al profiles in both compression and tension with exception of profile 8-2B-AP with adjustment connections, where the preload of profile 8-2B-AP was assumed. As this method required several simulations per profile, automatic meshing was used, resulting in tetrahedron meshing for all elements except the preloaded bolts, where the system defaulted to hex dominant meshing as shown in Figure 3-9.

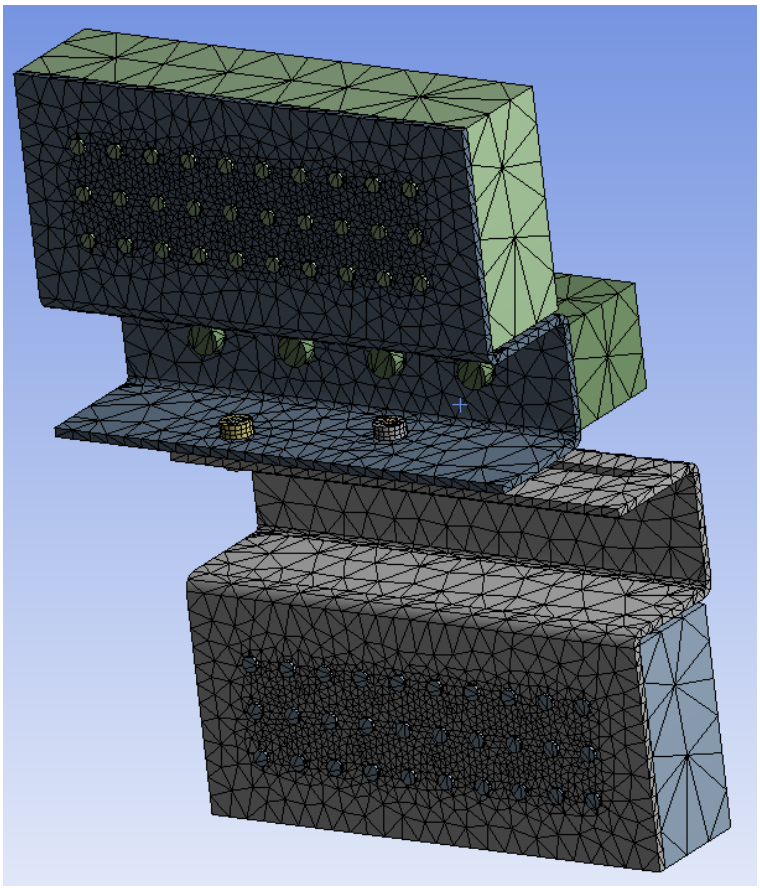

Figure 3-9: Meshing for moment reaction simulation. (Images used courtesy of ANSYS, Inc.)

The second simulation type was performed to determine the profile stresses, deformation as well as the force reactions of the critical connectors at support A,B and D for the different loading situations. As the force reaction distribution of the connectors were dependent on the deformation of the support elements, the forces and supports were applied on the edges of the support elements as shown in Figure 3-10 and Figure 3-11 for profile 8-2B and 8-2B-R.

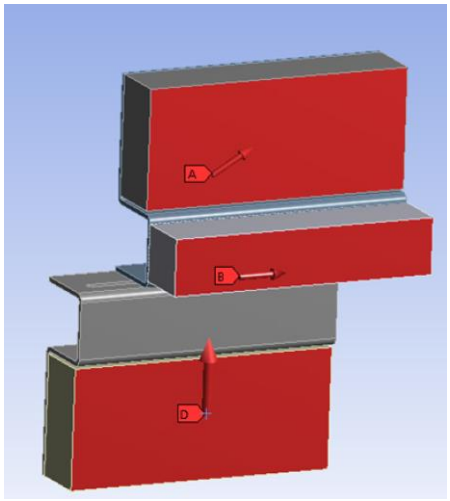

Figure 3-10: Surface force application for stress simulation. (Images used courtesy of ANSYS, Inc.)

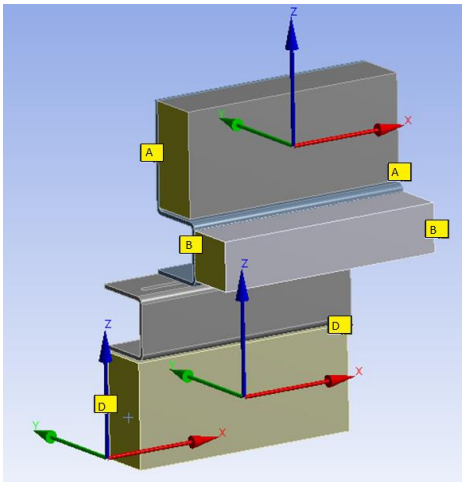

Figure 3-11: Surface support application for stress simulation. (Images used courtesy of ANSYS, Inc.)

For profile 8-2B-DP, the forces were applied on the top and bottom parts of the CLT elements for each plate. For Profile 8-2B-AP, the CLT elements were facing the other direction. As a result, the forces were applied to the outer most CLT face for this profile.

The required preload determined from the moment reaction calculations were used for these simulations. To increase the accuracy of the simulation for stresses at the friction connection for the different profiles, mesh refinement was applied to the edges of the elongated holes as shown in Figure 3-12.

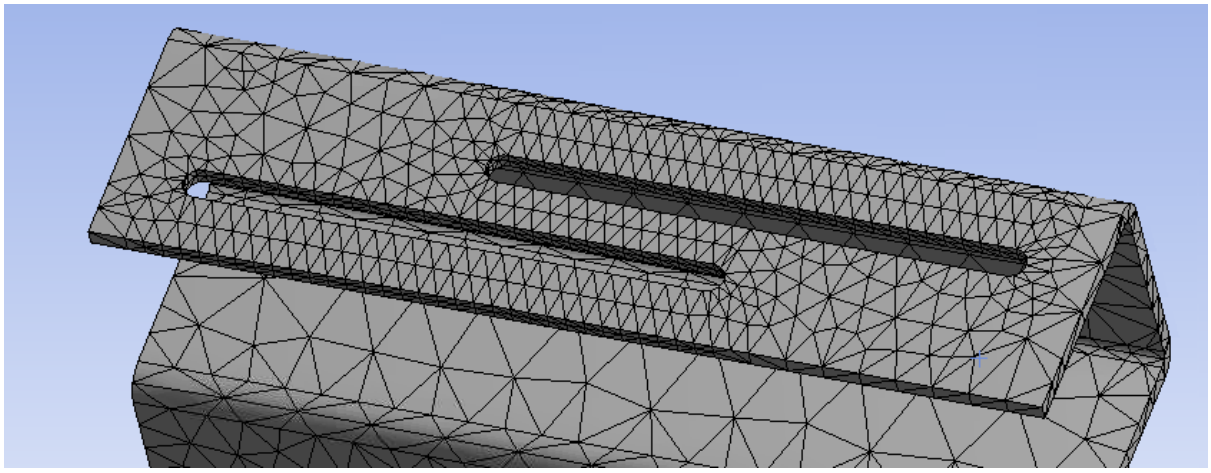

Figure 3-12: Mesh refinement of elongated holes.

After running a stress simulation, the location of the critical connector at each support was determined by looking at the plate stresses, as demonstrated in Figure 3-13. The force reaction of the critical connector was then found applying the probe Force Reaction function to the surfaces of the critical connector as shown in Figure 3-14.

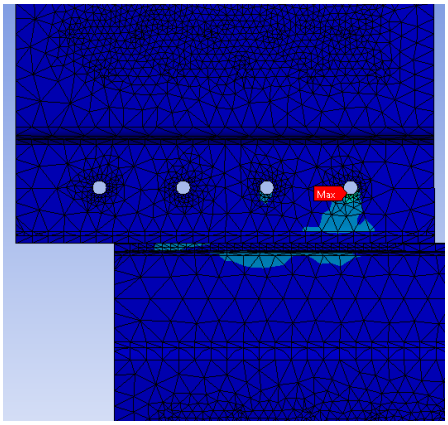

Figure 3-13: Example of plate stress in hole for connector. (Images used courtesy of ANSYS, Inc.)

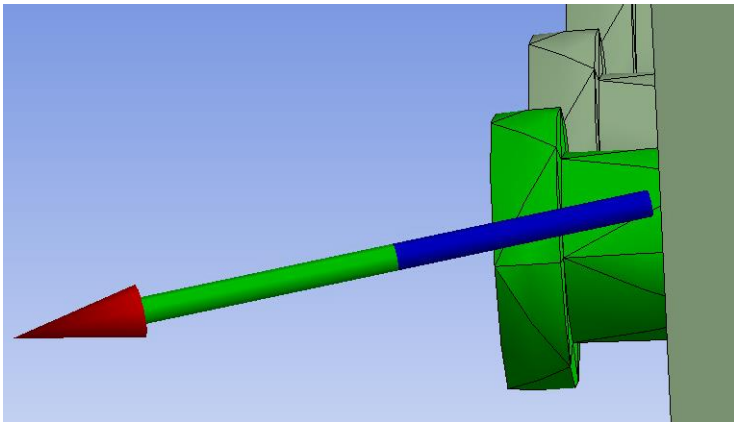

Figure 3-14: Surfaces used for calculation of force reaction of critical connectors. (Images used courtesy of ANSYS, Inc.)

For profile 8-2B-AP with adjustment connections, only the resulting stresses were simulated using the method and forces of profile 8-2B with the same preload determined from profile 8-2B-AP.

Hand calculations:

Hand calculations for moment reactions and connection capacity utilization were performed for profile 8-2B, 8-2B-R and 8-2B-AP. All the moment reactions were calculated considering the preloaded bolts fully shifted to the left edge of the elongated holes. The adjusted support conditions based on the Ansys simulations, for the moment calculations of the different profiles summarized in Table 3-3 to Table 3-5.

Table 3-3: support conditions for hand calculations of profile 8-2B.

Reactions	Supports			
	A	B	C	D
Δx	Free	Free	Free	Fixed
Δy	Free	Fixed	Free	Free
Δz	Free	Fixed	Free	Free
ϕx	Fixed	Fixed	Free	Fixed
ϕy	Fixed	Fixed	Fixed	Fixed
ϕz	Fixed	Fixed	Free	Fixed

Table 3-4: support conditions for hand calculations of profile 8-2B-R.

Reactions	Supports			
	A	B	C	D
Δx	Free	Free	Free	Fixed
Δy	Free	Fixed	Free	Free
Δz	Free	Fixed	Free	Free
ϕx	Fixed	Fixed	Free	Fixed
ϕy	Fixed	Fixed	Free	Fixed
ϕz	Fixed	Fixed	Free	Fixed

Table 3-5: Support conditions for hand calculations of profile 8-2B-AP.

Reactions	Supports			
	A	B	C	D
Δx	Free	Free	Free	Fixed
Δy	Free	Free	Fixed	Free
Δz	Free	Free	Fixed	Free
ϕx	Fixed	Free	Fixed	Fixed
ϕy	Fixed	Free	Fixed	Fixed
ϕz	Fixed	Free	Fixed	Fixed

For the profiles in tension, the vertical and horizontal force reaction of the friction connections were calculated as acting at the center between the two preloaded bolts. The horizontal force reactions of the friction connection for the profiles in compression were also assumed to act at the midpoint between the preloaded bolts.

For the profiles in compression, the vertical force center of the friction connections was assumed to act at the point along the x-axis as shown in Figure 3-15.

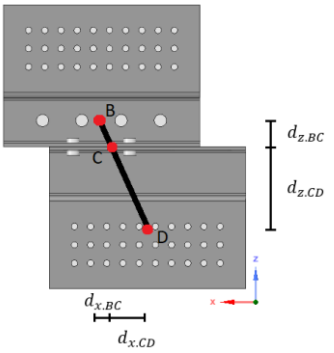

Figure 3-15: Vertical force center of friction connection C. (Images used courtesy of ANSYS, Inc.)

The force center was calculated using linear interpolation for the relative horizontal and vertical distances between support B,C and D for profile 8-2B and 8-2B-R using the following equation.

$$d_{x.BC} = \frac{d_{z.BC}}{(d_{z.BC} + d_{z.BD})} d_{x.BD} \tag{3.6}$$

d	Distance
x & z	Along either axis
AB & BC	From support to support

The same equation was used for 8-2B-AP calculating the distance $\mathrm{d_{x.AB}}$ as the friction connection was in support B for the profile.

The approximation of the vertical compression force center along the y-axis of the friction connections, were based on the resulting moment reactions found from the Ansys simulations. The force centers were summarized in Table 3-6.

Table 3-6: Force center of vertical reaction force along the y-axis of friction connection relative to previous connection.

Profile	vertical force center y-axis
8-2B	$\frac{1}{3} d_{y.BD}$
8-2B-R	$\frac{2}{3} d_{y.BD}$
8-2B-AP	$d_{y.AB}$

The CLT-steel capacity calculations were performed for both the critical compression and tension load criteria. Rothoblaas plate 8x80 were utilized for the CLT-steel connection. The measurements and characteristic capacities were summarized in Figure 3-16 and Table 3-7.

Table 3-7: Rothoblaas plate 8x80 characteristics. (ETA-Danmark, 2019)

Properties	Size	Unit	Description
d_1	8	mm	Nominal diameter
d_2	5.4	mm	Tip diameter
d_s	58	mm	Shank diameter
d_{uk}	10	mm	Under-head diameter
d_v	5	mm	Pre-drilling diameter
d_k	14.5	mm	Head diameter
b	55	mm	Thread length
L	80	mm	Screw length
t_1	3.4	mm	Head thickness
$M_{y.k}$	20.1	kNmm	Characteristic yield moment
$f_{ax.k}$	11.7	N/mm^2	Characteristic withdrawal
ρ_a	350	kg/m^3	reference density of characteristic values
f_{head}	10.5	N/mm^2	Characteristic head-pull through resistance
$f_{tens.k}$	21.1	N/mm^2	Characteristic tensile strength

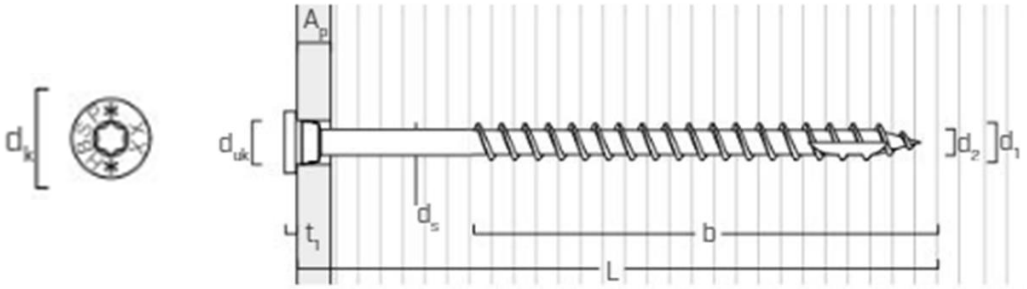

Figure 3-16: Rothoblaas plate 8x80. (ETA-Danmark, 2019)

The characteristic capacity was calculated for the Rothoblaas plate 8x80 using the method described in *2.9 ETA-11/0030 and EN 1995-1-1:2008.*

A five layered CLT panel was considered for the system shear wall. The CLT wall consisted of five perpendicular alternate layers of 20 mm thick boards with vertical outer boards. The CLT properties used for the connection calculations were summarized in Table 3-8.

Table 3-8: CLT characteristics.

Properties	Size	Unit	Description
ρ_k	385.0	kg/m^3	Density of CLT
$f_{c.90.k}$	2.5	N/mm^2	compressive strength perpendicular to grain
t_{CLT}	100	mm	Element thickness
$E_{90.g.mean}$	300	N/mm^2	Elastic modulus perpendicular to grain

The resulting reaction forces of the screws and compression stress in the CLT were calculated according to the theory described in chapter *2.8 Out of plane eccentrically loaded bolt connections.* The strain of the Rothoblaas screws at their characteristic tension capacity were assumed to be equal to the yield strain of CLT in compression, which was calculated from the CLT yield strength and elastic modulus described in Table 3-8 using Hooke's law (Hibbeler, 2013).

The critical characteristic and design connection utilization were calculated using the design criteria from *2.9 ETA-11/0030 and EN 1995-1-1:2008.* In addition, the characteristic utilization was controlled for the sum of the compression stress in the CLT from the two out of plane moments. The characteristic preloaded bolt capacity was calculated according to EN 1993-1-8:2005 table 3.4.

The concrete-steel connection calculations were performed for the compression load criteria of the three profiles. For the concrete connection, four Hilti HIT-Z anchors were calculated using the characteristic capacities and dimensions of the anchors described in ETA-12/0028 (DIBt, 2012). The dimensions not found in the ETA for this specific connection were summarized in Figure 3-17 and Table 3-9.

Table 3-9: Specific connection characteristics.

Properties	Size	Unit	Description
l_{nom}	120	mm	Nominal anchor depth
H_c	400	mm	Height of concrete cross section
B_c	100	mm	Width of concrete section
c_{min}	0.5 H_c	mm	Minimum vertical concrete edge distance
A_s	84.3	mm	Threaded stress area
$f_{c.cubed}$	25	N/mm^2	Cubed concrete yield strength
E_s	200 000	N/mm^2	Modulus of elasticity for steel
E_c	29 962	N/mm^2	Elasticity of modulus for concrete

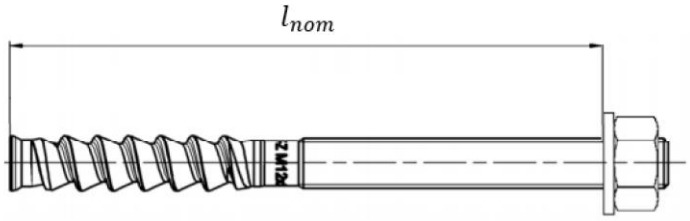

Figure 3-17: Hilti HIT-Z (DIBt, 2012).

The force reactions of the concrete connections were calculated using the same method as the CLT-steel connection. For the out of plane calculations, the linear strain curve was calculated assuming the modulus of elasticity for C20-25 concrete in the compression part of the profile, and modulus of elasticity of steel for the anchors as shown in Table 3-9.

3.4 Estimation of optimal slip load

The lateral force method of EN 1998-1:2004 clause 4.3.3.2 was performed for the four-story RC structure with the layout in Figure 3-18 and dimensions of Table 3-10. All floors and frames were equally spaced. Type two elastic response spectra for ground type C was assumed. The weight of the building was assumed to be concentrated in the floor of each story with the mass calculated as the weight of a concrete floor with constant thickness H_{cb} over the entire floor area. In addition, live

loads are imposed in the form of an imposed load. The structure was considered to be situated outside Scandinavia, resulting in the wind and snow loads to be ignored. In addition, the roof was considered as a story for the live load calculation.

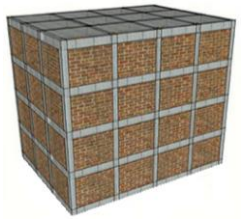

Figure 3-18: Building layout for base shear calculation.

Table 3-10: Building dimensions and characteristics.

Properties	Size	Unit	Description
H	12	m	Total structure height
A_{story}	18x26	m^2	Floor area of each story
H_{cb}	0.3	m	Average floor thickness
ρ_c	2500	kg/m^3	concrete density

The equivalent building seismic base shear F_b was calculated for a PGA of 0.1 and 0.35, and the resulting optimal friction system slip force was calculated as 0.2 F_b. The required number of friction columns were then estimated considering all friction dissipating elements experiencing the characteristic slip load calculated for profile 8-2B in Appendix C.

3.5 Limitations

Several simplifications and limitations were made for the approach of this thesis. These are summarized in the following lists.

External forces:

- Simplified lateral force method might not be representable for all real-world load cases.
- Reduced slip force of the overlaying CLT-element was assumed for the simulations and hand calculations. If even distribution of slip force is to be implemented, this assumption will result in a slight underestimate of the vertical loads acting in point A of the profiles.
- Profile 8-2B-AP is estimated for the CLT-element second from the bottom.

Ansys simulations:

- Preloaded bolts modeled with same diameter as holes. The same applied for the Rothoblaas screws.
- $\mu = 0.3$ were assumed for all friction surfaces.
- Supports and corresponding connectors were combined as one element with an estimated elastic modulus for the entire element.
- CLT elements simplified as either fixed or free for rotation and translation.
- Ansys supports applied to surface of element facing steel plate for moment simulation, prohibiting compression of the support element.

Hand calculations:

- Two shear plains with equal contribution were assumed per bolt, with $\mu = 0.3$.
- Elastic strain curve used for concrete
- Estimated linear strain curve for Rothoblaas screws with critical strain value at axial tensile capacity equal to yield strain of compressed glulam perpendicular to grain.
- Profile supports and connections simplified either fixed or free for translation and rotation.
- Steel plates assumed perfectly rigid.
- Concrete beam assumed indefinitely wide.

4 Results and discussion

4.1 Torsion behavior at bend

The torsion simulation was devised for to study the of the torsion behavior as a result of the Large M_y acting in the horizontal plate sections of the front mounted profiles.

To do this, a deformable M_y of 3 kNm was applied at the edge of the model flange. A deformable moment allowed the applied moment surface to deform. This was done to simulate the deformation caused by pure St Venant torsion at the support as described in *2.4 Torsion stress*. If a rigid moment had been applied, moment would have caused the surface to twist as one rigid element, thus restraining the applied moment for warping. The resulting shear stress of the test yielded a critical shear stress of 150 N/mm^2 as shown in Figure 4-1.

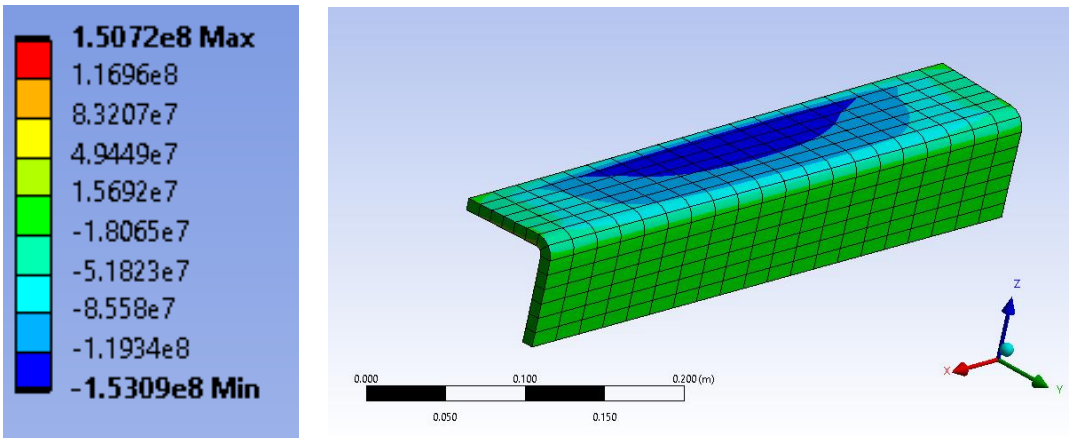

Figure 4-1: Resulting xy-shear stress. [N/m^2] (Images used courtesy of ANSYS, Inc.)

This was less than half the critical shear stress of 313 N/mm^2 expected for a cross-section resisting the entirety of the torsion with St Venant shear stress. The shear distribution near the applied moment did on the other hand reflect the distribution expected for an infinitely long plate affected by a torsion moment.

The low critical shear stress and decreasing shear stress indicated that the plate bend acted as a restraint for warping. Studying the normal forces along the y-axis revealed large stress concentrations of 316 N/mm^2 at the ends of the plate bends in Figure 4-2 as expected from a warping moment acting at the bend. As the shear force of Figure 4-1 was around 100 N/mm^2 at the support, this insinuated a combination of St Venant and warping moment acting at the bend, with the majority of the applied torsion moment being resisted by the warping effect.

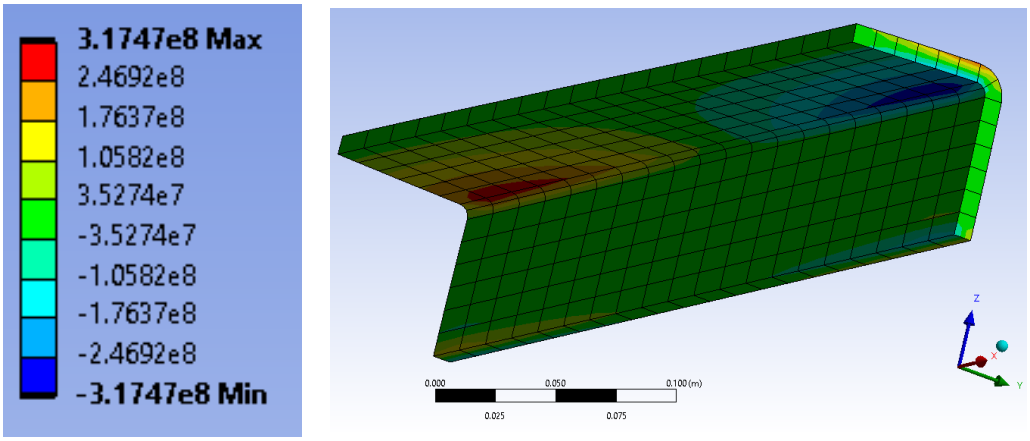

Figure 4-2: Equivalent normal stress along x-axis. [N/m^2] (Images used courtesy of ANSYS, Inc.)

The normal stresses were also transferred from the horizontal plate to the vertical plate as shown in Figure 4-3. These stresses were likely a reaction caused by the twisting of the horizontal plate. The stresses at the bend were observed to be distributed around the middle of the plate, but also near the rigid bottom connection. As a result of these two effects, a critical normal stress of 383 N/mm^2 was observed for the element web.

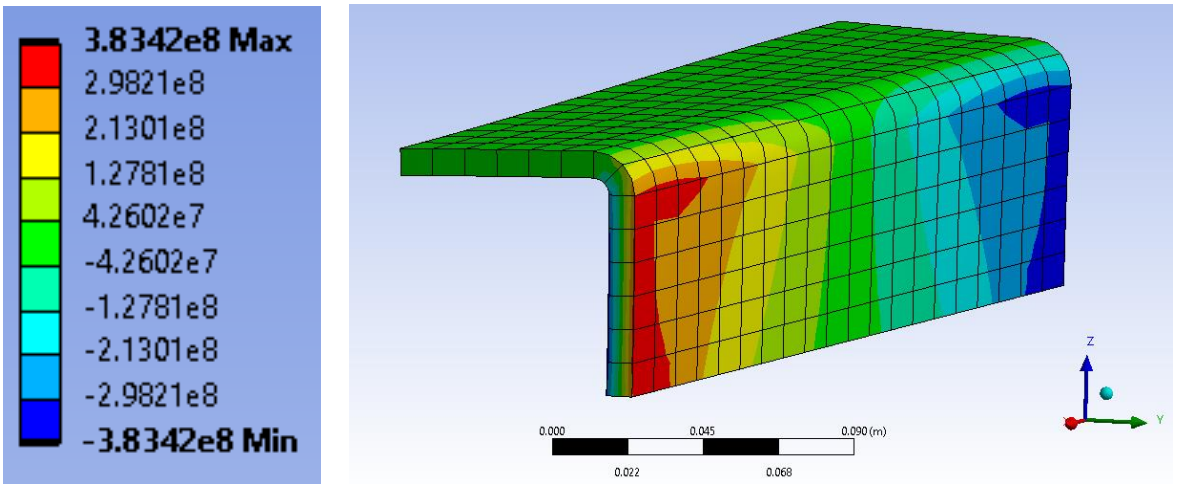

Figure 4-3: Equivalent normal stress along z-axis. [N/m^2] (Images used courtesy of ANSYS, Inc.)

4.2 Preloaded friction system

The friction test was devised to get a better understanding of how external forces and moments would affect the friction connections of the different profiles. It also served as a test for the theory and formulas derived in *2.5 Preloaded bolts in tension and shear capacity* and 2.6 External force application of profiles.

Table 4-1: Friction capacity of hand calculations and Ansys model.

Load case		Hand calculation	Ansys		Hole factor
		Friction capacity [kN]	Friction capacity [kN]	Deformation [mm]	k_s
A [1 n_f]	22 kN preloading	6.80	6.80	0.24	1.00
A	22 kN preloading	13.20	13.20	0.33	1.00
B	22 kN preloading + 10 kN tensile force	10.20	10.20	0.48	1.00
C	22 kN preloading + 1 kNm M_y	13.20	13.20	0.36	1.00
D	22 kN preloading + 10 kN tensile force + 1 kNm M_y	-	10.30	0.47	1.01

From the friction plate theory of EN 1993-1-8:2005, one would traditionally disregard the shear surface between the bolt and plate. Instead, one would only consider shear surface between the plates. For this thesis, this assumption was assumed to be too conservative as both the surface between the plates and the surface between the bolt and plate would have to yield for the plate to slide freely. To test this, load case A [1 n_f] was modeled reducing the friction coefficient to 0.01 for the surface between the bolt and plate.

From the model, a critical shear force of 6.80 kN was found from Table 4-1, which was the same shear capacity as was found for the hand calculations. This capacity was almost half that of the 13.20 kN found for load case A, where both the surfaces were modeled with a friction constant of 0.3. These results indicated that there would be two effective shear surfaces per preloaded bolt.

On the other hand, these results were found from a simulation, not physical testing. As a result, the shear capacities of the models could have been the result of Ansys applying friction theory with disregard for the effective area required to achieve friction capacity in a shear plane. The modeling assumed equal friction coefficient for all the friction surfaces, which would likely not be the case.

The contribution of the bolt shear surface would likely be dependent on the bolt deflection along the x-axis relative to the plate deformation as shown in Figure 4-4 for load case A. Small relative deformations were observed for the upper bolt-plate shear surface, resulting in the surfaces contributing to the system shear force for small connection deflections. This would likely not be the case for real-world testing, as the simulation prohibited deformation of the bolt by having the same diameter of the holes as the bolt shafts. The increased relative deformation as well as differing friction coefficient would likely be the reasons why the outer shear force normally would be neglected for static systems.

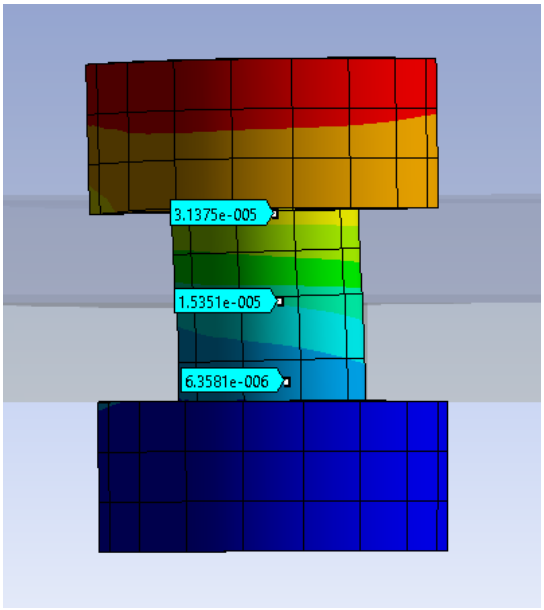

Figure 4-4: Bolt deflection for load case A. (Images used courtesy of ANSYS, Inc.)

As the friction connection assumed for the profiles would have to slide freely for both the shear planes, the contribution of the outer bolt would likely have to be considered, as both the bolt-plate and plate-plate shear surfaces would have to slip for the system to slide. On the other hand, that would not necessarily mean that the slip force would be the sum of the two shear surfaces, as they might not slip at the same time, and the kinetic friction constant would likely be smaller than the static friction constant.

The friction capacities of cases A to C for the models yielded approximately the same results as the hand calculations considering a critical plate deformation of 0.5 mm. This resulted in a friction reduction factor of 1.0 for the elongated hole instead of the factor 0.93 expected from theory. These results could indicate that the reduction factor based on the shape of the hole would be negligible, or they could indicate that the Ansys simulations would not take these effects in to account with the assumptions made for the analysis.

A base assumption for the simulation was that plate slippage would occur with relative deformation between the plates of 0.5 mm. This assumption was based on the (Husson, 2008) study shown in Figure 2-17, where exponential slip increase was experienced for increased tensile loading at around 0.5 mm of deflection.

From load case A, the friction capacity was approximated to be 13.2 kN with a relative deformation of 0.33 mm from the model. This was the lowest increment of 100 N resulting in this deformation being less than 0.5 mm. Increasing the applied shear force to 13.3 kN for the model, resulted in a deformation of 0.74 mm as shown in Figure 4-5. The large relative deformation increase reflected the large increase of deformation near the friction capacity seen in Figure 2-17, strengthening the assumption of slippage occurring at a relative deformation of around 0.5 mm.

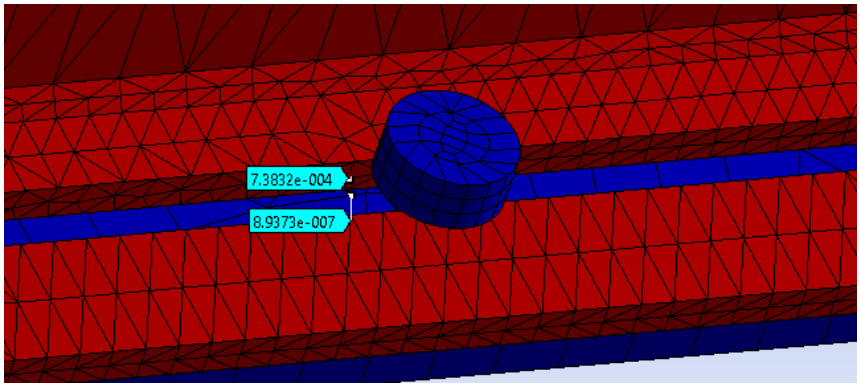

Figure 4-5: Load case A with a shear force of 13.3 kN. (Images used courtesy of ANSYS, Inc.)

For load case D, the additional moment introduced to the connection in tension, resulted in a slight increased friction capacity. This indicated, that the combination of connection tension and moment forces would not decrease the connection friction capacity.

For load case A, a critical stress concentration of 172 N/mm^2 was found in Figure 4-6. The resulting stresses were mostly centered around the preloaded bolt.

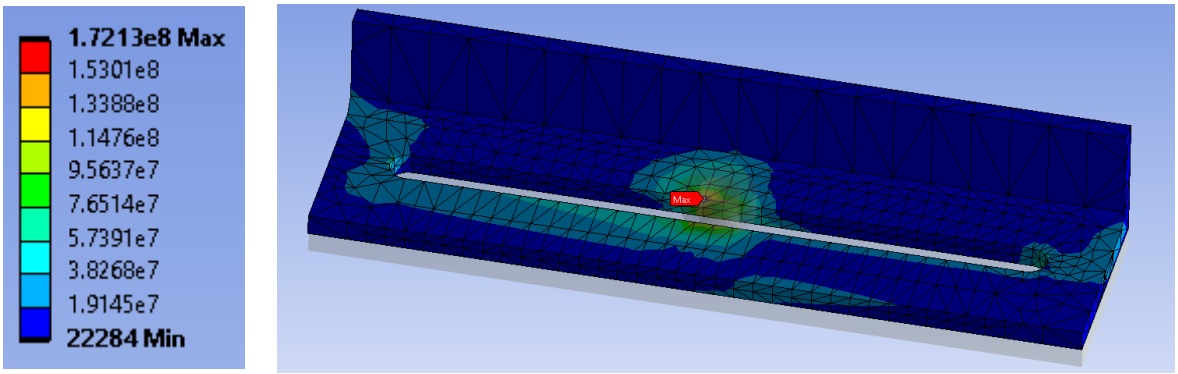

Figure 4-6: Equivalent stress for load case A. (Images used courtesy of ANSYS, Inc.)

For load case B in Figure 4-7, the additional tension force of 10 kN acting on the top edge of the L-bracket increased the critical stress for the connection to 596 N/mm^2. These stress concentrations were situated on each end of the elongated holes and were likely the result of the tension force creating a moment reaction M_x compressing the outer part of the profile. This would in turn create extra tension in the bolts.

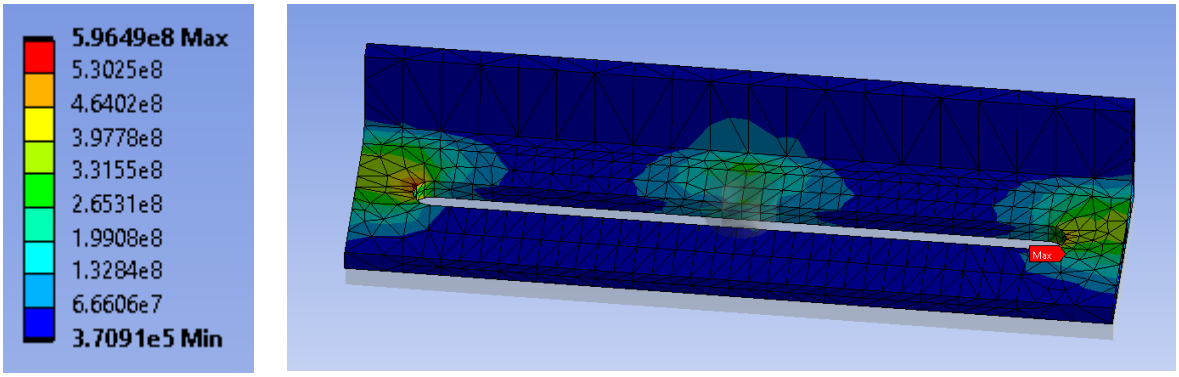

Figure 4-7: Equivalent stress for load case B. (Images used courtesy of ANSYS, Inc.)

Load case B for a normal hole, resulted in a critical stress of 340 N/mm^2, as observed in Figure 4-8. This reduction in critical stress was likely the result of having a larger moment of inertia about the x-axis as a result of the increased cross-section compared to the slim edges around the elongated hole in Figure 4-7.

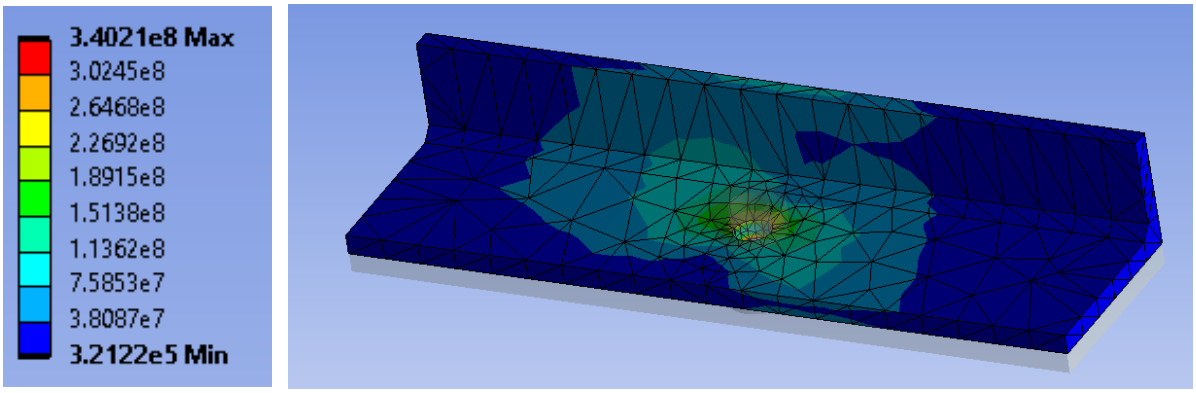

Figure 4-8: Equivalent stress for load case B with normal hole. (Images used courtesy of ANSYS, Inc.)

For load case C, a critical stress of 201 N/mm^2 was observed from Figure 4-9. This was only a 30 N/mm^2 increase in comparison to load case A. unlike load case A, the critical stress concentrations were found at the bend plate bend. These stresses could potentially be the result of a torsion warping effect acting at the bend.

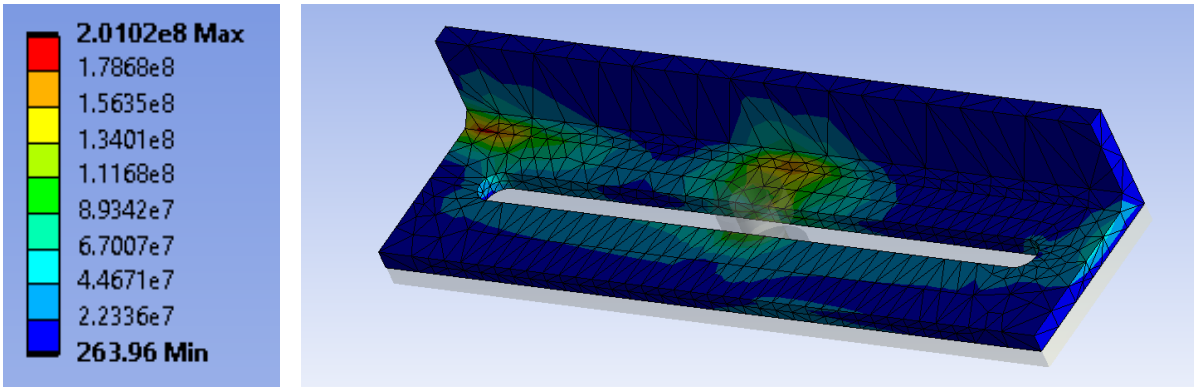

Figure 4-9: Equivalent stress for load case C. (Images used courtesy of ANSYS, Inc.)

The stresses resulting from load case D of the elongated hole shown in Figure 4-10, gave a critical stress concentration of 769 N/mm^2. Compared to load case B, this was a stress increase of more than 170 N/mm^2, which was approximately equal to the increased stress seen for load case C. Additionally, it was observed that most of the stress had shifted to the edge of the compressed side for M_y. This reflected the stress concentrations seen for load case C.

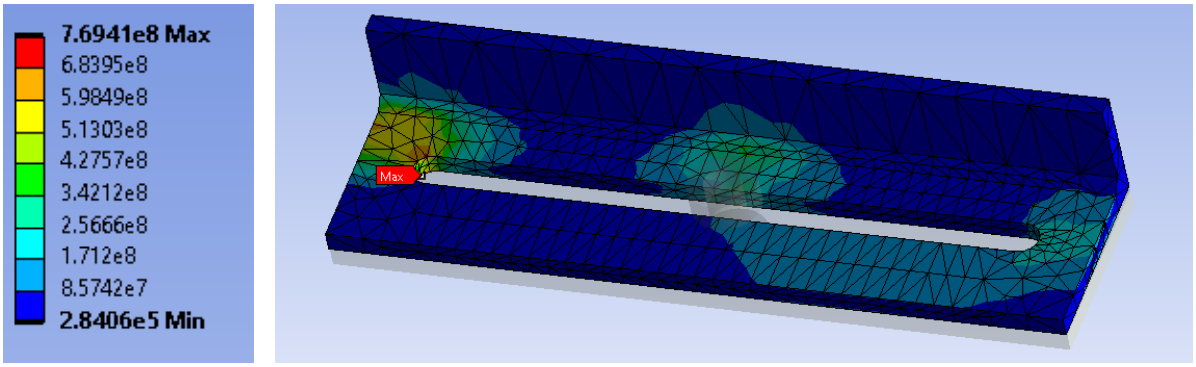

Figure 4-10: Equivalent stress for load case D. (Images used courtesy of ANSYS, Inc.)

The critical stress for the design shear capacity of a normal hole yielded a critical stress concentration of 639 N/mm^2 as shown in Figure 4-11. This stress concentration was far greater than the ultimate material strength of S235, and would have failed if plastic behavior of the plates was considered unacceptable.

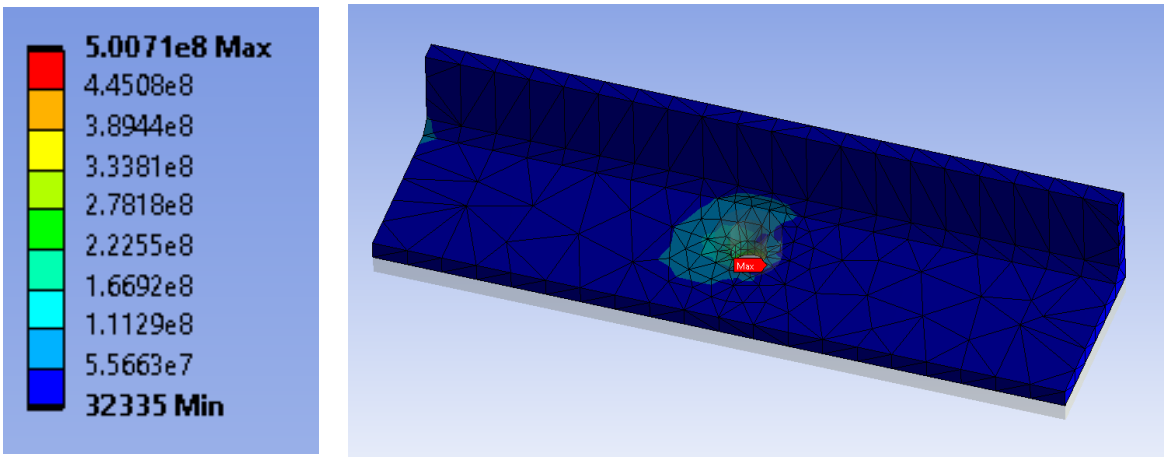

Figure 4-11: M14 design shear capacity loading. (Images used courtesy of ANSYS, Inc.)

The design shear capacity of the M14 preloaded bolt with a friction constant of 0.5 was calculated to be 32.2 kN in Appendix B, according to EN 1993-1-8:2005. This meant that the local stress concentrations derived from the shear load in the model of Figure 4-11 would not result in connection failure, even if the critical stress was considerably larger than the ultimate capacity. This was likely the case as EN 1993-1-8:2005 use the plastic material strength when estimating these capacities. If the models had been calculated using an elastic perfect plastic material, yield stress acting over a larger area would likely have been observed.

As a result, the critical stresses seen for the elongated holes, would not necessarily mean that a failure would appear at the edges of the elongated holes. Instead the stress concentrations, could merely be the result of the perfectly elastic model not being able to distribute the stresses plastically.

On the other hand, increased stresses were observed for Figure 4-10 compared to Figure 4-7 as a result of the imposed moment. As the connection would have to resist this imposed moment force and the moment induced by the eccentrically loaded tension force, portions of the stresses seen at the ends of the elongated holes could be the result of moment stresses as well as the shear stresses.

4.3 Force and moment tables for Profiles

In this section the general behaviors for the hand calculations and Ansys® *Academic Research Mechanical, Release 19.2* simulations of the different profiles were summarized. These tables were discussed in depth for the different profiles in their respectable subchapters.

The forces of Table 4-2 were calculated from the hand calculations. These forces were used as the external forces applied in the simulations of the FEM models, with exception of the preloads, which were summarized in Table 4-3.

Table 4-2: Resulting external forces and preloads calculated from hand calculations.

Load conditions		Forces [N]					
		P_{xA}	P_{zA}	P_{xB}	P_{xC}	P_{zD}	Preload
Top mounted concrete connection	Compression	27000	17100	3000	-	19100	21700
	Tension	-16400	-19600	-1800	-	-21600	
Bottom mounted concrete connection	Compression	27000	-19300	-	3000	-21300	19000
	Tension	-15800	16850	-	-1750	18850	

Table 4-3: preload required to run Ansys simulations for the three original profiles with approximate relative plate deformations. Unforeseen behavior marked in red .

Profiles	Load case			
	Compression		Tension	
	Preload [kN]	Deformation [mm]	Preload [kN]	Deformation [mm]
8-2B	21	0.5	25	0.1
8-2B-R	22-25	≈ 1	22.5	0.5
8-2B-DP	20	0.5	20	0.5
8-2B-SR	21	0.4	21	0.4
8-2B-AP	16	0.5	19	0.5

Table 4-5 and Table 4-4 show the moment reactions found from the Ansys® *Academic Research Mechanical, Release 19.2* moment simulations and hand calculations.

Table 4-4: Moment reactions from hand calculations.

Profiles	support	[Moment reactions kNm]					
		$M_{x.c}$	$M_{y.c}$	$M_{z.c}$	$M_{x.t}$	$M_{y.t}$	$M_{z.t}$
8-2B	B	-1.8	-6.5	-0.4	-	-	-
	D	-1.5	-4.8	-1.6	1.2	3.0	1.2
8-2B-R	B	-2.6	-4.2	-0.4	-	-	-
	D	-0.8	-7.8	-1.6	1.2	6.0	1.2
8-2B-AP	A	0.5	-6.5	0.7	0.5	-4.8	-0.4
	C	1.0	-4.2	-0.9	-	-	-

Table 4-5: Ansys moment reactions for profiles in compression and tension.

Profiles	support	[Moment reactions kNm]					
		$M_{x.c}$	$M_{y.c}$	$M_{z.c}$	$M_{x.t}$	$M_{y.t}$	$M_{z.t}$
8-2B	A	-0.6	-3	0.1	1.2	1.9	-1.8
	B	-1.8	-7.8	2.7	2	4.2	-0.2
	D	-1.7	-4.4	-1.8	1.4	4.3	1.3
8-2B-R	A	-0.3	-2.3	0	0.4	0.2	-0.7
	B	-3.3	-5.5	3.5	3.9	3.6	-1
	D	-0.5	-7.2	-2.3	0.4	6.3	1
8-2B-DP	A	-0.9	-4.1	1.1	1.1	2.4	-0.8
	B	-0.3	-3.6	0	0.9	2.1	0.6
	D	-1	-7.4	-1.2	0.5	5.7	0.3
8-2B-SR	A	-1.5	-5.4	1.7	1.4	1.6	-1.3
	B	-0.9	-4	0.2	2.3	1.7	0.7
	D	-1.7	-5.6	-0.8	0.9	6.9	0.0
8-2B-AP	A	0.1	-6.5	0.2	0.3	5.6	0.2
	C	0.4	-3.2	0.1	-0.7	1.7	-0.4
	D	0.1	-4.1	-0.3	-0.1	2.2	0.1

The reaction forces of the critical connectors found from the Ansys® *Academic Research Mechanical, Release 19.2* simulations and hand calculations are summarized in Table 4-6 and Table 4-7.

Table 4-6: Absolute value of the reaction forces, for critical connector of each support calculated in Ansys. Position of concrete reaction for profile 8-2B-AP marked in red.

Profile	Force reaction [kN]	Support					
		A		B/C		D	
		Compression	Tension	Compression	Tension	Compression	Tension
8-2B	F_x	1.55	1.32	2.51	22.18	2.44	1.35
	F_y	5.10	5.68	10.69	13.00	9.85	4.54
	F_z	0.38	1.43	41.09	0.58	2.49	3.25
8-2B-R	F_x	1.46	0.81	0.03	0.55	2.35	1.55
	F_y	1.31	1.74	23.9	23.64	8.54	7.78
	F_z	0.31	0.70	1.97	0.50	5.26	1.17
8-2B-DP	F_x	1.63	0.94	1.51	0.11	0.74	0.14
	F_y	0.35	0.09	1.18	4.83	0.24	0.23
	F_z	3.28	2.68	25.76	18.29	5.98	4.76
8-2B-SR	F_x	1.88	0.38	2.06	0.60	0.44	1.62
	F_y	2.92	4.99	3.59	11.18	8.78	4.31
	F_z	3.35	1.49	27.83	16.49	3.30	4.45
8-2B-AP	Fx	1.99	1.36	0.39	1.00	1.69	0.87
	Fy	0.29	0.00	2.46	1.48	0.04	0.71
	Fz	3.91	3.48	25.82	15.47	2.63	1.69

Table 4-7: absolute value of critical connector force reaction from hand calculations. Critical connections for 8-2B-AP marked in red.

Profile	Critical force reaction [kN]	Support		
		B/C	D/A	
		Compression	Compression	Tension
8-2B	F_x	0.75	1.54	0.94
	F_y	9.16	1.53	1.16
	F_z	30.62	2.77	2.04
8-2B-R	F_x	0.75	1.87	1.27
	F_y	12.78	0.99	1.16
	F_z	23.11	4.11	3.36
8-2B-AP	F_x	0.75	1.63	1.07
	F_y	6.62	0.58	0.45
	F_z	21.70	3.55	2.71

Table 4-8 show the characteristic connection utilizations found from the hand calculations of the CLT-steel and concrete connections, for both characteristic and design connection resistances. Table 4-9 show the approximated characteristic connection utilizations found for the critical connectors of the CLT-steel connections of the profiles.

Table 4-8: Connection utilization from hand calculations, for characteristic and design resistance and characteristic loading P_x using $\gamma = 1.25$ for CLT-steel connections and $\gamma = 1.5$ for concrete connection.

Connection utilization						
Profile	8-2B		8-2B-R		8-2B-AP	
Criteria	$Ek/_{Rk}$	$Ek/_{Rd}$	$Ek/_{Rk}$	$Ek/_{Rd}$	$Ek/_{Rk}$	$Ek/_{Rd}$
CLT-steel [compression]	0.43	0.68	0.64	1	0.45	0.71
CLT-steel [tension]	0.23	0.36	0.45	0.7	0.25	0.39
Concrete [compression]	1.35	3.04	1.31	2.95	0.46	1.04

Table 4-9: Characteristic CLT-steel utilization for worst connector according to Ansys models.

Connection utilization					
Profile	8-2B	8-2B-R	8-2B-DP	8-2B-SR	8-2B-AP
Criteria	$Ek/_{Rk}$	$Ek/_{Rk}$	$Ek/_{Rk}$	$Ek/_{Rk}$	$Ek/_{Rk}$
CLT-steel [compression]	6.55	5.60	1.03	5.24	0.55
CLT-steel [tension]	1.67	3.98	0.64	1.82	0.39

4.4 Profile 8-2B

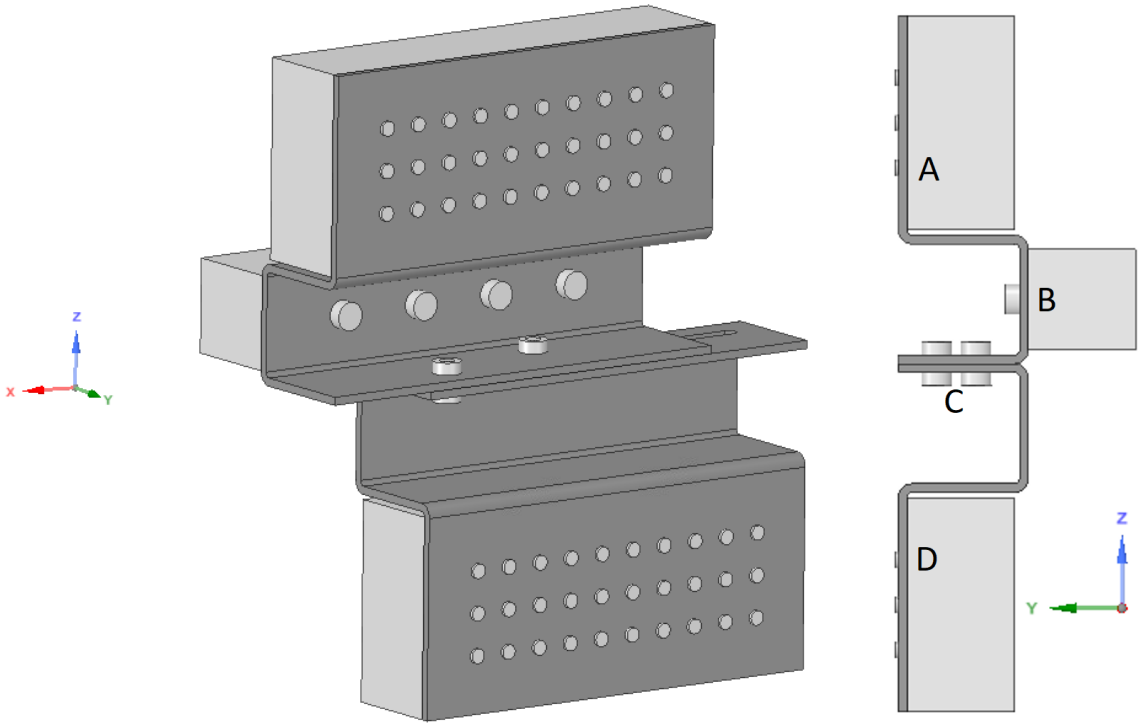

Figure 4-12: Profile 8-2B. (Images used courtesy of ANSYS, Inc.)

Profile 8-2B was the base profile for this thesis as shown in Figure 4-12. The resulting reaction moments from the Ansys simulation for the supports of profile 8-2B were summarized in Table 4-5. A moment reaction $M_{y.c}$ at support D of -4.38 kNm was observed for profile 8-2B in compression. This was lower than what was expected if the friction connection C was acting pinned, thereby it indicated a semi rigid behavior of the connection. The large moment reaction $M_{y.c}$ in the concrete support B of -7.78 kN further indicated that the friction connection was transferring moment forces about the y-axis.

The friction connection was assumed fixed for $M_{y.c}$ in the hand calculations, which yielded a slightly smaller $M_{y.c}$ of 6.47 kN for support B, and a slightly larger $M_{y.c}$ of 4.81 kNm for support D compared to the simulation. This might have been a result of the increased elastic modulus of the concrete connection in B compared to the CLT-steel connection, even though the CLT-steel connection had more connectors. It might also have been a result of the varying stiffness about the y-axis of the steel profile along the z-axis.

The assumption of moment resistance for the friction connection was further strengthened by looking at the equivalent stresses for the profile in compression shown in Figure 4-13. The figure showed a clear increase of stress at the inner left edge of the top plate. The stress concentration indicated that the friction connection resisted moment forces $M_{y.c}$ by pivoting about the stress concentration area with the preloaded bolts resisting the resulting moment tension forces.

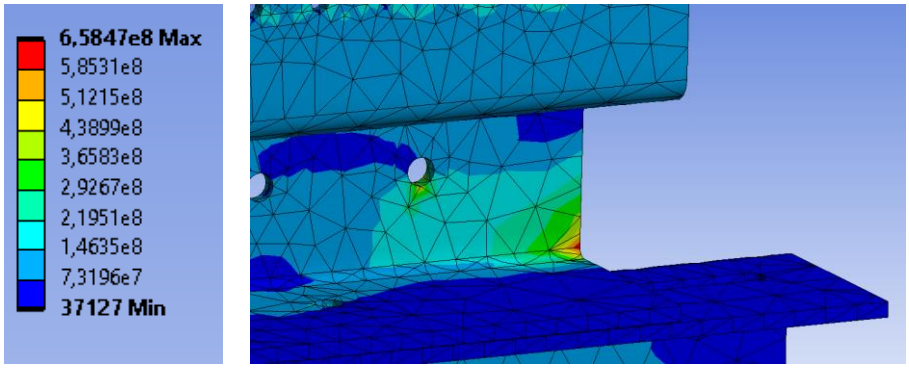

Figure 4-13: Stress concentration between top and bottom profiles of 8-2B in compression [N/m²]. (Images used courtesy of ANSYS, Inc.)

For the tension profile, a $M_{y.t}$ of 4.26 kNm at support D and 4.18 kNm at support B were observed from the ANSYS simulation. From the hand calculations of Table 4-4, a $M_{y.t}$ of 2.9 kNm was found calculating connection C fixed for profile 8-2B, while a $M_{y.t}$ of 5.95 was found for profile 8-2B-R, which was calculated using a pinned friction connection at C. This indicated that the friction connection at C was acting less rigid for $M_{y.t}$ than it did for the connection in $M_{y.c}$, but still semi rigid.

The moment reactions of $M_{x.c}$ from the Ansys simulation in Table 4-5 yielded a larger moment reaction in support D and smaller reaction in support B than initially assumed for a pinned connection with a vertical concentric force acting at the midpoint between the preloaded bolts. The resulting moment reactions $M_{x.c}$ indicated a low stiffness of the friction connection in relation to the plate bends, which resulted in the vertical force reaction in support C shifting towards the inner bend of the connection along the y-axis.

The moment reactions M_z at support C and D from Table 4-5 of the Ansys simulation indicated an uneven distribution of horizontal forces between the two preloaded bolts. This result was initially unexpected as the hand calculations assumed the horizontal concentric force reaction for the friction connection located at the mid-point between the preloaded bolts. This was assumed to be the case in the hand calculations as both friction bolts were calculated with the same preload force, thus having the same friction capacity. As a result, both bolts would have to transfer equal amounts of forces along the x-axis for the friction connection to be slipping.

The reason for the uneven distribution was determined to be the result of simulating the system statically with approximated preloaded forces higher than the model required to experience slip. As a result, the inner preloaded bolt would resist a greater portion of the horizontal forces. This resulted in unrepresentative reaction moments M_z found for support B and D, as they would not reflect the real behavior of the friction system in motion.

The resulting moment reactions $M_{z.c}$ in Table 4-5 for connection A, were on the other hand considered representative to the real system as the equivalent horizontal force center of connection C would have little to no effect on the behavior of connection A. The resulting moment reaction indicated that the top CLT-steel connection at point A acted pinned for $M_{z.c}$ as it only had a moment reaction force of 0.1 kNm. This could have been the result of the increased plate stiffness at support B as a result of the U-shaped steel plate of the connection. Another reason could have been the increased elastic modulus of the concrete support compared to the CLT-connection.

For the profile in tension, the opposite effect was observed with support A having a $M_{z.t}$ of -1.8 kNm. Figure 4-14 show a concentration of normal stresses on the bottom row of screws for connection A. This was unexpected, as stress concentrations were expected in the outer right rows, on account of the large $M_{z.t}$ in the connection. This indicated that the plate was not able to distribute the forces evenly among the connectors.

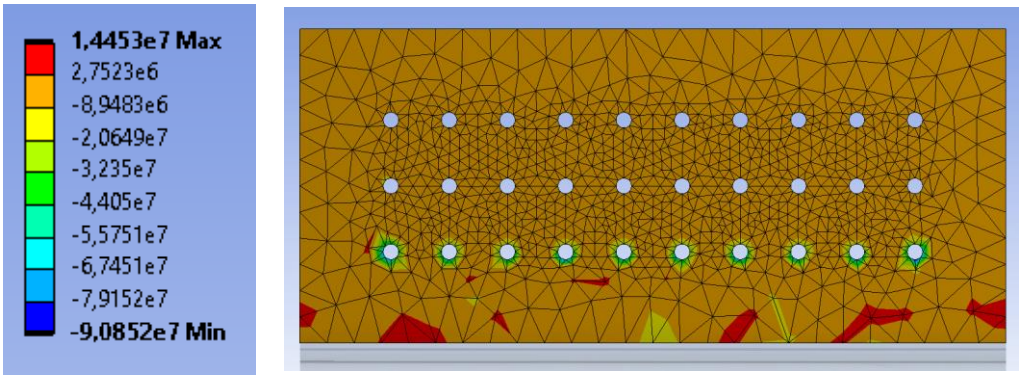

Figure 4-14: Normal stress along y-axis for support A of 8-2B in tension [N/m²]. (Images used courtesy of ANSYS, Inc.)

A required preload of 21 kN was estimated for the profile in compression as shown in Table 4-3. This was close to the 21.7 kN expected from the hand calculations. For the tension profile on the other hand, the lowest preload found to make the simulation converge was 25 kN. As a result, the relative deformation between the top and bottom plate of the friction connection was only 0.1 mm. It had been assumed that the friction connection would not slip before the deformation hit 0.5 mm based on the theory of *2.5 Preloaded bolts in tension and shear capacity.* This indicated an overestimate for the preload force.

It was found that increasing the refinement of the model mesh to the meshing used for the stress simulations reduced the required preload by around 1 kN. As a result, it might have been possible to reduce the required preload further, but the mesh used for the approximation of preloads was the finest mesh deemed practical based on rendering time per simulation.

The resulting stresses of profile 8-2B in compression as shown in Figure 4-15 gave a maximum equivalent von-Mises stress of 658 N/mm^2. This stress concentration was situated at the left edge of connection C for the top plate. This stress was 2.8 times the characteristic yield capacity of the S235 steel intended for use in the profiles. Figure 4-15 also indicated stress concentrations in the bottom row of screws for support A and the top row for support D.

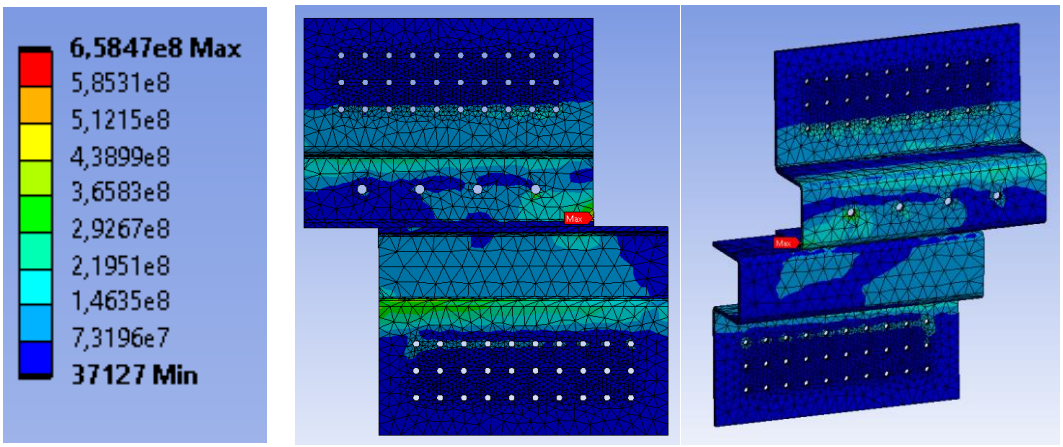

Figure 4-15: Equivalent von-Mises stress for profile 8-2B in compression from front and rear [N/m²]. (Images used courtesy of ANSYS, Inc.)

The second most critical stress observed for profile 8-2B in compression was found at the left edge of the lower bend of the bottom plate, with a critical stress of 469 N/mm^2. This stress was likely the result of the large moment $M_{x.c}$ in the profile resulting from the large eccentricity of the vertical force acting in the friction connection C, as well as the torsion effect discussed in *4.2 Preloaded friction system* as a result of the large $M_{y.c}$. This effect was confirmed in Figure 4-16 and Figure 4-17 as the plates were twisting, resulting in both tension and compression of the plate at each end of the lower bend.

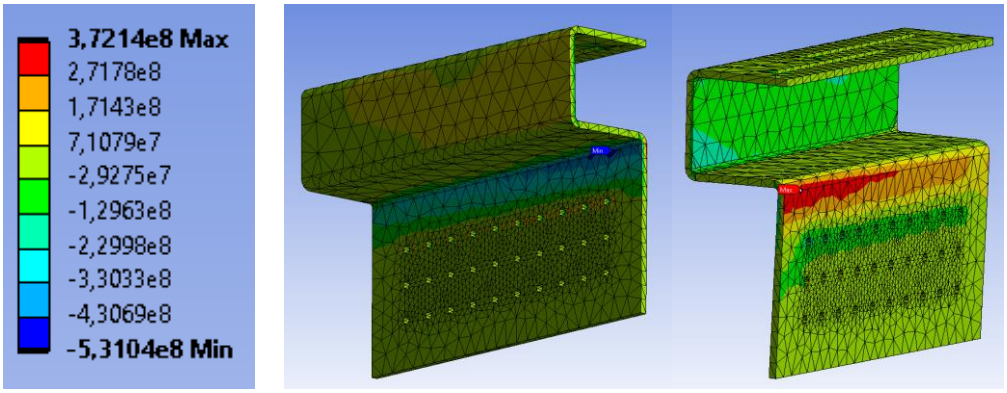

Figure 4-16: Equivalent stress along Z-axis for 8-2B bottom profile in compression [N/m^2]. (Images used courtesy of ANSYS, Inc.)

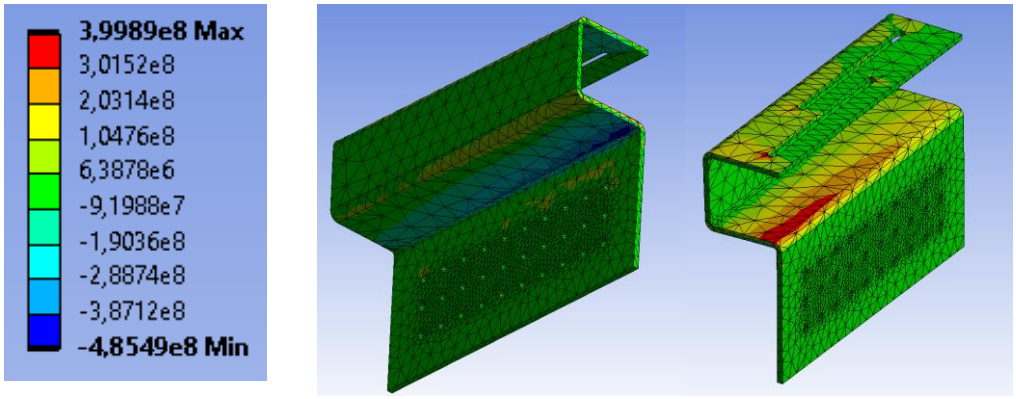

Figure 4-17: Equivalent stress along Y-axis for 8-2B bottom profile in compression [N/m^2]. (Images used courtesy of ANSYS, Inc.)

For the tension profile, the resulting Ansys stresses were displayed in Figure 4-18 with a critical plate stress of 739 N/m^2. This stress was situated at the end of the inner of the two elongated holes. Figure 4-19 showed how there was a larger stress concentration located at the inner preloaded bolt compared to the outer bolt. This could be a result of the inner bolt being located closer to the vertical bend of the plate, resulting in greater stiffness compared to the outer bolt. The result of this behavior was a center of the vertical reaction force situated close to the inner bolt as indicated by the moment calculations for profile 8-2B in tension.

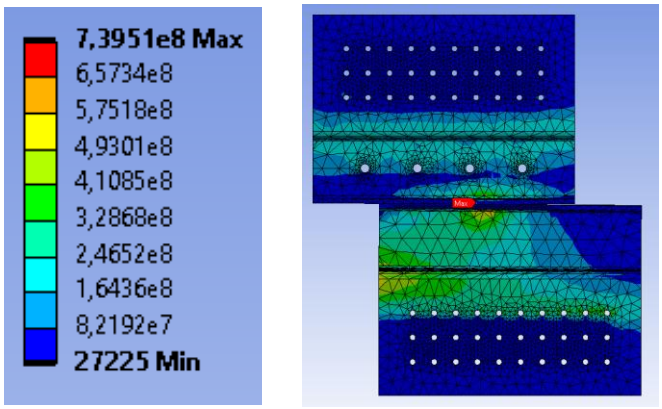

Figure 4-18: Equivalent von-Mises stress for 8-2B in tension [N/m^2]. (Images used courtesy of ANSYS, Inc.)

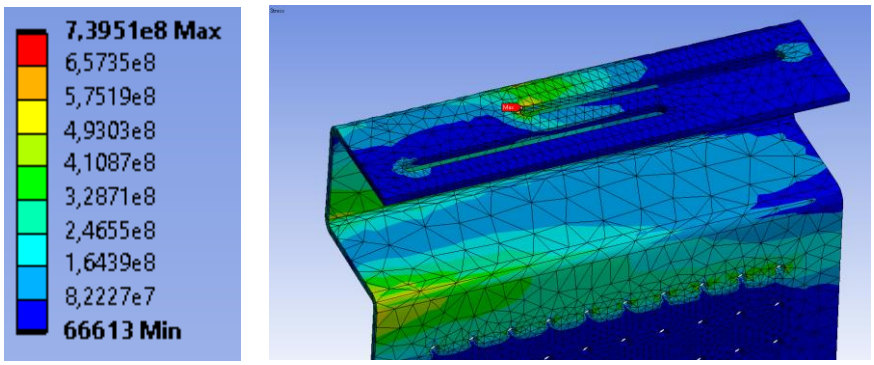

Figure 4-19: Equivalent stress for 8-2B bottom profile in tension [N/m^2]. (Images used courtesy of ANSYS, Inc.)

The increased tension reaction force of the inner bolt compared to the outer also resulted in a large vertical stress concentration of 687 N/m^2 in the vertical side of the bend of connection C for the top and bottom plate as shown in Figure 4-18. The figure also indicated that the torsion problem and bending about the weak axis, seen for the compressed profile, persisted for the plate bends of profile 8-2B in tension. The resulting deformations of the Ansys simulations for profile 8-2B in compression in Figure 4-20 and Figure 4-21, provided a critical deformation of more than 1.5 mm along the x-axis, and more than 2.4 mm along the z-axis.

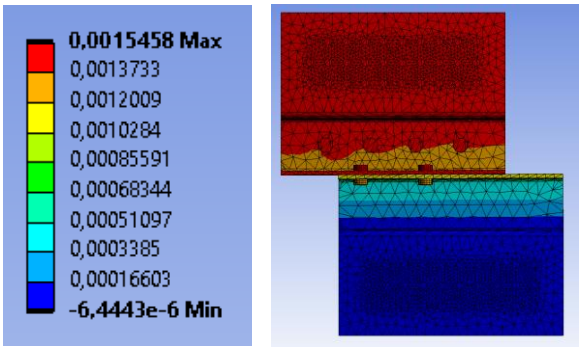

Figure 4-20: Deformation of 8-2B in compression along X-axis [m]. (Images used courtesy of ANSYS, Inc.)

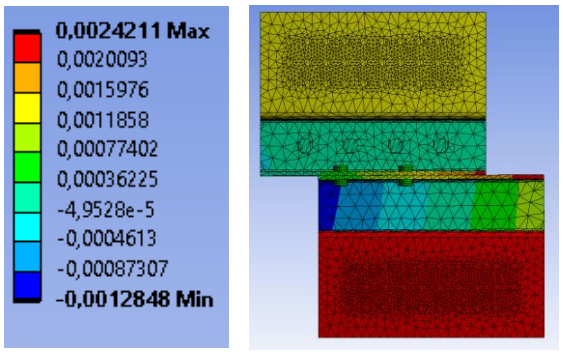

Figure 4-21: Deformation of 8-2B in compression along Z-axis [m]. (Images used courtesy of ANSYS, Inc.)

The deformations from the Ansys simulation of profile 8-2B in tension, as shown in Figure 4-22 and Figure 4-23, yielded a maximum deformation along the x-axis of more than -1.3 mm, as well as a deformation of the bottom plate of more than -5.5 mm along the z-axis.

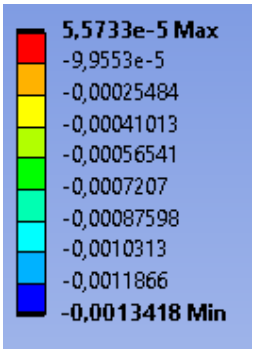

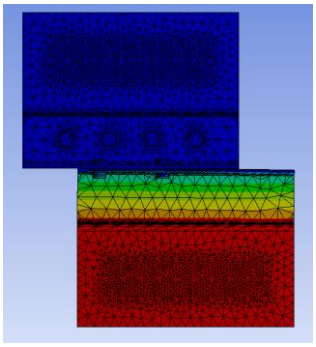

Figure 4-22: Deformation of 8-2B in tension along X-axis [m]. (Images used courtesy of ANSYS, Inc.)

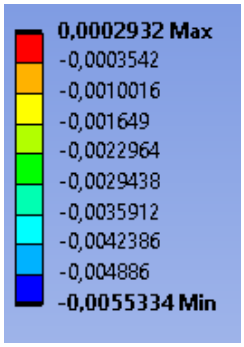

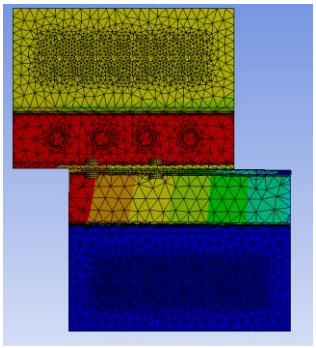

Figure 4-23: Deformation of 8-2B in tension along Z-axis [m]. (Images used courtesy of ANSYS, Inc.)

These deformations were the result of the large stresses observed in the plates. For the real profiles these deformations could be even greater, as the Ansys simulations were performed using perfectly elastic materials, while the S235 steel proposed for use in the plates would have a yield strength of 235 N/mm^2 and a high ductility.

For the moment hand calculations of profile 8-2B, it was determined to only to change the properties of the friction connection, despite the varying M_x and M_z support behaviors observed from the Ansys simulations. Adjusting the hand calculation moments for these moment reactions could result in misleading connection behaviors. This was thought to be the case, as the M_x and M_z distribution seen for the supports were more affected by the lack of plate stiffness than the behavior of the connectors themselves. This behavior would have to be eliminated for a final profile, as the CLT-connectors would not have the capacity to handle the force concentrations resulting from the lack of plate stiffness.

The resulting utilizations of profile 8-2B in Table 4-8 gave a critical characteristic utilization of 0.43 for the CLT-steel connection at D in tension, which resulted in a critical design utilization of 0.68 which was well below the critical capacity of the connection. For the concrete connection the hand calculations yielded a characteristic utilization of 1.35 in compression, which was well above the characteristic capacity of the system. In addition, the Hilti HIT-Z anchors required a qama factor of 1.5 for the design value, bringing the utilization to 3.04 for the design resistance.

The resulting shear forces of the critical 8-2B connection were almost equal for the hand calculations summarized in Table 4-7 and the Ansys simulation from Table 4-6. The tables also showed a large increase in axial force reaction for the compressed profile in the Ansys simulation compared to the hand calculations. The Ansys axial reaction force of 9.85 kN was more than 6 times higher than the critical axial force calculated for the same connector in the hand calculations. This increase was determined be the result of a lack of stiffness for the connection plate against moment M_x. As a result of these concentrations for the compressed profile, the characteristic utilization was found to be 6.55 for the CLT-steel connection, as shown in Table 4-9.

For the concrete calculations of profile 8-2B, the axial force reactions of the critical concrete anchor were approximately the same for the hand calculations as for the Ansys simulations. The critical shear forces were around 30 % greater for the Ansys simulation. These force reactions could have been the result of a force concentration in the critical anchor as a result of the steel plate not acting fully rigid for the moment forces about the y-axis, but having sufficient stiffness about the other axis as a result of the U-shape of plate bends increasing the effective moment of inertia.

4.5 Profile 8-2B-R

Profile 8-2B-R was based on profile 8-2B with the same profile dimensions. In addition to the original dimensions, profile 8-2B-R had added reinforcement as shown in Figure 4-24.

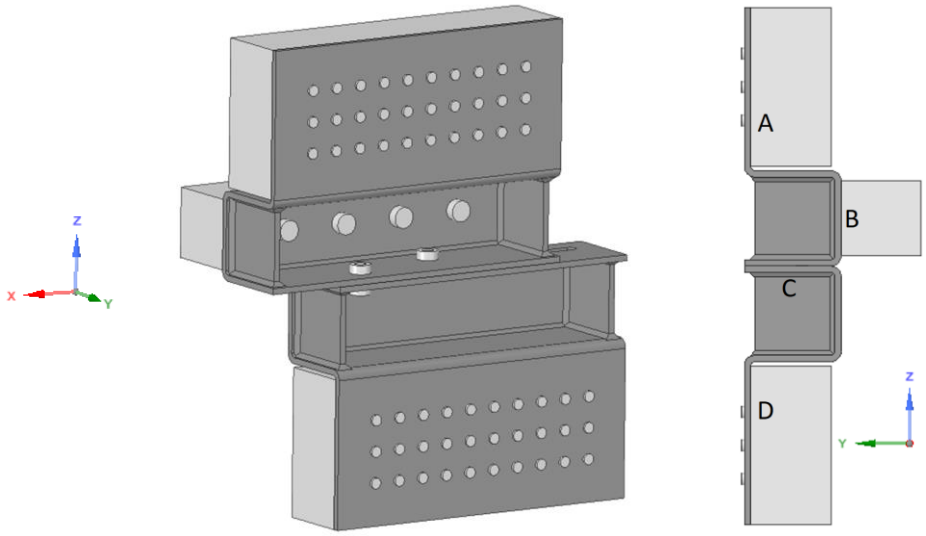

Figure 4-24: Profile 8-2B-R. (Images used courtesy of ANSYS, Inc.)

From Table 4-5, a $M_{y.c}$ of -7.2 kNm was found from the simulation at support D, while a reaction $M_{y.c}$ of -3.5 kNm was observed for the concrete support in B. Calculating the $M_{y.c}$ for connection C as pinned for profile 8-2B-R in the hand calculations yielded a $M_{y.c}$ of -7.8 kNm for support D and -4.2 kNm for support B, as shown in Table 4-4. This indicated a pinned behavior for the friction connection of profile 8-2B-R in compression.

The resulting moment reactions presented in Table 4-5 for the tension profile, also indicated the friction connection acting pinned for $M_{y.t}$. In addition, almost no moment resistance $M_{y.t}$ was observed for support A in tension, as well as a low resistance $M_{y.c}$ for support A in compression from the Ansys simulations. This behavior was unexpected, and was not observed for any of the other profiles tested. One possible reasoning for this, could have been the increased stiffness for the concrete support, as a result of the reinforcement.

The resulting $M_{x.c}$ for support D of -0.5 kNm seen in Table 4-5, indicated a low eccentricity between the vertical force center of the friction connection C and the bottom CLT-steel connection at point B along the y-axis for the Ansys simulation. This was likely caused by the stress concentration in the reinforcement of the profile as a result of the local stiffness increase, as shown in Figure 4-25.

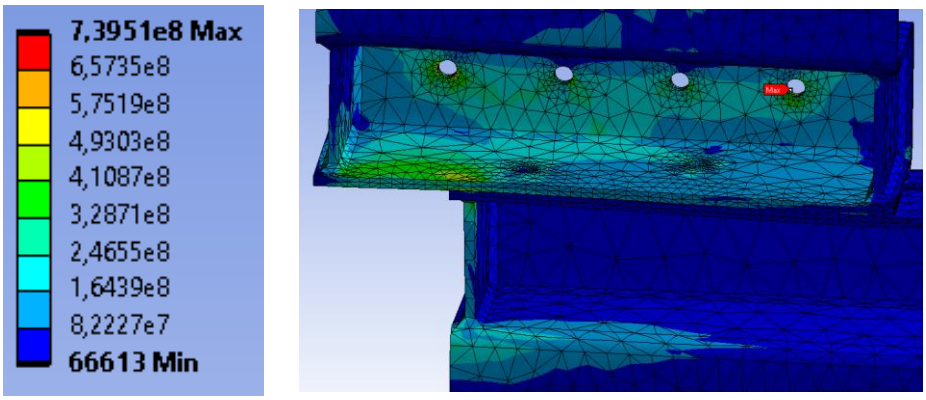

Figure 4-25: Stress concentration of 8-2B-R in compression, in top profile above reinforcement of bottom profile [N/m²]. (Images used courtesy of ANSYS, Inc.)

A similar behavior was observed for profile 8-2B-R in tension. Figure 4-26 showed a stress concentration twice as large around the outer friction bolt as the inner one. This was likely a result of the increased vertical stiffness relative to support D for the reinforcement compared to the remaining plate where the stresses would have to be transferred through the horizontal parts of the plate.

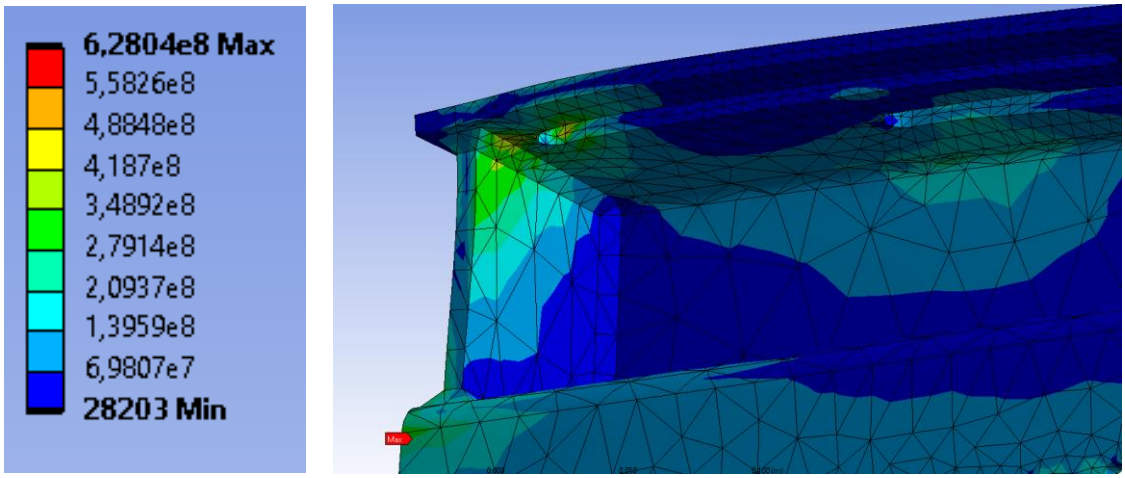

Figure 4-26: Equivalent stress concentration in reinforcement of 8-2B-R bottom profile in tension [N/m^2]. (Images used courtesy of ANSYS, Inc.)

The $M_{z.A}$ at support A, shown in Table 4-5 was 0.03 kNm. For the tension profile, a reaction $M_{z.t}$ of only -0.7 kNm was found from the simulation. The reduced M_z in compression compared to tension was unexpected, as M_z would be dependent on the horizontal force application. The applied system $P_{x.A}$ shown in Table 4-2, was larger for the compressed profile, which should have result in a larger M_z for the compressed profile. One explanation for this behavior, could have been the lack of plate stiffness for M_z at support A for larger moment reactions. This could result in the connection being able to resist smaller moment reactions, but experience force concentration seen from profile 8-2B for larger moment. This could result in insignificant relative stiffness of support A compared to support B for larger applied moments.

For the simulation, a required bolt preload of 22.5 kN was found for the profile in compression, as shown in Table 4-3. This was close to the 21.7 kN found from the hand calculations shown in Table 4-2 using a factor k_s of 0.93 for a pinned connection. For the compressed behavior, the lowest preload found to converge the system was 22 kN with a relative plate deformation of 1 mm. When increasing the preload to 25 kN, little to no change in relative deformation was observed. This was likely a result of the twisting experienced for the friction connection plates, as a result of the reinforcement.

The resulting stresses for the compressed 8-2B-R profile Ansys simulation, found in Figure 4-27, gave a maximum stress of 717 N/mm^2 acting at the left hole of the concrete connection. This increase of stress for the plate at support B compared to profile 8-2B was likely a result of the increased $M_{x.c}$ for support B, as the low vertical edge distance of the concrete support would result in a large increases of tension forces of the anchors. The moment reaction would likely be marginally smaller for the system in real life, as the connection element at B was calculated with an elastic modulus of 200 GPa for the Ansys simulations. This was far greater than the elastic modulus of the concrete in compression, resulting in an overestimated stiffness for the concrete connection.

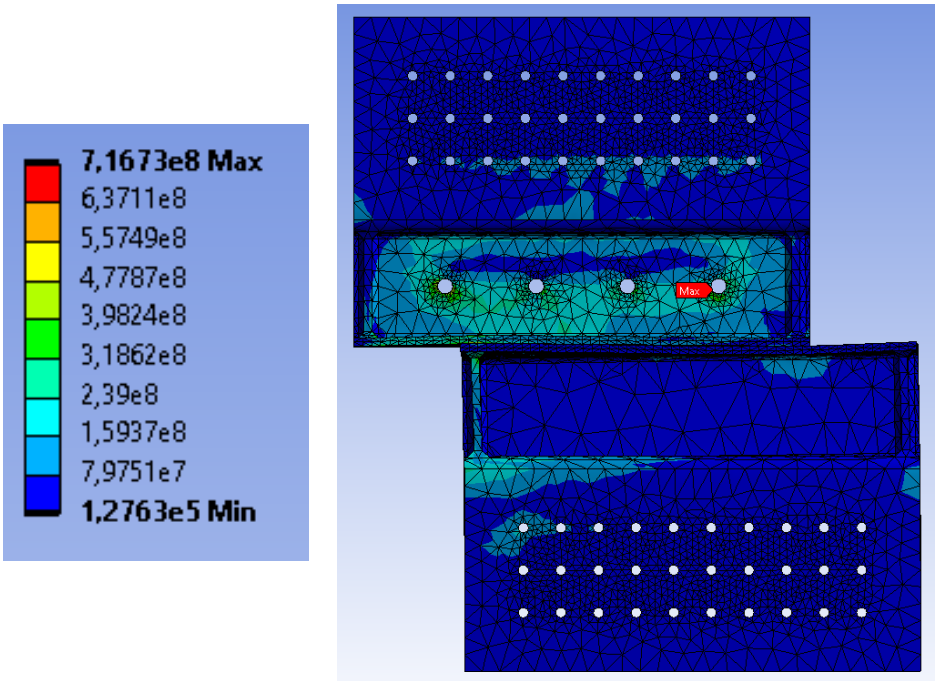

Figure 4-27: Equivalent von-Mises stress for 8-2B-R in compression [N/m²]. (Images used courtesy of ANSYS, Inc.)

The stress concentration above the left reinforcement of the bottom profile, shown in Figure 4-25, resulted in a critical stress of around 450 N/mm^2. This stress concentration was likely due to the large moment stresses caused by a vertical point load from the reinforcement. As these stresses were far greater than the material capacity, the plastic moment stress distribution of the top plate in connection C would likely cause irreversible plastic plate deformation.

In addition, a critical stress concentration of 442 N/mm^2 was observed beneath the same reinforcement at the bend of the plate as shown in Figure 4-28.

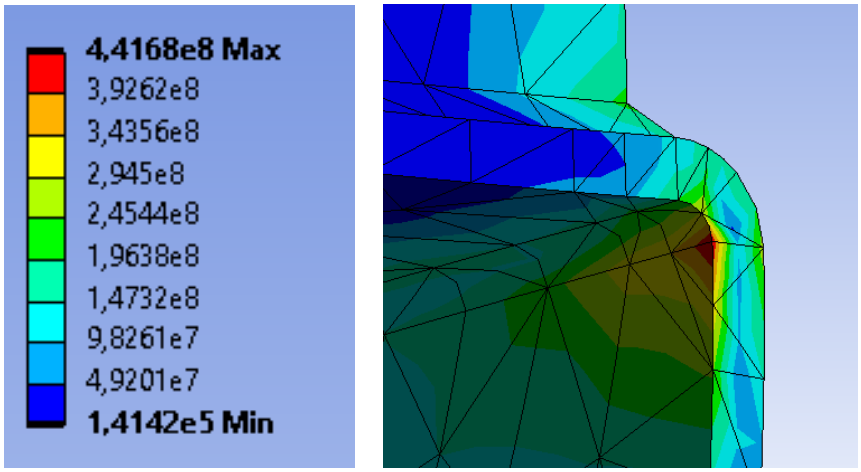

Figure 4-28: Maximum stress for bottom profile of 8-2B in compression, located beneath reinforcement. [N/mm²] (Images used courtesy of ANSYS, Inc.)

This concentration was further investigated in Figure 4-29, where a reduced torsion effect was observed for the outer bend as compared to profile 8-2B. The maximum vertical stress for the bend had been reduced in excess of 100 N/mm^2. The improved torsion behavior of the reinforced part of profile 8-2B-R was likely the result of the reinforcement creating a hollow rectangular cross-section

for the torsion moment, as this section shape experienced reduced warping in addition to having larger polar moments compared to long, thin rectangular cross-sections.

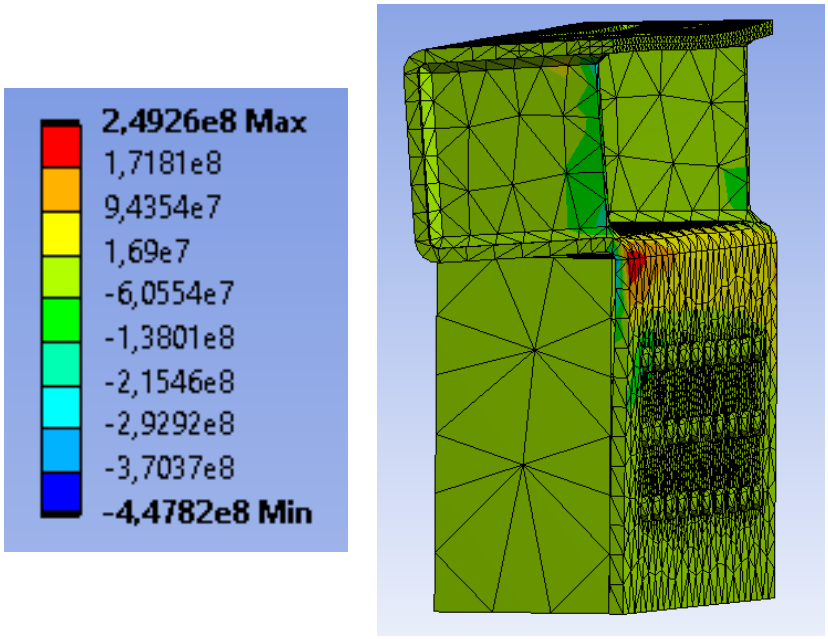

Figure 4-29: Equivalent stress along Z-axis for 8-2B-R bottom profile in compression. [N/mm²] (Images used courtesy of ANSYS, Inc.)

Figure 4-30 showed how the critical deformation for the compressed profile was more than 4.3 mm along the x-axis, which was almost three times greater than the deformation observed for the compressed 8-2B profile. Studying the vertical deformation more closely in Figure 4-31 revealed that the rear part of the left reinforcement of the bottom plate had a critical deformation of -5.1 mm along the z-axis, while the front of the plate had a deformation of 5.1 mm along the z-axis. This twisting of the plate was likely caused by the weakness of the bottom bend of the lower plate, as well as the low stiffness for the top plates of connection B, which allowed the outer part of the bottom plate to push up into the top plate. The twisting likely also caused the large deformation along the x-axis, as the deformation of the bottom plate along the x-axis increased quickly as it approached the friction connection in Figure 4-30.

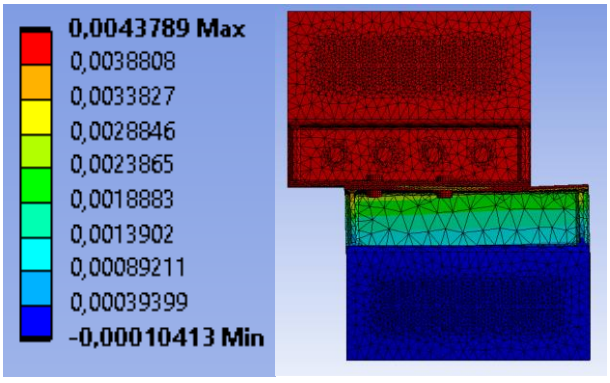

Figure 4-30: Deformation of 8-2B-R in Compression along X-axis [m]. (Images used courtesy of ANSYS, Inc.)

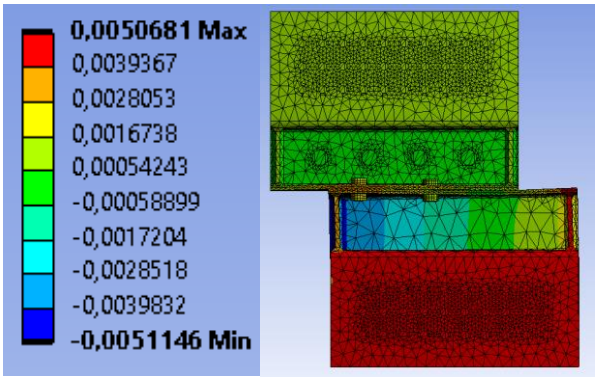

Figure 4-31: Deformation of 8-2B-R in compression along Z-axis [m]. (Images used courtesy of ANSYS, Inc.)

The equivalent stress for profile 8-2B-R in tension of the Ansys simulation showed a critical stress concentration of 668 N/mm^2 at the edge of the outer elongated hole as shown in Figure 4-32. This was likely a result of the increased vertical stiffness for the outer preloaded bolt compared to the inner bolt in relation to support D. From the tension simulation a critical stress of 628 N/mm^2 was

observed directly beneath the left reinforcement at the bend of the bottom plate. This stress was likely caused by the stress concentration in the reinforcement, as well as the torsion effect acting on the outer part of the bend.

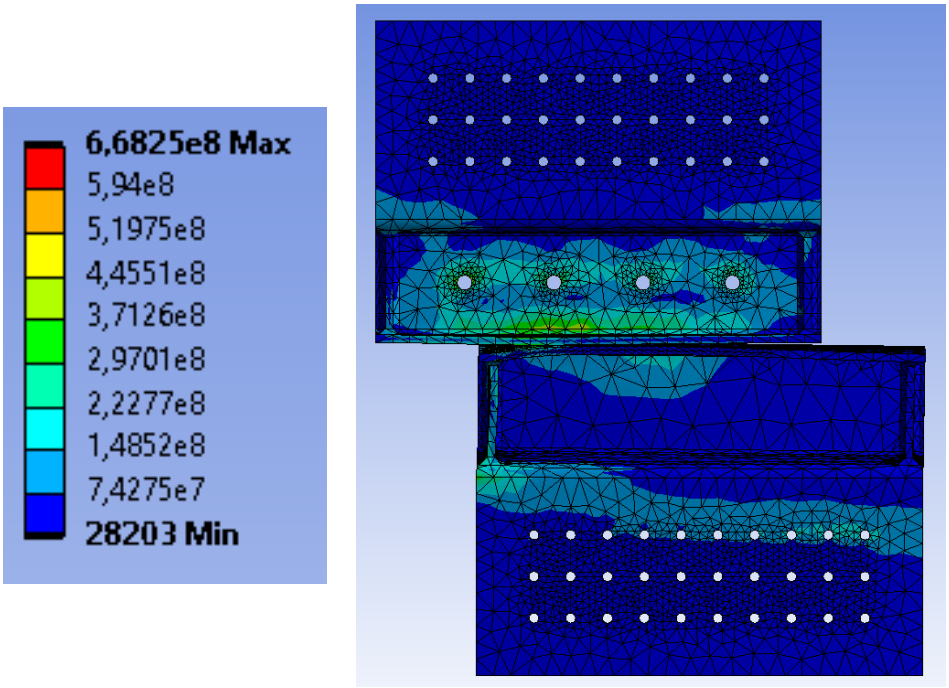

Figure 4-32: Equivalent von-Mises stress for 8-2B-R in tension [N/m²]. (Images used courtesy of ANSYS, Inc.)

Figure 4-33 showed how large vertical stresses were acting on the at the outer edges of the reinforcement. The figure also showed large plate deformations, as the model showed deformation in scare 1:1.

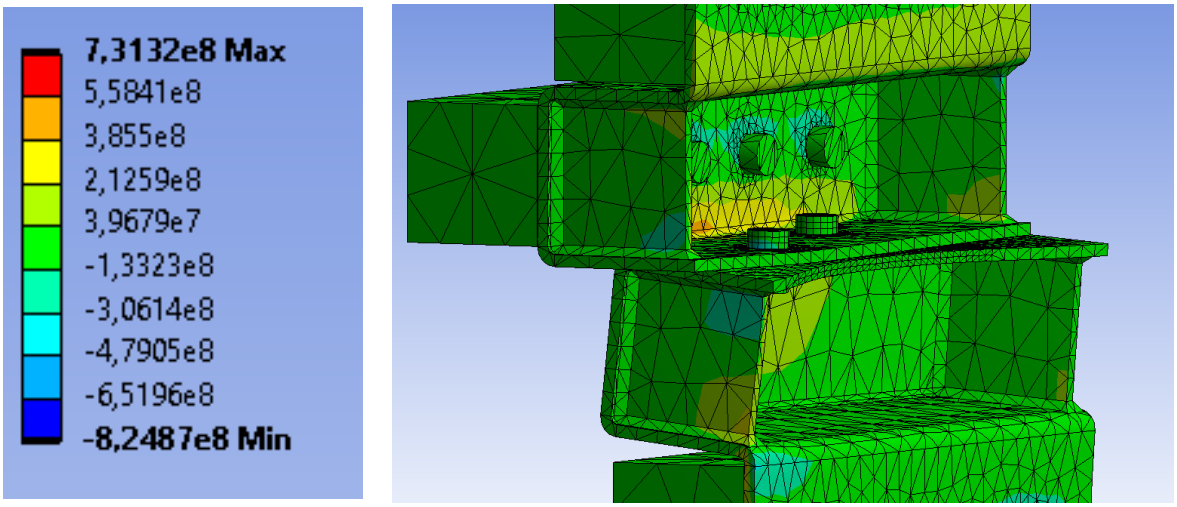

Figure 4-33: Equivalent stress along Z-axis for 8-2B-R bottom profile in compression [N/m²]. (Images used courtesy of ANSYS, Inc.)

Figure 4-34 gave a critical negative deformation along the z-axis of 12 mm at the front of the reinforcements for the bottom plate in tension. In addition to the large vertical deformation, a horizontal deformation along the x-axis of 4 mm was observed from Figure 4-35. The large deformation difference along the z-axis between the top and bottom steel plates was likely caused by the concrete connection increasing the stiffness for the rotation of the top plate about the x-axis

at the preloaded connection. As the inner vertical plate surface of the bottom plate was not restrained for this rotation, a lever arm resulted between the outer preloaded bolt and the vertical profile plates in compression.

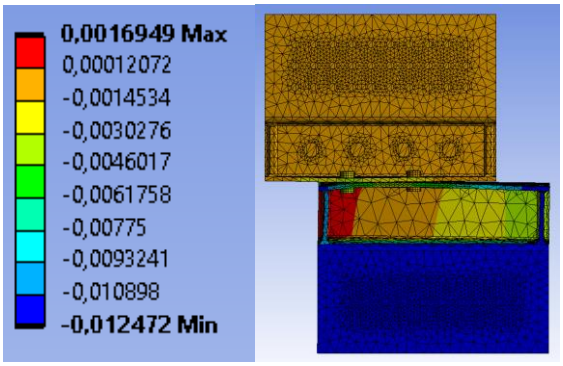

Figure 4-34: Deformation of 8-2B-R in tension along Z-axis [m]. (Images used courtesy of ANSYS, Inc.)

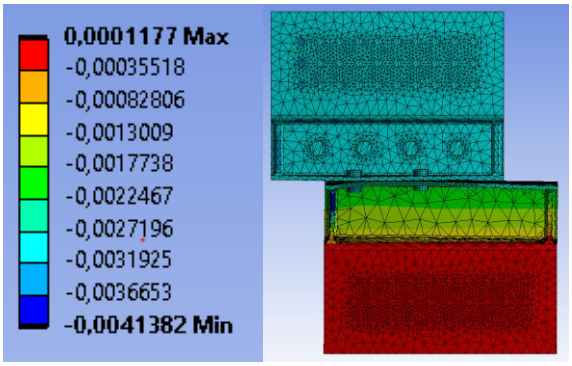

Figure 4-35: Deformation of 8-2B-R in tension along X-axis [m]. (Images used courtesy of ANSYS, Inc.)

For the CLT-steel connection of support D, the increased moments M_y and M_x of the compressed profile 8-2B-R compared to 8-2B resulted in a characteristic utilization from the hand calculations of 0.64 and a critical design value of 1.00 from Table 4-8. Even though the design value was at the criteria limit, the capacity could still be enough as the friction dissipating system was intended to be tested and sold as a product instead of a set of standalone components. The characteristic utilization of the concrete connection for 8-2B-R was found to be 1.54, while the design resistance gave a utilization of 3.46 for the hand calculations in Table 4-8.

For the critical connector at support D of the compressed profile, the simulations forces in Table 4-6 revealed a critical shear force of 5.76 kN, while 4.52 kN was found from the hand calculations as shown in Table 4-7. This was roughly a 20% increased shear force from the Ansys simulation, despite the hand calculations having utilized a larger $M_{y.c}$ for the connection. This indicated that the profile plate, was not behaving as perfectly rigid for moments about the y-axis. For the critical axial force reaction of the compressed connection, a force of 8.54 kN was observed from the Ansys simulation. This behavior was similar to that of profile 8-2B, and indicated a force concentration as a result of lack of stiffness for the plate of the connection. The same concentration was observed for the connection in tension.

As a result of these force concentrations in support D from the simulation, the critical characteristic utilization of the connection as shown in Table 4-9 was 5.60. This clearly indicated that failure of the connection would occur, unlike the hand calculations where the profile would have been strong enough for the assumptions made for the hand calculations.

The reaction force from the critical concrete anchor of profile 8-2B-R were different from the hand calculations. The critical anchor of the Ansys simulation experienced an axial force of 23.9 kN according to Table 4-6. This was an 80 % increase of the axial force compared to the equivalent hand calculations in Table 4-9. The increased axial force, was likely the result of the increased moments M_x and M_z for the Ansys calculations, compared to the hand calculations. Especially the increased M_x for the connection would increase the axial force of the connection greatly, as the steel plate only had a vertical edge distance of 60 mm, resulting in a small lever arm.

In addition to the large axial force, there were almost no shear force acting on the critical anchor for the simulation. This could have been a result of the increased moments out of plane, which would have created large compression forces in the concrete. As all the profile was calculated with a

friction coefficient of 0.3 for all friction surfaces, the concrete compression would result in a larger shear resistance of the concrete-steel surface.

This result revealed a weakness in the way the force reactions were retrieved from the model, as the friction between the plates would have to be ignored for the concrete connection. This was the case as the edge failure, which was dependent on the resulting connection shear force, was found to be the critical failure mode in the hand calculations of the concrete connection of profile 8-2B-R, as shown in Appendix C.

4.6 Profile 8-2B-DP

Profile 8-2B-DP differed from profile 8-2B in the CLT-steel connections, as an additional rear facing steel plate was utilized in combination with a front mounted plate as shown in Figure 4-36. In addition, the Rothoblaas screws of profile 8-2B had been distributed evenly between the two steel plates of the CLT-steel connection.

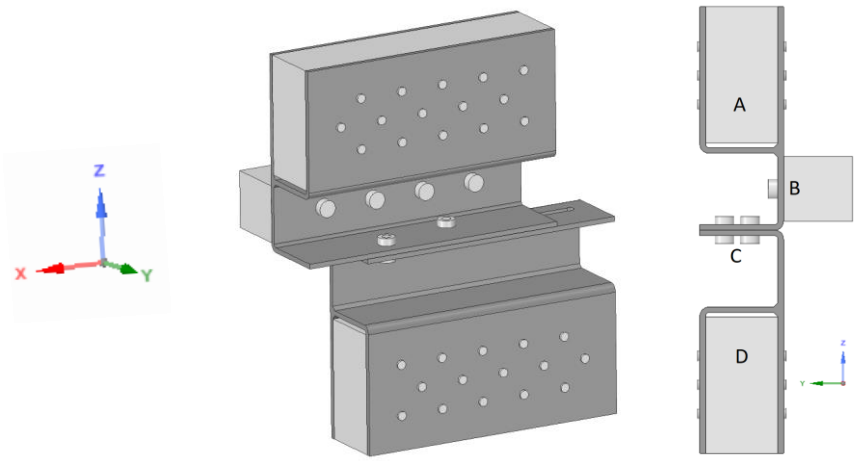

Figure 4-36: Profile 8-2B-DP (Images used courtesy of ANSYS, Inc.)

The moment reactions of the Ansys simulation for profile 8-2B-DP, seen in Table 4-5, resulted in a moment reaction $M_{y.c}$ of -7.4 kNm. This was in line with what would be expected from the friction connection at point C acting pinned. The concrete connection of support B was found to resist a smaller moment M_y compared to profile 8-2B-R, while support A resisted a larger M_y than 8-2B-R. This could be a result of the back plate of profile 8-2B-DP increasing the plate stiffness for M_y, which in turn would decrease the plate deformation between the concrete connection at point B and the CLT-steel connection in support A.

This behavior was supported by the shear forces found for the critical connector of the inner and outer plate at support D as shown in Table 4-10. The table showed how the critical connector of the inner plate resisted more than twice the shear force of the outer connector. This was the case for both compression and tension of the profile. As the front and back connections at support D had the same number of connectors with equal spacing, it was estimated that around 70 % of the total M_y of support D was resisted by the inner plate.

Table 4-10: shear force of critical connector found from simulation for inner and outer plate of support D.

Load case	Critical connector shear force reaction [kN]	
	Inner plate	Outer plate
Compression	6.03	2.86
Tension	4.76	1.91

The moments for M_x and M_z for support A and D in Table 4-5 for the Ansys simulations, yielded larger moment reactions than expected for the supports, as the rear plate had been found to resist most of the moment reactions. The large M_x and M_z were likely a result of the applied forces being evenly distributed between each CLT-steel connection face, while the moment reaction would be unevenly resisted for the two surfaces. The M_y observed in the Ansys simulations for support A and D on the other hand, were likely correct as the applied forces and supports were all symmetrical about the xz-plane.

Reaction $M_{x.c}$ and $M_{x.t}$ for the concrete connection B was also considered to be representative, as the support condition of this connection only acted on one surface. For the compressed profile 8-2B-DP, $M_{x.c}$ was almost non-existent, implying that the vertical force acted close to the inner edge for connection C, as well as most of the vertical force being transferred by the inner plate of support A.

For profile 8-2B-DP in tension profile, $M_{x.t}$ was found to be 0.6 kNm for connection B, which was likely a result of the vertical force center acting between the two preloaded bolts as it did for profile 8-2B, which also lacked reinforcement at support C.

The required preloads for the system were found to be 20 kN for the profile in both compression and tension as shown in Table 4-3. This was slightly lower than the estimate of 21.7 kN from the hand calculations. The difference indicated a factor k_s of around 1.0. This was likely a result of Ansys not considering a reduced slip force on account of the shape of the hole, as seen in *4.2 Preloaded friction system.*

The equivalent stress for profile 8-2B-DP in Figure 4-37 gave a maximum stress of 535 N/mm^2 at the right hole of the concrete anchors of support B. This was expected as high stress concentrations had been observed for all the previous profiles. It was determined that these stresses for the connector holes in the plates were not necessarily critical for the profiles, as EN 1993-1-8:2005 Table 3.4 proposes to calculate the punching an bearing strength of the holes using the plastic capacity of the plates (CEN, 2005). The stress concentration around the critical concrete connection of the plate, also indicated a large force reaction of the critical concrete anchor.

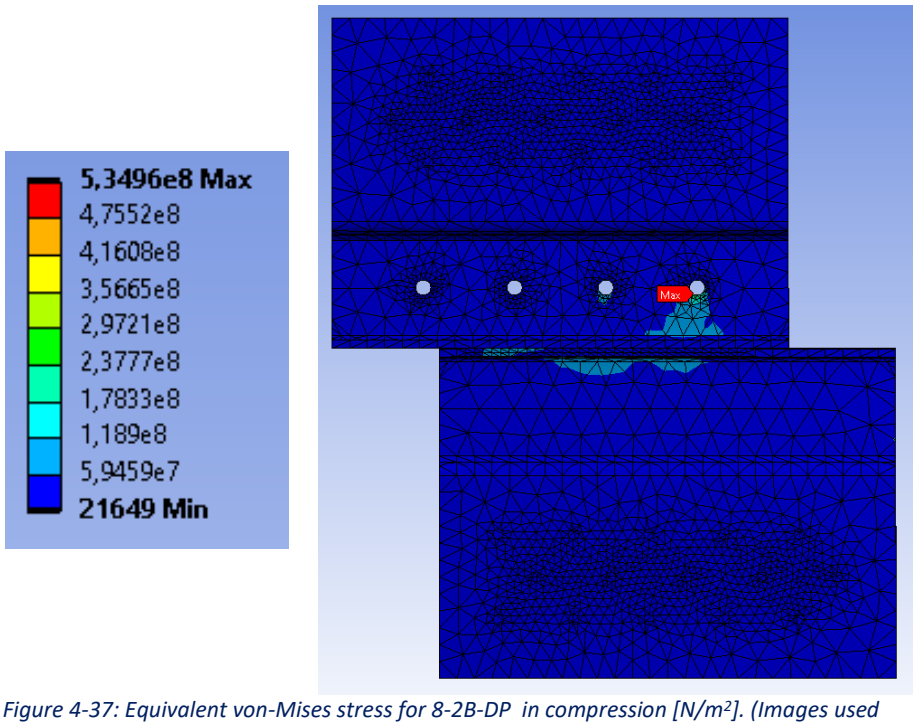

Figure 4-37: Equivalent von-Mises stress for 8-2B-DP in compression [N/m^2]. (Images used courtesy of ANSYS, Inc.)

With exception of the anchor stress concentration, Figure 4-37 indicated that the stresses of the plates were greatly reduced for the profile compared to profile 8-2B and 8-2B-R. Further investigation of profile 8-2B-DP in Figure 4-38, revealed a maximum stress of 209 N/mm^2 for the bottom plate of 8-2B-DP at the end of the elongated hole. This behavior resembled that of load case A from Figure 4-6, where the preloaded bolt was only affected by a shear force. For the remaining part of the plates, the equivalent stress barely exceeded 100 N/mm^2, far below the material yield strength of 235 N/mm^2. This behavior was excepted as $M_{x.c}$ and $M_{x.t}$ were greatly reduced compared to the two previous profiles, and the plate had a large moment of inertia for M_y thanks to the plate width of 450 mm.

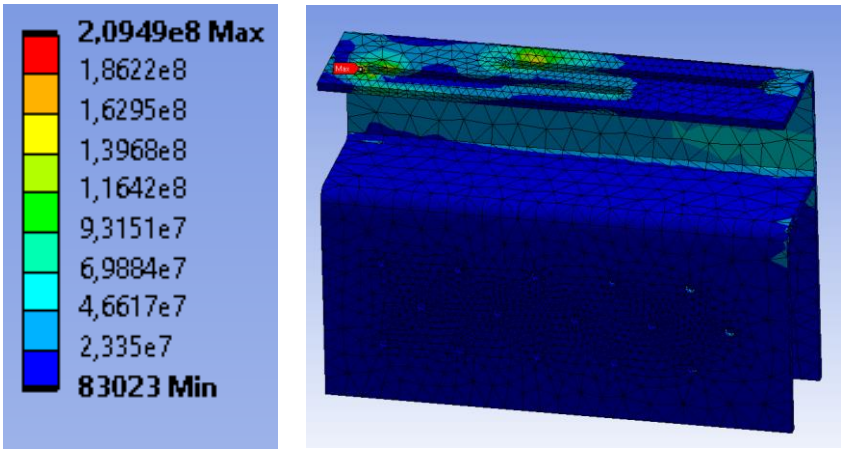

Figure 4-38: Equivalent stress for 8-2B-DP bottom profile [N/m^2]. (Images used courtesy of ANSYS, Inc.)

This decrease of stresses as well as increased stiffness was also observed for the combined total plate deformation of 1.1 mm as shown in Figure 4-39. This was a substantial reduction compared to profile 8-2B and 8-2B-R. In addition, profile 8-2B-DP would likely obtain a similar deformation during real world testing, as the maximum stresses did not exceed the material yield strength, with exception of the concrete connection.

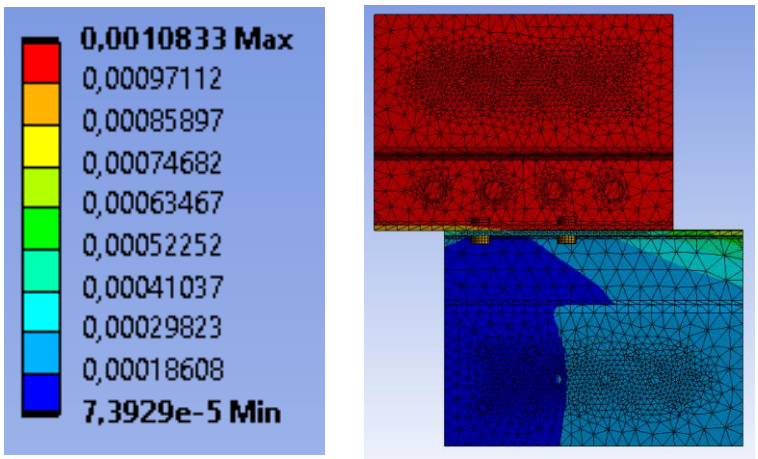

Figure 4-39: Total deformation of 8-2B-DP in compression [m]. (Images used courtesy of ANSYS, Inc.)

For the tension profile, Figure 4-40 showed a stress concentration of around 300 N/mm^2 for the vertical part of the bottom plate close to the inner preloaded bolt. This was an indication of the inner preloaded bolt of connection C resisting the majority of the vertical force reaction of the connection.

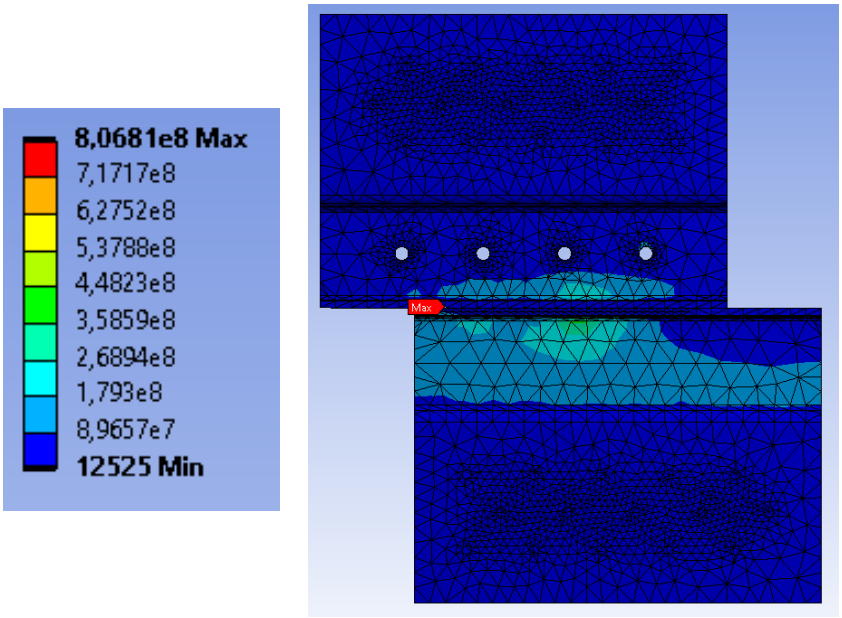

Figure 4-40: Equivalent von-Mises stress for 8-2B-DP in compression [N/m²]. (Images used courtesy of ANSYS, Inc.)

This uneven distribution of vertical forces between the outer and inner bolt, likely resulted in the large stress concentration around both preloaded bolts of more than 800 N/mm^2 as seen in Figure 4-41. These stress concentrations were large, but they were also situated locally around the edge of the elongated holes, reducing to less than 200 N/mm^2 at the edges of the plates as shown in Figure 4-41. As a result, it was unclear how these stress concentrations would distribute for the plastic behavior of S235.

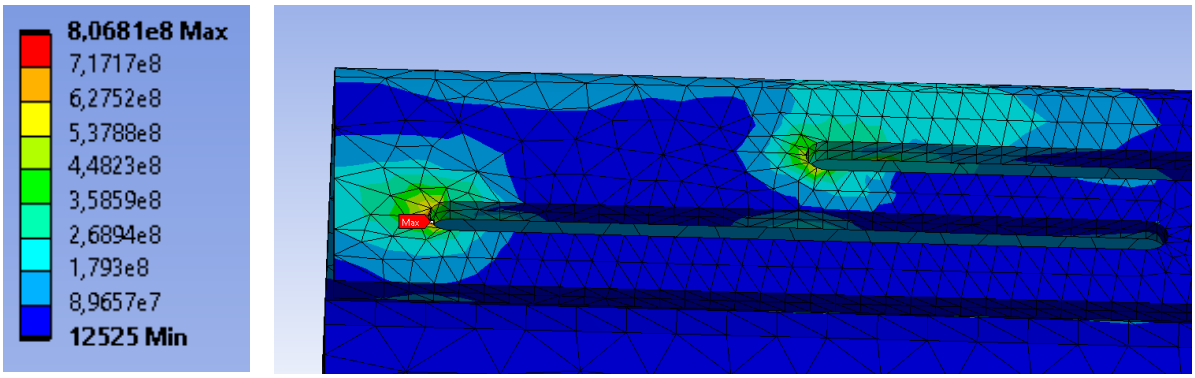

Figure 4-41: Stress concentration at end of elongated hole in bottom profile of 8-2B-DP in tension. [N/m²] (Images used courtesy of ANSYS, Inc.)

For the critical connector force reactions in support A and D in Table 4-6, the drastic increase in axial force reaction of the Ansys simulations observed for profile 8-2B and 8-2B-R were not observed for profile 8-2B-DP. This was likely due to the reduced reaction moments M_x and M_z acting in the supports for profile 8-2B-DP compared to profile 8-2B and 8-2B-R, resulting in the plates of the CLT-steel connections being stiff enough to behave close to rigid during system loading.

Profile 8-2B-DP and 8-2B-R from the Ansys simulations were initially assumed to behave roughly the same for M_y in support D, as both profiles resisted roughly the same amount of moments $M_{y.c}$ and $M_{y.t,}$ as well as having the same number of connectors with the same connector spacing in the xz-plane.

This turned out to be incorrect, as the Ansys shear force for the critical connector at support D in compression was almost 34% greater for profile 8-2B-DP critical shear force calculated from the hand calculations of profile 8-2B-R in Table 4-7. This increase in critical shear force, likely resulted from the rear plate of profile 8-2B-DP resisting around 70% of the reaction moment M_y for the CLT-steel supports.

As a result of these behaviors, a characteristic utilization of 1.03 was found for the compressed profile in Table 4-9. This was close to what would be expected from potential hand calculations following Navier's hypothesis with 70% of the moment acting on the inner plate, consisting of 15 connectors.

For the concrete connection of 8-2B-DP in compression, the resulting shear force of the critical connector in Table 4-6 from the Ansys simulation were larger than what was observed for connection 8-2B-R, even though the moment reaction observed for 8-2B-DP was smaller. This was likely a result of the reduced axial force acting on the anchor, which resulted in a smaller friction reaction force being taken by the compressed concrete surface. The resulting shear force was larger than would have been expected for hand calculations of the connection. This was likely caused by the insufficient plate stiffness about the y-axis.

4.7 Profile 8-2B-SR

Even though profile 8-2B and 8-2B-R larger stress concentrations, the two profiles were originally preferred to the concept of profile 8-2B-DP. This was mainly because of the mounting, and maintenance problems which could arise from not having access to the screws of a rear mounted CLT-steel connection. From profile 8-2B-R it was observed that the introduction of the reinforcement eliminated the torsion effect for the rear bend of the bottom plate, as well as reduce the effect on the outer bend. Unfortunately, the reinforcement also caused twisting of the entire reinforced area of the bottom plate, resulting in larger vertical deformations of more than 10 mm.

To avoid these problems profile 8-2B-SR was designed with side reinforcement stretching the entire height of the top and bottom plate of the profile as shown in Figure 4-42. This change was made in an attempt to reduce the torsion effect for the entire profile, in addition to increasing the profile stiffness for M_x and M_z.

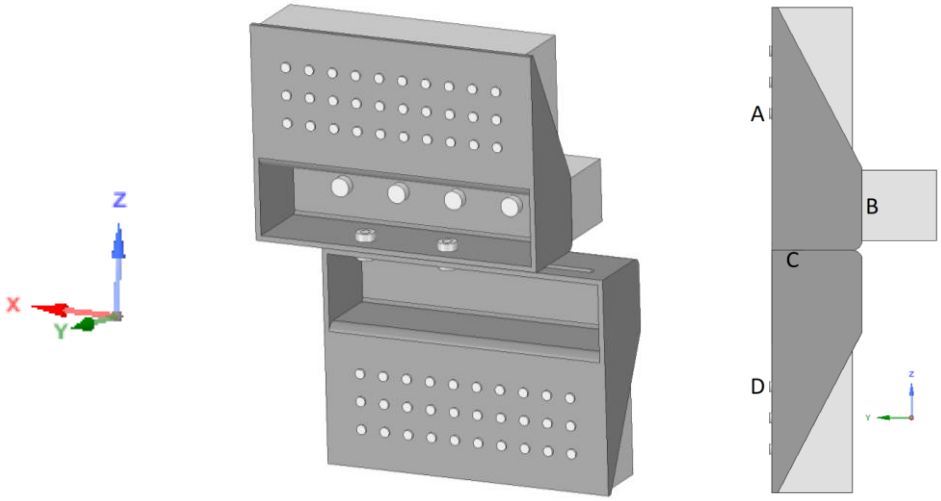

Figure 4-42:Profile 8-2B-SR (Images used courtesy of ANSYS, Inc.)

In addition to the side reinforcement, the width of the original profile was reduced with 16 mm, as the original edge distance of the CLT-steel connectors were 58 mm, when the hand calculations from

Appendix C only required a minimum edge distance of 48 mm. In addition to the reduced plate width, the two holes were moved to the outer edge to reduce the eccentrical vertical and horizontal loading of the CLT-steel connection at support D. The added reinforcement was also intended to reduce the stress concentration of the inner horizontal rows of the CLT-steel connections observed for profile 8-2B and 8-2B-R as a result of the moment M_x.

The resulting moments from the simulations summarized in Table 4-5, showed a reduced Moment reaction M_y of -4.0 kNm for support B and -5.6 kNm for D compared to profile 8-2B-R, while an increased M_y of -5.4 kNm was observed for support A. This indicated a moment resistant friction connection in C.

Figure 4-43 indicated that the increased stiffness of the plates distributed the resulting M_y evenly in the friction connection for the compressed profile 8-2B-SR, avoiding the force concentration seen in the friction connection for profile 8-2B.

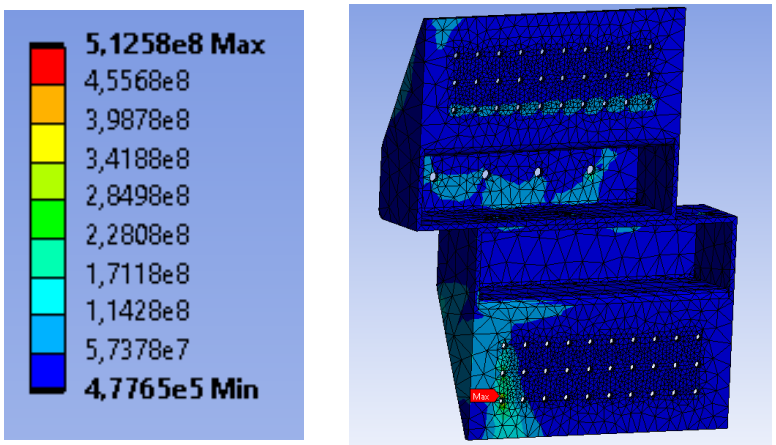

Figure 4-43: Equivalent von-Mises stress for the 8-2B-SR in compression [N/m²]. (Images used courtesy of ANSYS, Inc.)

$M_{x.c}$ was found to be around -1.5 kNm for support A and -1.7 kNm for support D, as seen in Table 4-5, while a $M_{x.c}$ of only -0.9 kNm was observed for the concrete support at B. This decrease of $M_{x.c}$ for the concrete connection indicated a fixed behavior for the friction connection about the x-axis, where the reinforcements of the CLT-steel connections were able to distribute larger $M_{x.c}$ than seen for the other profiles.

The equivalent stresses observed in Figure 4-43 showed a reduced stresses for the compressed profile 8-2B-SR compared to profile 8-2B-R with exception of the critical anchor at support B with a critical stress of 329 N/mm^2 and the critical Rothoblaas connector in support D experiencing 512 N/mm^2. For support connection D, the stress concentration was observed for the entire vertical left row of the connection.

This concentration was likely a result of the left reinforcement of the bottom profile leading most of the forces and moments into connection D while experiencing twisting as a result of the reduced stiffness in the outer part of the top plate for connection C. In turn the stiffness of the plate at support D, was insufficient to withstand the twisting without deforming, leading to most of the Moment M_x being taken by the closest vertical row of connectors. This effect was quite pronounced as seen in Figure 4-44, where the scaled deformation of the bottom profile shows a concentrated local deformation of 1.1 mm along the y-axis at the bottom left corner.

The resulting axial force of the worst connector of support D for profile 8-2B-SR in compression was 8.78 kN according to the results from the Ansys simulation in Table 4-6. In addition to the increased

axial force of the connector, a resulting shear force of 5.76 kN was observed for the connector, which was considerably higher than what was expected for a moment $M_{y.c}$ in the connection, if the shear force had been evenly distributed. The larger shear and axial forces of the critical connector in support D, resulted in a characteristic utilization of 5.24, as shown in Table 4-9.

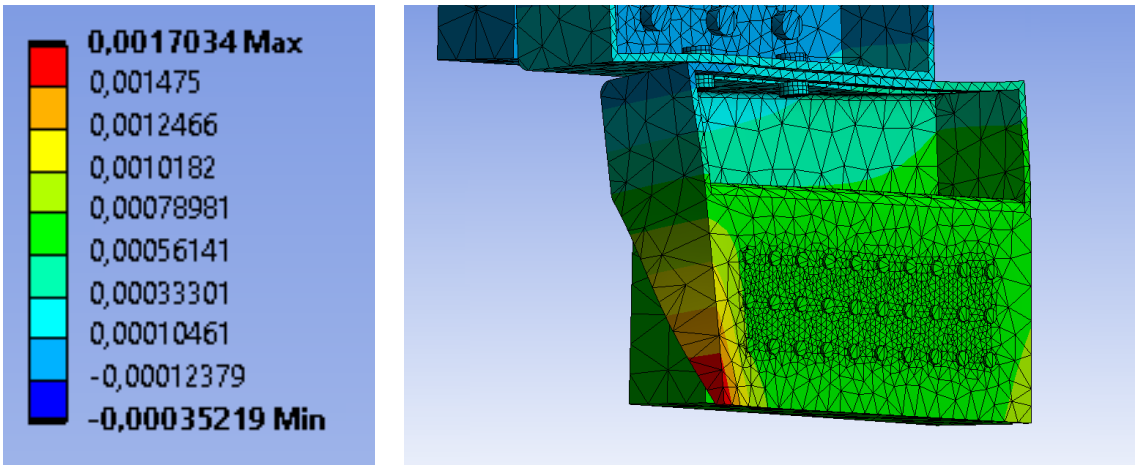

Figure 4-44: Deformation of 8-2B-SR bottom profile in compression along y-axis with 26 times graphical deformation scaling for visualization [m]. (Images used courtesy of ANSYS, Inc.)

For profile 8-2B-SR in tension, a pinned behavior was observed for the friction connection, resulting in a moment reaction $M_{y.t}$ of 6.9 kNm for support D. Figure 4-45 showed large stresses acting at the vertical edges of the top and bottom plate of the friction connection C in tension.

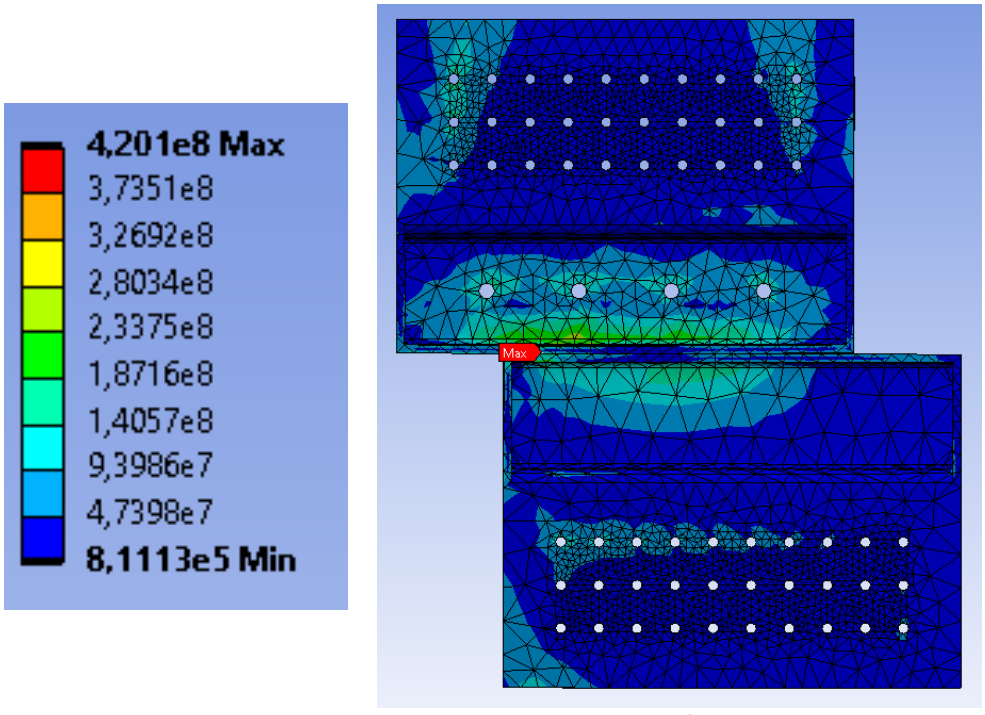

Figure 4-45: Equivalent von-Mises stress for the 8-2B-SR in tension [N/m²]. (Images used courtesy of ANSYS, Inc.)

These stresses were especially clear looking at Figure 4-46, where the entire top plate of the friction connection at point C experienced large stresses. These stresses seemed to concentrate at the inner plate bend, indicating large moment stresses occurring as a result of the span between the closest vertical support and the tension forces acting on the preloaded bolts.

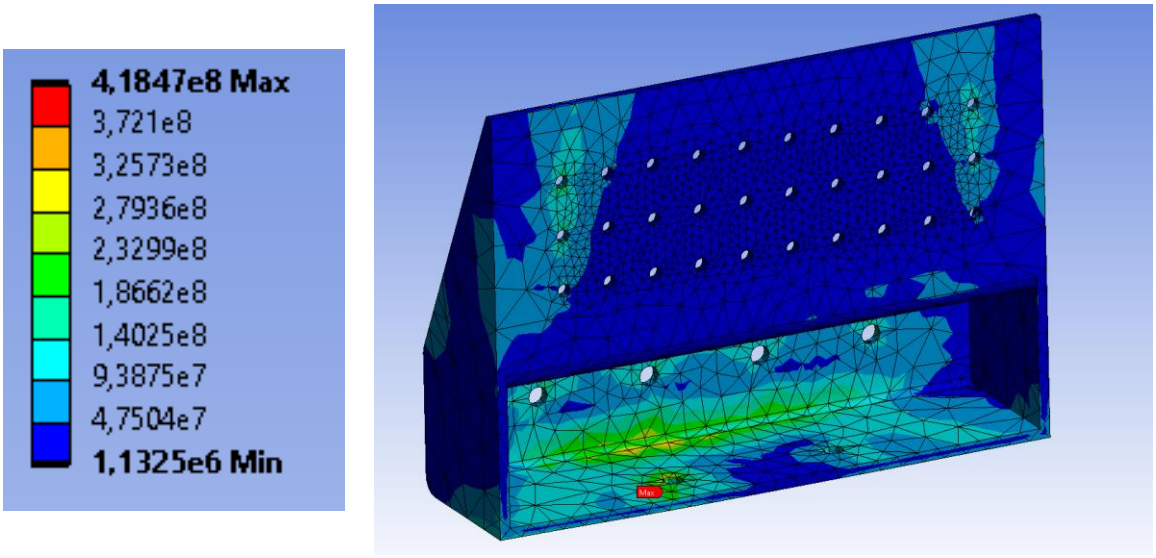

Figure 4-46: Equivalent stress for top profile of 8-2B-SR in tension [N/m²]. (Images used courtesy of ANSYS, Inc.)

Stress concentrations were also observed for the outer vertical screw rows of support A for the profile in tension shown in Figure 4-46. These stresses were likely a result of the $M_{x.t}$ reaction of 1.4 kNm acting in the connection. This moment reaction was larger than the $M_{x.t}$ found for the same simulation of profile 8-2B, and was likely a result of the reinforcement in A distributing the $M_{x.t}$ more evenly between support A and B, as the $M_{x.t}$ had decreased by almost half compared to profile 8-2B-R.

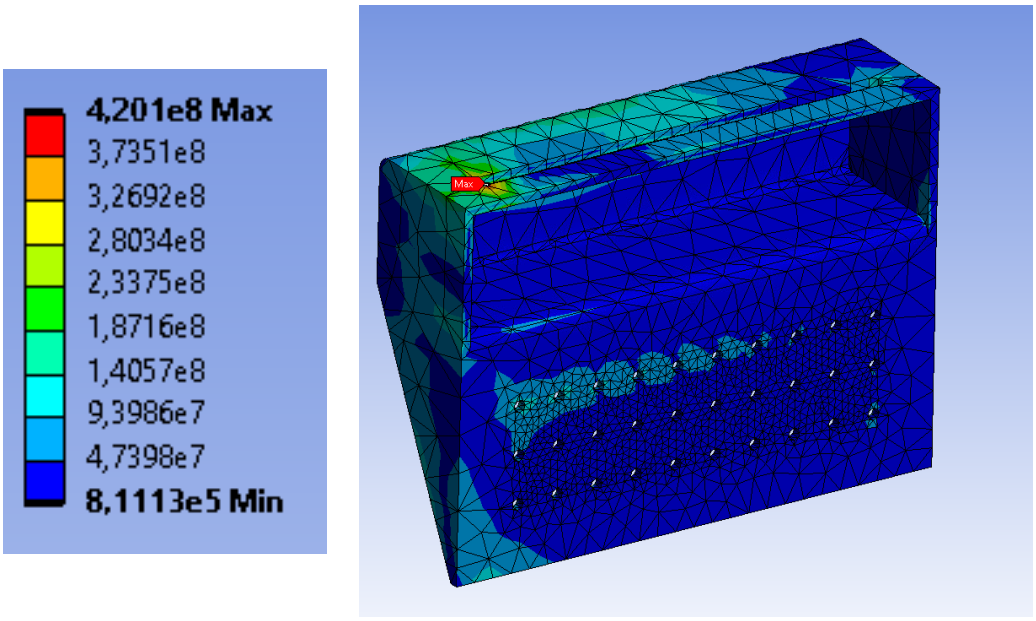

Figure 4-47: Equivalent stress for 8-2B-SR bottom profile in tension [N/m²]. (Images used courtesy of ANSYS, Inc.)

A stress concentration was also observed on both the outer vertical rows of connectors for support A of profile 8-2B-SR in tension in Figure 4-45. These were a result of the two profiles bulging out as a result of the vertical forces acting on the bolted connection. This effect is especially visible in Figure 4-48, where a graphical deformation scaling of 20 times shows the top plate deflecting downwards around the preloaded bolts, resulting in a deflection at the top of the reinforcement of 0.9 mm along the y-axis.

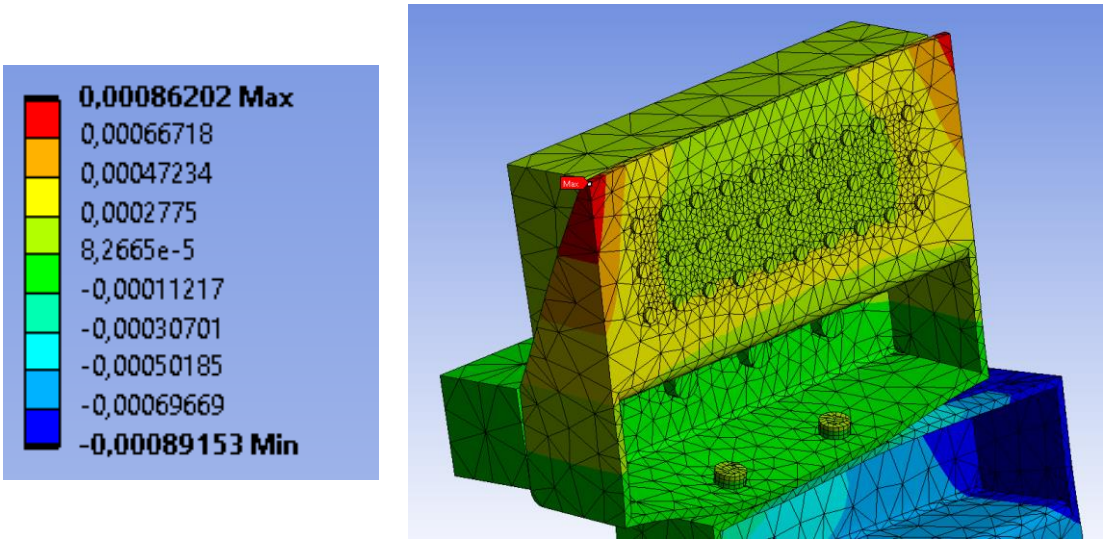

Figure 4-48: Deformation of 8-2B-SR top profile in tension along y-axis with 20 times graphical deformation scaling for visualization [m]. (Images used courtesy of ANSYS, Inc.)

For the profile deflection, Figure 4-49 and Figure 4-50 gave critical deformations along the x-axis for profile 8-2B-SR of less than 1 mm for both compression and tension, despite the large deformations observed along the y-axis.

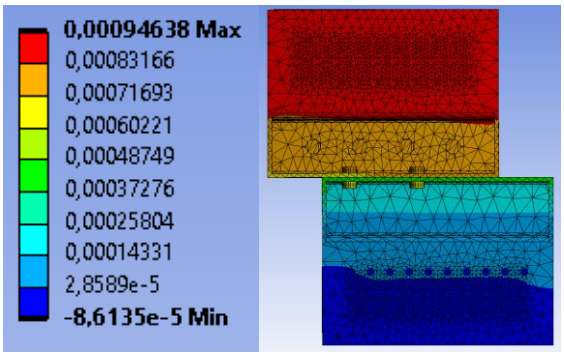

Figure 4-49: Deformation of 8-2B-SR in compression along X-axis [m]. (Images used courtesy of ANSYS, Inc.)

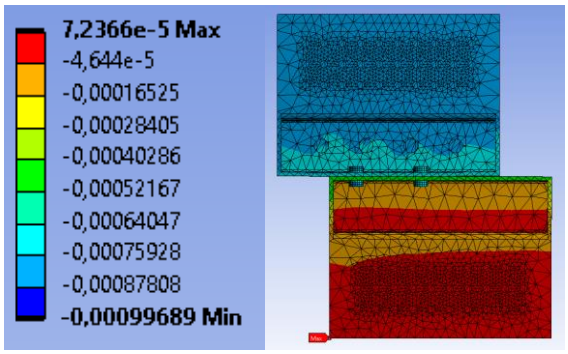

Figure 4-50: Deformation of 8-2B-SR in tension along X-axis [m]. (Images used courtesy of ANSYS, Inc.)

The resulting deformation along the z-axis were also greatly improved compared top profile 8-2B and 8-2B-R with Figure 4-51 and Figure 4-52 yielding critical deflection of 1.8 mm for the compressed profile 8-2B-SR.

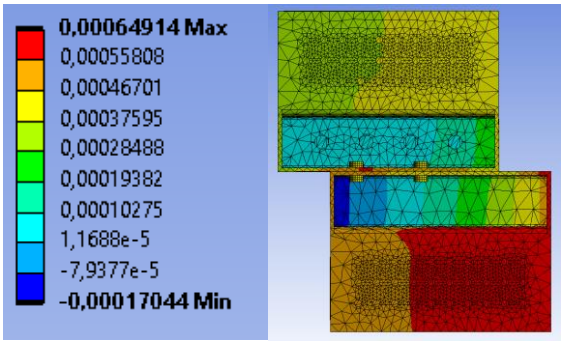

Figure 4-51: Deformation of 8-2B-SR in compression along Z-axis [m]. (Images used courtesy of ANSYS, Inc.)

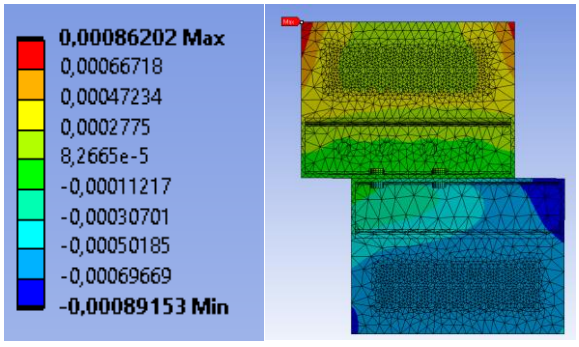

Figure 4-52: Deformation of 8-2B-SR in tension along Z-axis [m]. (Images used courtesy of ANSYS, Inc.)

The changes made to profile 8-2B-SR compared to profile 8-2B-R yielded both improvements and new problems which would have to be improved on for a final design. The new reinforcement,

seemed to resolve the large plate stresses which mainly occurred from the large eccentricities of the vertical and horizontal forces along the x- and y-axis, which resulted in critical torsion effects, as well as bending about the weak axis of the profile plates. Profile 8-2B-SR also highlighted the lack of stiffness for the steel plate in the CLT-steel connections, which resulted in large stress concentrations occurring either at the closes horizontal edge for M_x or at the vertical connector edges for M_z.

Lastly the profile showcased the problem of the placement of the friction connection along the y-axis. Having the bolts in the same hole, seemed to distribute the stresses more evenly. The reinforcement had the opposite effect, as it increased plate stiffness close to the reinforcement compared to the rest of the friction connection. This resulted in uneven reaction force distribution between the bolts when they approached the end of the slotted hole.

Having the bolts close to the edge, also resulted in large vertical moment stresses in the top plate of the friction connection, as the holes for the bolts, were located at the furthest point from the support. Moving the slotted inwards from the edge would likely negate these stress concentrations, as well as the fixed behavior for the M_x for the friction connection. On the other hand, this could result in larger $M_{x.t}$ for the CLT-steel connection at support D, which would be problematic as the CLT-steel connections still lacked stiffness for M_x and M_z, despite the improvements made to profile 8-2B. As a result, additional reinforcement of the CLT-steel connection would have to be added to the profile 8-2B-SR, if the design were to be proceeded with.

4.8 Profile 8-2B-AP

A second approach for improving the profile capacity of the friction dissipating system was profile 8-2B-AP shown in Figure 4-53.

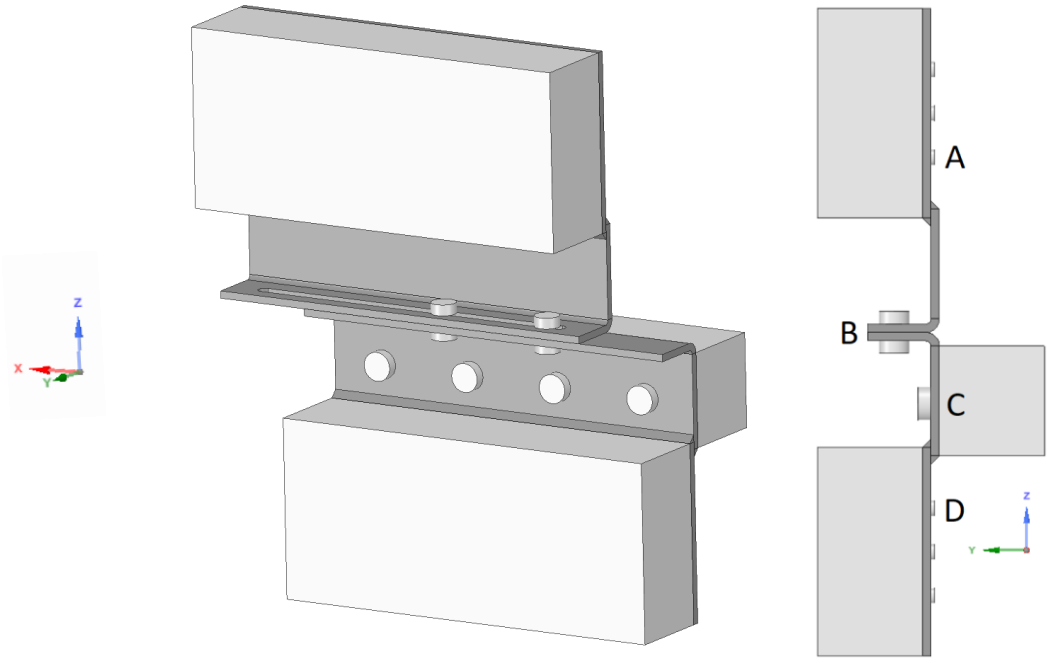

Figure 4-53: Profile 8-2B-AP (Images used courtesy of ANSYS, Inc.)

Profile 8-2B-AP was based on the results found from profile 8-2B-DP, where the M_x and M_z had been found to be reduced compared to the front mounted CLT-steel approach. As a result, the CLT-steel connection was moved to the back of the CLT element to decrease these moments. This would hopefully also decrease the shear stress of the critical connector in the CLT-steel connections, as 30

connectors were used for the one plate, instead of 15 connectors taking 70% of the shear forces as seen for profile 8-2B-DP.

To further reduce the eccentricity of the connection, the preloaded bolts were moved to the same elongated hole for profile 8-2B-AP located as close to the inner bend as possible to reduce moment stress concentrations in the vertical bends of the friction connection seen for profile 8-2B-SR. Avoiding reinforcement of the friction connection as well as having the bolts equally far from the bend would hopefully also result in a more even distribution of vertical forces in the preloaded bolts.

The concrete connection was also changed for profile 8-2B-AP, as the previous hand calculations and Ansys simulations had resulted in a lack of capacity for the concrete anchors. To improve the concrete connection capacity the anchor distancing was increased to 110 mm, close to the maximum allowable hole spacing of 112 mm for the steel plate according to EN 1993-1-8:2005 table 3.3 for steel exposed to climatic impacts. In addition, the anchors size was increased to M16 instead of the M14 anchors proposed in the initial profiles. These changes would result in reduced moment forces, as a result of the increased lever arm of the connectors as well as an increased concrete edge area.

From a practical point, the top and bottom plate were proposed welded with a small overlap at the end of the CLT-steel connections. This was done to create a gap large enough to fit the Rothoblaas screw heads without risking rubbing between the Profile and the RC beams or existing potential mortar infill. The last change made, was to move the concrete connection to the bottom plate of the profile. This was done for easier installation, and was discussed further in *4.9 Mounting procedure for profile 8-2B-AP with proposed adjustment connection.*

The switch of the concrete and friction connection would result in vertical forces acting negative along the z-axis (downwards) compressing the friction connection. Accounting for the system weight, this resulted in slightly larger vertical forces acting on the compressed profile and slightly smaller forces acting on the tension profile.

For the calculations of profile 8-2B-AP, the second friction dissipating system (CLT-element) from the bottom was chosen for the calculations, as the system of the ground floor would not be affected by vertical forces from below. This resulted in marginally lower vertical and horizontal forces acting on the friction connection as shown in Table 4-2. This was done as the ground friction system, would not be affected by an underlying friction system. If the profile was to be studied further, this load case should be studied as well. A lower estimate of the required preload of 19 kN for the friction bolts was also estimated in the Table 4-2 from the hand calculations compared to 21.7 kN for the other profiles.

This estimated preload turned out to be close to the required preload of 20 kN, estimated in the Ansys simulations for compression and tension in Table 4-3. The slight increase of the Ansys estimate could have been a result of the relative deformation assumption of 0.5 mm being a rough estimate, as the preload estimated for the different profiles fluctuated between being slight overestimates, to being slight underestimates. Table 4-5 for profile 8-2B-AP showed $M_{y.c}$ and $M_{y.t}$ expected for the friction connection acting pinned. In addition, $M_{y.c}$ for support A of profile 8-2B-AP was found to be the same for the hand calculations and the simulation, While $M_{y.t}$ was found to be underestimated by approximately 0.8 kNm for the Hand calculations.

The reduced profile eccentricity of profile 8-2B-AP compared to the profiles with front mounted CLT-steel connections, resulted in M_x and M_z never exceeding 0.3 kNm for support A and D in

compression or tension for the Ansys simulations. The low eccentricity also resulted in $M_{x.t}$ and $M_{z.t}$ never exceeding 0.7 kNm for the Ansys calculation.

For the hand calculations, all the vertical and horizontal forces were considered to act at the center of the preloaded bolts along the y-axis. This assumption resulted in quite an overestimate for the moment reactions M_x and M_z for the CLT-steel connection at support A, which was considered acceptable as the moment reactions were quite small for both the hand calculations and Ansys simulation. The overestimate would also ensure that the capacity of the connection would not be overestimated for these moment reactions.

Figure 4-54 gave a critical stress of 281 N/mm^2 for the compressed profile 8-2B-AP. This stress was the result of a stress concentration found in the plate at the left edge of the hole.

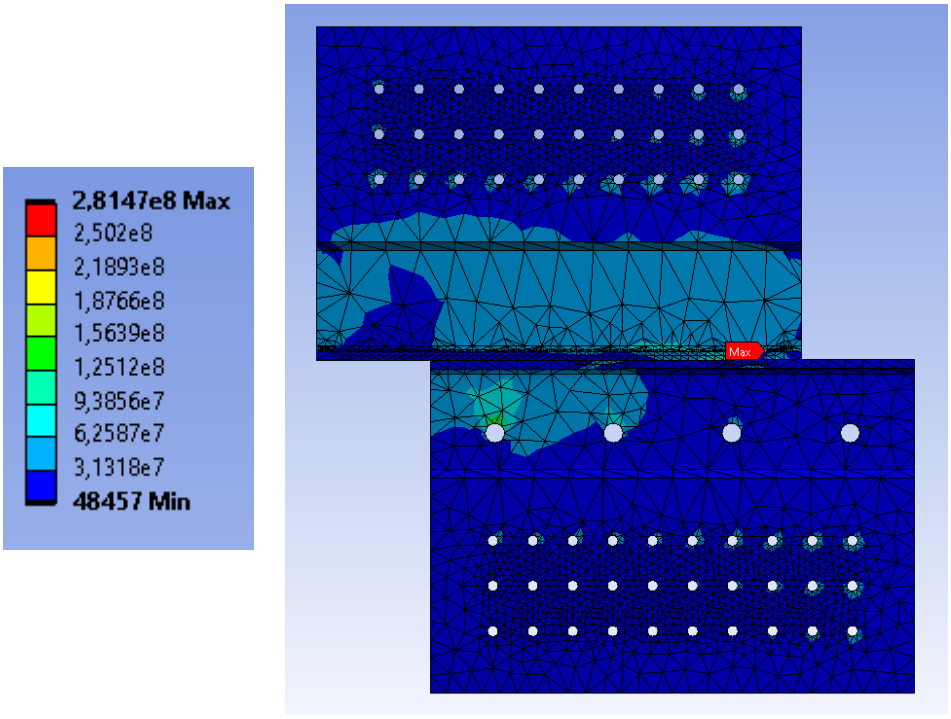

Figure 4-54: Equivalent von-Mises stress for the 8-2B-AP in compression [N/m^2]. (Images used courtesy of ANSYS, Inc.)

This stress concentration would likely not be a problem, as the concentration was localized in one small area as shown in Figure 4-55, as well as not exceeding the ultimate material strength. For the remaining parts of the profile in compression, stresses never exceeded 150 N/mm^2. An even stress distribution for the holes around the CLT-steel and concrete connections also indicated the connection plates behaving rigid. This was likely a result of the reduced moments M_x and M_z for profile 8-2B-AP compared to 8-2B and 8-2B-R.

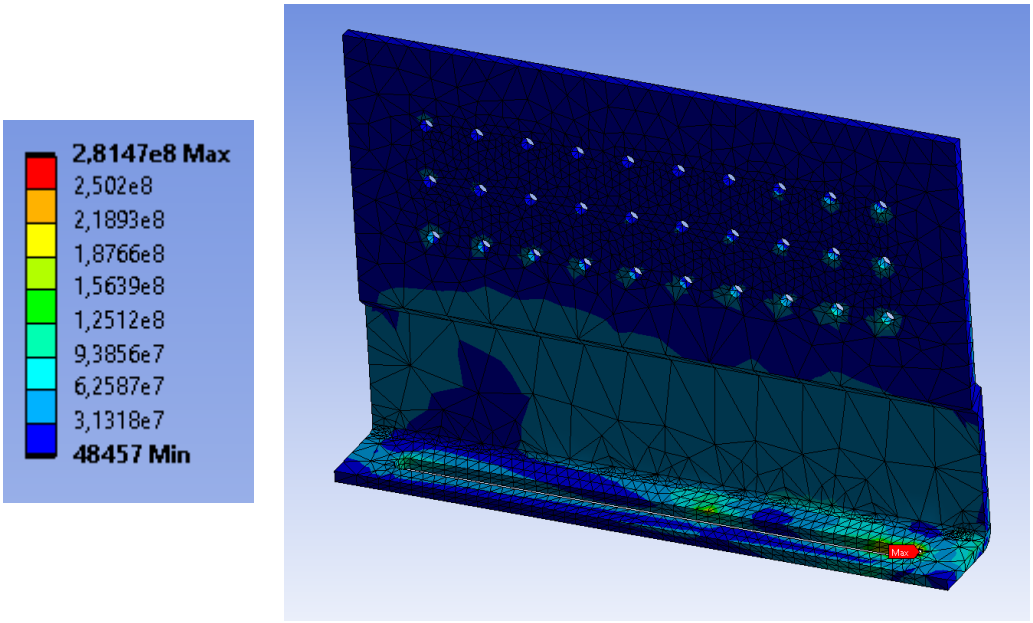

Figure 4-55: Equivalent stress for top profile of 8-2B-AP in compression [N/m²]. (Images used courtesy of ANSYS, Inc.)

The low stresses of the profile, also resulted in small deformation as shown in Figure 4-56 and Figure 4-57. The critical profile deformation along the x-axis was 0.7 mm and 0.4 mm along the z-axis for profile 8-2B-AP in compression.

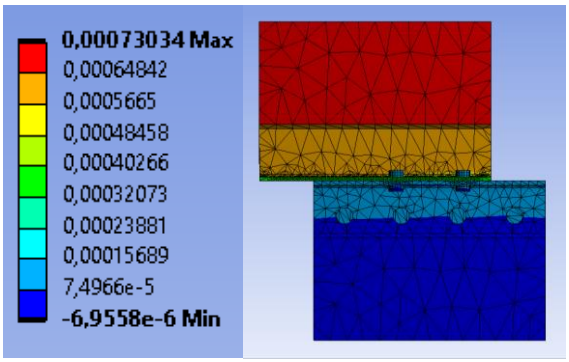

Figure 4-56: Deformation of 8-2B-AP in compression along X-axis [m]. (Images used courtesy of ANSYS, Inc.)

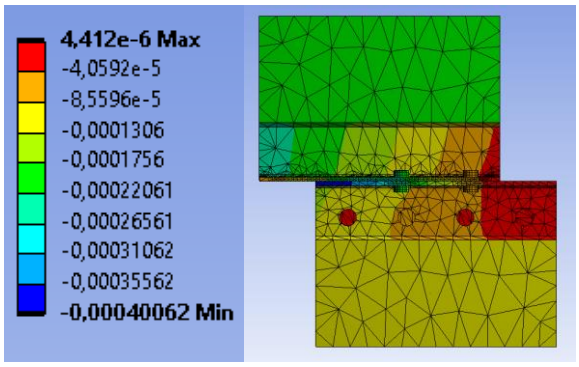

Figure 4-57: Deformation of 8-2B-AP in compression along Z-axis [m]. (Images used courtesy of ANSYS, Inc.)

For profile 8-2B-AP in tension, Figure 4-58 show a maximum stress concentration of 460 N/mm^2 appearing at the end of the elongated hole in the same way as the compressed profile 8-2B-AP.

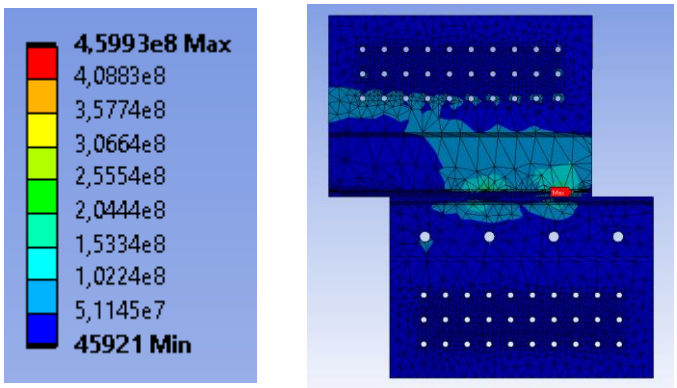

Figure 4-58: Equivalent von-Mises stress for the 8-2B-AP in tension [N/m²]. (Images used courtesy of ANSYS, Inc.)

A closer look at the stress concentrations in Figure 4-59 revealed the stress concentrations going all around the edge. This concentration could have been the result of both bolts leading most of the stresses of the outer plate past the edge of the elongated hole. A smaller stress concentration of 300 N/mm^2 was found for the right preloaded bolt hole of the bottom plate, as shown in Figure 4-60.

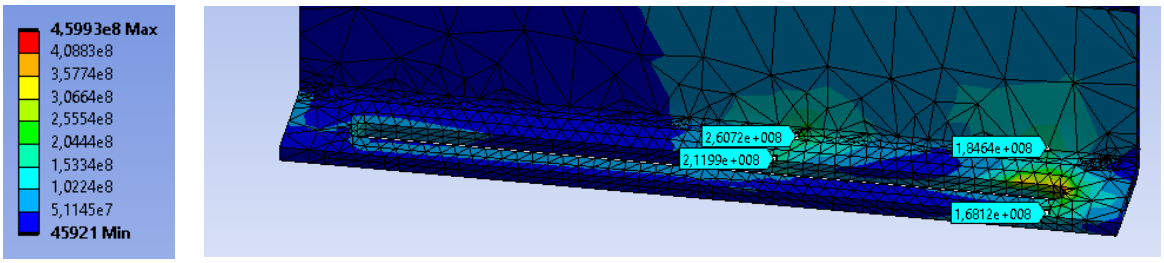

Figure 4-59: Stress concentrations for top profile of 8-2B-AP in tension [N/m^2]. (Images used courtesy of ANSYS, Inc.)

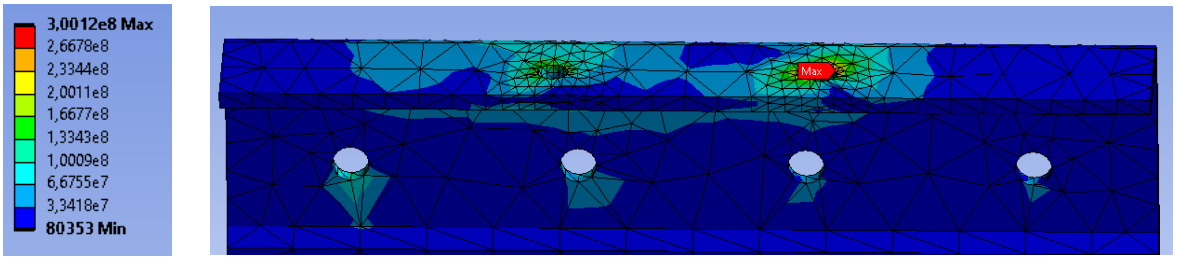

Figure 4-60: Stress concentrations for preloaded holes of bottom plate of profile 8-2B-AP in tension [N/m^2]. (Images used courtesy of ANSYS, Inc.)

Figure 4-59 also showed localized stress concentrations from each bolt at the vertical plate edge of the friction connection. For the inner bolt, the figure showed a stress concentration of 261 N/mm^2, while a critical stress of 185 N/mm^2 was observed for the outer bolt. As the plate would have residual strength to cope with the observed stresses by distributing them plasticly, it is unclear how critical the stress concentration behavior would be for the actual profile.

For profile 8-2B-AP in tension, critical deformations of 0.5 mm along the x-axis, as well as 0.8 mm along the z-axis were found from Figure 4-61 and Figure 4-62. The low 4vertical deformation of the friction connection, indicated that the decreased distance between the bolts and the vertical plate bend, had increased the system stiffness for vertical deformation compared to the profiles having two rows of bolts. The low deformation of the friction system also indicated that the stress concentrations at the inner edge were mainly caused by shear stresses, as opposed to moment stresses seen for profile 8-2B-SR.

In the case of the profile 8-2B-DP, an equally low vertical deformation was observed, but the stress concentration around the inner bolt was almost twice that of profile 8-2B-AP in tension.

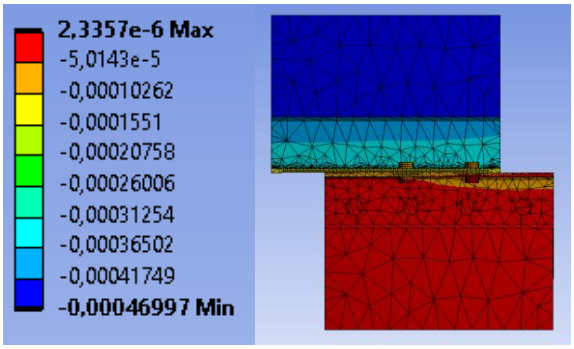

Figure 4-61: Deformation of 8-2B-AP in tension along X-axis [m]. (Images used courtesy of ANSYS, Inc.)

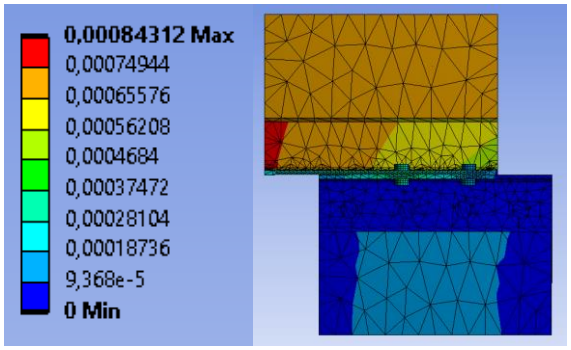

Figure 4-62: Deformation of 8-2B-AP in tension along Z-axis [m]. (Images used courtesy of ANSYS, Inc.)

The resulting shear stresses observed for the worst connector of connection A was found to be for the compressed profile 8-2B-AP. For the Ansys connection, a critical shear stress of 4.38 kN was estimated according to Table 4-6, compared to 3,91 kN, from the hand calculations summarized in Table 4-7. This indicated a shear concentration in the critical connector at support A for the Ansys simulation, as the $M_{y.c}$ found for the CLT-steel connection in Ansys was equal to the moment of the hand calculation.

An axial force of 0.58 kN was calculated for the critical connector at support A in compression, as shown in Table 4-7. A smaller axial force of 0.29 kN was found from the simulation, as shown in Table 4-6. This was likely a result of the increased eccentricities considered for the hand calculations, compared to what was observed in the Ansys model.

The resulting critical characteristic utilization for connection A was calculated to be 0.45 for the hand calculations summarized in Table 4-8, compared to a critical characteristic utilization estimate of 0.55 from the Ansys simulation from Table 4-9. This indicated that the steel plate would behave as relatively rigid for profile 8-2B-AP compared to the profiles with front mounted CLT-connection.

For the concrete connection at support C for the compressed profile 8-2B-AP, the hand calculations showed a critical shear force of 21,7 kN, summarized in Table 4-7. This was lower than the 25.8 kN observed from the simulation, shown in Table 4-6. This indicated a shear concentration in the critical connector, as a larger moment had been assumed for the hand calculations, compared to the simulation. For the axial force reaction of the critical concrete anchor, a critical force of only 2.46 kN was observed from the Ansys simulation, which was far lower than the critical axial force of 6.62 kN calculated from the hand calculations. This was likely a result of the increased eccentricity used for the hand calculations.

A resulting characteristic utilization of 0.46 was found for the concrete connection from the hand calculations in Table 4-8, indicating that the improvements made to the concrete connection compared to the other profiles were effective. As the Hilti HIT-Z anchors required a gamma factor of 1.5 compared to 1.25 assumed for the remaining profile system, the utilization considering characteristic loading and design resistance came to 1.04.

For this anchor capacity calculation, a cross-section height of 350 mm assumed. For an older building, the height could be less than that. In addition, a concrete reinforcement factor of $\psi_{\mathrm{re,V}}$ of 1.2 was utilized as the compressed profile would have the vertical force reaction pushing downward into the beam reinforcement. For a building with a lower concrete beam height, the concrete connection could become insufficient. For such a building, this system would likely not be an option, as the vertical shear forces applied to the RC-frame would likely exceed the shear capacity of the beam.

The $\psi_{re,V}$ factor for the compressed load case could also lead the concrete calculation in tension to become the critical load case as the factor could likely not be used for this load case. On the other hand, the external force reaction of the tension profile summarized in Table 4-2 resulted in reduced vertical and horizontal forces acting on the profile in tension compared to compression.

4.9 Mounting procedure for profile 8-2B-AP with proposed adjustment connection

The original proposal for mounting the friction dissipating system, was to mount the profiles first and then slide the CLT element in to place. After this had been done, the Rothoblaas screws of the CLT-steel connection could be installed. This approach would allow for around 10 mm of adjustment as a 58 mm CLT edge distance was used for the CLT-steel connections. ETA-11/0030 only required an edge distances of 48 mm. This clearance was important, as the friction dissipating system was mainly intended for use in older pre-existing buildings, where the floors might not be completely level or have differing heights. It would also be a challenge getting the Hilti HIT-Z concrete anchors perfectly aligned.

Even though this procedure would be quite simple in theory, there were several challenges with the procedure. From the Ansys simulations, the stresses induced on the front mounted CLT-connections of profile 8-2B were higher than the material capacity. The improved profile 8-2B-SR almost removed these stresses with exception of the stress concentrations of the CLT-steel connections.

These concentrations could be fixed by increasing the reinforcement of the connections, but this would add more weight to the profiles. This would likely be quite inconvenient as each plate likely would have to be lifted into place by hand, and each plate of the 8-2B-SR weighed 17.4 kg before any additional reinforcement of the CLT-steel connections.

In addition, the improved profile 8-2B-SR would not allow for the plate to be slid into place, as the reinforcements would block the CLT element. The element could be pivoted on to the bottom steel plate while the top plates were connected. This could potentially create a dangerous situation for the workers, as the plate would naturally want to pivot outwards towards the workers mounting the plate at the top of the CLT-element. Even if they were to do this, 120 holes would have to be pre-bored for the Rothoblaas screws of each profile, and then connecting all the screws. This would be a time consuming and cumbersome work, as it would have to be performed while the plate was hanging on the building.

As profile 8-2B-AP was the best performing profile under the loading conditions set for this thesis, an improved mounting method was desired for this profile. As the screw connections were inaccessible on when the profiles were mounted on the wall, the profile plates would have to be mounted to the CLT-elements before the system went up on the wall. This posed a challenge, as the original adjustment method depended on being able to adjust the CLT-element placement in relation to the Rothoblaas connectors of the plates to account for uneven spacing of the building floors.

As a result, the only clearance of the friction dissipating elements using the 8-2B-AP profile would be that of the hole clearance of the anchors. As 2 mm of clearance would be insufficient for CLT elements several meters high, profile 8-2B-AP would be impractical as tested in this thesis. To impose a greater level of adjustment to profile 8-2B-AP, a friction system as seen in Figure 4-63 is proposed.

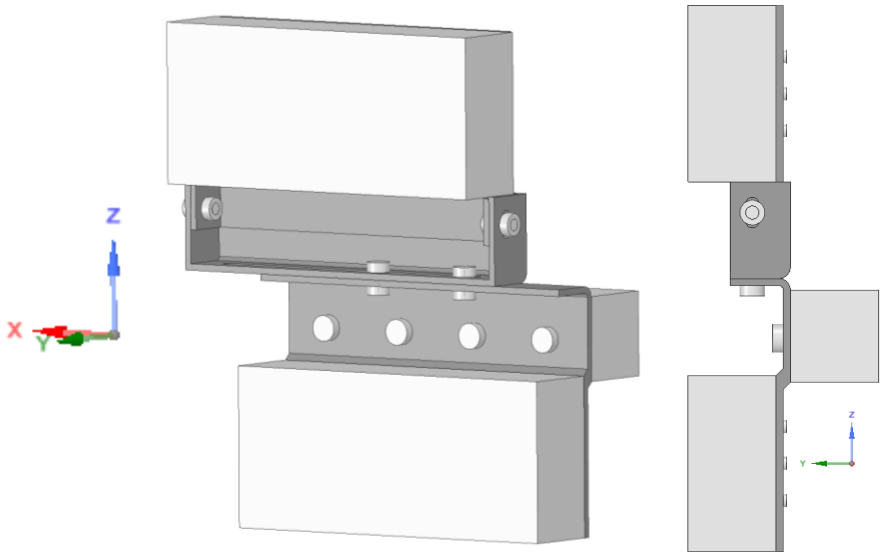

Figure 4-63: Profile 8-2B-AP with proposed adjustment system. (Images used courtesy of ANSYS, Inc.)

The proposed adjustment system would connect the overlapping plates in the top part of profile 8-2B-AP using preloaded bolts, in place of the welded connection proposed for profile 8-2B-AP. As profile 8-2B-AP had low eccentricity along the x- and y-axis, the reaction moments M_x and M_z imposed on the adjustment connections would be relatively small.

In addition, the pinned behavior of the friction connection for profile 8-2B-AP would result in a reduced moment acting at the adjustment connection as it would be located close to the friction connection. The characteristic friction capacity of the M14 Bolts with a preload of 70% would be around 30 kN per bolt for elongated holes according to EN 1993-1-8:2005 clause 3.9.1, if two effective shear surfaces were to be considered with a k_s of 0.68. The combined vertical load and moment reaction M_y acting in the connection would likely not exceed this capacity, as the lever arm between the connectors would be 450 mm. If friction testing were to reveal that only one shear surface contributes to the shear capacity, an additional steel plate could be welded to the top plate of the adjustment connection to create double lapped connections. If M_x turned out to be a problem for the connection, the plate overlap of the adjustment connection could be increased to create a larger lever arm resisting M_x.

As the proposed profile would have its own adjustment system, the holes of the CLT elements could be ordered predrilled from the factory. This would increase the precision of the predrilling, as well as reducing the mounting time for the CLT-steel connections on site. It would also allow mounting of the CLT-steel connection on the ground. The bottom mounted concrete connection for the profile, would allow the entire element to be hoisted in place, and be fastened securely to the RC-beam before fastening the preloaded bolts. A mounting procedure for the proposed friction dissipating system is shown in Figure 4-64.

Mounting procedure:

Step 1:

The bolts of the adjustment connection are loosely fastened.

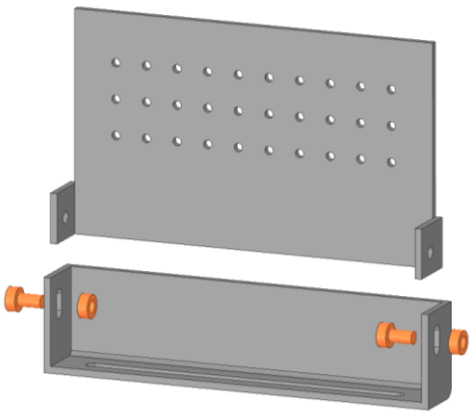

Step 2:

The Rothoblaas screws of the CLT-steel connections are fastened in the predrilled holes.

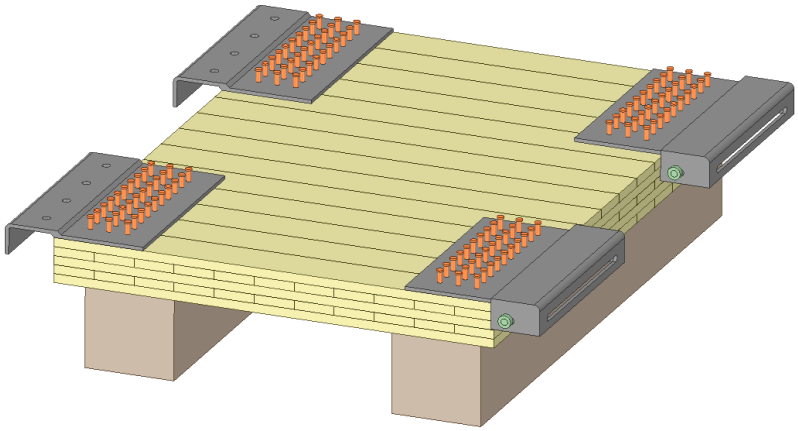

Step 3:

The element is lifted on to the pre-mounted concrete anchors.

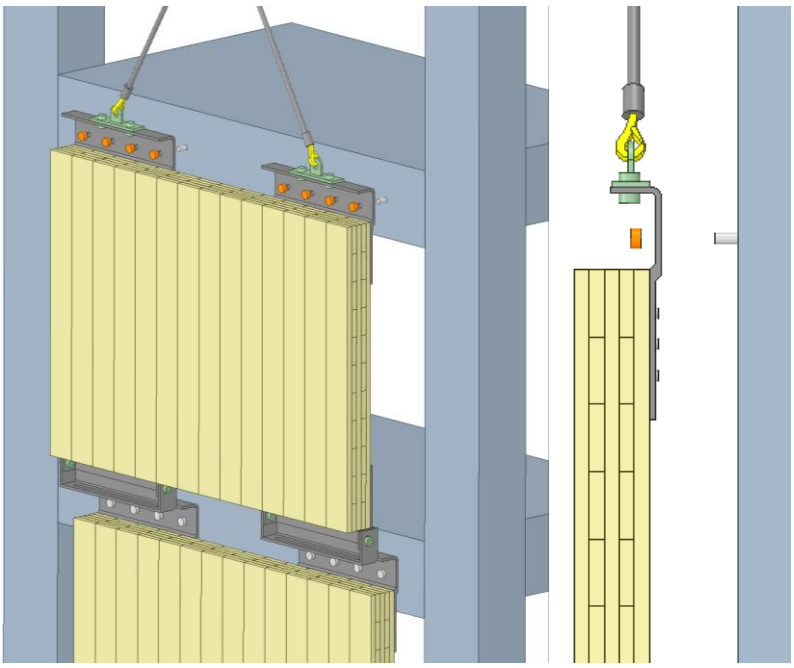

Step 3:

The bolts of the friction connections are preloaded to the required torque, aligning the adjustment system in the process.

Finally, the bolts of the adjustment system are preloaded.

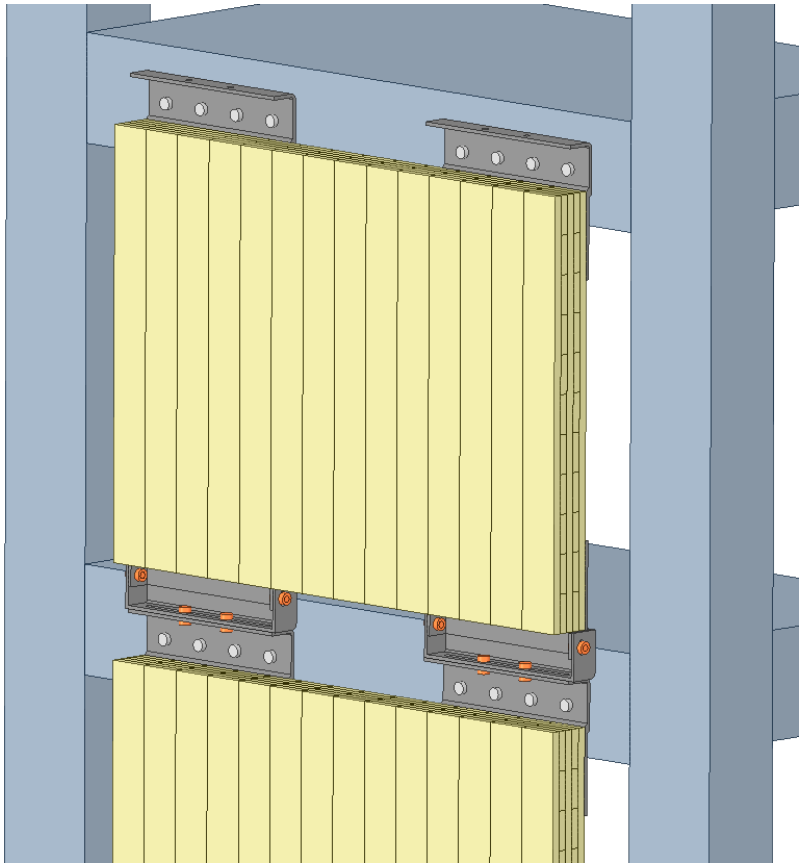

Step 5:

The element is fully mounted, ready for the next friction dissipating element to be mounted.

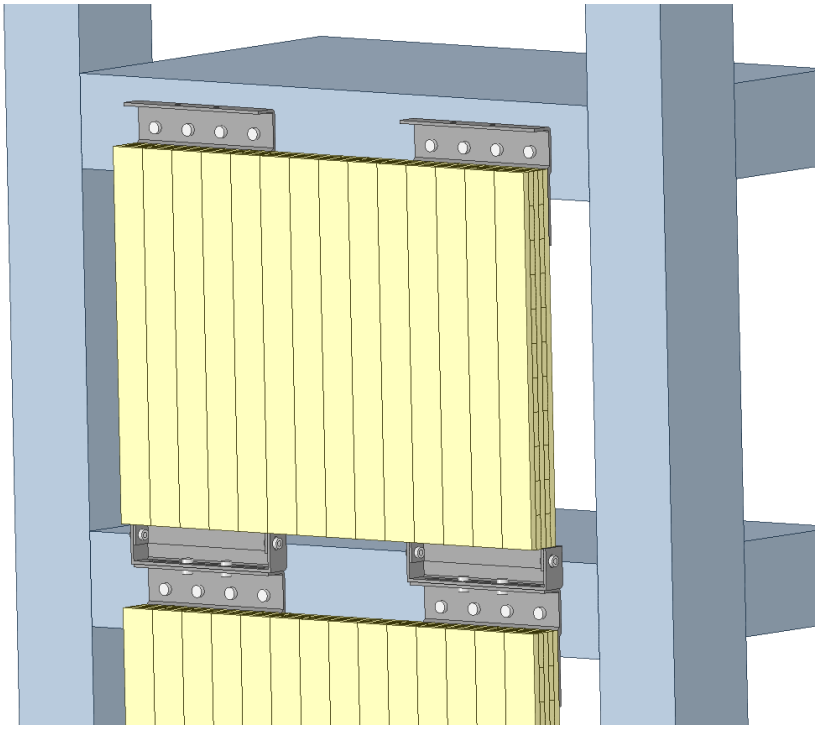

Figure 4-64: Proposed installation procedure for profile 8-2B-AP with adjustment mechanism. (Images used courtesy of ANSYS, Inc.)

Preliminary Ansys simulations were performed for the resulting stresses of the revised profile 8-2B-AP with the adjustment system in compression and tension. Figure 4-65 for the equivalent stress of the proposed profile showed stresses comparable to that of profile 8-2B-AP.

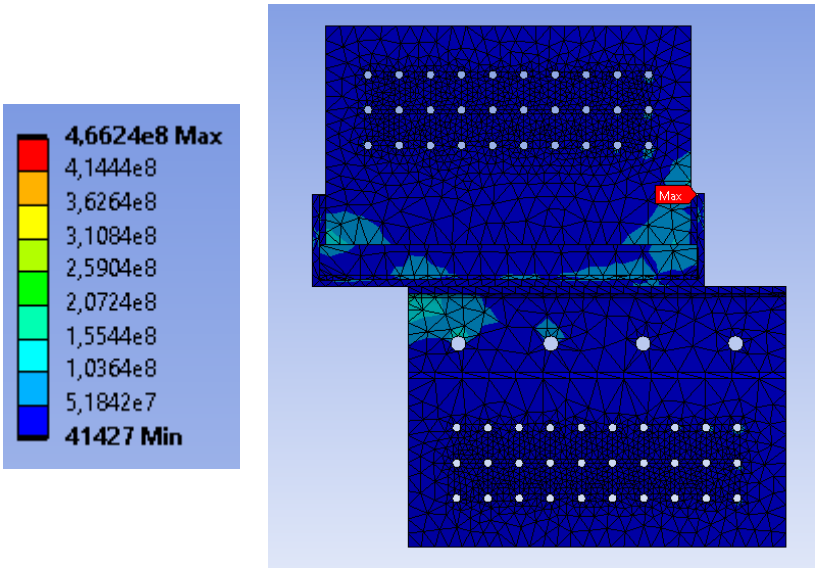

Figure 4-65: Equivalent von-Mises stress for the 8-2B-AP with proposed adjustment connection in compression [N/m^2]. (Images used courtesy of ANSYS, Inc.)

A stress concentration of 466 N/mm^2 was observed at the adjustment connection as shown in Figure 4-66. This stress concentration was observed at the edge and would therefor likely not pose a problem.

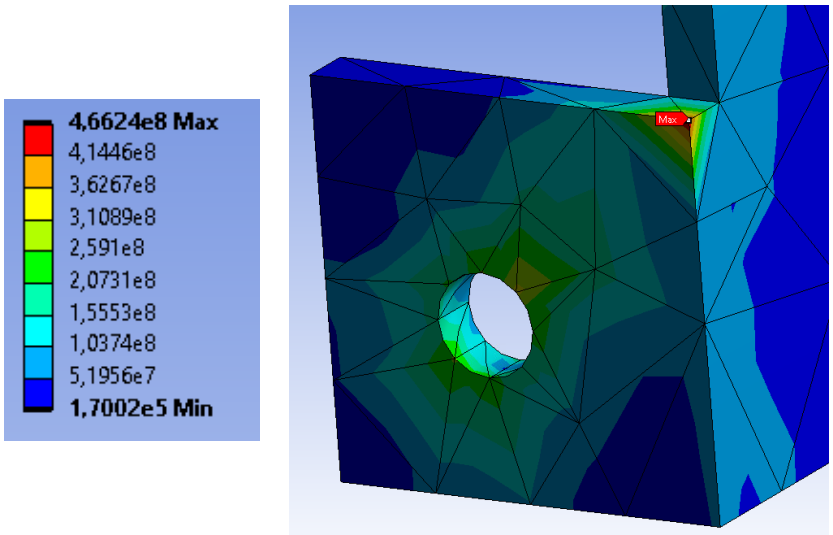

Figure 4-66: local stress concentration of top mounted adjustment plate in compression [N/m^2]. (Images used courtesy of ANSYS, Inc.)

The stresses of the profile in tension as showed in Figure 4-67, also resembled the critical stresses observed in profile 8-2B-AP.

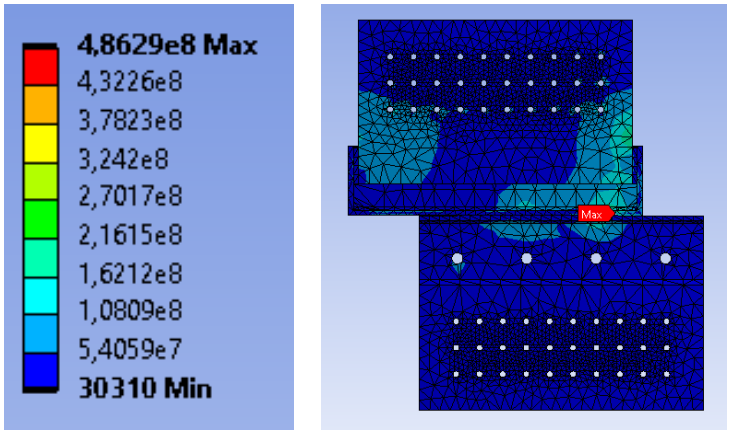

Figure 4-67: Equivalent von-Mises stress for the 8-2B-AP with proposed adjustment connection in tension [N/m2]. (Images used courtesy of ANSYS, Inc.)

A slight increase in the stress concentration around the end bolt was observed in Figure 4-68, compared with profile 8-2B-AP. This was likely a result of the increased moment stiffness introduced from the reinforcement. For a finalized design, it would be recommended to not connect the adjustment plate directly to the horizontal part of the friction connection to avoid this increase of stiffness.

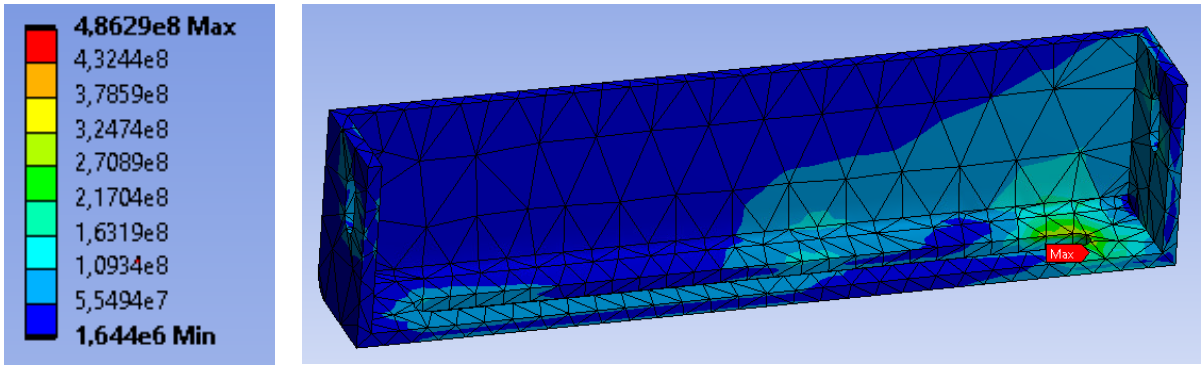

Figure 4-68: Equivalent stress of top element of friction connection in tension [N/m²]. (Images used courtesy of ANSYS, Inc.)

A stress concentration of 220 N/mm^2 was also observed above the adjustment connection for the top plate in Figure 4-69. This concentration could increase beyond the plate capacity for the profile calculation at the ground floor but should be quite easy to reduce in a potential finalizing of the profile by increasing the stiffness of the connection with horizontal reinforcement.

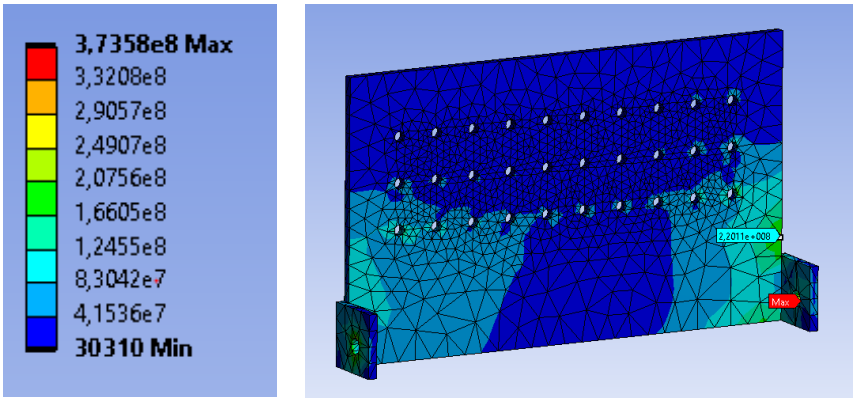

Figure 4-69: Stress for CLT-steel top plate in tension [N/m²]. (Images used courtesy of ANSYS, Inc.)

4.10 Estimated optimal slip load

The friction system of this thesis was intended to provide an affordable and convenient solution for improving the seismic capacity of existing buildings. *2.3 Friction damping,* described how a lateral stiffness of around three to ten times that of the undamped structure, would result in optimal damping. An estimate of the relative stiffness for the friction system was not performed for this thesis, but the proposed friction dissipating system would likely impose a large relative stiffness compared to the existing structure, as the CLT-elements would act like shear walls. This would likely be the case, as the CLT-elements would have a larger moment of inertia compared to the RC-columns, and small horizontal displacements of less than 1 mm were observed for the profile 8-2B-AP, as shown in Figure 4-56 and Figure 4-61. From the theory of *2.3 Friction damping,* a slip force of around 0.2 times the base shear of the undamped structure was found to result in optimal damping. The base shear and required number of friction dissipating system columns were summarized in Table 4-11 for the four floor structures. For the four-story structure assumed in this thesis, each column would consist of four friction dissipating CLT elements.

Table 4-11: Approximated base shear for four floor building, and required friction systems assuming evenly distributed slip force for each story.

PGA [g]	Base shear [kN]	required systems [even slip distribution]
0.10	2461	2.55
0.35	8616	8.93

From the low PGA of 0.1, the approximation of 2.26 fully utilized friction columns, were promising. Depending on the system damping effect, this would entail that only a few columns of these friction systems would be required when improving the seismic capacity of a building in a low seismic area. This would allow for these systems to be installed when renovating or adding new stories to an existing building. This would be especially convenient for older buildings originally designed without consideration of seismic loading, resulting in lack of capacity when conforming to the seismic load criteria of EN 1998-1:2004.

For the PGA of 0.35, almost eight columns of the proposed friction system would be required to impose an optimal level of damping to the building. As the short side of the building would only allow for the installation of six of these systems, it would be assumed that the system would be insufficient as proposed for this thesis. Possible ways of increasing the slip force of the friction dissipating system, could be to install four friction profiles per story instead of the two proposed in this thesis. Assuming enough width of the CLT-elements, two profiles could be installed on each side without compromising the lever arm of the significantly. This could potentially provide close to double the slip capacity for each element, effectively halving the required number of friction system columns.

On the other hand, this could potentially cause problems with shear capacity for the RC beams, as each beam would be required to resist a local vertical shear force of around 80 kN for fully utilized CLT-elements. As the required system slip force was calculated for an optimal damping effect, the force could likely be reduced for several buildings, as the required seismic capacity improvement for an existing building would likely not require optimal friction damping. Diverging too far from the optimal damper stiffness or slip force could on the other hand result in poor utilization of the friction system. This could in turn result in waste of material, installation time and money.

5 Conclusion

From the hand calculations and simulations of the three original profiles, all the profiles were determined to have insufficient capacity. Profile 8-2B was found to have insufficient plate stiffness to resist the large moment stresses occurring as a result of M_x and the large stresses resulting from the warping torsion induced on the profile bends. In addition, the friction connection was observed to resist moments, resulting in a large stress concentration of the compressive zone. Profile 8-2B-R experienced the same torsion problem, in addition to large twisting deformations as a result of the added reinforcement of the bottom plate. In addition to these problems, both profile 8-2B and 8-2B-R experienced large axial stress concentrations for the critical CLT-steel connectors, as a result of the low plate stiffness against M_x and M_z.

Profile 8-2B-DP did not experience these effects, and fared well for the critical plate stresses. The profile did on the other hand experience an uneven moment reaction distribution between the inner and outer plate of the CLT-steel connections, which resulted in shear failure of the connection. In addition to these problems, all the original profiles experienced uneven stress distribution between the preloaded bolts as a result of the relative distances to the vertical plate bends. All the original profiles were also found to have insufficient capacity for the concrete connections.

The proposed profile 8-2B-SR yielded reduced plate stresses as a result of the increased profile stiffness against torsion and M_x. On the other hand, moving the friction bolts to the outer part of the profile, resulted in large moment stresses for the plates in the friction connection. In addition, the lack of stiffness for M_z at the CLT-steel connections, resulted in large stress concentrations around the outer columns of connectors. As a result, it would be recommended increasing the stiffness of the plate in the CLT-steel connections, if a front mounted plate system were to be chosen for the friction dissipating system.

Profile 8-2B-AP fared far better than the other profiles with regards to plate stress and connection utilizations. The resulting critical characteristic connection utilizations were found to be around 0.5 for the CLT-steel and concrete-steel connections. Despite this, it was concluded that further improvements might be required for the concrete-steel connection, as the capacity had been calculated for a relatively tall concrete beam height of 350 mm. The connection was also calculated by hand, disregarding the shear concentration found for the outer anchors in the simulations.

From the simulations, it was concluded that the elastic behavior of the material defined for the model would result in larger stresses in the friction connection than would occur for the real-world elastic-elastic behavior implied by EN 1993-1-8. It was therefore determined that further testing of the friction connections would be required.

For the mounting of profile 8-2B-AP, it was determined that the profile lacked adequate adjustment. As a result, an adjustment mechanism was proposed for the profile in addition to a subjectively more convenient mounting procedure, compared to the original proposal.

From the initial calculations of the base shear force of a four floor RC-building, it was found that the CLT-elements, as tested in this thesis would likely have slip capacity to achieve optimal damping for a structure in less seismic regions, with PGA of around 0.1 g. For higher seismic regions with PGA's of around 0.35 g, it was found that a doubling of friction profiles per CLT-element would likely be required to achieve efficient damping of the structure.

6 Further work

Friction capacity testing:

The theory utilized for the calculations and simulations of the system friction behavior should be studied more closely, as the thesis assumed a friction coefficient of 0.3 for the shear surfaces. In addition, two effective shear surfaces were found from the modeling in this thesis. This needs to be tested, as traditional theory assumes one shear surfaces for single lap joints.

Determination of friction connection capacity:

The elastic behavior for the models of the Ansys® *Academic Research Workbench, Release 19.2* simulations, resulted in inconclusive data for the utilization of the friction connection. The effect of shear and tensile forces, as well as moments must be studied further. This could be done through elastic-perfect plastic modeling and or physical testing of the profile connection.

Estimate elements stiffness:

The stiffness of the resulting bracing effect of the friction dissipating elements were determined to be an important factor for the optimal structure damping as discussed in *4.10 Estimated optimal slip load.* As a result, the stiffness of each friction dissipating element should be estimated.

Estimate the impact of vertical forces on RC beams and columns.

As vertical forces were found to be transferred from the friction elements to the RC beams, the effect on the capacity of these elements during seismic events would have to be determined, as the RC capacity could be a determining factor for the critical slip load of the elements.

Dynamic modeling to determine efficiency of friction damping for structure:

As *4.10 Estimated optimal slip load* only determined an estimate for the optimal friction slip capacity and relative stiffness, a model for a representable structure should be created to study the effect of the proposed friction system. The dampers could be modeled as hysteretic approximations of the friction CLT-elements for each frame. The dynamic modeling could be performed according to EN 1998-1:2004 clause 4.3.3.4.3 Non-linear time-history analysis where artificial accelerograms could be used.

Models should be run for different seismic events, as well as different friction slip loads. This would be interesting, as it would give insight to how the slip load would affect the system damping effect. The effect of distributing the slip load according to shear force of each floor could also be experimented with.

Implementation of system with regards to EN 1998-1:2004:

How to implement the friction system with regards to EN 1998-1:2004 must be determined. Requiring the use of Non-linear time-history analysis would be one possibility, but this would be a comprehensive process to do for a project, and would require high levels of skill for an engineer.

Another possibility would be to determine a set of requirements which would have to be met for a structure, for the system implementation to be possible. Meeting these criteria could potentially allow for the use of a behavior factor which would reduce the shear forces of the seismic loading criteria.

7 List of figures

8 List of tables

9 References

CEN. (2004). *EN 1998-1*. Eurocode 8: Design of structures for earthquake resistance – Part 1: General rules, seismic actions and rules for buildings Brussels.

CEN. (2005). *EN 1993-1-8*. Eurocode 3: Design of steelstructures - Part 1-8: Design of joints. Brussels.

CEN. (2008). *EN 1995-1-1*. Eurocode 5: Design of timber structures - Part 1-1. Brussels.

CEN. (2014). *NS-EN 1998-1_2004/NA:2014 Nasjonalt tillegg NA*.

DIBt. (2012). *ETA-12/0028*. Injection system Hilti HIT-HY 200-R with HIT-Z / HIT-Z-R Berlin.

EOTA. (2007). *TR 029*. Technical Report: Design of Bonded Anchors. Brussels.

EOTA. (2010). *ETAG 001*. GUIDELINE FOR EUROPEAN TECHNICAL APPROVAL OF METAL ANCHORS FOR USE IN CONCRETE. Brussels.

ETA-Danmark. (2019). *ETA-11/0030*. Rotho Blaas Self-tapping screws and threaded rods Kopenhagen.

Hibbeler, R. C. (2013). *Mechanics of Materials*. 9th Edition ed. Singapore: Pearson Education South Asia Pte Ltd.

Hughes, I. a. M. (2011). *DESIGN OF STEEL BEAMS IN TORSION*. Berkshire: Steel Construction Institute.

Husson, W. V., M. (2008). *BEHAVIOUR OF A FRICTION CONNECTION USING TCB IN LONG SLOTTED HOLES* Sweeden: Luleå University of Technology.

L. Chiaraluce, R. D. S., E. Tinti, L. Scognamiglio, M. Michele, E. Casarotti, M. Cattaneo, P. De Gori, C. Chiarabba, G. Monachesi, A. Lombardi, L. Valoroso, D. Latorre, S. Marzorati. (2017). The 2016 Central Italy Seismic Sequence: A First Look at the Mainshocks, Aftershocks, and Source Models. *Seismological Research Letters*, 88.

MechaniCalc. *Bolt Pattern Force Distribution*. Available at: https://mechanicalc.com/reference/bolt-pattern-force-distribution.

NSC. (2005). *AD 286: Preloaded Bolts: The Net Effect of Applied Tension and Preload*: newsteelconstruction Available at: https://www.newsteelconstruction.com/wp/ad-286-preloaded-bolts-the-net-effect-of-applied-tension-and-preload/ (accessed: 29.05.2020).

P. Larsen , A. C., A. Aalberg. (2014). *Stålkonstruksjoner: Profiler of Formler*. 3 ed., vol. 2. Bergen: Fagbokforlaget.

Ruiqiang, S., Yue, L., & John, W.L (2014). *Impact of earthquake ground motion characteristics on collapse risk of post-mainshock buildings considering aftershocks*. In Gould, P. L. (ed.). Engineering Structures.

Sang-Hyun Lee, J.-H. P., Sung-Kyung Lee, Kyung-Won Min. (2008). Allocation and slip load of friction dampers for a seismically excited building structure based on storey shear force distribution. *ENGINEERING STRUCTURES*, 30 (4): 930-940.

Sawada, S. (2004). *A SIMPLIFIED EQUATION TO APPROXIMATE NATURAL PERIOD OF LAYERED GROUND ON THE ELASTIC BEDROCK FOR SEISMIC DESIGN OF STRUCTURES*. Vancouver: 13th World Conference on Earthquake Engineering

Shabana, A. (2019). *Theory of Vibration: An introduction. Third Edition*. Cham: Springer International Publishing.

Sørensen, S. (2013). *Betong Konstruksjoner*. 2 ed., vol. 3. Bergen: Fagbokforlaget.

Stibor, M. (2014). *Simple St. Venant and non uniform torsion with warping*: Paragon International University. Available at: https://structural-analyser.com/domains/SteelDesign/Torsion/.

Tipler, P. (2008). *Physics for Scientists and Engineers*. 6th ed., vol. Tenth volume. New York: W. H. Freeman and Company.

USGS. (2016). *M 6.6 - 7km N of Norcia, Italy*: U.S. Geological Survey. Available at: https://earthquake.usgs.gov/earthquakes/eventpage/us1000731j/executive.

VDC. (1999). *Izmit-Kocaeli 1999-08-17 00:01:40 UTC*. Strong-motion Viritual Data Center.

Woessner, J., Danciu L., D. Giardini and the SHARE consortium. (2015). *The 2013 European Seismix Hazard Model: key components and results*. Available at: http://www.efehr.org/en/Documentation/specific-hazard-models/europe/overview/ (accessed: 04.02.2020).

APPENDIX A:

Profile dimensions

8-2B BOTTOM PROFILE

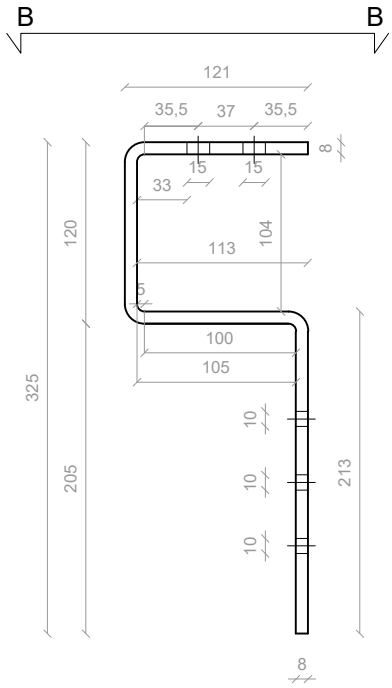

Lateral view

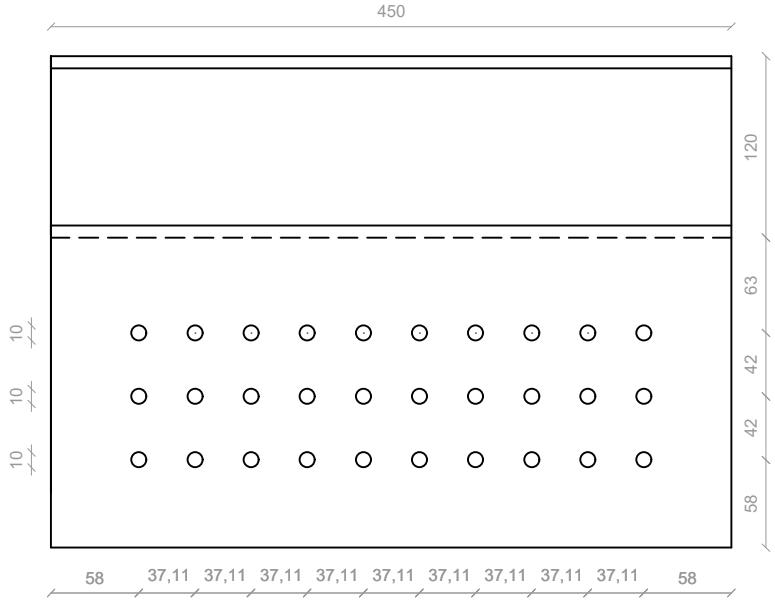

Front view

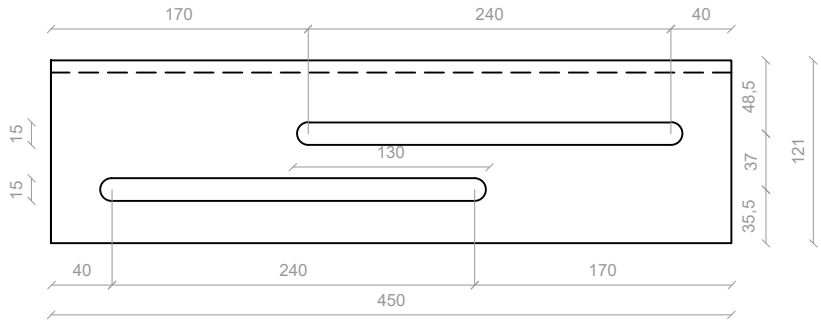

View B-B

8-2B UPPER PROFILE

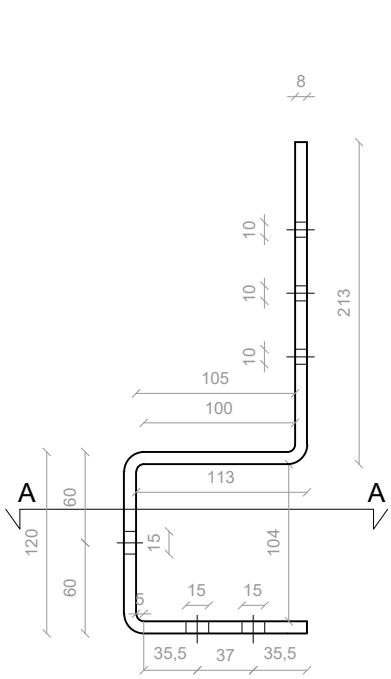

Lateral view

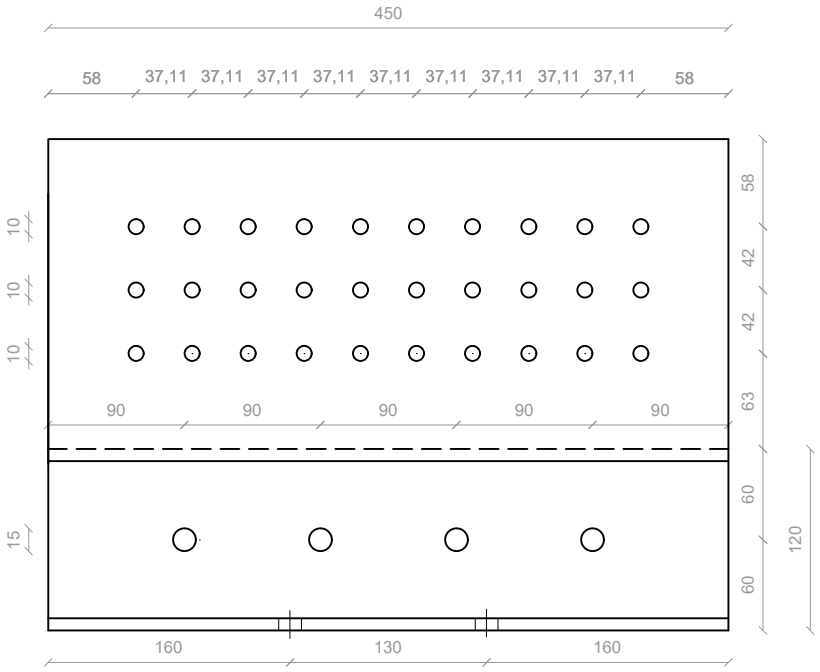

Front view

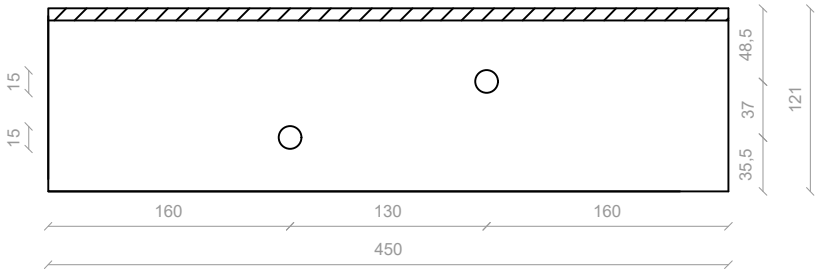

Section A-A

8-2B-R BOTTOM PROFILE

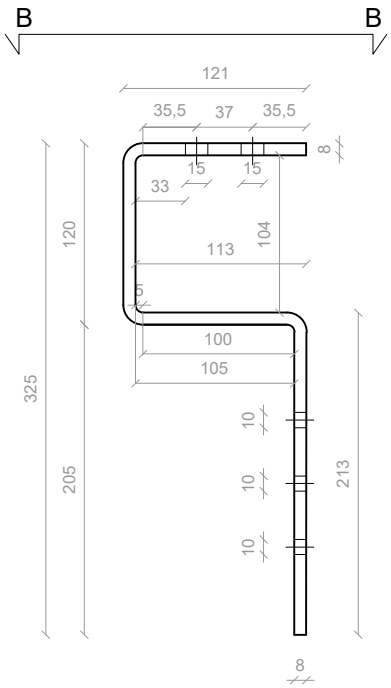

Lateral view

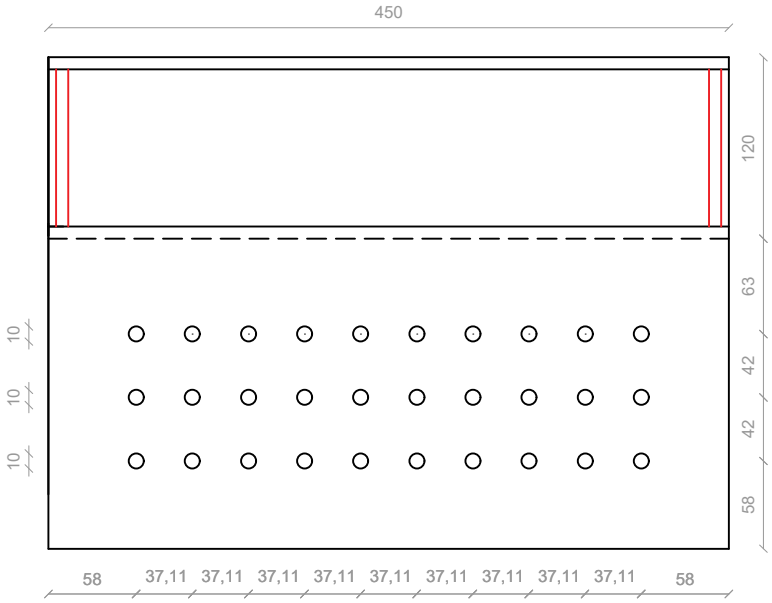

Front view

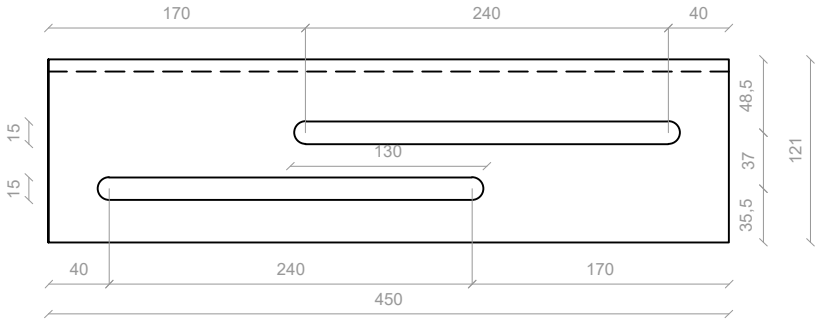

View B-B

PRODUCED BY AN AUTODESK STUDENT VERSION

PRODUCED BY AN AUTODESK STUDENT VERSION

8-2B-R UPPER PROFILE

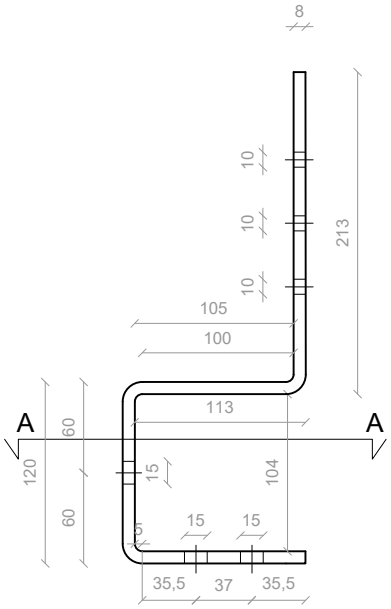

Lateral view

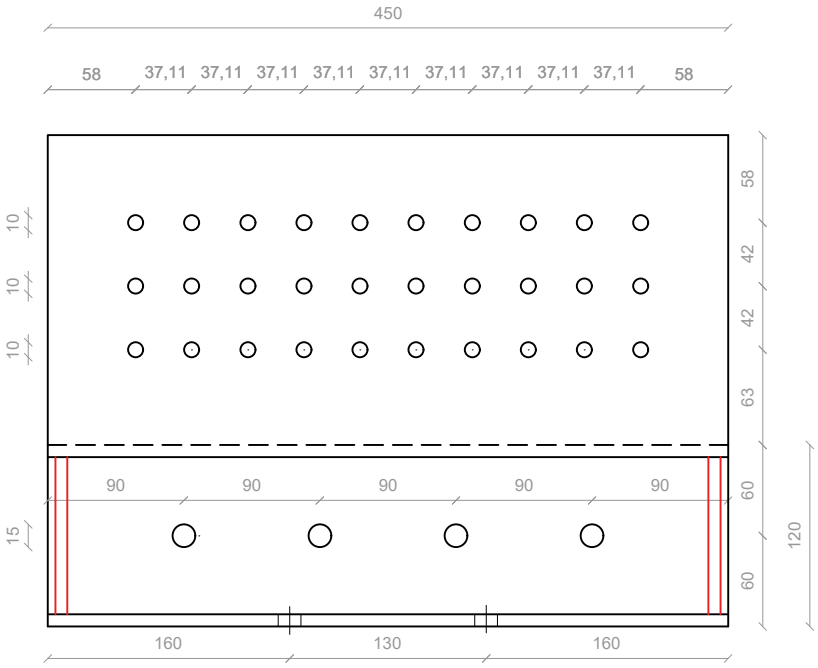

Front view

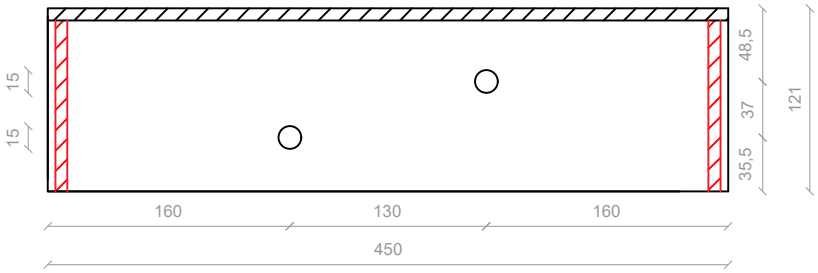

Section A-A

PRODUCED BY AN AUTODESK STUDENT VERSION

PRODUCED BY AN AUTODESK STUDENT VERSION

8-2B-DP BOTTOM PROFILE

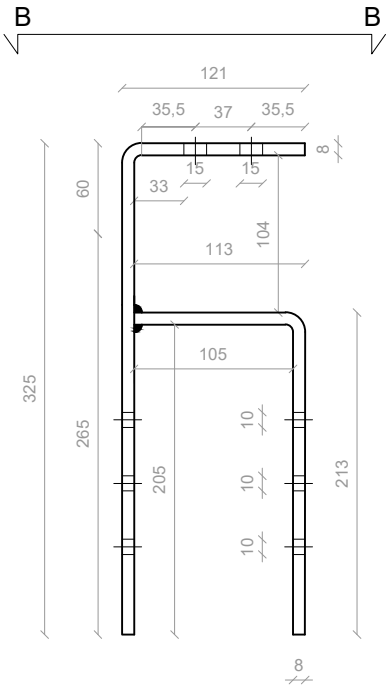

Lateral view

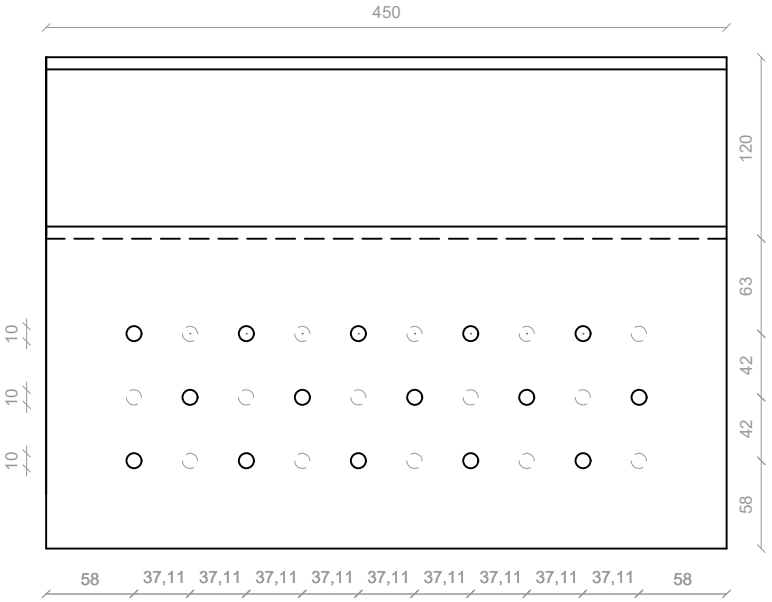

Front view

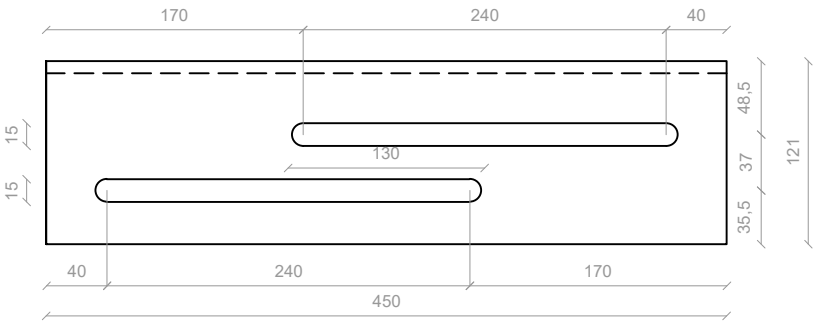

View B-B

8-2B-DP UPPER PROFILE

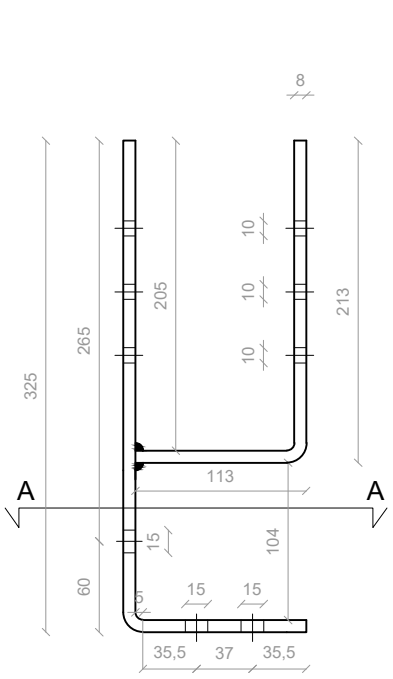

Lateral view

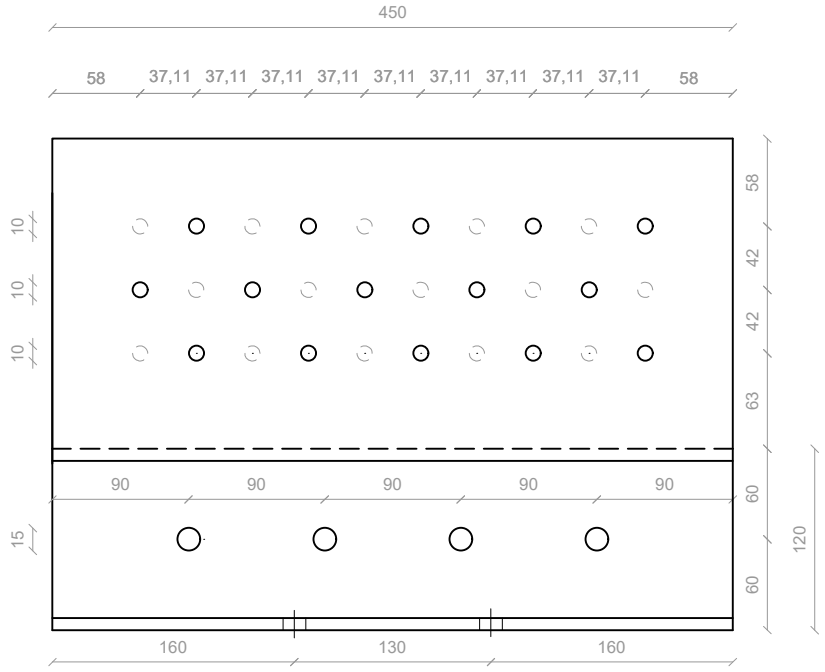

Front view

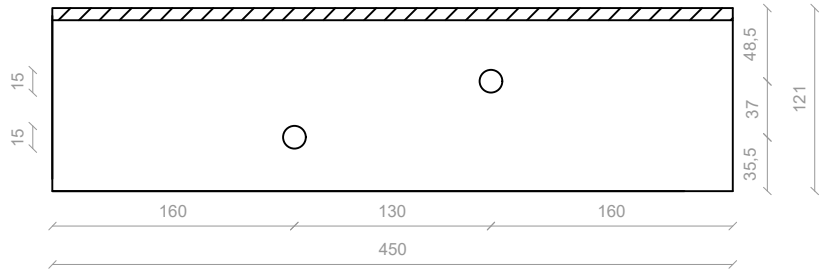

Section A-A

8-2B-AP BOTTOM PROFILE

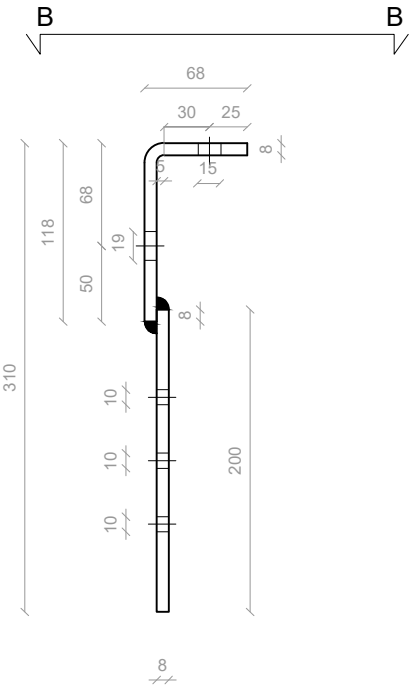

Lateral view

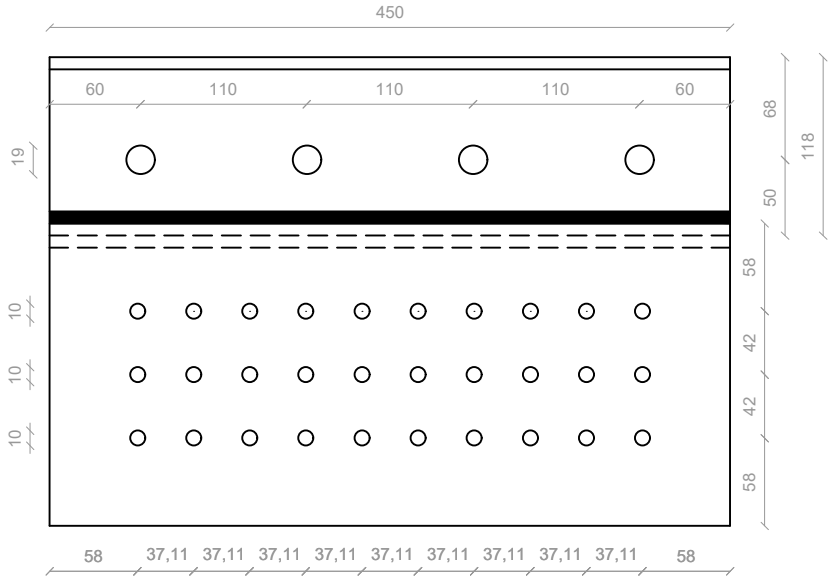

Front view

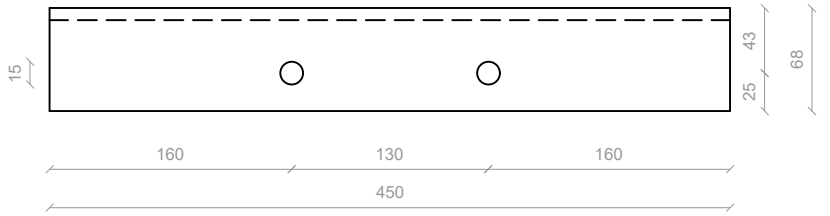

View B-B

8-2B-AP UPPER PROFILE

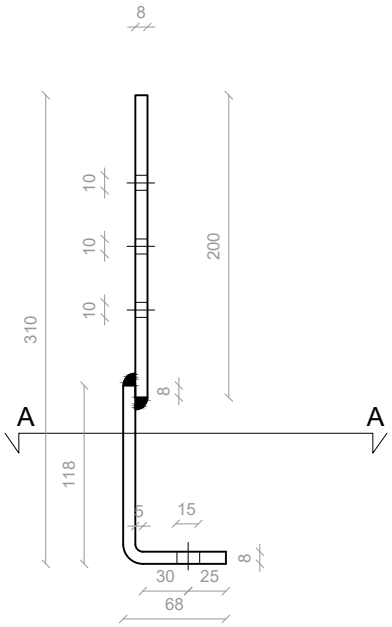

Lateral view

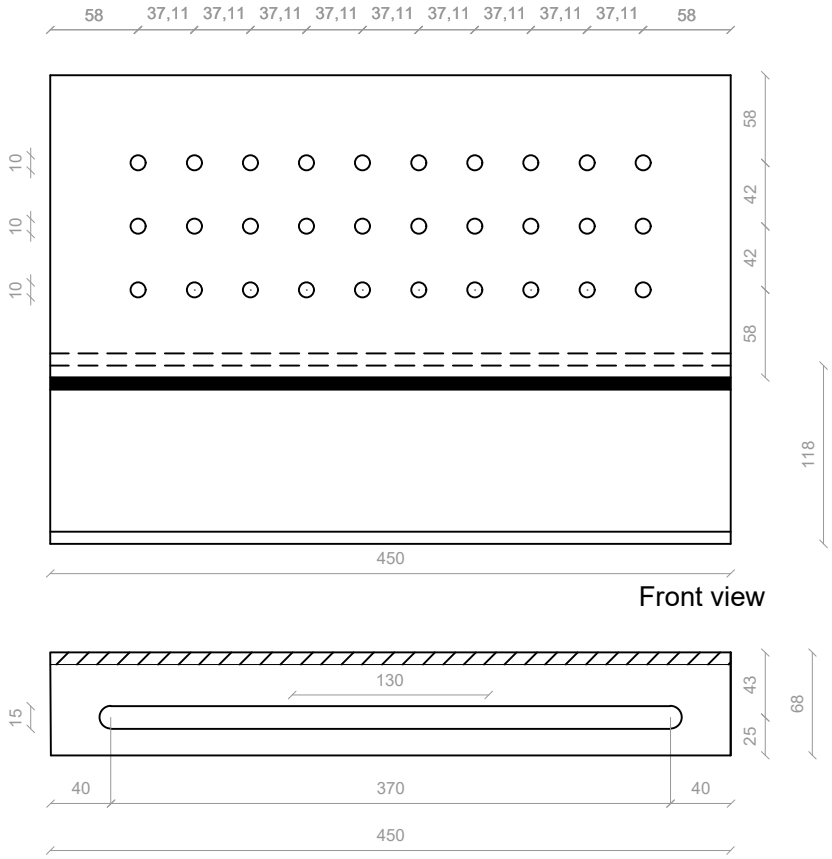

Front view

Section A-A

8-2B-SR BOTTOM PROFILE

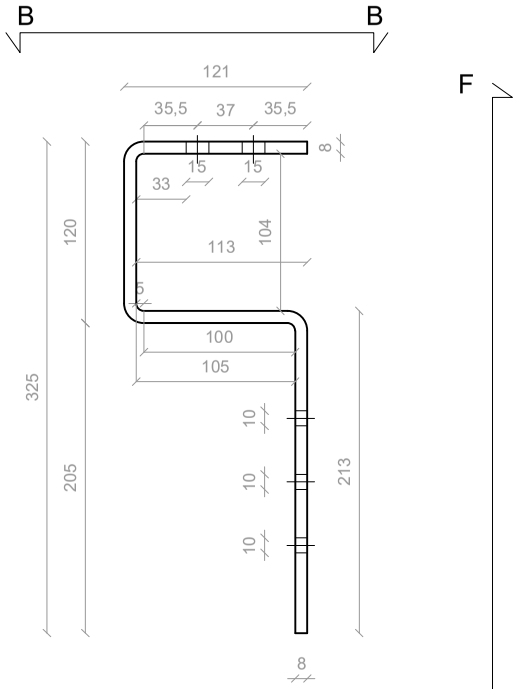

Lateral view G-G

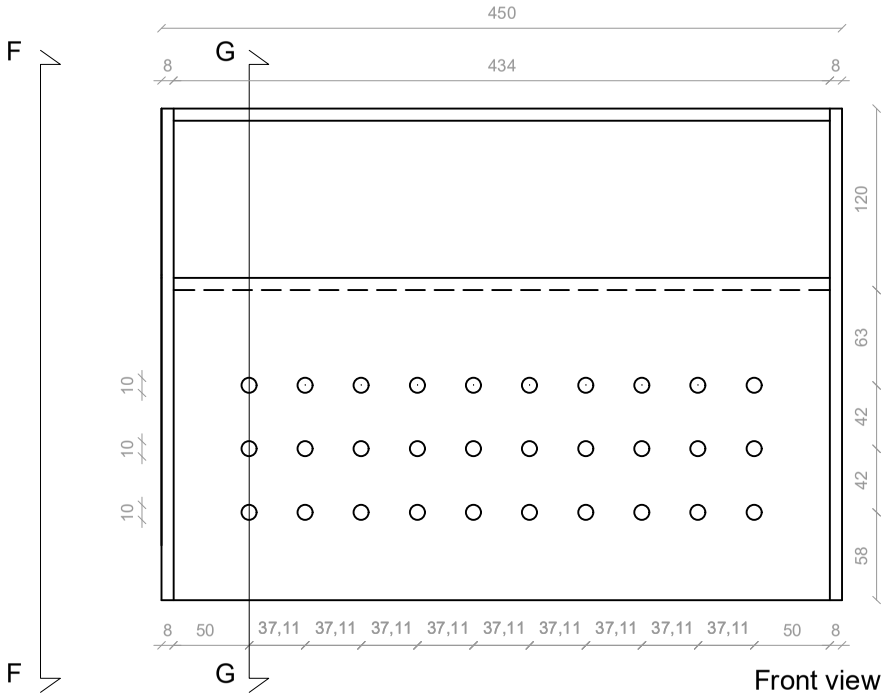

Front view

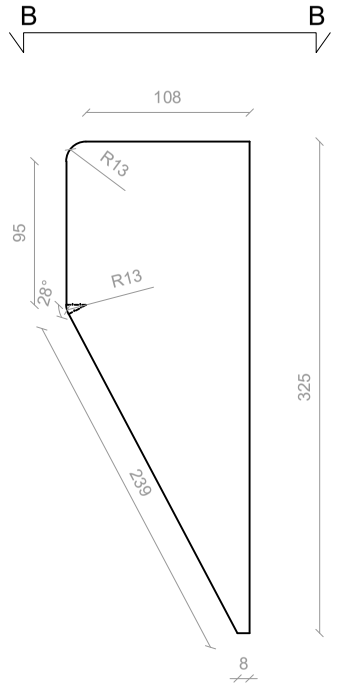

Lateral view F-F

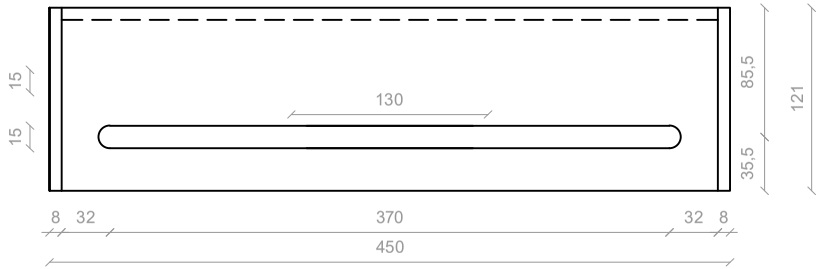

View B-B

PRODUCED BY AN AUTODESK STUDENT VERSION

PRODUCED BY AN AUTODESK STUDENT VERSION

8-2B-SR UPPER PROFILE

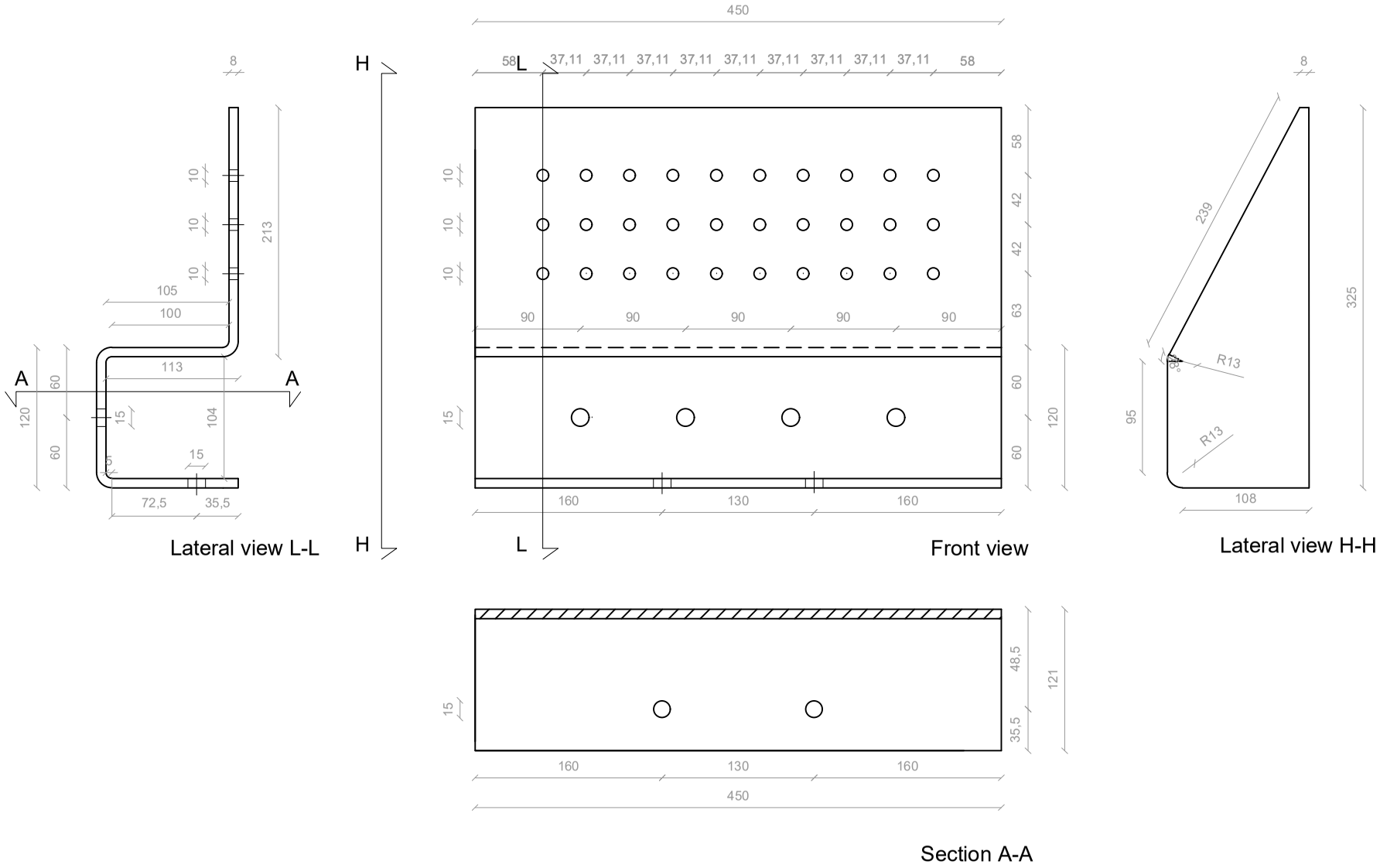

APPENDIX B:

Design capacity of friction connector

Friction bolts calculated according to design cirteria of EN 1993-1-8:2005 table 3.4.

$f_{ub} := 1000 \frac{N}{mm^2}$ "Ultimate strength of bolt"

$d_m := 28\ mm$ "Average head diameter"

$d_b := 14\ mm$ "Bolt diameter"

$n_C := 1$ "Number of friction bolts"

$A_s := 115\ mm^2$ "Hinged bolt area"

$t_p := 8\ mm$ "Plate thickness"

$d_0 := 15\ mm$ "Hole diameter"

$f_u := 360 \frac{N}{mm^2}$ "ultimate steel strength"

$f_y := 235 \frac{N}{mm^2}$ "Steel yield strength"

$\mu_f := 0.5$ "Slip factor for Class A, according to Tabel 3.7"

Design shear capactiy normal hole for shear test:

$e_{2.s} := 40\ mm$ "Edge distance shear test"

$k_s := 1$ "No reduction for normal holes"

$\gamma := 1.25$ "Equal for al factors used in calculations"

$F_{p.C} := 0.7 \cdot f_{ub} \cdot A_s = 80500\ N$ "Design pretensio according to clause 3.6.1(2)"

$F_{s.Rd} := \frac{k_s \cdot n_C \cdot \mu_f \cdot F_{p.C}}{\gamma} = 32200\ N$ "Design friction capacity is critical conneciton capacity"

For the connection, EN 1993-1-8:2005 3.4.1(c) and 3.4.2(b) are used in combination to determine the nesecary capacity controls. For the calculations of the indevidula fasteners EN 1993-1-8:2005 table 3.4 has been used with exeption for Fbrk where EN 1993-1-8:2005 stated that a one faced connection with a single row of bolts should be calculated acording to 3.6.1(10).

$F_{b.Rd} := \frac{1.5 \cdot f_u \cdot d_b \cdot t_p}{\gamma}$ "Characteristiv bearing resistance per hole for a single section connection with one screw row."

$F_{b.Rd} = 48.38\ kN$

Plate capacity is calculated according to EN 1993-1-1 clause 6.2.3 with estimated design plastic resistance and ultimate resistance calculated according to EN 1993-1-8 equation (3.11).

$N_{u.Rd} := \frac{2 \cdot \left(e_{2.s} - 0.5 \cdot d_0\right) \cdot t_p \cdot f_u}{\gamma} = 149.76\ kN$ "Equation (3.11) from EN 1993-1-8 for L-bracket"

$N_{pl.Rd} := \frac{2 \cdot e_{2.s} \cdot t_p \cdot f_y}{\gamma} = 120.32\ kN$ "Estimated design plastic resistance from area of bottom plate"

Characteristic connector capactiy for elongated hole of profile 8-2B-AP.

$e_1 := 40\ mm$

"smalest edge distance of 8-2B-AP"

$e_2 := 35.5\ mm$

$p_1 := 130\ mm$

"Approximated for bolt distance in same hole, even though EN 1993-1-8 specify hole distance"

$$\alpha_d := \text{Min}\left(\begin{bmatrix} \frac{e_1}{3 \cdot d_0} \\ \frac{p_1}{3 \cdot d_0} - \frac{1}{4} \\ 1 \end{bmatrix}\right) = 0.89$$

$$k_{1.el} := \text{Min}\left(\begin{bmatrix} 2.8 \cdot \frac{e_2}{d_0} - 1.7 \\ 2.5 \end{bmatrix}\right) = 2.5$$

The eurocode does not specify wether Clause 3.6.1(10) refering to figure 3.3 counts for all single section connections with a singular row of connectors, or only single row connections perpendicular to load dirrection. If not, Table 3.4 gives a higher connection capacity. For this thesis, the best case is assumed:

$$F_{b.Rd} := \frac{0.6 \cdot \alpha_d \cdot k_{1.el} \cdot f_u \cdot t_p \cdot d_b}{\gamma} = 43.01\ kN$$

"Tabel 3.4 calculation"

$$F_{b.Rd2} := \frac{0.6 \cdot 1.5 \cdot f_u \cdot d_b \cdot t_p}{\gamma} = 29.03\ kN$$

"Clause 3.6.1(10) for a single cut connection consisting of one row of screws. Becomes critical capacity"

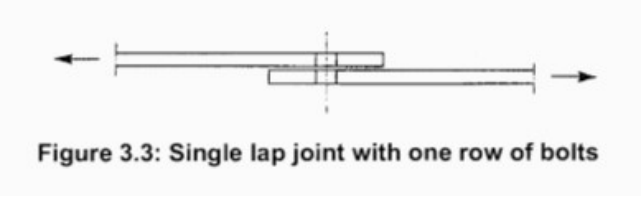

Figure 3.3: Single lap joint with one row of bolts

Can not find a reduciton factor for elongated holes, but should not really be a problem, as the punching strength would need to be reduced by more than 80% to pose a problem for the combined load of the two pretension bolts of profile 8-2B-AP.

$B_{p.Rk} := 0.6 \cdot \pi \cdot d_m \cdot t_p \cdot f_u$

"Ultimate characteristic punching strength"

$B_{p.Rk} = 152\ kN$

For a combined shear tension load situation, the two should be combined using the criteria of Table 3.4, but the combined loading of around 10 kN tensile force and shear of 15 kN would not come close to surpacing the criteria.

$\alpha_v := 0.5$

$F_{v.Rk} := \alpha_v \cdot f_{ub} \cdot A_s$

"Characteristic shear strength of bolt"

$F_{v.Rk} = 57.5\ kN$

$k_2 := 0.9$

$F_{t.Rk} := k_2 \cdot f_{ub} \cdot A_s$

"Characteristic tensile screw capactiy"

$F_{t.Rk} = 103.5\ kN$

APPENDIX C:

Profile hand calculations

Profile 8-2B: Clt to steel connection capacity, consisting of 30 Rothoblaas HBS Plate 8x80 screws

$g := 9.81 \frac{N}{kg}$

Dimensions and material characteristics:

Concrete-steel connection with C20/25 and M12 Anchors:

$d_{x.anchor} := 90\ mm$ "Horizontal screw distance as well as edge distance"

$e_{x.anchor} := 90\ mm$ "Steel edge distance of anchors"

$d_{z.anchor} := 60\ mm$ "Edge distance for concrete steel contact"

$n_{Bx} := 4$ "Number of horizontal anchors in support B"

$d_{anchor} := 12\ mm$ "Anchor diameter"

$f_{ck.cube} := 25 \frac{N}{mm^2}$ "Cubed compressive strength"

$E_{cm} := 29962 \frac{N}{mm^2}$ "C20/25 elastic modulus"

$E_s := 200000 \frac{N}{mm^2}$ "Elastic modulus of anchors"

$d_{anchor} = 0.012\ m$ "M12 anchor diameter"

CLT panel

$H_{CLT} := 3\ m$ "Height of CLT panel"

$B_{CLT} := 4\ m$ "Width of CLT panel"

$t_{CLT} := 0.1\ m$ "CLT thickness"

$\rho_{CLT} := 385 \frac{kg}{m^3}$ "CLT density"

$\rho_k := 385 \frac{N}{mm^2}$ $\boxed{\frac{kg}{m^3}}$ "Empirical units resulting from formula used later"

$f_{c.90.k} := 2.5 \frac{N}{mm^2}$ "CLT compression strength perpendicular to wood grain"

$m_{CLT} := H_{CLT} \cdot B_{CLT} \cdot t_{CLT} \cdot \rho_{CLT} = 462\ kg$ "CLT Element weight"

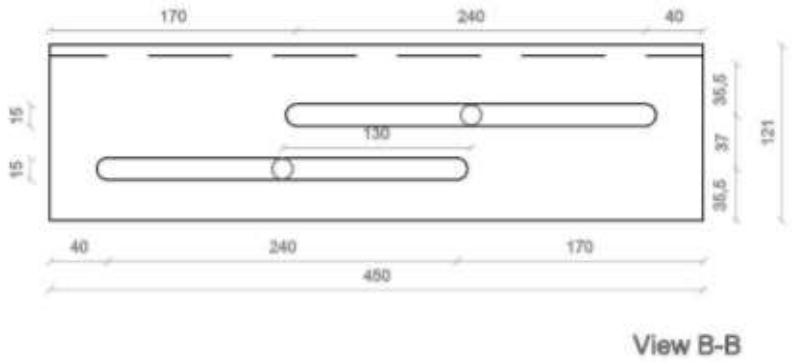

View B-B

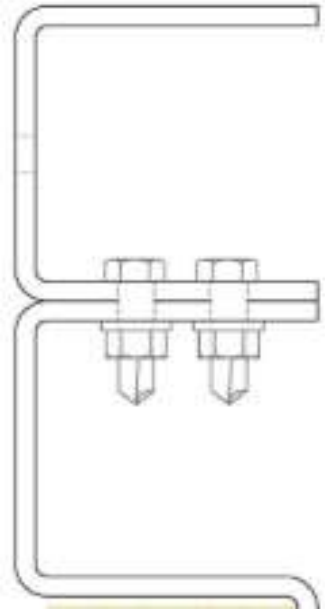

Profile and support D:

$e_1 := 58.00\ mm$ "horizontal edge distance end screw"

$e_2 := 58.00\ mm$ "Vertical edge distance of end screws"

$p_1 := 37.11\ mm$ "Internal horizontal screw distance"

$p_2 := 42.00\ mm$ "Internal vertical screw distance"

$H := 200\ mm$ "Vertical contact of underlying CLT"

$B := 450\ mm$ "Horizontal contact of underlying CLT"

$t_p := 8\ mm$ "Plate thickness"

$n_{xD} := 10$ "Number of screws per row"

$n_{zD} := 3$ "Number of screws per column"

$n_D := n_{xD} \cdot n_{zD}$ "Total number of screws"

$f_u := 235\ \frac{N}{mm^2}$ "Plate yield capacity"

$m_{8\_2B} := 11\ kg$ "Profile mass"

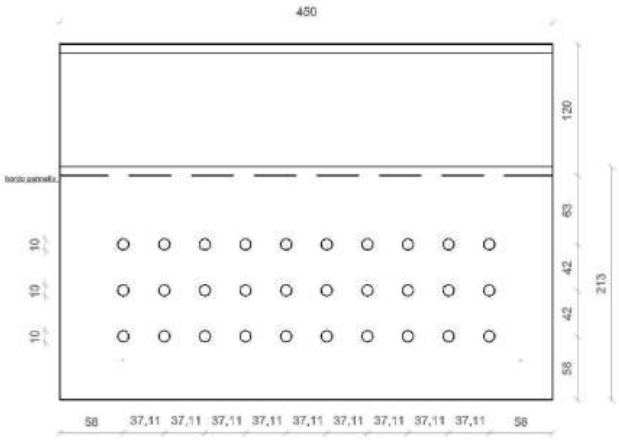

Front view

Concrete:

$f_{ck.cube} = 25\ \frac{N}{mm^2}$ "characteristic cubed strength"

HBS plate dimensions and static values:

"The values of the screws were retrived from the Rothoblaas catalog. Wil refere to the source in final paper."

$d_1 := 8\ mm$

$d_k := 14.5\ mm$

$d_2 := 5.4\ mm$

$d_s := 58\ mm$

$t_1 := 3.4\ mm$

$d_{uk} := 10\ mm$

$d_v := 5.0\ mm$

$L := 80\ mm$

$b := 55\ mm$

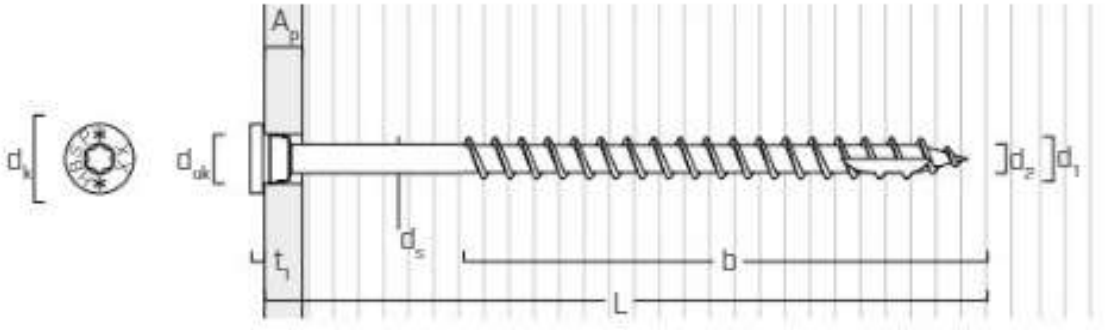

$n := 30$ "Number of screws"

$M_{y.k} := 20057\ N\ mm$ "Charicaristic yield moment"

$f_{ax.k} := 11.7\ \frac{N}{mm^2}$ "Charicaristic withdrawal resistance"

$\rho_a := 350\ \frac{N}{mm^2}$ "referance density for withdrawal resistance"

$f_{head} := 10.5\ \frac{N}{mm^2}$ "Characteristic head-pull through resistance"

$f_{tens.k} := 20.1\ kN$ "Characteristic tensile strenght"

$\alpha := 90\ deg$ "Angel of screws according to the grain"

$k_{ax} := 1$ "factor for angle 90 deg"

$K_\beta := 1$ "Factor for timber"

Friction bolts

$\mu_p := 0.3$ "Friction between plate and bolt"

$n_C := 2$ "Number of friction bolts"

$n_{fb} := 2$ "Number of friction surfaces per bolt"

Distances between supports and support criteria:

"All the distances to the centers of the connections were calculated according to the opper middle edge of conncetion D"

Reactions	Supports			
	A	B	C	D
Δx	Free	Free	Free	Fixed
Δy	Free	Fixed	Free	Free
Δz	Free	Fixed	Free	Free
ϕx	Fixed	Fixed	Free	Fixed
ϕy	Free	Fixed	Fixed	Fixed
ϕz	Free	Fixed	Free	Fixed

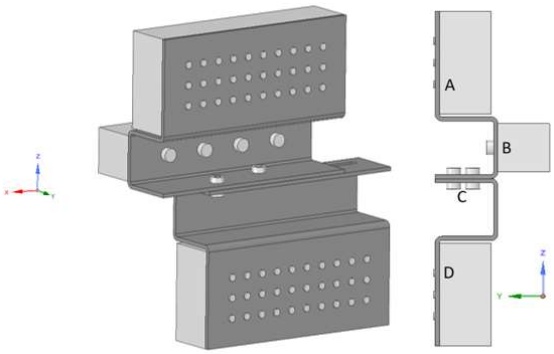

"Global distances between supports for tension profile"

$d_{yAB} := -0.121\ m$

$d_{zAB} := (-0.063 - 0.06)\ m$

$d_{yBC} := 0.067\ m$ "midd point between bolts"

$d_{zBC} := (-0.06)\ m$

$d_{xCD} := (-0.12)\ m$

$d_{yCD} := -d_{yBC} - d_{yAB} = 0.054\ m$

$d_{zCD} := (-0.184)\ m$

$d_{xBD} := d_{xCD}$

$d_{yBD} := -d_{yAB} = 0.121\ m$

$d_{zBD} := d_{zBC} + d_{zCD} = -0.244\ m$

"Ajusted distances with regards to the behaviour of support C for compressed profile"

$d_{yBC.c} := \left(d_{yBC}\right) = 67\ mm$ "Center of compression force acting on fricition connectort"

$d_{yCD.c} := d_{yCD} = 54\ mm$

$d_{xBC.c} := \frac{d_{zBC}}{\left(d_{zAB} + d_{zBC}\right)} \cdot d_{xBD} = -39.3443\ mm$ "Interpolated distaces for horizontal load center based on interpolated relative distance between support B and D"

$d_{xCD.c} := d_{xBD} - d_{xBC.c} = -80.6557\ mm$

$d_{yBC.cv} := \left(\frac{1}{3} \cdot d_{yBD}\right) = 40.3333\ mm$ "Vertical load center for support C approximated from Ansys"

$d_{yCD.cv} := -d_{yAB} - d_{yBC.cv} = 80.6667\ mm$

Formulas created for matrix calculations:

$Height_i(floors, floor\_height) :=$

```
Hp := matrix(1, floors)
for i ∈ [1..floors]
    Hp_{1,i} := floor_height · i
Hp
```

"Creates vector of evenly distributed floor heights (Ignoring ground floor)"

```
Prtoduct_ij(A, B) := | r := rows(A)
                     | c := cols(A)
                     | Hp := matrix(r, c)
                     | for i ∈ [1..r]
                     |   for j ∈ [1..c]
                     |     Hp_ij := (A_ij · B_ij)
                     | Hp
```

"Calculates the product of the matrix values A.ij and B.ij"

```
Division_ij(A, B) := | r := rows(A)
                     | c := cols(A)
                     | Hp := matrix(r, c)
                     | for i ∈ [1..r]
                     |   for j ∈ [1..c]
                     |     Hp_ij := A_ij / B_ij
                     | Hp
```

"Calculates the division of A.ij and B.ij"

```
SRSS_ij(A, B) := | r := rows(A)
                 | c := cols(A)
                 | Hp := matrix(r, c)
                 | for i ∈ [1..r]
                 |   for j ∈ [1..c]
                 |     Hp_ij := (√((A_ij)^2 + (B_ij)^2))
                 | Hp
```

"Sqare root of the sum of squares of individual values A.ij and B.ij"

```
Matrix_remove_negative_ij(A) := | r := rows(A)
                                | c := cols(A)
                                | Hp := matrix(r, c)
                                | for i ∈ [1..r]
                                |   for j ∈ [1..c]
                                |     if A_ij < 0
                                |       Hp_ij := 0
                                |     else
                                |       Hp_ij := A_ij
                                | Hp
```

"Removes negative values of a matrix"

```
Matrix_remove_positive_ij(A) := | r := rows(A)
                                | c := cols(A)
                                | Hp := matrix(r, c)
                                | for i ∈ [1..r]
                                |   for j ∈ [1..c]
                                |     if A_ij > 0
                                |       Hp_ij := 0
                                |     else
                                |       Hp_ij := A_ij
                                | Hp
```

"Removes positive values of a matrix"

External forces acting on system:

Forces acting on compression profile:

Following 2.2 External force application of profiles, an itnitial critical horizontal force is assumed:

$P_x := 30000\ \mathrm{N}$ "Total external horizontal force acting on compression profile"

For n.floors it is assumed that the mass distribution an floor height is constant equal to height of CLT element:

$n_{floors} := 4$ "Number of floors in building"

$z := Height_i\left(n_{floors}, H_{CLT}\right) = [\,3\ \ 6\ \ 9\ \ 12\,]\ \mathrm{m}$ "Floor height"

$P_{xB} := P_x \cdot \frac{z}{\sum_z 1} = 3000\ \mathrm{N}$ "Horizontal force in support B for profile in tension"

$P_{xA} := P_x - P_{xB} = 27000\ \mathrm{N}$ "Horizontal force in support A for compressed profile"

The average total force acting on the two profiles and on support A of the two profiles are approximated:

$\lambda := 0.608$ "Reduction factor for maximum vertical load in tension profile"

$P_{x.avg} := \frac{(1+\lambda)\cdot P_x}{2} = 24120\ \mathrm{N}$ "Total force on two profiles"

$P_{xA.avg} := \frac{(1+\lambda)\cdot P_{xA}}{2} = 21708\ \mathrm{N}$ "Total vertical force in connection A of the profiles"

Force from weight of a complete CLT element with four profile halfs:

$P_{element} := (-g)\cdot\left(m_{CLT} + m_{8\_2B}\cdot 4\right) = -4964\ \mathrm{N}$ "Equivalent system weight per profile"

Equivalent vertical force on tension and compression profiles:

$P_{zD} := P_{x.avg}\cdot\left(\frac{H_{CLT}}{B_{CLT}-B}\right) + \frac{P_{element}}{4} = 19142\ \mathrm{N}$ "Vertical force in compression support D accounting for system weight"

$P_{zD.t} := \left(-P_{x.avg}\right)\cdot\left(\frac{H_{CLT}}{B_{CLT}-B}\right) + \frac{P_{element}}{4} = -21624\ \mathrm{N}$ "Vertical force in tension support D"

$P_{xd} := P_x \cdot \frac{z}{\sum_z z} = \left[\,3000\ \frac{\mathrm{kg\ m}}{\mathrm{s}^2}\ \ 6000\ \frac{\mathrm{kg\ m}}{\mathrm{s}^2}\ \ 9000\ \frac{\mathrm{kg\ m}}{\mathrm{s}^2}\ \ 12000\ \frac{\mathrm{kg\ m}}{\mathrm{s}^2}\,\right]$

$P_{tot} := (1+\lambda)\cdot\left(P_{xd_4} + \left(P_{xd_4} + P_{xd_3}\right) + \left(P_{xd_4} + P_{xd_3} + P_{xd_2}\right) + \left(P_{xd_4} + P_{xd_3} + P_{xd_2} + P_{xd_1}\right)\right)$

$P_{tot} = 144.72\ \mathrm{kN}$

The vertical force of the system above is then approximated from P.xA.avg:

$$P_{zA} := P_{xA.avg} \cdot \left(\frac{H_{CLT}}{B_{CLT} - B} \right) + \frac{P_{element}}{4} = 17104 \text{ N}$$ "Vertical force in compression support A"

$$P_{zA.t} := \left(- P_{xA.avg} \right) \cdot \left(\frac{H_{CLT}}{B_{CLT} - B} \right) + \frac{P_{element}}{4} = -19586 \text{ N}$$ "Vertical force in tension support A"

Pretension of friction connection:

The pretension requrires for the compressed profile is calculated for the two bolts:

$k_s := 0.93$ "EC3 table 3.6 is to conservative"

$$F_{p.C.compression} := \frac{P_x - \left| P_{zD} \right| \cdot \mu_p}{\left(k_s \cdot n_{fb} \cdot n_C \cdot \mu_p \right)}$$

$F_{p.C.compression} = 21.736 \text{ kN}$ "Maximum pretension"

The friction force resulting from the bolt pretension is calculated for the tension connection:

$$F_{s.Rk.tension} := k_s \cdot \mu_p \cdot n_{fb} \cdot \left(n_C \cdot F_{p.C.compression} - \left| \frac{P_{zD.t}}{n_{fb}} \right| \right) = 18224.2462 \text{ N}$$

$F_{s.Rk.tension} = 18.2242 \text{ kN}$ "Resulting friction capactiy for profile in tension"

The total friction force of the system is calculated as the sum of the forur friction bolts:

$$F_{s.Rk.tot} := F_{s.Rk.tension} + P_x$$

$F_{s.Rk.tot} = 48.2242 \text{ kN}$ = $2 \cdot P_{x.avg} = 48.24 \text{ kN}$

Finally λ is adjusted until the average vertical force equals the friction force.

The horizontal force distribution for the tension profile is approximated:

$P_{xA.t} := \left(- P_{xA} \right) \cdot \lambda = -16416 \text{ N}$ "Horizontal force in support A for compressed profile"

$P_{xB.t} := \left(- P_{xB} \right) \cdot \lambda = -1824 \text{ N}$ "Horizontal force in support B for profile in tension"

$P_{x.t} := P_{xA.t} + P_{xB.t} = -18240 \text{ N}$ "Roughly equivalent to tension friction force"

Steel - CLT connection

For these calculations the Steel - CLT connection in support A and D was considered to be identical. Because of the increased horizontal and vertical forces acting on support D as well as the greater height differenc between support B and D compared to A-B, the critical steel - CLT connection was determined to be support D:

Minimum internal and edge distances of screws:

The minimum distances for screws were calculated in accordance with "ETA -11/0030" annex B:

Minimum distances:

$a_1 := 4 \cdot d_1$

$a_1 = 32\ \text{mm}$

$a_2 := 2.5 \cdot d_1$

$a_2 = 0.02\ \text{m}$

$a_{3.t} := 6 \cdot d_1$

$a_{3.t} = 48\ \text{mm}$

$a_{3.c} := 6 \cdot d_1$

$a_{3.c} = 48\ \text{mm}$

$a_{4.t} := 6 \cdot d_1$

$a_{4.t} = 48\ \text{mm}$

$a_{4.c} := 2.5 \cdot d_1$

$a_{4.c} = 20\ \text{mm}$

Connection distances:

$a_{1.c} := p_1$

$a_{1.c} = 37.11\ \text{mm}$

$a_{2.c} := p_2$

$a_{2.c} = 42\ \text{mm}$

$a_{3.t.c} := e_1$

$a_{3.t.c} = 58\ \text{mm}$

$a_{3.c.c} := e_1$

$a_{3.c.c} = 58\ \text{mm}$

$a_{4.t.c} := e_2$

$a_{4.t.c} = 58\ \text{mm}$

$a_{4.c.c} := e_2$

$a_{4.c.c} = 58\ \text{mm}$

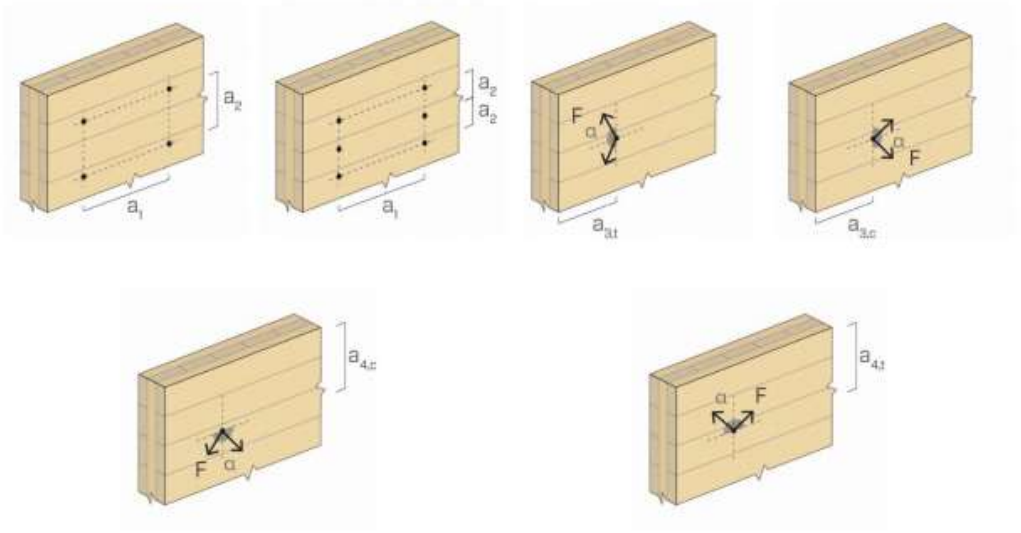

Al the minnimum distances were calculated to be well below the minimum distances of the plates.

Characteristic Rothoblaas HBS Plate 8x80 screw capacity

Characteristic tensile resistance:

"The tensile resistance was calculated in acordance with "ETA-11/0030" for axialy loades screws following the technical assesments equations and reference to EN 1995-1-1:2008:

$n_{ef} := n^{0.9} = 21.3506$ "Efficient number of tensile screws"

$F_{ax.Rk} := n_{ef} \cdot f_{ax.k} \cdot d_1 \cdot b \cdot \left(\frac{\rho_k}{\rho_a}\right)^{0.8}$ "Axial withdrawal capacity for system"

$F_{ax.Rk} = 118.6211\ \text{kN}$

$F_{ax.Rk.screw} := \frac{F_{ax.Rk}}{30} = 3.954\ \text{kN}$ "Axial withdrawal capacity per bolt"

Characteristic shear resistance:

"The shear resistance was calculated in accordance with "ETA-11/0030" which complyies with EN 1995-1-1:2008. Outer threaded diameter d.1 was used as effective diameter and non-predrilled holes were considered. The embeding strength was determined using the following "ETA-11/0030" equation:"

$d := 8$ Is used as d.1 for the empirical formula

$$f_{h.k} := \frac{\left(0.082 \cdot \rho_k \cdot \left(1 - 0.01 \cdot d\right)\right)}{2.5 \cdot \left(\cos(\alpha)\right)^2 + \left(\sin(\alpha)\right)^2}$$

$f_{h.k} = 29.0444\ \frac{\text{N}}{\text{mm}^2}$ "Characteristic predrill embedment strength"

"For the connection the plate thickness equaled the effective diameter, which resulted in the use of EN 1995-1-1:2008 eq. (8.10) for a single section thick steel plate:"

$$F_{vD.Rk} := \min\left(\left[\begin{array}{c} f_{h.k} \cdot L \cdot d_1 \cdot \left(\sqrt{2 + \frac{4 \cdot M_{y.k}}{f_{h.k} \cdot d_1 \cdot t_1^2}} - 1\right) + \frac{F_{ax.Rk.screw}}{4} \\ 2.3 \cdot \sqrt{M_{y.k} \cdot f_{h.k} \cdot d_1} + \frac{F_{ax.Rk.screw}}{4} \end{array}\right]\right)$$

$F_{vD.Rk} = 5.9537\ \text{kN}$ "Characteristic shear resistance per screw"

Characteristic head pull trugh capacity:

"In accordance with ETA-11/0030, head pull trugh capacity may be disregarded"

Compression profile:

Reaction forces and moments:

Shear reaction from applied shear force:

"Shear reaction in screws acting opposite of the applied shear force"

$$R_{xD.Ek} := -\frac{P_x}{n_D}$$ "Horizontal shear force per screw"

$$R_{xD.Ek} = -1\ \text{kN}$$

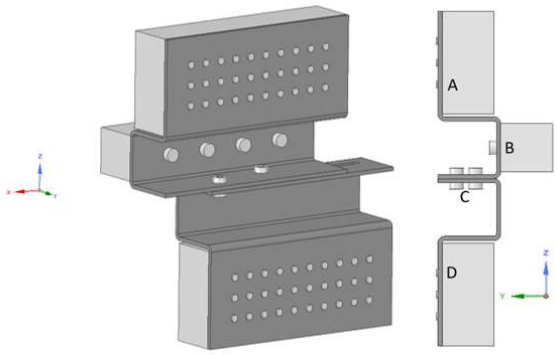

Shear reaction from applied normal force:

"Shear reaction acting opposite of applied force"

$$R_{zD.Ek} := -\frac{P_{zD}}{n_D}$$ "Vertical shear force per screw"

$$R_{zD.Ek} = -0.6381\ \text{kN}$$

Moment about y-axis:

"Because of the assumed moment resistance of connection C, the Moment M.yD was calculated as a fixed-fixed system from support B - D for My, but pinned for My and Mz at connection C.

$$R_{xBD} := P_x$$ "Vertical reaction force acting on system B-D"

$$R_{zBD} := P_{zD}$$ "Horizontal reaction froce in B for system B-D"

$$M_{yD} := \frac{1}{2} \cdot \left(R_{xBD} \cdot d_{zBD} + R_{zBD} \cdot d_{xBD} \right)$$

$$M_{yD} = -4.8085\ \text{kN m}$$

$$d_{zBD} = -0.244\ \text{m}$$

$$R_{xBD} \cdot d_{zBD} = -7320\ \text{J}$$

Moment about x-axis:

M.x was calculated as a cantilecer with a reactionforce R.zC.

$$R_{zCD} := -P_{zD}$$ "Vertical reaction force in C for system C-D"

$$M_{xD} := R_{zCD} \cdot d_{yCD.cv} = -1.54\ \text{kN m}$$

$$M_{xD} = -1.5441\ \text{kN m}$$

Moment about z-axis:

Reaction moment M.z was calculated as a cantilever with a reaction force R.xC

$$R_{xC} := P_x$$ "Horizontal reaction force in C for system C-D"

$$M_{zD} := R_{xC} \cdot \left(-d_{yCD.c} \right) = -1.62\ \text{kN m}$$

$$M_{zD} = -1.62\ \text{kN m}$$

Shear forces due to M.y

The shear forces ar calculated according to theory of In plane eccentrically loaded connections.

"Distances from geometrical connection center"

$$r_{Dz.My} := \begin{bmatrix} p_2 & p_2 & p_2 & p_2 & p_2 & p_2 & p_2 & p_2 & p_2 & p_2 \\ 0 & 0 & 0 & 0 & 0 & 0 & 0 & 0 & 0 & 0 \\ -p_2 & -p_2 & -p_2 & -p_2 & -p_2 & -p_2 & -p_2 & -p_2 & -p_2 & -p_2 \end{bmatrix}$$

$$r_{Dx.My} := \begin{bmatrix} 4.5\cdot p_1 & 3.5\cdot p_1 & 2.5\cdot p_1 & 1.5\cdot p_1 & 0.5\cdot p_1 & -(0.5\cdot p_1) & -(1.5\cdot p_1) & -(2.5\cdot p_1) & -(3.5\cdot p_1) & -(4.5\cdot p_1) \\ 4.5\cdot p_1 & 3.5\cdot p_1 & 2.5\cdot p_1 & 1.5\cdot p_1 & 0.5\cdot p_1 & -(0.5\cdot p_1) & -(1.5\cdot p_1) & -(2.5\cdot p_1) & -(3.5\cdot p_1) & -(4.5\cdot p_1) \\ 4.5\cdot p_1 & 3.5\cdot p_1 & 2.5\cdot p_1 & 1.5\cdot p_1 & 0.5\cdot p_1 & -(0.5\cdot p_1) & -(1.5\cdot p_1) & -(2.5\cdot p_1) & -(3.5\cdot p_1) & -(4.5\cdot p_1) \end{bmatrix}$$

Distance from connection center to screws:

$$r_{D.My} := SRSS_{ij}\left(r_{Dz.My}, r_{Dx.My}\right)$$ "Use the sum of square formula for the matrices"

$$r_{D.My} = \begin{bmatrix} 0.1722 & 0.1365 & 0.1018 & 0.0697 & 0.0459 & 0.0459 & 0.0697 & 0.1018 & 0.1365 & 0.1722 \\ 0.167 & 0.1299 & 0.0928 & 0.0557 & 0.0186 & 0.0186 & 0.0557 & 0.0928 & 0.1299 & 0.167 \\ 0.1722 & 0.1365 & 0.1018 & 0.0697 & 0.0459 & 0.0459 & 0.0697 & 0.1018 & 0.1365 & 0.1722 \end{bmatrix} \text{m}$$

The squared value of the distance:

$$r_{D.My.sq} := Prtoduct_{ij}\left(r_{D.My}, r_{D.My}\right)$$ "Use the product formula to calculate squared values"

$$r_{D.My.sq} = \begin{bmatrix} 0.0297 & 0.0186 & 0.0104 & 0.0049 & 0.0021 & 0.0021 & 0.0049 & 0.0104 & 0.0186 & 0.0297 \\ 0.0279 & 0.0169 & 0.0086 & 0.0031 & 0.0003 & 0.0003 & 0.0031 & 0.0086 & 0.0169 & 0.0279 \\ 0.0297 & 0.0186 & 0.0104 & 0.0049 & 0.0021 & 0.0021 & 0.0049 & 0.0104 & 0.0186 & 0.0297 \end{bmatrix} \text{m}^2$$

The torsion formula is the used to calculate the force distribution:

$$F_{Dv.My} := \frac{\left(-M_{yD}\right)\cdot r_{D.My}}{\sum r_{D.My.sq}}$$ "Shear distribution"

$$F_{Dv.My} = \begin{bmatrix} 2.2 & 1.75 & 1.3 & 0.89 & 0.59 & 0.59 & 0.89 & 1.3 & 1.75 & 2.2 \\ 2.13 & 1.66 & 1.19 & 0.71 & 0.24 & 0.24 & 0.71 & 1.19 & 1.66 & 2.13 \\ 2.2 & 1.75 & 1.3 & 0.89 & 0.59 & 0.59 & 0.89 & 1.3 & 1.75 & 2.2 \end{bmatrix} \text{kN}$$

"These forces were considerd to act positive in relation to the reaction moment, resulting in all forces being positive. As a result the direction of the shear in x- and y- axis had to be ajusted to fit the direction of forces of the reaction moment as shown in the figure below for the direction of reaction forces to a positive M.y (y-axis out of plane).

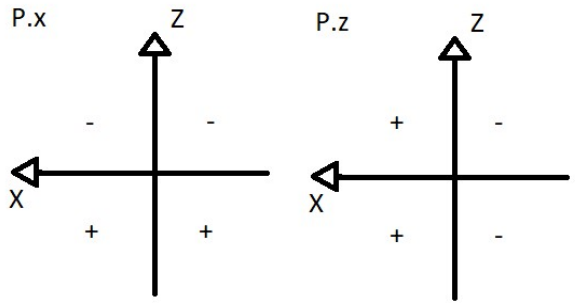

"Since the shear forces acts perpendicular the length vector from the mass center, the component forces in x and z direction were calculated trough geometry with the following formulas where Px and Py were vectors:

$$P_{xij} := P_{ij} \cdot \frac{r_{yij}}{r_{ij}} \qquad P_{yij} := P_{ij} \cdot \frac{r_{xij}}{r_{ij}}$$

Equivalent shear components:

$$F_{xD.My} := Division_{ij}\left(Prtoduct_{ij}\left(F_{Dv.My}, r_{Dz.My}\right), r_{D.My}\right)$$ "Shear component in x-axis"

$$F_{xD.My} = \begin{bmatrix} 0.54 & 0.54 & 0.54 & 0.54 & 0.54 & 0.54 & 0.54 & 0.54 & 0.54 & 0.54 \\ 0 & 0 & 0 & 0 & 0 & 0 & 0 & 0 & 0 & 0 \\ -0.54 & -0.54 & -0.54 & -0.54 & -0.54 & -0.54 & -0.54 & -0.54 & -0.54 & -0.54 \end{bmatrix} \text{kN}$$

$$F_{zD.My} := Division_{ij}\left(Prtoduct_{ij}\left(F_{Dv.My}, r_{Dx.My}\right), r_{D.My}\right)$$ "Shear component in z-axis"

$$F_{zD.My} = \begin{bmatrix} 2.13 & 1.66 & 1.19 & 0.71 & 0.24 & -0.24 & -0.71 & -1.19 & -1.66 & -2.13 \\ 2.13 & 1.66 & 1.19 & 0.71 & 0.24 & -0.24 & -0.71 & -1.19 & -1.66 & -2.13 \\ 2.13 & 1.66 & 1.19 & 0.71 & 0.24 & -0.24 & -0.71 & -1.19 & -1.66 & -2.13 \end{bmatrix} \text{kN}$$

screw tension and CLT compression due to M.x:

The method described in 2.4 out of plane eccentrically loaded bolt connection is ues with maximum elastic strain for screws at characteristical axial screw capactiy equal to maximum elastic strain of CLT at characteristic compression capacity:

The N.A distance percentage factor is calculated:

$\lambda_{CLT.Mx} := 0.549$ "Percentage of connection distance from CLT edge"

$c_{MxD} := \left(H - e_2\right) \cdot \lambda_{CLT.Mx} = 0.07796\ m$ "Edge distance for CLT"

The resulting distance from N.A to screws are calculated from the transposed matrix:

$$r\_initial_{D.Mx} := \begin{bmatrix} e_2 - c_{MxD} & e_2 + p_2 - c_{MxD} & e_2 + 2 \cdot p_2 - c_{MxD} \\ e_2 - c_{MxD} & e_2 + p_2 - c_{MxD} & e_2 + 2 \cdot p_2 - c_{MxD} \\ e_2 - c_{MxD} & e_2 + p_2 - c_{MxD} & e_2 + 2 \cdot p_2 - c_{MxD} \\ e_2 - c_{MxD} & e_2 + p_2 - c_{MxD} & e_2 + 2 \cdot p_2 - c_{MxD} \\ e_2 - c_{MxD} & e_2 + p_2 - c_{MxD} & e_2 + 2 \cdot p_2 - c_{MxD} \\ e_2 - c_{MxD} & e_2 + p_2 - c_{MxD} & e_2 + 2 \cdot p_2 - c_{MxD} \\ e_2 - c_{MxD} & e_2 + p_2 - c_{MxD} & e_2 + 2 \cdot p_2 - c_{MxD} \\ e_2 - c_{MxD} & e_2 + p_2 - c_{MxD} & e_2 + 2 \cdot p_2 - c_{MxD} \\ e_2 - c_{MxD} & e_2 + p_2 - c_{MxD} & e_2 + 2 \cdot p_2 - c_{MxD} \\ e_2 - c_{MxD} & e_2 + p_2 - c_{MxD} & e_2 + 2 \cdot p_2 - c_{MxD} \end{bmatrix}^T = \begin{bmatrix} -0.02\ m & \cdots \\ 0.022\ m & \\ 0.064\ m & \end{bmatrix}$$

"Distances from N.A for screws"

The screwes in the compression area are not allowed to contribute to moment resistance and are removed:

$r_{D.Mx} := Matrix\_remove\_negative_{ij}\left(r\_initial_{D.Mx}\right)$

$$r_{D.Mx} = \begin{bmatrix} 0 & 0 & 0 & 0 & 0 & 0 & 0 & 0 & 0 & 0 \\ 0.022 & 0.022 & 0.022 & 0.022 & 0.022 & 0.022 & 0.022 & 0.022 & 0.022 & 0.022 \\ 0.064 & 0.064 & 0.064 & 0.064 & 0.064 & 0.064 & 0.064 & 0.064 & 0.064 & 0.064 \end{bmatrix} m$$

The squared distance is calcutated:

$r_{D.Mx.sq} := Prtoduct_{ij}\left(r_{D.Mx}, r_{D.Mx}\right)$

Distance to screw force resultant is calculated from the sum of moments about the N.A:

$$dm_{screw.Mx} := \frac{\sum r_{D.Mx.sq}}{\sum r_{D.Mx}}$$

"Distance from neutral axis to resultant force in Screws"

$dm_{screw.Mx} = 53.29\ mm$

The resulting moment arm is calculated from the center of the screw force and the equivalent position of the triangular CLT compression force:

$$z_{D.Mx} := dm_{screw.Mx} + \frac{2}{3} \cdot c_{MxD}$$ "Connection moment arm"

$$z_{D.Mx} = 105.26 \text{ mm}$$

Resulting moments on compression and tension side from the N.A:

$$M_{x.screws} := \left| M_{xD} \right| \cdot \frac{dm_{screw.Mx}}{z_{D.Mx}} = 0.782 \text{ kN m}$$ "Moment acting on screws from N.A"

$$M_{x.CLT} := \left| M_{xD} \right| \cdot \frac{\frac{2}{3} \cdot c_{MxD}}{z_{D.Mx}} = 0.762 \text{ kN m}$$ "Moment acting on CLT from N.A"

Resulting tension forces in screws:

$$F_{Dax.Mx} := \frac{M_{x.screws} \cdot r_{D.Mx}}{\left(\sum r_{D.Mx.sq} \right)}$$ "Force distribution in screws"

$$F_{Dax.Mx} = \begin{bmatrix} 0 & 0 & 0 & 0 & 0 & 0 & 0 & 0 & 0 & 0 \\ 0.3756 & 0.3756 & 0.3756 & 0.3756 & 0.3756 & 0.3756 & 0.3756 & 0.3756 & 0.3756 & 0.3756 \\ 1.0914 & 1.0914 & 1.0914 & 1.0914 & 1.0914 & 1.0914 & 1.0914 & 1.0914 & 1.0914 & 1.0914 \end{bmatrix} \text{kN}$$

$$\sum F_{Dax.Mx} = 14669.7221 \text{ N}$$ "Sum of tension forces"

Maximum compression stress of CLT:

$$I_{z.CLT} := \frac{B \cdot c_{MxD}^{3}}{3} = 7.1068 \cdot 10^{-5} \text{ m}^4$$ "Moment of inertia of CLT about N.A"

$$\sigma_{max.CLT.Mx} := \frac{M_{x.CLT} \cdot c_{MxD}}{I_{z.CLT}} = 0.8363 \frac{\text{N}}{\text{mm}^2}$$ "Maximum stress acting on CLT"

Force resultant in CLT:

$$\frac{\sigma_{max.CLT.Mx} \cdot c_{MxD}}{2} \cdot B = 14669.7221 \text{ N}$$ "Sum of compression forces"

Maximum screw strain:

The maximum strain of the screws and CLT were both calculated considering the maximum CLT strain perpendicular to the grain, with the maximum strain asumed to act at the characteristic screw tension capacity:

$$\varepsilon_{CLT.Mx} := \frac{\sigma_{max.CLT.Mx}}{f_{c.90.k}} \cdot 0.0083 = 0.0028$$ "Maximum strain on CLT"

$$\varepsilon_{screw.Mx} := \frac{\max\left(F_{Dax.Mx} \right)}{F_{ax.Rk.screw}} \cdot 0.0083 = 0.0023$$ "Maximum strain in screws"

The strain ratio of change along the connecton is then calculated for the tension and compression part:

$$\varepsilon'_{CLT} := \frac{\varepsilon_{CLT.Mx}}{c_{MxD}} = 0.0356 \cdot \frac{1}{m}$$ "CLT strain/distrance ratio"

$$\varepsilon'_{screw} := \frac{\varepsilon_{screw.Mx}}{e_2 + 2 \cdot p_2 - c_{MxD}} = 0.0358 \cdot \frac{1}{m}$$ "Screw strain/distrance ratio"

The resulting rate of change should be zero when the neurtal axis has been determined correctly trough the ajustment of λ.CLT.Mx:

$$\varepsilon'_{CLT} - \varepsilon'_{screw} = -0.0002 \cdot \frac{1}{m}$$

screw tension and CLT compression due to M.z:

The same procedure as for M.x is used for the force calculations of M.z

$$\lambda_{CLT.Mz} := 0.248$$

$$c_{MzD} := \left(B - e_1\right) \cdot \lambda_{CLT.Mz} = 0.0972 \text{ m}$$

$$\left(r\_initial_{D.Mz}\right) := \begin{bmatrix} e_1 + 9 \cdot p_1 - c_{MzD} & e_1 + 9 \cdot p_1 - c_{MzD} & e_1 + 9 \cdot p_1 - c_{MzD} \\ e_1 + 8 \cdot p_1 - c_{MzD} & e_1 + 8 \cdot p_1 - c_{MzD} & e_1 + 8 \cdot p_1 - c_{MzD} \\ e_1 + 7 \cdot p_1 - c_{MzD} & e_1 + 7 \cdot p_1 - c_{MzD} & e_1 + 7 \cdot p_1 - c_{MzD} \\ e_1 + 6 \cdot p_1 - c_{MzD} & e_1 + 6 \cdot p_1 - c_{MzD} & e_1 + 6 \cdot p_1 - c_{MzD} \\ e_1 + 5 \cdot p_1 - c_{MzD} & e_1 + 5 \cdot p_1 - c_{MzD} & e_1 + 5 \cdot p_1 - c_{MzD} \\ e_1 + 4 \cdot p_1 - c_{MzD} & e_1 + 4 \cdot p_1 - c_{MzD} & e_1 + 4 \cdot p_1 - c_{MzD} \\ e_1 + 3 \cdot p_1 - c_{MzD} & e_1 + 3 \cdot p_1 - c_{MzD} & e_1 + 3 \cdot p_1 - c_{MzD} \\ e_1 + 2 \cdot p_1 - c_{MzD} & e_1 + 2 \cdot p_1 - c_{MzD} & e_1 + 2 \cdot p_1 - c_{MzD} \\ e_1 + p_1 - c_{MzD} & e_1 + p_1 - c_{MzD} & e_1 + p_1 - c_{MzD} \\ e_1 - c_{MzD} & e_1 - c_{MzD} & e_1 - c_{MzD} \end{bmatrix}^T$$

$$r\_initial_{D.Mz} = \begin{bmatrix} 294.8 & 257.7 & 220.6 & 183.4 & 146.3 & 109.2 & 72.1 & 35 & -2.1 & -39.2 \\ 294.8 & 257.7 & 220.6 & 183.4 & 146.3 & 109.2 & 72.1 & 35 & -2.1 & -39.2 \\ 294.8 & 257.7 & 220.6 & 183.4 & 146.3 & 109.2 & 72.1 & 35 & -2.1 & -39.2 \end{bmatrix} \text{ mm}$$

$$r_{D.Mz} := Matrix\_remove\_negative_{ij}\left(r\_initial_{D.Mz}\right)$$

$$r_{D.Mz.sq} := Prtoduct_{ij}\left(r_{D.Mz}, r_{D.Mz}\right)$$

$$F_{Dax.Mz} := \frac{M_{zD} \cdot r_{D.Mz}}{\sum r_{D.Mz.sq}}$$

$$F_{Dax.Mz} = \begin{bmatrix} -0.5781 & -0.5053 & -0.4325 & -0.3598 & -0.287 & -0.2142 & -0.1414 & -0.0686 & 0 & 0 \\ -0.5781 & -0.5053 & -0.4325 & -0.3598 & -0.287 & -0.2142 & -0.1414 & -0.0686 & 0 & 0 \\ -0.5781 & -0.5053 & -0.4325 & -0.3598 & -0.287 & -0.2142 & -0.1414 & -0.0686 & 0 & 0 \end{bmatrix} \text{ kN}$$

Distance to screw force resultant:

$$dm_{screw.Mz} := \frac{\sum r_{D.Mz.sq}}{\sum r_{D.Mz}}$$

$dm_{screw.Mz} = 208.74\ \text{mm}$ "Distance from neutral axis to resultant force in Screws"

Resulting moment arm:

$z_{D.Mz} := dm_{screw.Mz} + \frac{2}{3} \cdot c_{MzD}$ "Connection moment arm"

$z_{D.Mz} = 273.55\ \text{mm}$

Resulting moments on compression and tension side:

$M_{z.screws} := \left|M_{zD}\right| \cdot \frac{dm_{screw.Mz}}{z_{D.Mz}} = 1.236\ \text{kN m}$ "Moment acting on screws from N.A"

$M_{z.CLT} := \left|M_{zD}\right| \cdot \frac{\frac{2}{3} \cdot c_{MzD}}{z_{D.Mz}} = 0.384\ \text{kN m}$ "Moment acting on CLT from N.A"

Resulting tension forces in screws:

$F_{Dax.Mz} := \frac{M_{z.screws} \cdot r_{D.Mz}}{\left(\sum r_{D.Mz.sq}\right)}$ "Force distribution in screws"

$$F_{Dax.Mz} = \begin{bmatrix} 0.4411 & 0.3856 & 0.3301 & 0.2745 & 0.219 & 0.1635 & 0.1079 & 0.0524 & 0 & 0 \\ 0.4411 & 0.3856 & 0.3301 & 0.2745 & 0.219 & 0.1635 & 0.1079 & 0.0524 & 0 & 0 \\ 0.4411 & 0.3856 & 0.3301 & 0.2745 & 0.219 & 0.1635 & 0.1079 & 0.0524 & 0 & 0 \end{bmatrix} \text{kN}$$

$\sum F_{Dax.Mz} = 5922\ \text{N}$ "Sum of tension forces"

Maximum compression stress of CLT:

$I_{x.CLT} := \frac{H \cdot c_{MzD}^{3}}{3} = 6.1252 \cdot 10^{7}\ \text{mm}^{4}$ "Moment of inertia of CLT about N.A"

$\sigma_{max.CLT.Mz} := \frac{M_{z.CLT} \cdot c_{MzD}}{I_{x.CLT}} = 0.6092\ \frac{\text{N}}{\text{mm}^{2}}$ "Maximum stress acting on CLT"

Force resultant in CLT:

$\frac{\sigma_{max.CLT.Mz} \cdot c_{MzD}}{2} \cdot H = 5922\ \text{N}$ "Sum of compression forces"

Maximum screw strain:

$$\varepsilon_{CLT.Mz} := \frac{\sigma_{max.CLT.Mz}}{f_{c.90.k}} \cdot 0.0083 = 0.002$$ "Maximum strain on CLT"

$$\varepsilon_{screw.Mz} := \frac{\max\left(F_{Dax.Mz}\right)}{F_{ax.Rk.screw}} \cdot 0.0083 = 0.0009$$ Maximum strain in screws"

Strain ratio:

$$\varepsilon'_{CLT.Mz} := \frac{\varepsilon_{CLT.Mz}}{c_{MzD}} = 0.0208 \cdot \frac{1}{m}$$ "CLT strain/distrance ratio"

$$\varepsilon'_{screw.Mz} := \frac{\varepsilon_{screw.Mz}}{\left|e_2 + 2 \cdot p_2 - c_{MzD}\right|} = 0.0207 \cdot \frac{1}{m}$$ "Screw strain/distrance ratio"

$$\varepsilon'_{CLT.Mz} - \varepsilon'_{screw.Mz} = 0.0001 \cdot \frac{1}{m}$$

Tension profile:
Reaction forces and moments in

Shear reaction from applied shear force:

Shear reaction in screws acting opposite of the applied shear force:

$$R_{xD.t.Ek} := -\frac{P_{x.t}}{n_D}$$ "Horizontal shear force per screw"

$$R_{xD.t.Ek} = 0.608\ kN$$

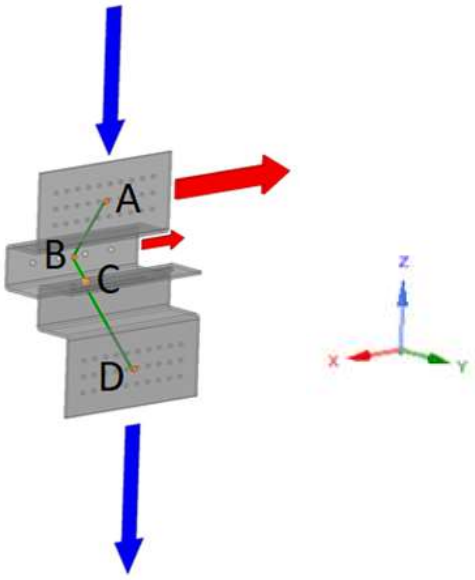

Shear reaction from applied normal force:

Shear reaction acting opposite of applied force

$$R_{zD.t.Ek} := -\frac{P_{zD.t}}{n_D}$$ "Vertical shear force per screw"

$$R_{zD.t.Ek} = 0.7208\ kN$$

Moment about y-axis:

Because of the assumed moment resistance of connection C, the Moment M.yD was calculated as a fixed-fixed system from support B - D.

$$R_{xBD.t} := P_{x.t}$$ "Vertical reaction force acting on system B-D"

$$R_{zCD.t} := P_{zD.t}$$ "Horizontal reaction froce in B for system B-D"

$$M_{yD.t} := 0.5 \cdot \left(R_{xBD.t} \cdot d_{zCD} + R_{zCD.t} \cdot d_{xCD}\right)$$

$$M_{yD.t} = 2.9755\ kN\ m$$

Moment about x-axis:

M.x was calculated as a cantilecer with a reactionforce R.zC.

$R_{zCD.t} := -P_{zD.t}$ "Vertical reaction force in C for system C-D"

$M_{xD.t} := R_{zCD.t} \cdot d_{yCD}$

$M_{xD.t} = 1.1677\ \text{kN m}$

Moment about z-axis:

Reaction moment M.z was calculated as a cantilever with a reaction force R.xC

$R_{xC.t} := -P_{x.t}$ "Horizontal reaction force in C for system C-D"

$M_{zD.t} := R_{xC.t} \cdot d_{yBC}$

$M_{zD.t} = 1.2221\ \text{kN m}$

Shear forces due to M.y

The placement of the critical screws for the different forces were ignored, since it was observed that the critical forces would always act at the same screw in one of the outer corners. The same distance matrix is used as for the compression profile:

$$F_{Dv.t.My} := \frac{\left(-M_{yD.t}\right) \cdot r_{D.My}}{\sum r_{D.My.sq}}$$ "Shear forces distribution"

$$F_{Dv.t.My} = \begin{bmatrix} -1.36 & -1.08 & -0.81 & -0.55 & -0.36 & -0.36 & -0.55 & -0.81 & -1.08 & -1.36 \\ -1.32 & -1.03 & -0.73 & -0.44 & -0.15 & -0.15 & -0.44 & -0.73 & -1.03 & -1.32 \\ -1.36 & -1.08 & -0.81 & -0.55 & -0.36 & -0.36 & -0.55 & -0.81 & -1.08 & -1.36 \end{bmatrix} \text{kN}$$

The shear components are calculated:

$F_{xD.t.My} := Division_{ij}\left(Prtoduct_{ij}\left(F_{Dv.t.My}, r_{Dz.My}\right), r_{D.My}\right)$

$$F_{xD.t.My} = \begin{bmatrix} -0.33 & -0.33 & -0.33 & -0.33 & -0.33 & -0.33 & -0.33 & -0.33 & -0.33 & -0.33 \\ 0 & 0 & 0 & 0 & 0 & 0 & 0 & 0 & 0 & 0 \\ 0.33 & 0.33 & 0.33 & 0.33 & 0.33 & 0.33 & 0.33 & 0.33 & 0.33 & 0.33 \end{bmatrix} \text{kN}$$

$F_{zD.t.My} := Division_{ij}\left(Prtoduct_{ij}\left(F_{Dv.t.My}, r_{Dx.My}\right), r_{D.My}\right)$

$$F_{zD.t.My} = \begin{bmatrix} -1.32 & -1.03 & -0.73 & -0.44 & -0.15 & 0.15 & 0.44 & 0.73 & 1.03 & 1.32 \\ -1.32 & -1.03 & -0.73 & -0.44 & -0.15 & 0.15 & 0.44 & 0.73 & 1.03 & 1.32 \\ -1.32 & -1.03 & -0.73 & -0.44 & -0.15 & 0.15 & 0.44 & 0.73 & 1.03 & 1.32 \end{bmatrix} \text{kN}$$

Screw tension and CLT compression due to M.x.t:

Resulting moments on compression and tension side:

$$M_{x.screws.t} := \left|M_{xD.t}\right| \cdot \frac{dm_{screw.Mx}}{z_{D.Mx}} = 0.591\ \text{kN m}$$ "Moment acting on screws from N.A"

$$M_{x.CLT.t} := \left|M_{xD.t}\right| \cdot \frac{\frac{2}{3} \cdot c_{MxD}}{z_{D.Mx}} = 0.577\ \text{kN m}$$ "Moment acting on CLT from N.A"

Resulting tension forces in screws:

$$F_{Dax.Mx.t} := \frac{M_{x.screws.t} \cdot r_{D.Mx}}{\left(\sum r_{D.Mx.sq}\right)}$$ "Force distribution in screws"

$$F_{Dax.Mx.t} = \begin{bmatrix} 0 & 0 & 0 & 0 & 0 & 0 & 0 & 0 & 0 & 0 \\ 0.2841 & 0.2841 & 0.2841 & 0.2841 & 0.2841 & 0.2841 & 0.2841 & 0.2841 & 0.2841 & 0.2841 \\ 0.8253 & 0.8253 & 0.8253 & 0.8253 & 0.8253 & 0.8253 & 0.8253 & 0.8253 & 0.8253 & 0.8253 \end{bmatrix} \text{kN}$$

$$\sum F_{Dax.Mx.t} = 11093.4978\ \text{N}$$ "Sum of tension forces"

Maximum compression stress of CLT:

$$I_{z.CLT.t} := \frac{B \cdot c_{MxD}^{3}}{3} = 7.1068 \cdot 10^{-5}\ \text{m}^4$$ "Moment of inertia of CLT about N.A"

$$\sigma_{max.CLT.Mx.t} := \frac{M_{x.CLT.t} \cdot c_{MxD}}{I_{z.CLT}} = 0.6324\ \frac{\text{N}}{\text{mm}^2}$$ "Maximum stress acting on CLT"

Force resultant in CLT:

$$\frac{\sigma_{max.CLT.Mx.t} \cdot c_{MxD}}{2} \cdot B = 11093.4978\ \text{N}$$ "Sum of compression forces"

Maximum screw strain:

The maximum strain of the bolts and CLT were both calculated considering the maximum compression perpendicular to the grain.

$$\varepsilon_{CLT.Mx.t} := \frac{\sigma_{max.CLT.Mx.t}}{f_{c.90.k}} \cdot 0.0083 = 0.0021$$ "Maximum strain on CLT"

$$\varepsilon_{screw.Mx.t} := \frac{\max\left(F_{Dax.Mx.t}\right)}{F_{ax.Rk.screw}} \cdot 0.0083 = 0.0017$$ "Maximum strain in screws"

Strain ratio:

$$\varepsilon'_{CLT.t} := \frac{\varepsilon_{CLT.Mx.t}}{c_{MxD}} = 0.0269 \cdot \frac{1}{m}$$ "CLT strain/distrance ratio"

$$\varepsilon'_{screw.t} := \frac{\varepsilon_{screw.Mx.t}}{e_2 + 2 \cdot p_2 - c_{MxD}} = 0.0271 \cdot \frac{1}{m}$$ "Screw strain/distrance ratio"

$$\varepsilon'_{CLT.t} - \varepsilon'_{screw.t} = -0.0001 \cdot \frac{1}{m}$$

screw tension and CLT compression due to M.z:

Resulting moments on compression and tension side:

$$M_{z.screws.t} := \left|M_{zD.t}\right| \cdot \frac{dm_{screw.Mz}}{z_{D.Mz}} = 0.933 \text{ kN m}$$ "Moment acting on screws from N.A"

$$M_{z.CLT.t} := \left|M_{zD.t}\right| \cdot \frac{\frac{2}{3} \cdot c_{MzD}}{z_{D.Mz}} = 0.29 \text{ kN m}$$ "Moment acting on CLT from N.A"

Resulting tension forces in screws:

$$F_{Dax.Mz.t} := \frac{M_{z.screws.t} \cdot r_{D.Mz}}{\left(\sum r_{D.Mz.sq}\right)}$$ "Force distribution in screws"

$$F_{Dax.Mz.t} = \begin{bmatrix} 0.3328 & 0.2909 & 0.249 & 0.2071 & 0.1652 & 0.1233 & 0.0814 & 0.0395 & 0 & 0 \\ 0.3328 & 0.2909 & 0.249 & 0.2071 & 0.1652 & 0.1233 & 0.0814 & 0.0395 & 0 & 0 \\ 0.3328 & 0.2909 & 0.249 & 0.2071 & 0.1652 & 0.1233 & 0.0814 & 0.0395 & 0 & 0 \end{bmatrix} \text{kN}$$

Maximum compression stress of CLT:

$$I_{x.CLT} := \frac{H \cdot c_{MzD}^{3}}{3} = 6.1252 \cdot 10^{-5} \text{ m}^4$$ "Moment of inertia of CLT about N.A"

$$\sigma_{max.CLT.Mz.t} := \frac{M_{z.CLT.t} \cdot c_{MzD}}{I_{x.CLT}} = 0.4595 \frac{\text{N}}{\text{mm}^2}$$ "Maximum stress acting on CLT"

Capacity control:

The axial forces acting on the system are a result Mx and Mz:

Resulting axial forces acting on screws:

"M.x and M.z are the only contributers to the axial forces of the system:

$$F_{Dax.tot} := F_{Dax.Mx} + F_{Dax.Mz} = \begin{bmatrix} 0.441 & 0.386 & 0.33 & 0.275 & 0.219 & 0.163 & 0.108 & 0.052 & 0 & 0 \\ 0.817 & 0.761 & 0.706 & 0.65 & 0.595 & 0.539 & 0.484 & 0.428 & 0.376 & 0.376 \\ 1.532 & 1.477 & 1.421 & 1.366 & 1.31 & 1.255 & 1.199 & 1.144 & 1.091 & 1.091 \end{bmatrix} \text{kN}$$

$F_{Dax.Ek} := \max\left(F_{Dax.tot}\right) = 1.5325\ \text{kN}$ "Critical axial force on screws in compression system"

$$F_{Dax.tot.t} := F_{Dax.Mx.t} + F_{Dax.Mz.t} = \begin{bmatrix} 0.333 & 0.291 & 0.249 & 0.207 & 0.165 & 0.123 & 0.081 & 0.04 & 0 & 0 \\ 0.617 & 0.575 & 0.533 & 0.491 & 0.449 & 0.407 & 0.365 & 0.324 & 0.284 & 0.284 \\ 1.158 & 1.116 & 1.074 & 1.032 & 0.99 & 0.949 & 0.907 & 0.865 & 0.825 & 0.825 \end{bmatrix} \text{kN}$$

$F_{Dax.Ek.t} := \max\left(F_{Dax.tot.t}\right) = 1.1581\ \text{kN}$ "Critical axial force on screws in tension system"

Resulting maximum CLT compression:

"Maximum compressive stress for CLT is considderd to act at the top right corner of the connection resulitng in the maximum compression being the sum of critical compression from M.z and M.y:"

$\sigma_{clt.Ek} := \sigma_{max.CLT.Mx} + \sigma_{max.CLT.Mz}$

$\sigma_{clt.Ek} = 1.4455\ \frac{\text{N}}{\text{mm}^2}$

$$\frac{\sigma_{clt.Ek}}{f_{c.90.k}} = 0.578$$

$\sigma_{clt.Ek.t} := \sigma_{max.CLT.Mx.t} + \sigma_{max.CLT.Mz.t}$

$\sigma_{clt.Ek.t} = 1.092\ \frac{\text{N}}{\text{mm}^2}$

$$\frac{\sigma_{clt.Ek.t}}{f_{c.90.k}} = 0.437$$

Resulting maximum shear force acting on screws:

"The maximum shear from moments M.x and M.z and forces R.px are summed for respective axes."

$$F_{xD.tot} := R_{xD.Ek} + F_{xD.My}$$

$$F_{xD.tot} = \begin{bmatrix} -0.463 & -0.463 & -0.463 & -0.463 & -0.463 & -0.463 & -0.463 & -0.463 & -0.463 & -0.463 \\ -1 & -1 & -1 & -1 & -1 & -1 & -1 & -1 & -1 & -1 \\ -1.537 & -1.537 & -1.537 & -1.537 & -1.537 & -1.537 & -1.537 & -1.537 & -1.537 & -1.537 \end{bmatrix} \text{kN}$$

$$F_{zD.tot} := R_{zD.Ek} + F_{zD.My}$$

$$F_{zD.tot} = \begin{bmatrix} 1.497 & 1.022 & 0.548 & 0.074 & -0.401 & -0.875 & -1.35 & -1.824 & -2.299 & -2.773 \\ 1.497 & 1.022 & 0.548 & 0.074 & -0.401 & -0.875 & -1.35 & -1.824 & -2.299 & -2.773 \\ 1.497 & 1.022 & 0.548 & 0.074 & -0.401 & -0.875 & -1.35 & -1.824 & -2.299 & -2.773 \end{bmatrix} \text{kN}$$

"As a result of the even distribution of shear forces from external forces and the maximum shear force from moments acting in corner scres, it is determined that the maximum shear wil act in one of the four corners resulting in the SRSS of the maximum shear force in x and z direction."

$$F_{vD.Ek} := \sqrt{\left(\text{Max}\left(\left|\text{mat2sys}\left(F_{xD.tot}\right)\right|\right)\right)^2 + \left(\text{Max}\left(\left|\text{mat2sys}\left(F_{zD.tot}\right)\right|\right)\right)^2}$$

$F_{vD.Ek} = 3170.445\ \text{N}$ "Critical shear force force of compression profile"

"The maximum shear from moments M.x.t and M.z.t and forces R.px are summed for their respective axes."

$$F_{xD.tot.t} := R_{xD.t.Ek} + F_{xD.t.My}$$

$$F_{xD.tot.t} = \begin{bmatrix} 0.276 & 0.276 & 0.276 & 0.276 & 0.276 & 0.276 & 0.276 & 0.276 & 0.276 & 0.276 \\ 0.608 & 0.608 & 0.608 & 0.608 & 0.608 & 0.608 & 0.608 & 0.608 & 0.608 & 0.608 \\ 0.94 & 0.94 & 0.94 & 0.94 & 0.94 & 0.94 & 0.94 & 0.94 & 0.94 & 0.94 \end{bmatrix} \text{kN}$$

$$F_{zD.tot.t} := R_{zD.t.Ek} + F_{zD.t.My}$$

$$F_{zD.tot.t} = \begin{bmatrix} -0.6 & -0.307 & -0.013 & 0.28 & 0.574 & 0.868 & 1.161 & 1.455 & 1.748 & 2.042 \\ -0.6 & -0.307 & -0.013 & 0.28 & 0.574 & 0.868 & 1.161 & 1.455 & 1.748 & 2.042 \\ -0.6 & -0.307 & -0.013 & 0.28 & 0.574 & 0.868 & 1.161 & 1.455 & 1.748 & 2.042 \end{bmatrix} \text{kN}$$

$$F_{vD.Ek.t} := \sqrt{\left(\text{Max}\left(\left|\text{mat2sys}\left(F_{xD.tot.t}\right)\right|\right)\right)^2 + \left(\text{Max}\left(\left|\text{mat2sys}\left(F_{zD.tot.t}\right)\right|\right)\right)^2}$$

$F_{vD.Ek.t} = 2247.9862\ \text{N}$ "Critical shear force of tension profile"

"EN 1995 1-1:2008 does not give an expression for the combined characteristic capacity of screws. As a result eq. (8.28) is adapted for characteristic values by exchanging the design values for characteristic values:"

$$\left(\frac{F_{Dax.Ek}}{F_{ax.Rk.screw}}\right)^2+\left(\frac{F_{vD.Ek}}{F_{vD.Rk}}\right)^2=0.4338$$

"Characteristic utilization for profile in compression: $P_x=30\ kN$

$$\left(\frac{F_{Dax.Ek.t}}{F_{ax.Rk.screw}}\right)^2+\left(\frac{F_{vD.Ek.t}}{F_{vD.Rk}}\right)^2=0.2283$$

"Characteristic utilization for profile in tension: $P_{x.t}=-18.24\ kN$

"Calculating the design utilization for a γ factor of 1.25, yields the following design utilization for a load P.x:

$$F_{vD.Rd}:=\frac{F_{vD.Rk}}{1.25}$$

"Design shear capacity"

$$F_{ax.Rd}:=\frac{F_{ax.Rk.screw}}{1.25}$$

"Design axial capacity"

$$\left(\frac{F_{Dax.Ek}}{F_{ax.Rd}}\right)^2+\left(\frac{F_{vD.Ek}}{F_{vD.Rd}}\right)^2=0.68$$

"Design utilization in compression"

$$\left(\frac{F_{Dax.Ek.t}}{F_{ax.Rd}}\right)^2+\left(\frac{F_{vD.Ek.t}}{F_{vD.Rd}}\right)^2=0.36$$

"Design utilization in tension"

Concrete connection calculations

"The moment in support B for the compression profile was considered to be the critical. This was because of the reduced horizontal forces and the short vertical span from B to C, resulting in a lower moment In B from the pinned system BC in tension than the fixed system BD for compression:

Forces acting on system

Reaction forces in connection C in regards to system BC:

$R_{xCB} := P_{xA} + P_{xB}$ "horizontal reaction force in connecton B"

$R_{zCB} := P_{zD}$ "Vertical reaction force in connection B"

The M.y in support B was calculated as the sum of the moments in B from a fixed-fixed moment system A-B and a fixed-fixed system B-D. This was done because support B prohibited any rotation in the support, thus prohibiting the transfer of moments. Point C was also considered moment resisting for moments about the y-axis.

$M_{yBab} := 0.5 \cdot P_{xA} \cdot d_{zAB} = -1.6605 \text{ kN m}$ "M.y from horizontal force in support A"

$M_{yBbd} := M_{yD} = -4.8085 \text{ kN m}$ "M.y from horizontal force in support D"

$M_{yB} := M_{yBab} + M_{yBbd}$ "Sum of M.y resisted by support B"

$M_{yB} = -6.469 \text{ kN m}$

M.x is calculated as the sum of the momet created from the vertical force acting in connection A and C:

$M_{xAB} := 0.5 \cdot P_{zA} \cdot d_{yAB} = -1.0348 \text{ kN m}$ "Fixed behavior"

$d_{yCB.cv} := -d_{yBC.cv}$ "Switch direction"

$M_{xCB} := R_{zCB} \cdot d_{yCB.cv} = -0.7721 \text{ kN m}$ "Cantilever"

$M_{xB} := \left(M_{xCB} + M_{xAB}\right)$ "Resultant moment"

$M_{xB} = -1.8068 \text{ kN m}$

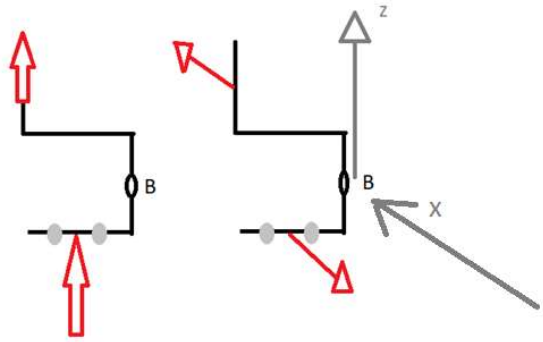

M.y is calculated as a sum of the force acting on

$M_{zAB} := 0.5 \cdot \left(-P_{xA}\right) \cdot d_{yAB} = 1.6335 \text{ kN m}$

$M_{zCB} := R_{xCB} \cdot \left(-d_{yBC.c}\right) = -2.01 \text{ kN m}$

"Resulting moments counteract each other"

$M_{zB} := \left(M_{zAB} + M_{zCB}\right)$

$M_{zB} = -0.3765 \text{ kN m}$

Because support B was the only connection considered to take vertical forces, the vertical force in support D would be the sum of all vertical system forces:

$$R_{zB} := -\left(P_{zA} + P_{zD}\right)$$

$$R_{zB} = -36.246\ \text{kN}$$

In additon to the the vertical reaction force, a horizontal force P.xB was considered to be transmited from the concrete to the system.

$$R_{xB} := -P_{xB} = -3000\ \text{N}$$

Reaction forces in concrete anchors due to M.y:

The calculation is done using the same principle as connection D for M.y with the center determined by symetri:

$$r_{B.My} := \left[\, 1.5 \cdot d_{x.anchor} \;\; 0.5 \cdot d_{x.anchor} \;\; (-0.5) \cdot d_{x.anchor} \;\; (-1.5) \cdot d_{x.anchor} \,\right]$$

$$r_{B.My} = \left[\, 0.135 \;\; 0.045 \;\; -0.045 \;\; -0.135 \,\right] \text{m}$$

$$r_{B.My.sq} := Prtoduct_{ij}\left(r_{B.My},\, r_{B.My}\right)$$

$$r_{B.My.sq} = \left[\, 0.0182 \;\; 0.002 \;\; 0.002 \;\; 0.0182 \,\right] \text{m}^2$$

The moment calculated was already the reaction of the screws resulting in the use of the moment exiting the connection being -M.yB:

$$F_{zB.My} := -\frac{M_{yB} \cdot r_{B.My}}{\sum r_{B.My.sq}}$$

$$F_{zB.My} = \left[\, 21.56 \;\; 7.19 \;\; -7.19 \;\; -21.56 \,\right] \text{kN}$$

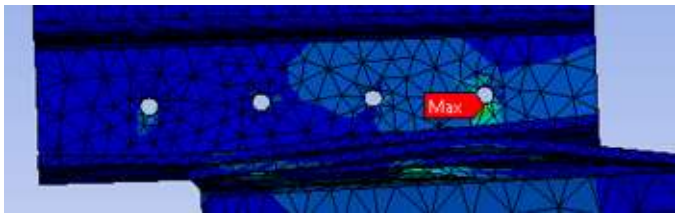

"Large force reaction because of the fixed behaviour of connection C"

Reaction forces in concrete anchors due to M.z:

The same procedure as for M.x is used for the force calculations of M.z

$n_{t.anchors} := 4$ "Number of anchors"

$\lambda_{Concrete.Mz} := 0.248$ "Relative distance from concrete edge"

$c_{MzB} := \left(\left(n_{t.anchors} - 1\right) \cdot d_{x.anchor} + e_{x.anchor}\right) \cdot \lambda_{Concrete.Mz} = 0.0893\ \text{m}$ "Concrete edge distance to neutral axis"

$$r\_initial_{B.Mz} := \begin{bmatrix} e_{x.anchor} + 3 \cdot d_{x.anchor} - c_{MzB} \\ e_{x.anchor} + 2 \cdot d_{x.anchor} - c_{MzB} \\ e_{x.anchor} + d_{x.anchor} - c_{MzB} \\ e_{x.anchor} - c_{MzB} \end{bmatrix}^{T}$$

$r\_initial_{B.Mz} = \begin{bmatrix} 270.7 & 180.7 & 90.7 & 0.7 \end{bmatrix}\ \text{mm}$

$r_{B.Mz} := Matrix\_remove\_negative_{ij}\left(r\_initial_{B.Mz}\right)$ "Compression screws are removed"

$r_{B.Mz.sq} := Prtoduct_{ij}\left(r_{B.Mz}, r_{B.Mz}\right)$ "Squared distances"

Distance to screw force resultant:

$$dm_{anchor.Mz} := \frac{\sum r_{B.Mz.sq}}{\sum r_{B.Mz}}$$

$dm_{anchor.Mz} = 210.32\ \text{mm}$ "Distance from neutral axis to resultant force in anchors"

Resulting moment arm:

$z_{B.Mz} := dm_{anchor.Mz} + \frac{2}{3} \cdot c_{MzB}$ "Connection moment arm"

$z_{B.Mz} = 269.84\ \text{mm}$

Resulting moments on compression and tension side:

$$M_{z.anchor} := \left|M_{zB}\right| \cdot \frac{dm_{anchor.Mz}}{z_{B.Mz}} = 0.293\ \text{kN m}$$ "Moment acting on anchors from N.A"

$$M_{z.Concrete} := \left|M_{zB}\right| \cdot \frac{\frac{2}{3} \cdot c_{MzB}}{z_{B.Mz}} = 0.083\ \text{kN m}$$ "Moment acting on concrete from N.A"

Resulting tension forces in screws:

$$F_{Bax.Mz} := \frac{M_{z.anchor} \cdot r_{B.Mz}}{\left(\sum r_{B.Mz.sq}\right)}$$ "Force distribution in anchors"

$$F_{Bax.Mz} = \left[\begin{array}{cccc} 0.6958 & 0.4645 & 0.2332 & 0.0019 \end{array}\right] \text{kN}$$

$$\sum F_{Bax.Mz} = 1395\ \text{N}$$ "Sum of tension forces"

Maximum compression stress of CLT:

$$I_{x.Concrete} := \frac{2 \cdot d_{z.anchor} \cdot c_{MzB}^{3}}{3} = 2.8466 \cdot 10^{-5}\ \text{m}^4$$ "Moment of inertia of concrete about N.A"

$$\sigma_{max.Concrete.Mz} := \frac{M_{z.Concrete} \cdot c_{MzB}}{I_{x.Concrete}} = 0.2605\ \frac{\text{N}}{\text{mm}^2}$$ "Maximum stress acting on concrete"

Force resultant in CLT:

$$\frac{\sigma_{max.Concrete.Mz} \cdot c_{MzB}}{2} \cdot 2 \cdot d_{z.anchor} = 1395\ \text{N}$$ "Sum of compression forces"

Maximum screw strain:

$$\varepsilon_{Concrete.Mz} := \frac{\sigma_{max.Concrete.Mz}}{E_{cm}} = 8.6932 \cdot 10^{-6}$$ "Maximum strain on concrete"

$$A_{anchor} := 84.3\ \text{mm}^2$$

$$\varepsilon_{anchor.Mz} := \frac{\max\left(F_{Bax.Mz}\right)}{A_{anchor} \cdot E_s} = 4.1268 \cdot 10^{-5}$$ Maximum strain in anchors"

Strain ratio:

$$\varepsilon'_{Concrete.Mz} := \frac{\varepsilon_{Concrete.Mz}}{c_{MzB}} = 9.737 \cdot 10^{-5} \cdot \frac{1}{\text{m}}$$ "concrete strain/distrance ratio"

$$\varepsilon'_{anchor.Mz} := \frac{\varepsilon_{anchor.Mz}}{\left|r\_initial_{B.Mz_1}\right|} = 0.0002 \cdot \frac{1}{\text{m}}$$ "anchors strain/distrance ratio"

$$\varepsilon'_{Concrete.Mz} - \varepsilon'_{anchor.Mz} = -5.5068 \cdot 10^{-5} \cdot \frac{1}{\text{m}}$$

Reaction forces in anchors due to M.xB

$n_{anchors} := 4$ "Number of anchors"

$H_B := d_{z.anchor} = 0.06\ m$ "Height of connection"

$\lambda_{Concrete.Mx} := 0.333$

$c_{MxB} := \left(H_B\right) \cdot \lambda_{Concrete.Mx} = 0.01998\ m$

Since the system only consists of one row of screws, the resultant tension force acts in the middle of the row.

$$dm_{anchor.Mx} := H_B - c_{MxB}$$

Resulting moment arm:

"When the system is linearly elastic the stress distribution of CLT is triangular, yielding the resultant force acting 2/3 of the distance from the neutral axis.

$z_{B.Mx} := dm_{anchor.Mx} + \frac{2}{3} \cdot c_{MxB}$ "Connection moment arm"

$z_{B.Mx} = 53.34\ mm$

Resulting moments on compression and tension side:

$M_{x.anchor} := \left|M_{xB}\right| \cdot \frac{dm_{anchor.Mx}}{z_{B.Mx}} = 1.356\ kN\ m$ "Moment acting on screws from N.A"

$M_{x.concrete} := \left|M_{xB}\right| \cdot \frac{\frac{2}{3} \cdot c_{MxB}}{z_{B.Mx}} = 0.451\ kN\ m$ "Moment acting on CLT from N.A"

Resulting tension forces in screws:

$F_{Bax.Mx.tot} := \frac{M_{x.anchor} \cdot dm_{anchor.Mx}}{dm_{anchor.Mx}^2}$ "Force distribution in screws"

$F_{Bax.Mx} := \frac{F_{Bax.Mx.tot}}{n_{anchors}} = 8.4685\ kN$

Maximum compression stress of concrete:

$I_{z.concrete} := \frac{B \cdot c_{MxB}^3}{3} = 1.1964 \cdot 10^{-6}\ m^4$ "Moment of inertia of CLT about N.A"

$\sigma_{max.concrete.Mx} := \frac{M_{x.concrete} \cdot c_{MxB}}{I_{z.concrete}} = 7.5351\ \frac{N}{mm^2}$ "Maximum stress acting on CLT"

The maximum strain of the bolts and CLT were both calculated considering the maximum compression perpendicular to the grain.

$$\varepsilon_{concrete.Mx} := \frac{\sigma_{max.concrete.Mx}}{E_{cm}} = 0.0003$$ "Maximum strain on CLT"

$$\varepsilon_{anchor.Mx} := \frac{F_{Bax.Mx}}{A_{anchor} \cdot E_s} = 0.0005$$ Maximum strain in screws"

Strain ratio:

For plates to remain plane, the rate of change in strain have to be equal for the tension and compression part of the connection.

$$\varepsilon'_{concrete} := \frac{\varepsilon_{concrete.Mx}}{c_{MxB}} = 0.0126 \cdot \frac{1}{m}$$ "CLT strain/distrance ratio"

$$\varepsilon'_{screw} := \frac{\varepsilon_{anchor.Mx}}{dm_{anchor.Mx}} = 0.0126 \cdot \frac{1}{m}$$ "Screw strain/distrance ratio"

Shear stress due to axial forces:

The shear forces due to axial forces were calculated as evenly distributed because the connection only consisted of one row of edge bolts. (Not two rows whtere the shear forces would be taken by the inner bolts to increase concrete tear out strength.)

Vertical force

$$R_{zB} = -36.246 \text{ kN}$$

$$F_{zB.Rz} := \frac{R_{zB}}{n_{Bx}} = -9.0615 \text{ kN}$$ "Vertical resistance per anchor"

Horizontal force

$$R_{xB} := -P_{xB} = -3000 \text{ N}$$

$$F_{xB.Rx} := \frac{R_{xB}}{n_{Bx}} = -0.75 \text{ kN}$$ "horizontal resistance per anchor"

Resulting forces in anchors due to applied forces:

Resulting vertical shear forces

$$F_{zB.Ek} := F_{zB.My} + F_{zB.Rz}$$

$$F_{zB.Ek} = [\, 12.5 \;\; -1.87 \;\; -16.25 \;\; -30.62 \,] \text{ kN}$$

Resulting horizontal shear forces:

$$F_{xB.Ek} := F_{xB.Rx} \cdot [1\ 1\ 1\ 1]$$

$$F_{xB.Ek} = [-0.75\ -0.75\ -0.75\ -0.75]\ \text{kN}$$

Resulting axial forces:

$$F_{axB.Ek} := F_{Bax.Mx} \cdot [1\ 1\ 1\ 1] + F_{Bax.Mz}$$

$$F_{axB.Ek} = [9.164\ 8.933\ 8.702\ 8.47]\ \text{kN}$$

From the results it was determined that the worst anchor was the right anchor because of the largest resulting vertical shear force.

Resulting reaction forces of worst anchor:

$$F_{zB.Ek.crit} := \text{Max}\left(\left|\text{mat2sys}\left(F_{zB.Ek}\right)\right|\right)$$

$$\boxed{F_{zB.Ek.crit} = 30.62\ \text{kN}}$$

$$F_{xB.Ek.crit} := \text{Max}\left(\left|\text{mat2sys}\left(F_{xB.Ek}\right)\right|\right)$$

$$\boxed{F_{xB.Ek.crit} = 0.75\ \text{kN}}$$

$$F_{axB.Ek.crit} := \text{Max}\left(F_{axB.Ek}\right)$$

$$\boxed{F_{axB.Ek.crit} = 9.1643\ \text{kN}}$$

Anchor capactiy control:

Can not find anchors of size M14: As a substitute, Hitist HIT-HY 200 M12 anchors are utilized. The calculations have been done for cracked concrete: No units are assigned, as the calculations are empirical:

$n_{t.anchors} := 4$ "Number of anchors"

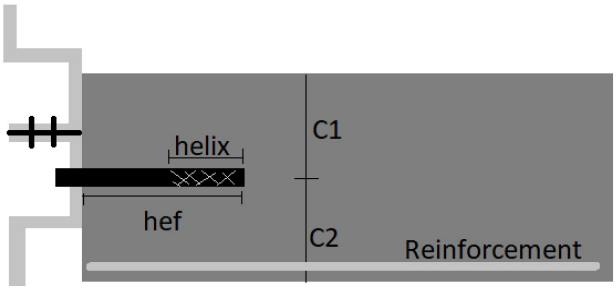

Concrete

$H_{concrete} := 350\ mm$ "Height of concrette beam"

$H_{concrete.depth} := 300\ mm$ "Concrete depth"

$c_{1.cap} := \frac{H_{concrete}}{2}$ "Upper edge distance"

$c_{2.cap} := c_{1.cap}$ "Lower edge distance" "Anchors assumed fixed in the middle"

$s_{1.cap} := 90\ mm$ "Anchor spacing"

$f_{ck.cube.cap} := 25\ \frac{N}{mm^2}$ "Characteristic cubed concrete capacity"

ETA-12/0028: HILTI HIT-HY 200R with HIT-Z: (Table values) "From catalog, not ETA"

$d_{anchor.cap} := 12\ mm$ "Anchor diameter"

$h_{nom} := 100\ mm$ "Anchor depth"

$h_{ef} := h_{nom}\ mm$ "Effective anchor depth"

$A_{s.anchor} := 84.3\ mm$ "Area of steel cross section"

$h_{helix} := 60\ mm$ "Length of helix part of anchor"

$C_{cr.sp} := 1.5 \cdot h_{ef} = 150\ mm$

$S_{cr.sp} := 2 \cdot C_{cr.sp} = 300\ mm$

"Pull out area distances valid for : H.concrete.depth / h.nom > 2.3"

$\tau_{rk.ucr} := 22\ \frac{N}{mm^2}$ "Anchor bond resistance"

$f_{uk} := 650\ \frac{N}{mm^2}$ "Characteristic capactiy of anchor"

$f_{yk.anchor} := 520\ \frac{N}{mm^2}$ "Yield strength of anchor"

$S_{cr.Np} := \mathrm{Min}\left(20 \cdot d_{anchor.cap}, 3 \cdot h_{helix}\right)$

$C_{cr.Np} := 0.5 \cdot S_{cr.Np} = 90$

"Group pull-out distances"

$k_{\psi 0.g.Np} := 2.3$ "Concrete factor according to ETA-12/0028"

$gamma := 1.5$ "Anchor safety factor"

$c_{min} := 90$

$s_{min} := 60$

"Minimum and maximum anchor distances for M12"

$h_{nom.max} := 144$

Distances and factors determined by ETAG 001:

"Pry out distances"

$S_{cr.N} := 3 \cdot h_{ef} = 300$

$C_{cr.N} := 0.5 \cdot S_{cr.N} = 150$

Concrete factors for cracked concrete ETAG 001:

$k_{N0.Rk.c} := 7.2$

$k_{V.Rk.cp} := 2$

$k_{V0.Rk.c} := 1.7$

Tension capactiy

Steel failure:

$N_{Rk.s} := n_{t.anchors} \cdot A_{s.anchor} \cdot f_{uk} = 2.1918 \cdot 10^{5}$ N "Steel capacity"

$\frac{\sum F_{axB.Ek}}{N_{Rk.s}} \text{ N} = 0.1609$ "Steel utilization for tension"

Eccentricity of resulting axial forces on anchors is determined:

$F_{axB.Ek} = [\, 9.1643 \;\; 8.933 \;\; 8.7017 \;\; 8.4704 \,]$ kN "Resultant tension forces on anchors"

$r_{nB} := [\, 1.5 \cdot s_{1.cap} \;\; 0.5 \cdot s_{1.cap} \;\; (-0.5) \cdot s_{1.cap} \;\; (-1.5) \cdot s_{1.cap} \,]$ "Distance from geometrical connector center"

$r_{nB} = [\, 135 \;\; 45 \;\; -45 \;\; -135 \,]$

$e_n := \frac{\sum Prtoduct_{ij}\left(r_{nB},\, F_{axB.Ek}\right)}{\sum F_{axB.Ek}} = 2.9513 \;\; mm$ "Eccentricity"

Group pull-out failure:

Next the different group pull out factors are calulated:

$\psi_{re.Np} := \text{Min}\left(0.5 + \frac{h_{ef}}{200},\, 1\right) = 1$ "Spalling factor"

$\psi_{ec.Np} := \text{Min}\left(\frac{1}{1 + 2 \cdot \frac{e_n}{S_{cr.Np}}},\, 1\right) = 0.9682$ "Eccentricity factor"

$\psi 0_{g.Np} := \text{Max}\left(\left(\sqrt{n_{t.anchors}} - \left(\sqrt{n_{t.anchors}} - 1\right) \cdot \frac{d_{anchor.cap} \cdot \tau_{rk.ucr}}{k_{\psi 0.g.Np} \cdot \sqrt{h_{ef} \cdot f_{ck.cube.cap}}}\right),\, 1\right) = 1$

$\psi_{g.Np} := \text{Max}\left(\psi 0_{g.Np} - \left(\frac{s}{S_{cr.Np}}\right)^{0.5} \cdot \left(\psi 0_{g.Np} - 1\right)\right) = 1$ "Surface factor"

$\psi_{s.Np} := 0.7 + 0.3 \cdot \frac{c_{1.cap}}{C_{cr.Np}} = 1.2833$ "Edge distance factor"

$A0_{p.N} := S_{cr.Np}^{2} = 32400$ "Ideal pull out area"

$A_{p.N} := 2 \cdot \text{Min}\left(c_{1.cap}, C_{cr.Np}\right) \cdot \left(2 \cdot C_{cr.Np} + \left(n_{t.anchors} - 1\right) \cdot s_{1.cap}\right) = 81000$ "Group pull out area"

$N0_{Rk.p} := \pi \cdot d_{anchor.cap} \cdot h_{helix} \cdot \tau_{rk.ucr} = 49762.8276$ "Ideal anchor pull out capacity"

$N_{Rk.p} := N0_{Rk.p} \cdot \frac{A_{p.N}}{A0_{p.N}} \cdot \psi_{s.Np} \cdot \psi_{g.Np} \cdot \psi_{ec.Np} \cdot \psi_{re.Np} = 1.5459 \cdot 10^{5}$ "Group pull out capacity"

$\frac{\sum F_{axB.Ek}}{N_{Rk.p}}_{N} = 0.2282$ "Characteristic pull out utilization"

Concrete cone failure:

$\psi_{ec.N} := \text{Min}\left(\frac{1}{1 + 2 \cdot \frac{e_n}{S_{cr.N}}}, 1\right) = 0.9807$ "Eccentricity factor"

$\psi_{re.N} := \text{Min}\left(0.5 + \frac{h_{ef}}{200}, 1\right) = 1$ "Spalling factor"

$\psi_{s.N} := \text{Min}\left(0.7 + 0.3 \cdot \frac{c_{1.cap}}{C_{cr.N}}, 1\right) = 1$ "Edge distance factor"

$A0_{c.N} := S_{cr.N}^{2} = 90000$ "Ideal cone area"

$A_{c.N} := 2 \cdot \text{Min}\left(c_{1.cap}, C_{cr.N}\right) \cdot \left(2 \cdot C_{cr.N} + \left(n_{t.anchors} - 1\right) \cdot s_{1.cap}\right) = 1.71 \cdot 10^{5}$ "Group cone area"

$N0_{Rk.c} := k_{N0.Rk.c} \cdot \sqrt{f_{ck.cube.cap}} \cdot h_{ef}^{1.5} = 36000$ "Ideal cone capacity"

$N_{Rk.c} := N0_{Rk.c} \cdot \frac{A_{c.N}}{A0_{c.N}} \cdot \psi_{s.N} \cdot \psi_{re.N} \cdot \psi_{ec.N} = 67080.1907$ "Cone group capacity"

$\frac{\sum F_{axB.Ek}}{N_{Rk.c}}_{N} = 0.5258$ "Characteristic cone group capcatiy"

Splitting failure:

$\psi_{ec.N.sp} := \text{Min}\left(\frac{1}{1 + 2 \cdot \frac{e_n}{S_{cr.N}}}, 1\right) = 0.9807$ "Eccentricity factor"

$\psi_{re.N.sp} := \text{Min}\left(0.5 + \frac{h_{ef}}{200}, 1\right) = 1$ "Spalling factor"

$\psi_{s.N.sp} := \text{Min}\left(0.7 + 0.3 \cdot \frac{c_{1.cap}}{C_{cr.sp}}, 1\right) = 1$ "Edge distance factor"

$$\psi_{h.sp} := \mathrm{Min}\left(\frac{H_{concrete.depth}}{\mathrm{Min}\left(C_{cr.sp}, c_{1.cap}\right) + \mathrm{Min}\left(C_{cr.sp}, c_{2.cap}\right)}, 1.5\right) = 1$$ "concrete depth factor"

"ideal anchor splitting area"

$$A0_{c.N.sp} := S_{cr.sp}{}^{2} = 90000$$

$$A_{c.N.sp} := 2 \cdot \mathrm{Min}\left(c_{1.cap}, C_{cr.sp}\right) \cdot \left(2 \cdot C_{cr.sp} + \left(n_{t.anchors} - 1\right) \cdot s_{1.cap}\right) = 1.71 \cdot 10^{5}$$ "Group splitting area"

$$N0_{Rk.c.sp} := k_{N0.Rk.c} \cdot \sqrt{f_{ck.cube.cap}} \cdot h_{ef}{}^{1.5} = 36000$$ "Ideal anchor splitting capacity"

$$N_{Rk.c.sp} := N0_{Rk.c.sp} \cdot \frac{A_{c.N.sp}}{A0_{c.N.sp}} \cdot \psi_{s.N.sp} \cdot \psi_{re.N.sp} \cdot \psi_{ec.N.sp} \cdot \psi_{h.sp} = 67080.1907$$ "Group splitting capacity"

$$\frac{\sum F_{axB.Ek}}{N_{Rk.c.sp}}\,\mathrm{N} = 0.5258$$ "Characteristic splitting utilization"

Shear capacity:

Eccentricity and equivalent critical size and dirrection of shear force:

$$F_{zB.Ek} = \left[\begin{array}{cccc} 12.5 & -1.87 & -16.25 & -30.62 \end{array}\right] \mathrm{kN}$$ "Resulting vertical force"

$$Forces_{V.C} := Matrix\_remove\_positive_{ij}\left(F_{zB.Ek}\right)$$ "Resulting negative values"

$$Forces_{V.C} = \left[\begin{array}{cccc} 0 & -1.8737 & -16.2493 & -30.6249 \end{array}\right] \mathrm{kN}$$

$$F_{xB.Ek} = \left[\begin{array}{cccc} -0.75 & -0.75 & -0.75 & -0.75 \end{array}\right] \mathrm{kN}$$ "Horizontal shear forces"

$$r_{vertical} := \left[\begin{array}{cccc} 1.5 \cdot s_{1.cap} & 0.5 \cdot s_{1.cap} & (-0.5) \cdot s_{1.cap} & (-1.5) \cdot s_{1.cap} \end{array}\right]$$ "Placement of anchors from center of anchors"

$$e_{v.x} := \frac{\sum Prtoduct_{ij}\left(r_{vertical}, Forces_{V.C}\right)}{\sum Forces_{V.C}} = -98.0815$$ "Vertical eccentricity of shear force"

$$Force_{\alpha} := \mathrm{atan}\left(\frac{\sum F_{xB.Ek}}{\sum Forces_{V.C}}\right)$$ "Angle of resulting shear force

$$Force_{\alpha} = 0.0615 \ rad$$

$$e_{v} := \cos\left(Force_{\alpha}\right) \cdot e_{v.x}$$ "equivalent anchor group eccentricity"

$$e_{v} = -97.9 \ mm$$

$$F_{shear.concrete.tot} := \sqrt{\left(\sum Forces_{V.C}\right)^{2} + \left(\sum F_{xB.Ek}\right)^{2}}$$

$$F_{shear.concrete.tot} = 48840.1192 \ \mathrm{N}$$ "Equivalent anchor shear force"

Steel failure:

$V_{Rk.s} := n_{t.anchors} \cdot 0.5 \cdot A_{s.anchor} \cdot f_{uk} = 1.0959 \cdot 10^{5}$ "Characteristic steel capacity"

$\frac{F_{shear.concrete.tot}}{N_{Rk.s}} = 0.2228$ "Characteristic steel utilization"

Pry-out failure:

Because the anchor group is affected by a torsion moment, the critical pry-out capactiy is calculated for the critical bolt:

$\psi_{ec.N.crit} := 1$ "No eccentricity of loading for a singular bolt" "Eccentricity factor"

$\psi_{re.N} := \text{Min}\left(0.5 + \frac{h_{ef}}{200}, 1\right) = 1$ "Spalling factor"

$\psi_{s.N} := \text{Min}\left(0.7 + 0.3 \cdot \frac{c_{1.cap}}{C_{cr.N}}, 1\right) = 1$ "Edge distance factor"

$A0_{c.N} := S_{cr.N}^{2} = 90000$ "Ideal tension pry out area"

$A_{c.N.crit} := 2 \cdot \text{Min}\left(c_{1.cap}, C_{cr.N}\right) \cdot \left(C_{cr.N} + \frac{s_{1.cap}}{2}\right) = 58500$ "Tension pry-out area for critical anchor"

$N0_{Rk.c.crit} := k_{N0.Rk.c} \cdot \sqrt{f_{ck.cube.cap}} \cdot h_{ef}^{1.5} = 36000$ "Characteristic tension pry-out capactiy"

$N_{Rk.c.crit} := N0_{Rk.c} \cdot \frac{A_{c.N.crit}}{A0_{c.N}} \cdot \psi_{s.N} \cdot \psi_{re.N} \cdot \psi_{ec.N} = 22948.4863$ "Concrete tension cone failure of critical shear anchor"

Using the tension capactiy of the critical anchor, the pry-out failure for the critical anchor is calculated as:

$V_{Rk.cp} := k_{V.Rk.cp} \cdot N_{Rk.c.crit} = 45896.9726$ "Pry out faillure capacity"

$V_{Ek.crit.anchor} := \sqrt{F_{zB.Ek.crit}^{2} + F_{xB.Ek.crit}^{2}} = 30634.0984\ \text{N}$ "Characteristic load acting on critical shear anchor"

$\frac{V_{Ek.crit.anchor}}{V_{Rk.cp}} = 0.6675$ "Characteristic pry out utilization"

Concrete edge failure:

"Using the eccentriceties and force angel the factors are calculated"

$\psi_{ec.V} := \text{Min}\left(\sqrt{\frac{1}{1 + \frac{2 \cdot e_{v}}{3 \cdot c_{1.cap}}}}, 1\right) = 1$

$$\psi_{\alpha.V} := \mathrm{Max}\left(\sqrt{\frac{1}{\left(\cos\left(Force_{\alpha}\right)\right)^2 + \left(\frac{\sin\left(Force_{\alpha}\right)}{2.5}\right)^2}}, 1\right) = 1.0016$$ "Resultant force angel factor"

$$\psi_{h.V} := \mathrm{Max}\left(\left(\frac{1.5 \cdot c_{1.cap}}{\mathrm{Min}\left(H_{concrete.depth}, 1.5 \cdot c_{1.cap}\right)}\right)^{\frac{1}{2}}, 1\right) = 1$$ "Concrete depth factor"

$$A0_{c.V} := 4.5 \cdot c_{1.cap}{}^2 = 1.3781 \cdot 10^5$$ "Ideal anchor edge area"

$$A_{c.V} := 1.5 \cdot c_{1.cap} \cdot \left(2 \cdot 1.5 \cdot c_{1.cap} + 3 \cdot s_{1.cap}\right) = 2.0869 \cdot 10^5$$ "Anhor group edge area"

$$\alpha_{V0.Rk.c} := 0.1 \cdot \left(\frac{h_{ef}}{c_{1.cap}}\right)^{\frac{1}{2}} = 0.0756$$

$$\beta_{V0.Rk.c} := 0.1 \cdot \left(\frac{d_{anchor.cap}}{c_{1.cap}}\right)^{0.2} = 0.0585$$

$$V0_{Rk.c} := k_{V0.Rk.c} \cdot d_{anchor.cap}{}^{\alpha_{V0.Rk.c}} \cdot h_{ef}{}^{\beta_{V0.Rk.c}} \cdot \sqrt{f_{ck.cube.cap}} \cdot c_{1.cap}{}^{1.5} = 31086.6583$$

$$V_{Rk.c} := V0_{Rk.c} \cdot \frac{A_{c.V}}{A0_{c.V}} \cdot \psi_{h.V} \cdot \psi_{\alpha.V} \cdot \psi_{ec.V} = 47148.8572 \ N$$ "Concrete edge shear capacity"

$$\frac{F_{shear.concrete.tot}}{V_{Rk.c}\ \mathrm{N}} = 1.0359$$ "Characteristic edge capactiy utilization"

Combined shear and tension:

The critical capactiy ration is calculated from the critical uti8lization of tension and shear":

$$\left(\frac{F_{shear.concrete.tot}}{V_{Rk.c}\ \mathrm{N}}\right)^2 + \left(\frac{\sum F_{axB.Ek}}{N_{Rk.c}\ \mathrm{N}}\right)^2 = 1.3495$$ "Characteristic anchor utilization"

The characteristic capactiy for the anchor group is far exceeded...

Design utilization of characteristic load:

$$\left(\frac{1.5 \cdot F_{shear.concrete.tot}}{V_{Rk.c}\ \mathrm{N}}\right)^2 + \left(\frac{1.5 \cdot \left(\sum F_{axB.Ek}\right)}{N_{Rk.c}\ \mathrm{N}}\right)^2 = 3.0363$$ "Design anchor utilization"

Profile 8-2B-R

$g := 9.81 \frac{N}{kg}$

Dimensions and material characteristics:

Concrete-steel connection with C20/25 and M12 Anchors:

$d_{x.anchor} := 90\ mm$ "Horizontal screw distance as well as edge distance"

$e_{x.anchor} := 90\ mm$ "Steel edge distance of anchors"

$d_{z.anchor} := 60\ mm$ "Edge distance for concrete steel contact"

$n_{Bx} := 4$ "Number of horizontal anchors in support B"

$d_{anchor} := 12\ mm$ "Anchor diameter"

$f_{ck.cube} := 25 \frac{N}{mm^2}$ "Cubed compressive strength"

$E_{cm} := 29962 \frac{N}{mm^2}$ "C20/25 elastic modulus"

$E_s := 200000 \frac{N}{mm^2}$ "Elastic modulus of anchors"

CLT panel

$H_{CLT} := 3\ m$ "Height of CLT panel"

$B_{CLT} := 4\ m$ "Width of CLT panel"

$t_{CLT} := 0.1\ m$ "CLT thickness"

$\rho_{CLT} := 385 \frac{kg}{m^3}$ "CLT density"

$f_{c.90.k} := 2.5 \frac{N}{mm^2}$ "CLT compression strength perpendicular to wood grain"

$m_{CLT} := H_{CLT} \cdot B_{CLT} \cdot t_{CLT} \cdot \rho_{CLT} = 462\ kg$ "Element weight"

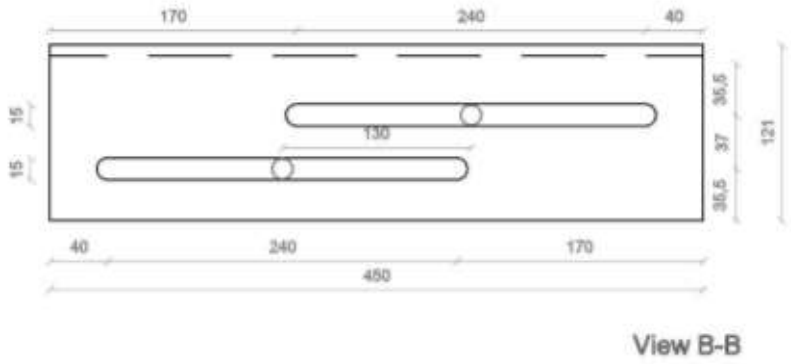

View B-B

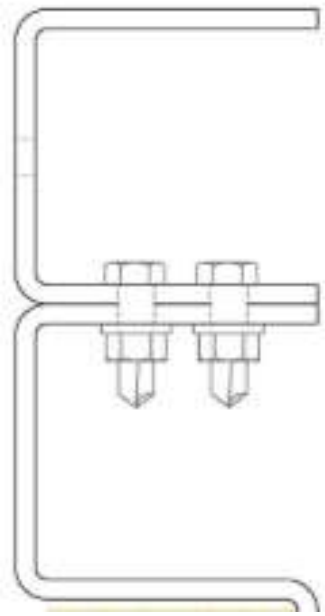

Profile and support D:

$e_1 := 58.00\ mm$ "horizontal edge distance end screw"

$e_2 := 58.00\ mm$ "Vertical edge distance of end screws"

$p_1 := 37.11\ mm$ "Internal horizontal screw distance"

$p_2 := 42.00\ mm$ "Internal vertical screw distance"

$H := 200\ mm$ "Vertical contact of underlying CLT"

$B := 450\ mm$ "Horizontal contact of underlying CLT"

$t_p := 8\ mm$ "Plate thickness"

$n_{xD} := 10$ "Number of screws per row"

$n_{zD} := 3$ "Number of screws per column"

$n_D := n_{xD} \cdot n_{zD}$ "Total number of screws"

$f_u := 235\ \frac{N}{mm^2}$ "Plate yield capacity"

$m_{8\_2B} := 11\ kg$ "Profile mass"

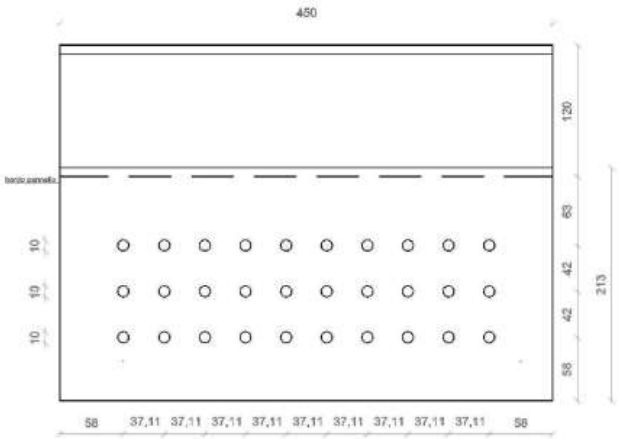

Front view

Concrete:

$f_{ck.cube} = 25\ \frac{N}{mm^2}$ "characteristic cubed strength"

HBS plate dimensions and static values:

"The values of the screws were retrived from the Rothoblaas catalog. Wil refere to the source in final paper."

$d_1 := 8\ mm$

$d_k := 14.5\ mm$

$d_2 := 5.4\ mm$

$d_s := 58\ mm$

$t_1 := 3.4\ mm$

$d_{uk} := 10\ mm$

$d_v := 5.0\ mm$

$L := 80\ mm$

$b := 55\ mm$

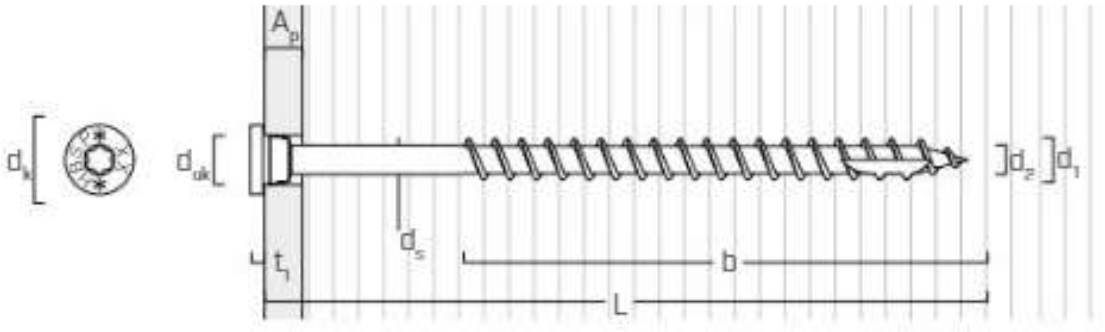

$n := 30$ "Number of screws"

$M_{y.k} := 20057\ N\ mm$ "Charicaristic yield moment"

$f_{ax.k} := 11.7\ \frac{N}{mm^2}$ "Charicaristic withdrawal resistance"

$\rho_a := 350\ \frac{N}{mm^2}$ "referance density for withdrawal resistance"

$f_{head} := 10.5\ \frac{N}{mm^2}$ "Characteristic head-pull through resistance"

$f_{tens.k} := 20.1\ kN$ "Characteristic tensile strenght"

$\alpha := 90\ deg$ "Angel of screws according to the grain"

$k_{ax} := 1$ "For angle 90 deg"

$K_\beta := 1$ "For timber"

$F_{ax.Rk.screw} := 3.954\ kN$ "Axial withdrawal capacity per bolt"

$F_{vD.Rk} := 5.9537\ kN$ “Characteristic shear resistance per screw”

Friction bolts

$\mu_p := 0.3$ "Friction between plate and bolt"

$n_C := 2$ "Number of friction bolts"

$n_{fb} := 2$ "Number of friction surfaces per bolt"

Distances between supports and support criteria:

"Distances from connection A and D were calculated from the center of the outer edge of the screw row facing inwards towards the profile.

Reactions	Supports			
	A	B	C	D
Δx	Free	Free	Free	Fixed
Δy	Free	Fixed	Free	Free
Δz	Free	Fixed	Free	Free
ϕx	Fixed	Fixed	Free	Fixed
ϕy	Fixed	Fixed	Free	Fixed
ϕz	Fixed	Fixed	Free	Fixed

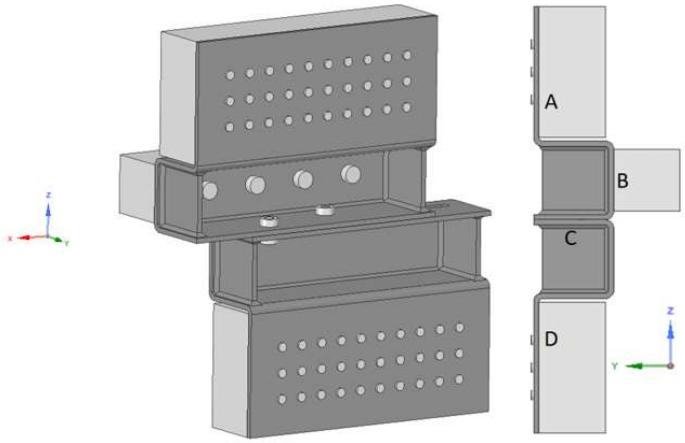

"Global distances for tension profile"

$d_{yAB} := -0.121\ \text{m}$

$d_{zAB} := (-0.063 - 0.06)\ \text{m}$

$d_{yBC} := 0.067\ \text{m}$

"midd point between bolts"

$d_{zBC} := (-0.06)\ \text{m}$

$d_{xCD} := (-0.12)\ \text{m}$

$d_{yCD} := -d_{yBC} - d_{yAB} = 0.054\ \text{m}$

$d_{zCD} := (-0.184)\ \text{m}$

$d_{xBD} := d_{xCD}$

$d_{yBD} := -d_{yAB} = 0.121\ \text{m}$

"Vertical load center for support C approximated from Ansys"

$d_{zBD} := d_{zBC} + d_{zCD} = -0.244\ \text{m}$

"Ajusted distances with regards to the behaviour of support C for compressed profile"

$d_{yBC.c} := \left(d_{yBC}\right) = 67\ \text{mm}$

"Center of horizontal force acting on fricition connectort"

$d_{yCD.c} := -d_{yAB} - d_{yBC.c} = 54\ \text{mm}$

$d_{xBC.c} := \frac{d_{zBC}}{\left(d_{zAB} + d_{zBC}\right)} \cdot d_{xBD} = -39.3443\ \text{mm}$

"Interpolated distaces for horizontal load center based on interpolated relative distance between support B and D"

$d_{xCD.c} := d_{xBD} - d_{xBC.c} = -80.6557\ \text{mm}$

$d_{yBC.cv} := \left(\frac{2}{3} \cdot d_{yBD}\right) = 80.6667\ \text{mm}$

"Center of vertical force acting on fricition connectort"

$d_{yCD.cv} := -d_{yAB} - d_{yBC.cv} = 40.3333\ \text{mm}$

External forces acting on system:

Forces acting on compression profile:

Following the theory of external force application of profiles, an itnitial critical horizontal force is assumed:

$P_x := 30000\ \text{N}$ "Total external horizontal force acting on compression profile"

For n.floors it is assumed that the mass distribution an floor height is constant equal to height of CLT element:

$n_{floors} := 4$ "Number of floors in building"

$z := Height_i\left(n_{floors}, H_{CLT}\right) = [\,3\ \ 6\ \ 9\ \ 12\,]\ \text{m}$ "Floor height"

$P_{xB} := P_x \cdot \frac{\sum_z 1}{z} = 3000\ \text{N}$ "Horizontal force in support B for profile in tension"

$P_{xA} := P_x - P_{xB} = 27000\ \text{N}$ "Horizontal force in support A for compressed profile"

The average total force acting on the two profiles and on support A of the two profiles are approximated:

$\lambda := 0.608$ "Reduction factor for maximum vertical load in tension profile"

$P_{x.avg} := \frac{(1+\lambda)\cdot P_x}{2} = 24120\ \text{N}$ "Total force on two profiles"

$P_{xA.avg} := \frac{(1+\lambda)\cdot P_{xA}}{2} = 21708\ \text{N}$ "Total vertical force in connection A of the profiles"

Force from weight of a complete CLT element with four profile halfs:

$P_{element} := (-g)\cdot\left(m_{CLT} + m_{8\_2B}\cdot 4\right) = -4964\ \text{N}$ "Equivalent system weight per profile"

Equivalent vertical force on tension and compression profiles:

$P_{zD} := P_{x.avg}\cdot\left(\frac{H_{CLT}}{B_{CLT}-B}\right) + \frac{P_{element}}{4} = 19142\ \text{N}$ "Vertical force in compression support D accounting for system weight"

$P_{zD.t} := \left(-P_{x.avg}\right)\cdot\left(\frac{H_{CLT}}{B_{CLT}-B}\right) + \frac{P_{element}}{4} = -21624\ \text{N}$ "Vertical force in tension support D"

The vertical force of the system above is then approximated from P.xA.avg:

$$P_{zA} := P_{xA.avg} \cdot \left(\frac{H_{CLT}}{B_{CLT} - B} \right) + \frac{P_{element}}{4} = 17104 \text{ N}$$ "Vertical force in compression support A"

$$P_{zA.t} := \left(- P_{xA.avg} \right) \cdot \left(\frac{H_{CLT}}{B_{CLT} - B} \right) + \frac{P_{element}}{4} = -19586 \text{ N}$$ "Vertical force in tension support A"

Pretension of friction connection:

The pretension requrires for the compressed profile is calculated for the two bolts:

$k_s := 0.93$ EC3 table 3.6 is to conservative

$$F_{p.C.compression} := \frac{P_x - \left| P_{zD} \right| \cdot \mu_p}{\left(k_s \cdot n_{fb} \cdot n_C \cdot \mu_p \right)}$$

$F_{p.C.compression} = 21.736 \text{ kN}$ "Maximum pretension"

The friction force resulting from the bolt pretension is calculated for the tension connection:

$$F_{s.Rk.tension} := k_s \cdot \mu_p \cdot n_{fb} \cdot \left(n_C \cdot F_{p.C.compression} - \left| \frac{P_{zD.t}}{n_{fb}} \right| \right) = 18224.2462 \text{ N}$$

$F_{s.Rk.tension} = 18.2242 \text{ kN}$ "Resulting friction capactiy for profile in tension"

The total friction force of the system is calculated as the sum of the forur friction bolts:

$$F_{s.Rk.tot} := F_{s.Rk.tension} + P_x$$

$F_{s.Rk.tot} = 48.2242 \text{ kN}$ = $2 \cdot P_{x.avg} = 48.24 \text{ kN}$

Finally λ is adjusted until the average vertical force equals the friction force.

The horizontal force distribution for the tension profile is approximated:

$P_{xA.t} := \left(- P_{xA} \right) \cdot \lambda = -16416 \text{ N}$ "Horizontal force in support A for compressed profile"

$P_{xB.t} := \left(- P_{xB} \right) \cdot \lambda = -1824 \text{ N}$ "Horizontal force in support B for profile in tension"

$P_{x.t} := P_{xA.t} + P_{xB.t} = -18240 \text{ N}$ "Roughly equivalent to tension friction force"

Steel - CLT connection

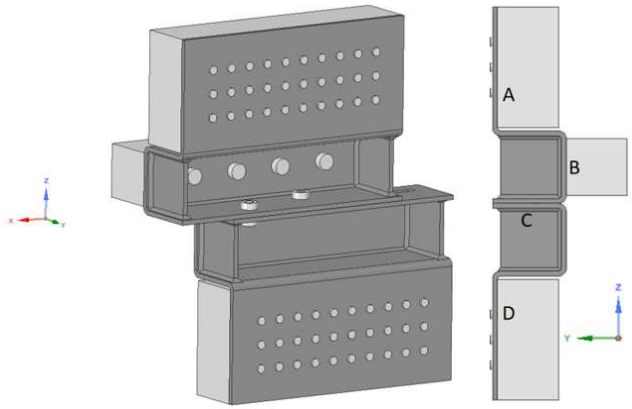

Compression profile:

Reaction forces and moments:

Shear reaction from applied shear force:

"Shear reaction in screws acting opposite of the applied shear force"

$$R_{xD.Ek} := -\frac{P_x}{n_D}$$ "Horizontal shear force per screw"

$$R_{xD.Ek} = -1\ \text{kN}$$

Shear reaction from applied normal force:

"Shear reaction acting opposite of applied force"

$$R_{zD.Ek} := -\frac{P_{zD}}{n_D}$$ "Vertical shear force per screw"

$$R_{zD.Ek} = -0.6381\ \text{kN}$$

The moment reaction is calculated as a canitlever with point loads in point C:

Moment about y-axis:

$$R_{xBD} := P_x$$ "Vertical reaction force acting on system B-D"

$$R_{zBD} := P_{zD}$$ "Horizontal reaction froce in B for system B-D"

$$M_{yD} := R_{xBD} \cdot d_{zCD} + R_{zBD} \cdot d_{xCD}$$

$$M_{yD} = -7.8171\ \text{kN m}$$

Moment about x-axis:

M.x was calculated as a cantilecer with a reactionforce R.zC.

$$R_{zCD} := -P_{zD}$$ "Vertical reaction force in C for system C-D"

$$M_{xD} := R_{zCD} \cdot d_{yCD.cv} = -0.77\ \text{kN m}$$

$$M_{xD} = -0.7721\ \text{kN m}$$

Moment about z-axis:

Reaction moment M.z was calculated as a cantilever with a reaction force R.xC

$$R_{xC} := P_x$$ "Horizontal reaction force in C for system C-D"

$$M_{zD} := R_{xC} \cdot \left(-d_{yCD.c}\right) = -1.62\ \text{kN m}$$

$$M_{zD} = -1.62\ \text{kN m}$$

Shear forces due to M.y

The shear forces ar calculated according to 2.3 In plane eccentrically loaded connections is used for these calculations:

The distances from geometrical connection center

$$r_{Dz.My} := \begin{bmatrix} p_2 & p_2 & p_2 & p_2 & p_2 & p_2 & p_2 & p_2 & p_2 & p_2 \\ 0 & 0 & 0 & 0 & 0 & 0 & 0 & 0 & 0 & 0 \\ -p_2 & -p_2 & -p_2 & -p_2 & -p_2 & -p_2 & -p_2 & -p_2 & -p_2 & -p_2 \end{bmatrix}$$

$$r_{Dx.My} := \begin{bmatrix} 4.5\cdot p_1 & 3.5\cdot p_1 & 2.5\cdot p_1 & 1.5\cdot p_1 & 0.5\cdot p_1 & -(0.5\cdot p_1) & -(1.5\cdot p_1) & -(2.5\cdot p_1) & -(3.5\cdot p_1) & -(4.5\cdot p_1) \\ 4.5\cdot p_1 & 3.5\cdot p_1 & 2.5\cdot p_1 & 1.5\cdot p_1 & 0.5\cdot p_1 & -(0.5\cdot p_1) & -(1.5\cdot p_1) & -(2.5\cdot p_1) & -(3.5\cdot p_1) & -(4.5\cdot p_1) \\ 4.5\cdot p_1 & 3.5\cdot p_1 & 2.5\cdot p_1 & 1.5\cdot p_1 & 0.5\cdot p_1 & -(0.5\cdot p_1) & -(1.5\cdot p_1) & -(2.5\cdot p_1) & -(3.5\cdot p_1) & -(4.5\cdot p_1) \end{bmatrix}$$

Distance from connection center to screws:

$$r_{D.My} := SRSS_{ij}\left(r_{Dz.My}, r_{Dx.My}\right)$$ "Use the sum of square formula for the matrices"

$$r_{D.My} = \begin{bmatrix} 0.1722 & 0.1365 & 0.1018 & 0.0697 & 0.0459 & 0.0459 & 0.0697 & 0.1018 & 0.1365 & 0.1722 \\ 0.167 & 0.1299 & 0.0928 & 0.0557 & 0.0186 & 0.0186 & 0.0557 & 0.0928 & 0.1299 & 0.167 \\ 0.1722 & 0.1365 & 0.1018 & 0.0697 & 0.0459 & 0.0459 & 0.0697 & 0.1018 & 0.1365 & 0.1722 \end{bmatrix} \text{m}$$

The squared value of the distance:

$$r_{D.My.sq} := Prtoduct_{ij}\left(r_{D.My}, r_{D.My}\right)$$ "Use the product formula to calculate squared values"

$$r_{D.My.sq} = \begin{bmatrix} 0.0297 & 0.0186 & 0.0104 & 0.0049 & 0.0021 & 0.0021 & 0.0049 & 0.0104 & 0.0186 & 0.0297 \\ 0.0279 & 0.0169 & 0.0086 & 0.0031 & 0.0003 & 0.0003 & 0.0031 & 0.0086 & 0.0169 & 0.0279 \\ 0.0297 & 0.0186 & 0.0104 & 0.0049 & 0.0021 & 0.0021 & 0.0049 & 0.0104 & 0.0186 & 0.0297 \end{bmatrix} \text{m}^2$$

The torsion formula is the used to calculate the force distribution:

$$F_{Dv.My} := \frac{\left(-M_{yD}\right)\cdot r_{D.My}}{\sum r_{D.My.sq}}$$ "Shear distribution"

$$F_{Dv.My} = \begin{bmatrix} 3.58 & 2.84 & 2.12 & 1.45 & 0.95 & 0.95 & 1.45 & 2.12 & 2.84 & 3.58 \\ 3.47 & 2.7 & 1.93 & 1.16 & 0.39 & 0.39 & 1.16 & 1.93 & 2.7 & 3.47 \\ 3.58 & 2.84 & 2.12 & 1.45 & 0.95 & 0.95 & 1.45 & 2.12 & 2.84 & 3.58 \end{bmatrix} \text{kN}$$

As the critical connector would always be one of the four outer connectors, the sign convention would be trivial.

Equivalent shear components:

$$F_{xD.My} := Division_{ij}\left(Prtoduct_{ij}\left(F_{Dv.My}, r_{Dz.My}\right), r_{D.My}\right)$$ "Shear component in x-axis"

$$F_{xD.My} = \begin{bmatrix} 0.87 & 0.87 & 0.87 & 0.87 & 0.87 & 0.87 & 0.87 & 0.87 & 0.87 & 0.87 \\ 0 & 0 & 0 & 0 & 0 & 0 & 0 & 0 & 0 & 0 \\ -0.87 & -0.87 & -0.87 & -0.87 & -0.87 & -0.87 & -0.87 & -0.87 & -0.87 & -0.87 \end{bmatrix} \text{kN}$$

$$F_{zD.My} := Division_{ij}\left(Prtoduct_{ij}\left(F_{Dv.My}, r_{Dx.My}\right), r_{D.My}\right)$$ "Shear component in z-axis"

$$F_{zD.My} = \begin{bmatrix} 3.47 & 2.7 & 1.93 & 1.16 & 0.39 & -0.39 & -1.16 & -1.93 & -2.7 & -3.47 \\ 3.47 & 2.7 & 1.93 & 1.16 & 0.39 & -0.39 & -1.16 & -1.93 & -2.7 & -3.47 \\ 3.47 & 2.7 & 1.93 & 1.16 & 0.39 & -0.39 & -1.16 & -1.93 & -2.7 & -3.47 \end{bmatrix} \text{kN}$$

screw tension and CLT compression due to M.x:

The method described in 2.4 out of plane eccentrically loaded bolt connection is ues with maximum elastic strain for screws at characteristical axial screw capactiy equal to maximum elastic strain of CLT at characteristic compression capacity:

The N.A distance percentage factor is calculated:

$\lambda_{CLT.Mx} := 0.549$ "Percentage of connection distance from CLT edge"

$c_{MxD} := \left(H - e_2\right) \cdot \lambda_{CLT.Mx} = 0.07796\ m$ "Edge distance for CLT"

The resulting distance from N.A to screws are calculated from the transposed matrix:

$$r\_initial_{D.Mx} := \begin{bmatrix} e_2 - c_{MxD} & e_2 + p_2 - c_{MxD} & e_2 + 2 \cdot p_2 - c_{MxD} \\ e_2 - c_{MxD} & e_2 + p_2 - c_{MxD} & e_2 + 2 \cdot p_2 - c_{MxD} \\ e_2 - c_{MxD} & e_2 + p_2 - c_{MxD} & e_2 + 2 \cdot p_2 - c_{MxD} \\ e_2 - c_{MxD} & e_2 + p_2 - c_{MxD} & e_2 + 2 \cdot p_2 - c_{MxD} \\ e_2 - c_{MxD} & e_2 + p_2 - c_{MxD} & e_2 + 2 \cdot p_2 - c_{MxD} \\ e_2 - c_{MxD} & e_2 + p_2 - c_{MxD} & e_2 + 2 \cdot p_2 - c_{MxD} \\ e_2 - c_{MxD} & e_2 + p_2 - c_{MxD} & e_2 + 2 \cdot p_2 - c_{MxD} \\ e_2 - c_{MxD} & e_2 + p_2 - c_{MxD} & e_2 + 2 \cdot p_2 - c_{MxD} \\ e_2 - c_{MxD} & e_2 + p_2 - c_{MxD} & e_2 + 2 \cdot p_2 - c_{MxD} \\ e_2 - c_{MxD} & e_2 + p_2 - c_{MxD} & e_2 + 2 \cdot p_2 - c_{MxD} \end{bmatrix}^T = \begin{bmatrix} -0.02\ m \\ 0.022\ m & \cdots \\ 0.064\ m \end{bmatrix}$$

"Distances from N.A for screws"

The screwes in the compression area are not allowed to contribute to moment resistance and are removed:

$$r_{D.Mx} := Matrix\_remove\_negative_{ij}\left(r\_initial_{D.Mx}\right)$$

$$r_{D.Mx} = \begin{bmatrix} 0 & 0 & 0 & 0 & 0 & 0 & 0 & 0 & 0 & 0 \\ 0.022 & 0.022 & 0.022 & 0.022 & 0.022 & 0.022 & 0.022 & 0.022 & 0.022 & 0.022 \\ 0.064 & 0.064 & 0.064 & 0.064 & 0.064 & 0.064 & 0.064 & 0.064 & 0.064 & 0.064 \end{bmatrix} m$$

The squared distance is calcutated:

$$r_{D.Mx.sq} := Prtoduct_{ij}\left(r_{D.Mx}, r_{D.Mx}\right)$$

Distance to screw force resultant is calculated from the sum of moments about the N.A:

$$dm_{screw.Mx} := \frac{\sum r_{D.Mx.sq}}{\sum r_{D.Mx}}$$

$dm_{screw.Mx} = 53.29\ mm$ "Distance from neutral axis to resultant force in Screws"

The resulting moment arm is calculated from the center of the screw force and the equivalent position of the triangular CLT compression force:

$$z_{D.Mx} := dm_{screw.Mx} + \frac{2}{3} \cdot c_{MxD} \qquad \text{"Connection moment arm"}$$

$$z_{D.Mx} = 105.26 \text{ mm}$$

Resulting moments on compression and tension side from the N.A:

$$M_{x.screws} := \left| M_{xD} \right| \cdot \frac{dm_{screw.Mx}}{z_{D.Mx}} = 0.391 \text{ kN m} \qquad \text{"Moment acting on screws from N.A"}$$

$$M_{x.CLT} := \left| M_{xD} \right| \cdot \frac{\frac{2}{3} \cdot c_{MxD}}{z_{D.Mx}} = 0.381 \text{ kN m} \qquad \text{"Moment acting on CLT from N.A"}$$

Resulting tension forces in screws:

$$F_{Dax.Mx} := \frac{M_{x.screws} \cdot r_{D.Mx}}{\left(\sum r_{D.Mx.sq} \right)} \qquad \text{"Force distribution in screws"}$$

$$F_{Dax.Mx} = \begin{bmatrix} 0 & 0 & 0 & 0 & 0 & 0 & 0 & 0 & 0 & 0 \\ 0.1878 & 0.1878 & 0.1878 & 0.1878 & 0.1878 & 0.1878 & 0.1878 & 0.1878 & 0.1878 & 0.1878 \\ 0.5457 & 0.5457 & 0.5457 & 0.5457 & 0.5457 & 0.5457 & 0.5457 & 0.5457 & 0.5457 & 0.5457 \end{bmatrix} \text{kN}$$

$$\sum F_{Dax.Mx} = 7334.8611 \text{ N} \qquad \text{"Sum of tension forces"}$$

Maximum compression stress of CLT:

$$I_{z.CLT} := \frac{B \cdot c_{MxD}^{3}}{3} = 7.1068 \cdot 10^{-5} \text{ m}^4 \qquad \text{"Moment of inertia of CLT about N.A"}$$

$$\sigma_{max.CLT.Mx} := \frac{M_{x.CLT} \cdot c_{MxD}}{I_{z.CLT}} = 0.4182 \frac{\text{N}}{\text{mm}^2} \qquad \text{"Maximum stress acting on CLT"}$$

Force resultant in CLT:

$$\frac{\sigma_{max.CLT.Mx} \cdot c_{MxD}}{2} \cdot B = 7334.8611 \text{ N} \qquad \text{"Sum of compression forces"}$$

Maximum screw strain:

The maximum strain of the screws and CLT were both calculated considering the maximum CLT strain perpendicular to the grain, with the maximum strain asumed to act at the characteristic screw tension capacity:

$$\varepsilon_{CLT.Mx} := \frac{\sigma_{max.CLT.Mx}}{f_{c.90.k}} \cdot 0.0083 = 0.0014 \qquad \text{"Maximum strain on CLT"}$$

$$\varepsilon_{screw.Mx} := \frac{\max\left(F_{Dax.Mx} \right)}{F_{ax.Rk.screw}} \cdot 0.0083 = 0.0011 \qquad \text{Maximum strain in screws"}$$

The strain ratio of change along the connecton is then calculated for the tension and compression part:

$$\varepsilon'_{CLT} := \frac{\varepsilon_{CLT.Mx}}{c_{MxD}} = 0.0178 \cdot \frac{1}{m}$$ "CLT strain/distrance ratio"

$$\varepsilon'_{screw} := \frac{\varepsilon_{screw.Mx}}{e_2 + 2 \cdot p_2 - c_{MxD}} = 0.0179 \cdot \frac{1}{m}$$ "Screw strain/distrance ratio"

The resulting rate of change should be zero when the neurtal axis has been determined correctly trough the ajustment of λ.CLT.Mx:

$$\varepsilon'_{CLT} - \varepsilon'_{screw} = -7.7455 \cdot 10^{-5} \cdot \frac{1}{m}$$

screw tension and CLT compression due to M.z:

The same procedure as for M.x is used for the force calculations of M.z

$$\lambda_{CLT.Mz} := 0.248$$

$$c_{MzD} := \left(B - e_1\right) \cdot \lambda_{CLT.Mz} = 0.0972 \text{ m}$$

$$\left(r\_initial_{D.Mz}\right) := \begin{bmatrix} e_1 + 9 \cdot p_1 - c_{MzD} & e_1 + 9 \cdot p_1 - c_{MzD} & e_1 + 9 \cdot p_1 - c_{MzD} \\ e_1 + 8 \cdot p_1 - c_{MzD} & e_1 + 8 \cdot p_1 - c_{MzD} & e_1 + 8 \cdot p_1 - c_{MzD} \\ e_1 + 7 \cdot p_1 - c_{MzD} & e_1 + 7 \cdot p_1 - c_{MzD} & e_1 + 7 \cdot p_1 - c_{MzD} \\ e_1 + 6 \cdot p_1 - c_{MzD} & e_1 + 6 \cdot p_1 - c_{MzD} & e_1 + 6 \cdot p_1 - c_{MzD} \\ e_1 + 5 \cdot p_1 - c_{MzD} & e_1 + 5 \cdot p_1 - c_{MzD} & e_1 + 5 \cdot p_1 - c_{MzD} \\ e_1 + 4 \cdot p_1 - c_{MzD} & e_1 + 4 \cdot p_1 - c_{MzD} & e_1 + 4 \cdot p_1 - c_{MzD} \\ e_1 + 3 \cdot p_1 - c_{MzD} & e_1 + 3 \cdot p_1 - c_{MzD} & e_1 + 3 \cdot p_1 - c_{MzD} \\ e_1 + 2 \cdot p_1 - c_{MzD} & e_1 + 2 \cdot p_1 - c_{MzD} & e_1 + 2 \cdot p_1 - c_{MzD} \\ e_1 + p_1 - c_{MzD} & e_1 + p_1 - c_{MzD} & e_1 + p_1 - c_{MzD} \\ e_1 - c_{MzD} & e_1 - c_{MzD} & e_1 - c_{MzD} \end{bmatrix}^T$$

$$r\_initial_{D.Mz} = \begin{bmatrix} 294.8 & 257.7 & 220.6 & 183.4 & 146.3 & 109.2 & 72.1 & 35 & -2.1 & -39.2 \\ 294.8 & 257.7 & 220.6 & 183.4 & 146.3 & 109.2 & 72.1 & 35 & -2.1 & -39.2 \\ 294.8 & 257.7 & 220.6 & 183.4 & 146.3 & 109.2 & 72.1 & 35 & -2.1 & -39.2 \end{bmatrix} \text{ mm}$$

$$r_{D.Mz} := Matrix\_remove\_negative_{ij}\left(r\_initial_{D.Mz}\right)$$

$$r_{D.Mz.sq} := Prtoduct_{ij}\left(r_{D.Mz}, r_{D.Mz}\right)$$

$$F_{Dax.Mz} := \frac{M_{zD} \cdot r_{D.Mz}}{\sum r_{D.Mz.sq}}$$

$$F_{Dax.Mz} = \begin{bmatrix} -0.5781 & -0.5053 & -0.4325 & -0.3598 & -0.287 & -0.2142 & -0.1414 & -0.0686 & 0 & 0 \\ -0.5781 & -0.5053 & -0.4325 & -0.3598 & -0.287 & -0.2142 & -0.1414 & -0.0686 & 0 & 0 \\ -0.5781 & -0.5053 & -0.4325 & -0.3598 & -0.287 & -0.2142 & -0.1414 & -0.0686 & 0 & 0 \end{bmatrix} \text{ kN}$$

Distance to screw force resultant:

$$dm_{screw.Mz} := \frac{\sum r_{D.Mz.sq}}{\sum r_{D.Mz}}$$

$dm_{screw.Mz} = 208.74\ \text{mm}$ "Distance from neutral axis to resultant force in Screws"

Resulting moment arm:

$z_{D.Mz} := dm_{screw.Mz} + \frac{2}{3} \cdot c_{MzD}$ "Connection moment arm"

$z_{D.Mz} = 273.55\ \text{mm}$

Resulting moments on compression and tension side:

$M_{z.screws} := \left|M_{zD}\right| \cdot \frac{dm_{screw.Mz}}{z_{D.Mz}} = 1.236\ \text{kN m}$ "Moment acting on screws from N.A"

$M_{z.CLT} := \left|M_{zD}\right| \cdot \frac{\frac{2}{3} \cdot c_{MzD}}{z_{D.Mz}} = 0.384\ \text{kN m}$ "Moment acting on CLT from N.A"

Resulting tension forces in screws:

$F_{Dax.Mz} := \frac{M_{z.screws} \cdot r_{D.Mz}}{\left(\sum r_{D.Mz.sq}\right)}$ "Force distribution in screws"

$$F_{Dax.Mz} = \begin{bmatrix} 0.4411 & 0.3856 & 0.3301 & 0.2745 & 0.219 & 0.1635 & 0.1079 & 0.0524 & 0 & 0 \\ 0.4411 & 0.3856 & 0.3301 & 0.2745 & 0.219 & 0.1635 & 0.1079 & 0.0524 & 0 & 0 \\ 0.4411 & 0.3856 & 0.3301 & 0.2745 & 0.219 & 0.1635 & 0.1079 & 0.0524 & 0 & 0 \end{bmatrix} \text{kN}$$

$\sum F_{Dax.Mz} = 5922\ \text{N}$ "Sum of tension forces"

Maximum compression stress of CLT:

$I_{x.CLT} := \frac{H \cdot c_{MzD}^{3}}{3} = 6.1252 \cdot 10^{7}\ \text{mm}^{4}$ "Moment of inertia of CLT about N.A"

$\sigma_{max.CLT.Mz} := \frac{M_{z.CLT} \cdot c_{MzD}}{I_{x.CLT}} = 0.6092\ \frac{\text{N}}{\text{mm}^{2}}$ "Maximum stress acting on CLT"

Force resultant in CLT:

$\frac{\sigma_{max.CLT.Mz} \cdot c_{MzD}}{2} \cdot H = 5922\ \text{N}$ "Sum of compression forces"

Maximum screw strain:

$$\varepsilon_{CLT.Mz} := \frac{\sigma_{max.CLT.Mz}}{f_{c.90.k}} \cdot 0.0083 = 0.002$$ "Maximum strain on CLT"

$$\varepsilon_{screw.Mz} := \frac{\max\left(F_{Dax.Mz}\right)}{F_{ax.Rk.screw}} \cdot 0.0083 = 0.0009$$ Maximum strain in screws"

Strain ratio:

$$\varepsilon'_{CLT.Mz} := \frac{\varepsilon_{CLT.Mz}}{c_{MzD}} = 0.0208 \cdot \frac{1}{m}$$ "CLT strain/distrance ratio"

$$\varepsilon'_{screw.Mz} := \frac{\varepsilon_{screw.Mz}}{\left|e_2 + 2 \cdot p_2 - c_{MzD}\right|} = 0.0207 \cdot \frac{1}{m}$$ "Screw strain/distrance ratio"

$$\varepsilon'_{CLT.Mz} - \varepsilon'_{screw.Mz} = 0.0001 \cdot \frac{1}{m}$$

Tension profile:
Reaction forces and moments in

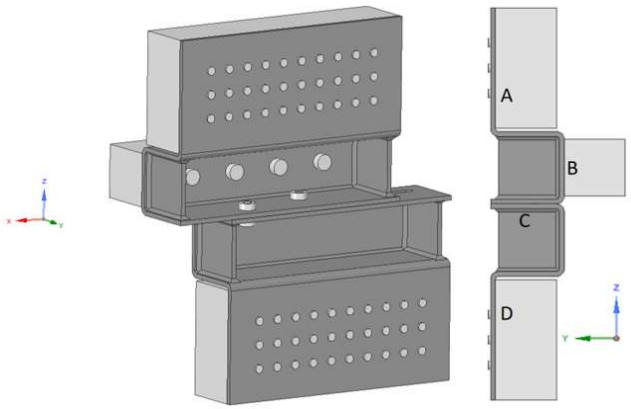

Shear reaction from applied shear force:

Shear reaction in screws acting opposite of the applied shear force:

$$R_{xD.t.Ek} := -\frac{P_{x.t}}{n_D}$$ "Horizontal shear force per screw"

$$R_{xD.t.Ek} = 0.608\ \text{kN}$$

Shear reaction from applied normal force:

Shear reaction acting opposite of applied force

$$R_{zD.t.Ek} := -\frac{P_{zD.t}}{n_D}$$ "Vertical shear force per screw"

$$R_{zD.t.Ek} = 0.7208\ \text{kN}$$

The moment reaction about the y-axis is calculated as a cantilever with loadingin point C:
Moment about y-axis:

$$R_{xBD.t} := P_{x.t}$$ "Vertical reaction force acting on system B-D"

$$R_{zCD.t} := P_{zD.t}$$ "Horizontal reaction froce in B for system B-D"

$$M_{yD.t} := R_{xBD.t} \cdot d_{zCD} + R_{zCD.t} \cdot d_{xCD}$$

$$M_{yD.t} = 5.951\ \text{kN m}$$

Moment about x-axis:

M.x was calculated as a cantilecer with a reactionforce R.zC.

$R_{zCD.t} := -P_{zD.t}$ "Vertical reaction force in C for system C-D"

$M_{xD.t} := R_{zCD.t} \cdot d_{yCD}$

$M_{xD.t} = 1.1677\ \text{kN m}$

Moment about z-axis:

Reaction moment M.z was calculated as a cantilever with a reaction force R.xC

$R_{xC.t} := P_{x.t}$ "Horizontal reaction force in C for system C-D"

$M_{zD.t} := \left(-R_{xC.t}\right) \cdot d_{yBC}$

$M_{zD.t} = 1.2221\ \text{kN m}$

Shear forces due to M.y

The placement of the critical screws for the different forces were ignored, since it was observed that the critical forces would always act at the same screw in one of the outer corners. The same distance matrix is used as for the compression profile:

$$F_{Dv.t.My} := \frac{\left(-M_{yD.t}\right) \cdot r_{D.My}}{\sum r_{D.My.sq}}$$ "Shear forces distribution"

$$F_{Dv.t.My} = \begin{bmatrix} -2.72 & -2.16 & -1.61 & -1.1 & -0.73 & -0.73 & -1.1 & -1.61 & -2.16 & -2.72 \\ -2.64 & -2.06 & -1.47 & -0.88 & -0.29 & -0.29 & -0.88 & -1.47 & -2.06 & -2.64 \\ -2.72 & -2.16 & -1.61 & -1.1 & -0.73 & -0.73 & -1.1 & -1.61 & -2.16 & -2.72 \end{bmatrix} \text{kN}$$

The shear components are calculated:

$F_{xD.t.My} := Division_{ij}\left(Prtoduct_{ij}\left(F_{Dv.t.My}, r_{Dz.My}\right), r_{D.My}\right)$

$$F_{xD.t.My} = \begin{bmatrix} -0.66 & -0.66 & -0.66 & -0.66 & -0.66 & -0.66 & -0.66 & -0.66 & -0.66 & -0.66 \\ 0 & 0 & 0 & 0 & 0 & 0 & 0 & 0 & 0 & 0 \\ 0.66 & 0.66 & 0.66 & 0.66 & 0.66 & 0.66 & 0.66 & 0.66 & 0.66 & 0.66 \end{bmatrix} \text{kN}$$

$F_{zD.t.My} := Division_{ij}\left(Prtoduct_{ij}\left(F_{Dv.t.My}, r_{Dx.My}\right), r_{D.My}\right)$

$$F_{zD.t.My} = \begin{bmatrix} -2.64 & -2.06 & -1.47 & -0.88 & -0.29 & 0.29 & 0.88 & 1.47 & 2.06 & 2.64 \\ -2.64 & -2.06 & -1.47 & -0.88 & -0.29 & 0.29 & 0.88 & 1.47 & 2.06 & 2.64 \\ -2.64 & -2.06 & -1.47 & -0.88 & -0.29 & 0.29 & 0.88 & 1.47 & 2.06 & 2.64 \end{bmatrix} \text{kN}$$

Screw tension and CLT compression due to M.x.t:

Resulting moments on compression and tension side:

$$M_{x.screws.t} := \left|M_{xD.t}\right| \cdot \frac{dm_{screw.Mx}}{z_{D.Mx}} = 0.591\ \text{kN m}$$ "Moment acting on screws from N.A"

$$M_{x.CLT.t} := \left|M_{xD.t}\right| \cdot \frac{\frac{2}{3} \cdot c_{MxD}}{z_{D.Mx}} = 0.577\ \text{kN m}$$ "Moment acting on CLT from N.A"

Resulting tension forces in screws:

$$F_{Dax.Mx.t} := \frac{M_{x.screws.t} \cdot r_{D.Mx}}{\left(\sum r_{D.Mx.sq}\right)}$$ "Force distribution in screws"

$$F_{Dax.Mx.t} = \begin{bmatrix} 0 & 0 & 0 & 0 & 0 & 0 & 0 & 0 & 0 & 0 \\ 0.2841 & 0.2841 & 0.2841 & 0.2841 & 0.2841 & 0.2841 & 0.2841 & 0.2841 & 0.2841 & 0.2841 \\ 0.8253 & 0.8253 & 0.8253 & 0.8253 & 0.8253 & 0.8253 & 0.8253 & 0.8253 & 0.8253 & 0.8253 \end{bmatrix} \text{kN}$$

$$\sum F_{Dax.Mx.t} = 11093.4978\ \text{N}$$ "Sum of tension forces"

Maximum compression stress of CLT:

$$I_{z.CLT.t} := \frac{B \cdot c_{MxD}^{3}}{3} = 7.1068 \cdot 10^{-5}\ \text{m}^4$$ "Moment of inertia of CLT about N.A"

$$\sigma_{max.CLT.Mx.t} := \frac{M_{x.CLT.t} \cdot c_{MxD}}{I_{z.CLT}} = 0.6324\ \frac{\text{N}}{\text{mm}^2}$$ "Maximum stress acting on CLT"

Force resultant in CLT:

$$\frac{\sigma_{max.CLT.Mx.t} \cdot c_{MxD}}{2} \cdot B = 11093.4978\ \text{N}$$ "Sum of compression forces"

Maximum screw strain:

The maximum strain of the bolts and CLT were both calculated considering the maximum compression perpendicular to the grain.

$$\varepsilon_{CLT.Mx.t} := \frac{\sigma_{max.CLT.Mx.t}}{f_{c.90.k}} \cdot 0.0083 = 0.0021$$ "Maximum strain on CLT"

$$\varepsilon_{screw.Mx.t} := \frac{\max\left(F_{Dax.Mx.t}\right)}{F_{ax.Rk.screw}} \cdot 0.0083 = 0.0017$$ "Maximum strain in screws"

Strain ratio:

$$\varepsilon'_{CLT.t} := \frac{\varepsilon_{CLT.Mx.t}}{c_{MxD}} = 0.0269 \cdot \frac{1}{m}$$ "CLT strain/distrance ratio"

$$\varepsilon'_{screw.t} := \frac{\varepsilon_{screw.Mx.t}}{e_2 + 2 \cdot p_2 - c_{MxD}} = 0.0271 \cdot \frac{1}{m}$$ "Screw strain/distrance ratio"

$$\varepsilon'_{CLT.t} - \varepsilon'_{screw.t} = -0.0001 \cdot \frac{1}{m}$$

screw tension and CLT compression due to M.z:

Resulting moments on compression and tension side:

$$M_{z.screws.t} := \left|M_{zD.t}\right| \cdot \frac{dm_{screw.Mz}}{z_{D.Mz}} = 0.933 \text{ kN m}$$ "Moment acting on screws from N.A"

$$M_{z.CLT.t} := \left|M_{zD.t}\right| \cdot \frac{\frac{2}{3} \cdot c_{MzD}}{z_{D.Mz}} = 0.29 \text{ kN m}$$ "Moment acting on CLT from N.A"

Resulting tension forces in screws:

$$F_{Dax.Mz.t} := \frac{M_{z.screws.t} \cdot r_{D.Mz}}{\left(\sum r_{D.Mz.sq}\right)}$$ "Force distribution in screws"

$$F_{Dax.Mz.t} = \begin{bmatrix} 0.3328 & 0.2909 & 0.249 & 0.2071 & 0.1652 & 0.1233 & 0.0814 & 0.0395 & 0 & 0 \\ 0.3328 & 0.2909 & 0.249 & 0.2071 & 0.1652 & 0.1233 & 0.0814 & 0.0395 & 0 & 0 \\ 0.3328 & 0.2909 & 0.249 & 0.2071 & 0.1652 & 0.1233 & 0.0814 & 0.0395 & 0 & 0 \end{bmatrix} \text{kN}$$

Maximum compression stress of CLT:

$$I_{x.CLT} := \frac{H \cdot c_{MzD}^{3}}{3} = 6.1252 \cdot 10^{-5} \text{ m}^4$$ "Moment of inertia of CLT about N.A"

$$\sigma_{max.CLT.Mz.t} := \frac{M_{z.CLT.t} \cdot c_{MzD}}{I_{x.CLT}} = 0.4595 \frac{\text{N}}{\text{mm}^2}$$ "Maximum stress acting on CLT"

Capacity control:

The axial forces acting on the system are a result Mx and Mz:

Resulting axial forces acting on screws:

"M.x and M.z are the only contributers to the axial forces of the system:

$$F_{Dax.tot} := F_{Dax.Mx} + F_{Dax.Mz} = \begin{bmatrix} 0.441 & 0.386 & 0.33 & 0.275 & 0.219 & 0.163 & 0.108 & 0.052 & 0 & 0 \\ 0.629 & 0.573 & 0.518 & 0.462 & 0.407 & 0.351 & 0.296 & 0.24 & 0.188 & 0.188 \\ 0.987 & 0.931 & 0.876 & 0.82 & 0.765 & 0.709 & 0.654 & 0.598 & 0.546 & 0.546 \end{bmatrix} \text{kN}$$

$$F_{Dax.Ek} := \max\left(F_{Dax.tot}\right) = 0.9868 \text{ kN}$$ "Axial force on screws in compression system"

$$F_{Dax.tot.t} := F_{Dax.Mx.t} + F_{Dax.Mz.t} = \begin{bmatrix} 0.333 & 0.291 & 0.249 & 0.207 & 0.165 & 0.123 & 0.081 & 0.04 & 0 & 0 \\ 0.617 & 0.575 & 0.533 & 0.491 & 0.449 & 0.407 & 0.365 & 0.324 & 0.284 & 0.284 \\ 1.158 & 1.116 & 1.074 & 1.032 & 0.99 & 0.949 & 0.907 & 0.865 & 0.825 & 0.825 \end{bmatrix} \text{kN}$$

$$F_{Dax.Ek.t} := \max\left(F_{Dax.tot.t}\right) = 1.1581 \text{ kN}$$ "Axial force on screws in tension system"

Resulting maximum CLT compression:

"Maximum compressive stress for CLT is considderd to act at the top right corner of the connection resulitng in the maximum compression being the sum of critical compression from M.z and M.y:"

$$\sigma_{clt.Ek} := \sigma_{max.CLT.Mx} + \sigma_{max.CLT.Mz}$$

$$\sigma_{clt.Ek} = 1.0273 \frac{\text{N}}{\text{mm}^2}$$

$$\boxed{\frac{\sigma_{clt.Ek}}{f_{c.90.k}} = 0.411}$$

$$\sigma_{clt.Ek.t} := \sigma_{max.CLT.Mx.t} + \sigma_{max.CLT.Mz.t}$$

$$\sigma_{clt.Ek.t} = 1.092 \frac{\text{N}}{\text{mm}^2}$$

$$\boxed{\frac{\sigma_{clt.Ek.t}}{f_{c.90.k}} = 0.437}$$

Resulting maximum shear force acting on screws:

"The maximum shear from moments M.x and M.z and forces R.px are summed for respective axes."

$$F_{xD.tot} := R_{xD.Ek} + F_{xD.My}$$

$$F_{xD.tot} = \begin{bmatrix} -0.127 & -0.127 & -0.127 & -0.127 & -0.127 & -0.127 & -0.127 & -0.127 & -0.127 & -0.127 \\ -1 & -1 & -1 & -1 & -1 & -1 & -1 & -1 & -1 & -1 \\ -1.873 & -1.873 & -1.873 & -1.873 & -1.873 & -1.873 & -1.873 & -1.873 & -1.873 & -1.873 \end{bmatrix} \text{kN}$$

$$F_{zD.tot} := R_{zD.Ek} + F_{zD.My}$$

$$F_{zD.tot} = \begin{bmatrix} 2.833 & 2.061 & 1.29 & 0.519 & -0.252 & -1.024 & -1.795 & -2.566 & -3.337 & -4.109 \\ 2.833 & 2.061 & 1.29 & 0.519 & -0.252 & -1.024 & -1.795 & -2.566 & -3.337 & -4.109 \\ 2.833 & 2.061 & 1.29 & 0.519 & -0.252 & -1.024 & -1.795 & -2.566 & -3.337 & -4.109 \end{bmatrix} \text{kN}$$

"As a result of the even distribution of shear forces from external forces and the maximum shear force from moments acting in corner scres, it is determined that the maximum shear wil act in one of the four corners resulting in the SRSS of the maximum shear force in x and z direction."

$$F_{vD.Ek} := \sqrt{\left(\text{Max}\left(\left|\text{mat2sys}\left(F_{xD.tot}\right)\right|\right)\right)^2 + \left(\text{Max}\left(\left|\text{mat2sys}\left(F_{zD.tot}\right)\right|\right)\right)^2}$$

$F_{vD.Ek} = 4515.478\ \text{N}$ "Critical shear force force of compression profile"

"The maximum shear from moments M.x.t and M.z.t and forces R.px are summed for their respective axes."

$$F_{xD.tot.t} := R_{xD.t.Ek} + F_{xD.t.My}$$

$$F_{xD.tot.t} = \begin{bmatrix} -0.057 & -0.057 & -0.057 & -0.057 & -0.057 & -0.057 & -0.057 & -0.057 & -0.057 & -0.057 \\ 0.608 & 0.608 & 0.608 & 0.608 & 0.608 & 0.608 & 0.608 & 0.608 & 0.608 & 0.608 \\ 1.273 & 1.273 & 1.273 & 1.273 & 1.273 & 1.273 & 1.273 & 1.273 & 1.273 & 1.273 \end{bmatrix} \text{kN}$$

$$F_{zD.tot.t} := R_{zD.t.Ek} + F_{zD.t.My}$$

$$F_{zD.tot.t} = \begin{bmatrix} -1.921 & -1.334 & -0.747 & -0.16 & 0.427 & 1.014 & 1.602 & 2.189 & 2.776 & 3.363 \\ -1.921 & -1.334 & -0.747 & -0.16 & 0.427 & 1.014 & 1.602 & 2.189 & 2.776 & 3.363 \\ -1.921 & -1.334 & -0.747 & -0.16 & 0.427 & 1.014 & 1.602 & 2.189 & 2.776 & 3.363 \end{bmatrix} \text{kN}$$

$$F_{vD.Ek.t} := \sqrt{\left(\text{Max}\left(\left|\text{mat2sys}\left(F_{xD.tot.t}\right)\right|\right)\right)^2 + \left(\text{Max}\left(\left|\text{mat2sys}\left(F_{zD.tot.t}\right)\right|\right)\right)^2}$$

$F_{vD.Ek.t} = 3595.6991\ \text{N}$ "Critical shear force of tension profile"

"EN 1995 1-1:2008 does not give an expression for the combined characteristic capacity of screws. As a result eq. (8.28) is adapted for characteristic values by exchanging the design values for characteristic values:"

$$\left(\frac{F_{Dax.Ek}}{F_{ax.Rk.screw}}\right)^2 + \left(\frac{F_{vD.Ek}}{F_{vD.Rk}}\right)^2 = 0.6375$$

"Characteristic utilization for profile in compression: $P_x = 30\ \text{kN}$

$$\left(\frac{F_{Dax.Ek.t}}{F_{ax.Rk.screw}}\right)^2 + \left(\frac{F_{vD.Ek.t}}{F_{vD.Rk}}\right)^2 = 0.4505$$

"Characteristic utilization for profile in tension: $P_{x.t} = -18.24\ \text{kN}$

Utilization from characteristic load Px and design capacity:

$$F_{vD.Rd} := \frac{F_{vD.Rk}}{1.25} \qquad F_{ax.Rd} := \frac{F_{ax.Rk.screw}}{1.25}$$

$$\left(\frac{F_{Dax.Ek}}{F_{ax.Rd}}\right)^2 + \left(\frac{F_{vD.Ek}}{F_{vD.Rd}}\right)^2 = 0.996$$

$$\left(\frac{F_{Dax.Ek.t}}{F_{ax.Rd}}\right)^2 + \left(\frac{F_{vD.Ek.t}}{F_{vD.Rd}}\right)^2 = 0.704$$

Concrete connection calculations

"The moment in support B for the compression profile was considered to be the critical. This was because of the reduced horizontal forces and the short vertical span from B to C, resulting in a lower moment In B from the pinned system BC in tension than the fixed system BD for compression:

Forces acting on system

Reaction forces in connection C in regards to system BC:

$R_{xCB} := P_{xA} + P_{xB}$ "horizontal reaction force in connecton B"

$R_{zCB} := P_{zD}$ "Vertical reaction force in connection B"

The M.y in support B was calculated as the sum of the moments in B from a fixed-fixed moment system A-B and a fixed-fixed system B-D. This was done because support B prohibited any rotation in the support, thus prohibiting the transfer of moments. Point C was also considered moment resisting for moments about the y-axis.

$M_{yBab} := 0.5 \cdot P_{xA} \cdot d_{zAB} = -1.6605 \text{ kN m}$ "M.y from horizontal force in support A"

$M_{yBbc} := \left(-P_x\right) \cdot \left(-d_{zBC}\right) + R_{zCD} \cdot \left(-d_{xBC.c}\right) = -2.5531 \text{ kN m}$ "M.y from horizontal force in support D"

$M_{yB} := M_{yBab} + M_{yBbc}$ "Sum of M.y resisted by support B"

$M_{yB} = -4.2136 \text{ kN m}$

M.x is calculated as the sum of the momet created from the vertical force acting in connection A and C:

$M_{xAB} := 0.5 \cdot P_{zA} \cdot d_{yAB} = -1.0348 \text{ kN m}$

$d_{yCB.cv} := -d_{yBC.cv}$ "Switch direction"

$M_{xCB} := R_{zCB} \cdot d_{yCB.cv} = -1.5441 \text{ kN m}$

$M_{xB} := \left(M_{xCB} + M_{xAB}\right)$ "Resultant moment"

$M_{xB} = -2.5789 \text{ kN m}$

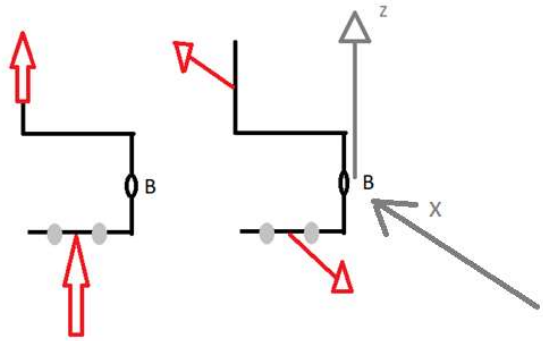

M.y is calculated as a sum of the force acting on

$M_{zAB} := 0.5 \cdot \left(-P_{xA}\right) \cdot d_{yAB} = 1.6335 \text{ kN m}$

$M_{zCB} := R_{xCB} \cdot \left(-d_{yBC.c}\right) = -2.01 \text{ kN m}$

$M_{zB} := \left(M_{zAB} + M_{zCB}\right)$

$M_{zB} = -0.3765 \text{ kN m}$

Because support B was the only connection considered to take vertical forces, the vertical force in support D would be the sum of all vertical system forces:

$$R_{zB} := -\left(P_{zA} + P_{zD}\right)$$

$$R_{zB} = -36.246\ \text{kN}$$

In additon to the the vertical reaction force, a horizontal force P.xB was considered to be transmited from the concrete to the system.

$$R_{xB} := -P_{xB} = -3000\ \text{N}$$

Reaction forces in concrete anchors due to M.y:

The calculation is done using the same principle as connection D for M.y with the center determined by symetri:

$$r_{B.My} := \left[\, 1.5 \cdot d_{x.anchor} \;\; 0.5 \cdot d_{x.anchor} \;\; (-0.5) \cdot d_{x.anchor} \;\; (-1.5) \cdot d_{x.anchor} \,\right]$$

$$r_{B.My} = \left[\, 0.135 \;\; 0.045 \;\; -0.045 \;\; -0.135 \,\right]\ \text{m}$$

$$r_{B.My.sq} := Prtoduct_{ij}\left(r_{B.My},\, r_{B.My}\right)$$

$$r_{B.My.sq} = \left[\, 0.0182 \;\; 0.002 \;\; 0.002 \;\; 0.0182 \,\right]\ \text{m}^2$$

$$F_{zB.My} := -\frac{M_{yB} \cdot r_{B.My}}{\sum r_{B.My.sq}}$$

$$F_{zB.My} = \left[\, 14.05 \;\; 4.68 \;\; -4.68 \;\; -14.05 \,\right]\ \text{kN}$$

"Shear force distributions from My"

Reaction forces in concrete anchors due to M.z:

The same procedure as for M.x is used for the force calculations of M.z

$n_{t.anchors} := 4$ "Number of anchors"

$\lambda_{Concrete.Mz} := 0.248$ "Connection percentage distance from concrete edge"

$c_{MzB} := \left(\left(n_{t.anchors} - 1\right) \cdot d_{x.anchor} + e_{x.anchor}\right) \cdot \lambda_{Concrete.Mz} = 0.0893\ \text{m}$ "Concrete edge distance to neutral axis"

$$r\_initial_{B.Mz} := \begin{bmatrix} e_{x.anchor} + 3 \cdot d_{x.anchor} - c_{MzB} \\ e_{x.anchor} + 2 \cdot d_{x.anchor} - c_{MzB} \\ e_{x.anchor} + d_{x.anchor} - c_{MzB} \\ e_{x.anchor} - c_{MzB} \end{bmatrix}^{T}$$

$r\_initial_{B.Mz} = \begin{bmatrix} 270.7 & 180.7 & 90.7 & 0.7 \end{bmatrix}\ \text{mm}$

$r_{B.Mz} := Matrix\_remove\_negative_{ij}\left(r\_initial_{B.Mz}\right)$ "Compression screws are removed"

$r_{B.Mz.sq} := Prtoduct_{ij}\left(r_{B.Mz}, r_{B.Mz}\right)$ "Squared distances"

Distance to screw force resultant:

$$dm_{anchor.Mz} := \frac{\sum r_{D.Mz.sq}}{\sum r_{D.Mz}}$$

$dm_{anchor.Mz} = 208.74\ \text{mm}$ "Distance from neutral axis to resultant force in anchors"

Resulting moment arm:

$z_{B.Mz} := dm_{anchor.Mz} + \frac{2}{3} \cdot c_{MzB}$ "Connection moment arm"

$z_{B.Mz} = 268.26\ \text{mm}$

Resulting moments on compression and tension side:

$$M_{z.anchor} := \left|M_{zB}\right| \cdot \frac{dm_{anchor.Mz}}{z_{B.Mz}} = 0.293\ \text{kN m}$$ "Moment acting on anchors from N.A"

$$M_{z.Concrete} := \left|M_{zB}\right| \cdot \frac{\frac{2}{3} \cdot c_{MzB}}{z_{B.Mz}} = 0.084\ \text{kN m}$$ "Moment acting on concrete from N.A"

Resulting tension forces in screws:

$$F_{Bax.Mz} := \frac{M_{z.anchor} \cdot r_{B.Mz}}{\left(\sum r_{B.Mz.sq}\right)}$$ "Force distribution in anchors"

$$F_{Bax.Mz} = \begin{bmatrix} 0.6946 & 0.4637 & 0.2328 & 0.0018 \end{bmatrix}\ \text{kN}$$

$$\sum F_{Bax.Mz} = 1393\ \text{N}$$ "Sum of tension forces"

Maximum compression stress of CLT:

$$I_{x.Concrete} := \frac{2 \cdot d_{z.anchor} \cdot c_{MzB}^{3}}{3} = 2.8466 \cdot 10^{-5}\ \text{m}^4$$ "Moment of inertia of concrete about N.A"

$$\sigma_{max.Concrete.Mz} := \frac{M_{z.Concrete} \cdot c_{MzB}}{I_{x.Concrete}} = 0.262\ \frac{\text{N}}{\text{mm}^2}$$ "Maximum stress acting on concrete"

Force resultant in CLT:

$$\frac{\sigma_{max.Concrete.Mz} \cdot c_{MzB}}{2} \cdot 2 \cdot d_{z.anchor} = 1404\ \text{N}$$ "Sum of compression forces"

Maximum screw strain:

$$\varepsilon_{Concrete.Mz} := \frac{\sigma_{max.Concrete.Mz}}{E_{cm}} = 8.7446 \cdot 10^{-6}$$ "Maximum strain on concrete"

$$A_{anchor} := 84.3\ \text{mm}^2$$

$$\varepsilon_{anchor.Mz} := \frac{\max\left(F_{Bax.Mz}\right)}{A_{anchor} \cdot E_s} = 4.1199 \cdot 10^{-5}$$ Maximum strain in anchors"

Strain ratio:

$$\varepsilon'_{Concrete.Mz} := \frac{\varepsilon_{Concrete.Mz}}{c_{MzB}} = 9.7945 \cdot 10^{-5} \cdot \frac{1}{\text{m}}$$ "concrete strain/distrance ratio"

$$\varepsilon'_{anchor.Mz} := \frac{\varepsilon_{anchor.Mz}}{\left|r\_initial_{B.Mz_1}\right|} = 0.0002 \cdot \frac{1}{\text{m}}$$ "anchors strain/distrance ratio"

$$\varepsilon'_{Concrete.Mz} - \varepsilon'_{anchor.Mz} = -5.4238 \cdot 10^{-5} \cdot \frac{1}{\text{m}}$$

Reaction forces in anchors due to M.xB

$n_{anchors} := 4$ "Number of anchors"

$H_B := d_{z.anchor} = 0.06\ \text{m}$ "Height of connection"

$\lambda_{Concrete.Mx} := 0.333$

$c_{MxB} := \left(H_B\right) \cdot \lambda_{Concrete.Mx} = 0.01998\ \text{m}$

Since the system only consists of one row of screws, the resultant tension force acts in the middle of the row.

$$dm_{anchor.Mx} := H_B - c_{MxB}$$

Resulting moment arm:

"When the system is linearly elastic the stress distribution of CLT is triangular, resulting in the resultant force acting 2/3 of the distance from the neutral axis.

$z_{B.Mx} := dm_{anchor.Mx} + \frac{2}{3} \cdot c_{MxB}$ "Connection moment arm"

$z_{B.Mx} = 53.34\ \text{mm}$

Resulting moments on compression and tension side:

$M_{x.anchor} := \left|M_{xB}\right| \cdot \frac{dm_{anchor.Mx}}{z_{B.Mx}} = 1.935\ \text{kN m}$ "Moment acting on screws from N.A"

$M_{x.concrete} := \left|M_{xB}\right| \cdot \frac{\frac{2}{3} \cdot c_{MxB}}{z_{B.Mx}} = 0.644\ \text{kN m}$ "Moment acting on CLT from N.A"

Resulting tension forces in screws:

$F_{Bax.Mx.tot} := \frac{M_{x.anchor} \cdot dm_{anchor.Mx}}{dm_{anchor.Mx}^2}$ "Force distribution in screws"

$F_{Bax.Mx} := \frac{F_{Bax.Mx.tot}}{n_{anchors}} = 12.0871\ \text{kN}$

Maximum compression stress of concrete:

$I_{z.concrete} := \frac{B \cdot c_{MxB}^3}{3} = 1.1964 \cdot 10^{-6}\ \text{m}^4$ "Moment of inertia of CLT about N.A"

$\sigma_{max.concrete.Mx} := \frac{M_{x.concrete} \cdot c_{MxB}}{I_{z.concrete}} = 10.7549\ \frac{\text{N}}{\text{mm}^2}$ "Maximum stress acting on CLT"

The maximum strain of the bolts and CLT were both calculated considering the maximum compression perpendicular to the grain.

$$\varepsilon_{concrete.Mx} := \frac{\sigma_{max.concrete.Mx}}{E_{cm}} = 0.0004$$ "Maximum strain on CLT"

$$\varepsilon_{anchor.Mx} := \frac{F_{Bax.Mx}}{A_{anchor} \cdot E_s} = 0.0007$$ Maximum strain in screws"

Strain ratio:

For plates to remain plane, the rate of change in strain have to be equal for the tension and compression part of the connection.

$$\varepsilon'_{concrete} := \frac{\varepsilon_{concrete.Mx}}{c_{MxB}} = 0.018 \cdot \frac{1}{m}$$ "CLT strain/distrance ratio"

$$\varepsilon'_{screw} := \frac{\varepsilon_{anchor.Mx}}{dm_{anchor.Mx}} = 0.0179 \cdot \frac{1}{m}$$ "Screw strain/distrance ratio"

Shear stress due to axial forces:

The shear forces due to axial forces were calculated as evenly distributed because the connection only consisted of one row of edge bolts. (Not two rows whtere the shear forces would be taken by the inner bolts to increase concrete tear out strength.)

Vertical force

$$R_{zB} = -36.246 \text{ kN}$$

$$F_{zB.Rz} := \frac{R_{zB}}{n_{Bx}} = -9.0615 \text{ kN}$$ "Vertical resistance per anchor"

Horizontal force

$$R_{xB} := -P_{xB} = -3000 \text{ N}$$

$$F_{xB.Rx} := \frac{R_{xB}}{n_{Bx}} = -0.75 \text{ kN}$$ "horizontal resistance per anchor"

Resulting forces in anchors due to applied forces:

Resulting vertical shear forces

$$F_{zB.Ek} := F_{zB.My} + F_{zB.Rz}$$

$$F_{zB.Ek} = \begin{bmatrix} 4.98 & -4.38 & -13.74 & -23.11 \end{bmatrix} \text{kN}$$

Resulting horizontal shear forces

$$F_{xB.Ek} := F_{xB.Rx} \cdot [1\ 1\ 1\ 1]$$

$$F_{xB.Ek} = [-0.75\ -0.75\ -0.75\ -0.75]\ \text{kN}$$

Resulting axial forces

$$F_{axB.Ek} := F_{Bax.Mx} \cdot [1\ 1\ 1\ 1] + F_{Bax.Mz}$$

$$F_{axB.Ek} = [12.782\ 12.551\ 12.32\ 12.089]\ \text{kN}$$

From the results it was determined that the worst anchor was the right anchor because of the largest resulting vertical shear force.

Resulting reaction forces of worst anchor:

$$F_{zB.Ek.crit} := \text{Max}\left(\left|\text{mat2sys}\left(F_{zB.Ek}\right)\right|\right)$$

$$\boxed{F_{zB.Ek.crit} = 23.11\ \text{kN}}$$

$$F_{xB.Ek.crit} := \text{Max}\left(\left|\text{mat2sys}\left(F_{xB.Ek}\right)\right|\right)$$

$$\boxed{F_{xB.Ek.crit} = 0.75\ \text{kN}}$$

$$F_{axB.Ek.crit} := \text{Max}\left(F_{axB.Ek}\right)$$

$$\boxed{F_{axB.Ek.crit} = 12.7818\ \text{kN}}$$

Anchor capactiy control:

Can not find anchors of size M14: As a substitute, Hitist HIT-HY 200 M12 anchors are utilized. The calculations have been done for cracked concrete: No units are assigned, as the calculations are empirical:

$n_{t.anchors} := 4$ "Number of anchors"

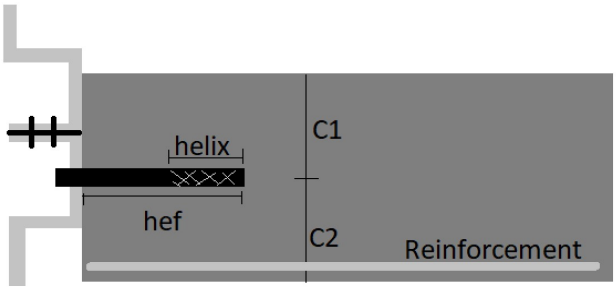

Concrete

$H_{concrete} := 350\ mm$ "Height of concrette beam"

$H_{concrete.depth} := 300\ mm$ "Concrete depth"

$c_{1.cap} := \frac{H_{concrete}}{2}$ "Upper edge distance"

$c_{2.cap} := c_{1.cap}$ "Lower edge distance" "Assumed to be fixed in the middle"

$s_{1.cap} := 90\ mm$ "Anchor spacing"

$f_{ck.cube.cap} := 25\ \frac{N}{mm^2}$ "Characteristic cubed concrete capacity"

ETA-12/0028: HILTI HIT-HY 200R with HIT-Z: (Table values)

$d_{anchor.cap} := 12\ mm$ "Anchor diameter"

$h_{nom} := 100\ mm$ "Anchor depth"

$h_{ef} := h_{nom}\ mm$ "Effective anchor depth"

$A_{s.anchor} := 84.3\ mm$ "Area of steel cross section"

$h_{helix} := 60\ mm$ "Length of helix part of anchor"

$C_{cr.sp} := 1.5 \cdot h_{ef} = 150\ mm$

$S_{cr.sp} := 2 \cdot C_{cr.sp} = 300\ mm$

"Pull out area distances valid for : H.concrete.depth / h.nom > 2.3"

$\tau_{rk.ucr} := 22\ \frac{N}{mm^2}$ "Anchor bond resistance"

$f_{uk} := 650\ \frac{N}{mm^2}$ "Characteristic capactiy of anchor"

$f_{yk.anchor} := 520\ \frac{N}{mm^2}$ "Yield strength of anchor"

$S_{cr.Np} := \mathrm{Min}\left(20 \cdot d_{anchor.cap}, 3 \cdot h_{helix}\right)$ "Group pull-out distances"

$C_{cr.Np} := 0.5 \cdot S_{cr.Np} = 90$

$k_{\psi 0.g.Np} := 2.3$ "Concrete factor according to ETA-12/0028"

$gamma := 1.5$ "Anchor safety factor"

$c_{min} := 90$

$s_{min} := 60$

"Minimum and maximum anchor distances for M12"

$h_{nom.max} := 144$

"From catalog, not ETA"

Distances and factors determined by ETAG 001:

"Pry out distances"

$S_{cr.N} := 3 \cdot h_{ef} = 300$

$C_{cr.N} := 0.5 \cdot S_{cr.N} = 150$

Concrete factors for cracked concrete ETAG 001:

$k_{N0.Rk.c} := 7.2$

$k_{V.Rk.cp} := 2$

$k_{V0.Rk.c} := 1.7$

Tension capactiy

Steel failure:

$N_{Rk.s} := n_{t.anchors} \cdot A_{s.anchor} \cdot f_{uk} = 2.1918 \cdot 10^{5}$ N "Steel capacity"

$\frac{\sum F_{axB.Ek}}{N_{Rk.s}} = 0.2269$ N "Steel utilization for tension"

Eccentricity of resulting axial forces on anchors is determined:

$F_{axB.Ek} = [\,12.7818 \;\; 12.5508 \;\; 12.3199 \;\; 12.089\,]$ kN "Resultant tension forces on anchors"

$r_{nB} := [\,1.5 \cdot s_{1.cap} \;\; 0.5 \cdot s_{1.cap} \;\; (-0.5) \cdot s_{1.cap} \;\; (-1.5) \cdot s_{1.cap}\,]$ "Distance from geometrical connector center"

$r_{nB} = [\,135 \;\; 45 \;\; -45 \;\; -135\,]$

$e_n := \frac{\sum Prtoduct_{ij}(r_{nB}, F_{axB.Ek})}{\sum F_{axB.Ek}} = 2.0891$ mm "Eccentricity"

Group pull-out failure:

Next the different group pull out factors are calulated:

$\psi_{re.Np} := \mathrm{Min}\left(0.5 + \frac{h_{ef}}{200}, 1\right) = 1$ "Spalling factor"

$\psi_{ec.Np} := \mathrm{Min}\left(\frac{1}{1 + 2 \cdot \frac{e_n}{S_{cr.Np}}}, 1\right) = 0.9773$ "Eccentricity factor"

$\psi 0_{g.Np} := \mathrm{Max}\left(\left(\sqrt{n_{t.anchors}} - \left(\sqrt{n_{t.anchors}} - 1\right) \cdot \frac{d_{anchor.cap} \cdot \tau_{rk.ucr}}{k_{\psi 0.g.Np} \cdot \sqrt{h_{ef} \cdot f_{ck.cube.cap}}}\right), 1\right) = 1$

$\psi_{g.Np} := \mathrm{Max}\left(\psi 0_{g.Np} - \left(\frac{s}{S_{cr.Np}}\right)^{0.5} \cdot \left(\psi 0_{g.Np} - 1\right)\right) = 1$ "Surface factor"

$$\psi_{s.Np} := 0.7 + 0.3 \cdot \frac{c_{1.cap}}{C_{cr.Np}} = 1.2833$$ "Edge distance factor"

$$A0_{p.N} := S_{cr.Np}{}^{2} = 32400$$ "Ideal pull out area"

$$A_{p.N} := 2 \cdot \mathrm{Min}\left(c_{1.cap}, C_{cr.Np}\right) \cdot \left(2 \cdot C_{cr.Np} + \left(n_{t.anchors} - 1\right) \cdot s_{1.cap}\right) = 81000$$ "Group pull out area"

$$N0_{Rk.p} := \pi \cdot d_{anchor.cap} \cdot h_{helix} \cdot \tau_{rk.ucr} = 49762.8276$$ "Ideal anchor pull out capacity"

$$N_{Rk.p} := N0_{Rk.p} \cdot \frac{A_{p.N}}{A0_{p.N}} \cdot \psi_{s.Np} \cdot \psi_{g.Np} \cdot \psi_{ec.Np} \cdot \psi_{re.Np} = 1.5603 \cdot 10^{5}$$ "Group pull out capacity"

$$\frac{\sum F_{axB.Ek}}{N_{Rk.p}}_{\mathrm{N}} = 0.3188$$ "Characteristic pull out utilization"

Concrete cone failure:

$$\psi_{ec.N} := \mathrm{Min}\left(\frac{1}{1 + 2 \cdot \frac{e_n}{S_{cr.N}}}, 1\right) = 0.9863$$ "Eccentricity factor"

$$\psi_{re.N} := \mathrm{Min}\left(0.5 + \frac{h_{ef}}{200}, 1\right) = 1$$ "Spalling factor"

$$\psi_{s.N} := \mathrm{Min}\left(0.7 + 0.3 \cdot \frac{c_{1.cap}}{C_{cr.N}}, 1\right) = 1$$ "Edge distance factor"

$$A0_{c.N} := S_{cr.N}{}^{2} = 90000$$ "Ideal cone area"

$$A_{c.N} := 2 \cdot \mathrm{Min}\left(c_{1.cap}, C_{cr.N}\right) \cdot \left(2 \cdot C_{cr.N} + \left(n_{t.anchors} - 1\right) \cdot s_{1.cap}\right) = 1.71 \cdot 10^{5}$$ "Group cone area"

$$N0_{Rk.c} := k_{N0.Rk.c} \cdot \sqrt{f_{ck.cube.cap}} \cdot h_{ef}{}^{1.5} = 36000$$ "Ideal cone capacity"

$$N_{Rk.c} := N0_{Rk.c} \cdot \frac{A_{c.N}}{A0_{c.N}} \cdot \psi_{s.N} \cdot \psi_{re.N} \cdot \psi_{ec.N} = 67460.4528$$ "Cone group capacity"

$$\frac{\sum F_{axB.Ek}}{N_{Rk.c}}_{\mathrm{N}} = 0.7373$$ "Characteristic cone group capcatiy"

Splitting failure:

$$\psi_{ec.N.sp} := \mathrm{Min}\left(\frac{1}{1 + 2 \cdot \frac{e_n}{S_{cr.N}}}, 1\right) = 0.9863$$ "Eccentricity factor"

$$\psi_{re.N.sp} := \mathrm{Min}\left(0.5 + \frac{h_{ef}}{200}, 1\right) = 1$$ "Spalling factor"

$$\psi_{s.N.sp} := \mathrm{Min}\left(0.7 + 0.3 \cdot \frac{c_{1.cap}}{C_{cr.sp}}, 1\right) = 1$$ "Edge distance factor"

$$\psi_{h.sp} := \mathrm{Min}\left(\frac{H_{concrete.depth}}{\mathrm{Min}\left(C_{cr.sp}, c_{1.cap}\right) + \mathrm{Min}\left(C_{cr.sp}, c_{2.cap}\right)}, 1.5\right) = 1$$

"concrete depth factor"

"ideal anchor splitting area"

$$A0_{c.N.sp} := S_{cr.sp}{}^{2} = 90000$$

$$A_{c.N.sp} := 2 \cdot \mathrm{Min}\left(c_{1.cap}, C_{cr.sp}\right) \cdot \left(2 \cdot C_{cr.sp} + \left(n_{t.anchors} - 1\right) \cdot s_{1.cap}\right) = 1.71 \cdot 10^{5}$$

"Group splitting area"

$$N0_{Rk.c.sp} := k_{N0.Rk.c} \cdot \sqrt{f_{ck.cube.cap}} \cdot h_{ef}{}^{1.5} = 36000$$

"Ideal anchor splitting capacity"

$$N_{Rk.c.sp} := N0_{Rk.c.sp} \cdot \frac{A_{c.N.sp}}{A0_{c.N.sp}} \cdot \psi_{s.N.sp} \cdot \psi_{re.N.sp} \cdot \psi_{ec.N.sp} \cdot \psi_{h.sp} = 67460.4528$$

"Group splitting capacity"

$$\frac{\sum F_{axB.Ek}}{N_{Rk.c.sp}}_{\mathrm{N}} = 0.7373$$

"Characteristic splitting utilization"

Shear capacity:

Eccentricity and equivalent critical size and dirrection of shear force:

$$F_{zB.Ek} = [\, 4.98 \;\; -4.38 \;\; -13.74 \;\; -23.11 \,]\ \mathrm{kN}$$

"Resulting vertical force"

$$Forces_{V.C} := Matrix\_remove\_positive_{ij}\left(F_{zB.Ek}\right)$$

"Resulting negative values"

$$Forces_{V.C} = [\, 0 \;\; -4.3797 \;\; -13.7433 \;\; -23.1069 \,]\ \mathrm{kN}$$

$$F_{xB.Ek} = [\, -0.75 \;\; -0.75 \;\; -0.75 \;\; -0.75 \,]\ \mathrm{kN}$$

"Horizontal shear forces"

$$r_{vertical} := \left[\, 1.5 \cdot s_{1.cap} \;\; 0.5 \cdot s_{1.cap} \;\; (-0.5) \cdot s_{1.cap} \;\; (-1.5) \cdot s_{1.cap} \,\right]$$

"Placement of anchors from center of anchors"

$$e_{v.x} := \frac{\sum Prtoduct_{ij}\left(r_{vertical}, Forces_{V.C}\right)}{\sum Forces_{V.C}} = -85.8794$$

"Vertical eccentricity of shear force"

$$Force_{\alpha} := \mathrm{atan}\left(\frac{\sum F_{xB.Ek}}{\sum Forces_{V.C}}\right)$$

"Angle of resulting shear force

$$Force_{\alpha} = 0.0726 \;\; rad$$

$$e_{v} := \cos\left(Force_{\alpha}\right) \cdot e_{v.x}$$

"equivalent anchor group eccentricity"

$$e_{v} = -85.7 \;\; mm$$

$$F_{shear.concrete.tot} := \sqrt{\left(\sum Forces_{V.C}\right)^{2} + \left(\sum F_{xB.Ek}\right)^{2}}$$

$$F_{shear.concrete.tot} = 41338.9117\ \mathrm{N}$$

"Equivalent anchor shear force"

Steel failure:

$V_{Rk.s} := n_{t.anchors} \cdot 0.5 \cdot A_{s.anchor} \cdot f_{uk} = 1.0959 \cdot 10^{5}$ "Characteristic steel capacity"

$\frac{F_{shear.concrete.tot}}{N_{Rk.s}}\ \mathrm{N} = 0.1886$ "Characteristic steel utilization"

Pry-out failure:

Because the anchor group is affected by a torsion moment, the critical pry-out capactiy is calculated for the critical bolt:

$\psi_{ec.N.crit} := 1$ "No eccentricity for a singular bolt" "Eccentricity factor"

$\psi_{re.N} := \mathrm{Min}\left(0.5 + \frac{h_{ef}}{200}, 1\right) = 1$ "Spalling factor"

$\psi_{s.N} := \mathrm{Min}\left(0.7 + 0.3 \cdot \frac{c_{1.cap}}{C_{cr.N}}, 1\right) = 1$ "Edge distance factor"

$A0_{c.N} := S_{cr.N}^{2} = 90000$ "Ideal tension pry out area"

$A_{c.N.crit} := 2 \cdot \mathrm{Min}\left(c_{1.cap}, C_{cr.N}\right) \cdot \left(C_{cr.N} + \frac{s_{1.cap}}{2}\right) = 58500$ "Tension pry-out area for critical anchor"

$N0_{Rk.c.crit} := k_{N0.Rk.c} \cdot \sqrt{f_{ck.cube.cap}} \cdot h_{ef}^{1.5} = 36000$ "Characteristic tension pry-out capactiy"

$N_{Rk.c.crit} := N0_{Rk.c} \cdot \frac{A_{c.N.crit}}{A0_{c.N}} \cdot \psi_{s.N} \cdot \psi_{re.N} \cdot \psi_{ec.N} = 23078.576$ "Concrete tension cone failure of critical shear anchor"

Using the tension capactiy of the critical anchor, the pry-out failure for the critical anchor is calculated as:

$V_{Rk.cp} := k_{V.Rk.cp} \cdot N_{Rk.c.crit} = 46157.1519$ "Pry out faillure capacity"

$V_{Ek.crit.anchor} := \sqrt{F_{zB.Ek.crit}^{2} + F_{xB.Ek.crit}^{2}} = 23119.1015\ \mathrm{N}$ "Characteristic load acting on critical shear anchor"

$\frac{V_{Ek.crit.anchor}}{V_{Rk.cp}}\ \mathrm{N} = 0.5009$ "Characteristic pry out utilization"

Concrete edge failure:

"Using the eccentriceties and force angel the factors are calculated"

$$\psi_{ec.V} := \mathrm{Min}\left(\sqrt{\frac{1}{1+\frac{2\cdot e_v}{3\cdot c_{1.cap}}}}, 1\right) = 1$$

$$\psi_{\alpha.V} := \mathrm{Max}\left(\sqrt{\frac{1}{\left(\cos\left(Force_\alpha\right)\right)^2+\left(\frac{\sin\left(Force_\alpha\right)}{2.5}\right)^2}}, 1\right) = 1.0022$$

"Resultant force angel factor"

$$\psi_{h.V} := \mathrm{Max}\left(\left(\frac{1.5\cdot c_{1.cap}}{\mathrm{Min}\left(H_{concrete.depth}, 1.5\cdot c_{1.cap}\right)}\right)^{\frac{1}{2}}, 1\right) = 1$$

"Concrete depth factor"

$$A0_{c.V} := 4.5\cdot c_{1.cap}{}^2 = 1.3781\cdot 10^5$$

"Ideal anchor edge area"

$$A_{c.V} := 1.5\cdot c_{1.cap}\cdot\left(2\cdot 1.5\cdot c_{1.cap}+3\cdot s_{1.cap}\right) = 2.0869\cdot 10^5$$

"Anhor group edge area"

$$\alpha_{V0.Rk.c} := 0.1\cdot\left(\frac{h_{ef}}{c_{1.cap}}\right)^{\frac{1}{2}} = 0.0756$$

$$\beta_{V0.Rk.c} := 0.1\cdot\left(\frac{d_{anchor.cap}}{c_{1.cap}}\right)^{0.2} = 0.0585$$

$$V0_{Rk.c} := k_{V0.Rk.c}\cdot d_{anchor.cap}{}^{\alpha_{V0.Rk.c}}\cdot h_{ef}{}^{\beta_{V0.Rk.c}}\cdot\sqrt{f_{ck.cube.cap}}\cdot c_{1.cap}{}^{1.5} = 31086.6583$$

$$V_{Rk.c} := V0_{Rk.c}\cdot\frac{A_{c.V}}{A0_{c.V}}\cdot\psi_{h.V}\cdot\psi_{\alpha.V}\cdot\psi_{ec.V} = 47178.5545\ N$$

"Concrete edge shear capacity"

$$\frac{F_{shear.concrete.tot}}{V_{Rk.c}\ \mathrm{N}} = 0.8762$$

"Characteristic edge capactiy utilization"

Combined shear and tension:

The critical capactiy ration is calculated from the critical uti8lization of tension and shear":

$$\left(\frac{F_{shear.concrete.tot}}{V_{Rk.c}\ \mathrm{N}}\right)^2+\left(\frac{\sum F_{axB.Ek}}{N_{Rk.c}\ \mathrm{N}}\right)^2 = 1.3114$$

"Characteristic anchor utilization"

The characteristic capactiy for the anchor group is far exceeded...

Design utilization of characteristic load:

$$\left(\frac{1.5\cdot F_{shear.concrete.tot}}{V_{Rk.c}\ \mathrm{N}}\right)^2+\left(\frac{1.5\cdot\left(\sum F_{axB.Ek}\right)}{N_{Rk.c}\ \mathrm{N}}\right)^2 = 2.9507$$

"Design anchor utilization"

Profile 8-2B-AP

$g := 9.81 \frac{N}{kg}$

Dimensions and material characteristics:

Concrete-steel connection with C20/25 and M16 Anchors:

$d_{x.anchor} := 110\ mm$ "Horizontal screw distance as well as edge distance"

$e_{x.anchor} := 60\ mm$ "Steel edge distance of anchors"

$d_{z.anchor} := 60\ mm$ "Edge distance for concrete steel contact"

$n_{Bx} := 4$ "Number of horizontal anchors in support B"

$d_{anchor} := 16\ mm$ "Anchor diameter"

$f_{y.anchor} := 900 \frac{N}{mm^2}$ "yield capacity of anchor "

$f_{u.anchor} := 1000 \frac{N}{mm^2}$ "Ultimate capacity of anchor"

$f_{ck.cube} := 25 \frac{N}{mm^2}$ "Cubed compressive strength"

$E_{cm} := 29962 \frac{N}{mm^2}$ "C20/25 elastic modulus"

$E_s := 200000 \frac{N}{mm^2}$ "Elastic modulus of anchors"

CLT panel

$H_{CLT} := 3\ m$ "Height of CLT panel"

$B_{CLT} := 4\ m$ "Width of CLT panel"

$t_{CLT} := 0.1\ m$ "CLT thickness"

$\rho_{CLT} := 385 \frac{kg}{m^3}$ "CLT density"

$f_{c.90.k} := 2.5 \frac{N}{mm^2}$ "CLT compression strength perpendicular to wood grain"

$m_{CLT} := H_{CLT} \cdot B_{CLT} \cdot t_{CLT} \cdot \rho_{CLT} = 462\ kg$ "Element weight"

Profile and support A:

$e_1 := 58.00\ mm$ "horizontal edge distance end screw"

$e_2 := 58.00\ mm$ "Vertical edge distance of end screws"

$p_1 := 37.11\ mm$ "Internal horizontal screw distance"

$p_2 := 42.00\ mm$ "Internal vertical screw distance"

$H := 200\ mm$ "Vertical contact of underlying CLT"

$B := 450\ mm$ "Horizontal contact of underlying CLT"

$t_p := 8\ mm$ "Plate thickness"

$n_{xD} := 10$ "Number of screws per row"

$n_{zD} := 3$ "Number of screws per column"

$n_D := n_{xD} \cdot n_{zD}$ "Total number of screws"

$f_y := 235\ \frac{N}{mm^2}$ "Plate yield capacity"

$f_u := 360\ \frac{N}{mm^2}$

$m_{8\_2B} := 11\ kg$ "Profile mass"

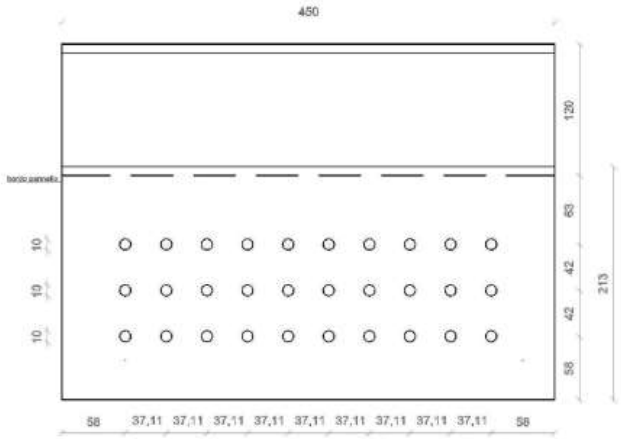

Front view

Concrete:

$f_{ck.cube} = 25\ \frac{N}{mm^2}$ "characteristic cubed strength"

HBS plate dimensions and static values:

"The values of the screws were retrived from the Rothoblaas catalog. Wil refere to the source in final paper."

$d_1 := 8\ mm$

$d_k := 14.5\ mm$

$d_2 := 5.4\ mm$

$d_s := 58\ mm$

$t_1 := 3.4\ mm$

$d_{uk} := 10\ mm$

$d_v := 5.0\ mm$

$L := 80\ mm$

$b := 55\ mm$

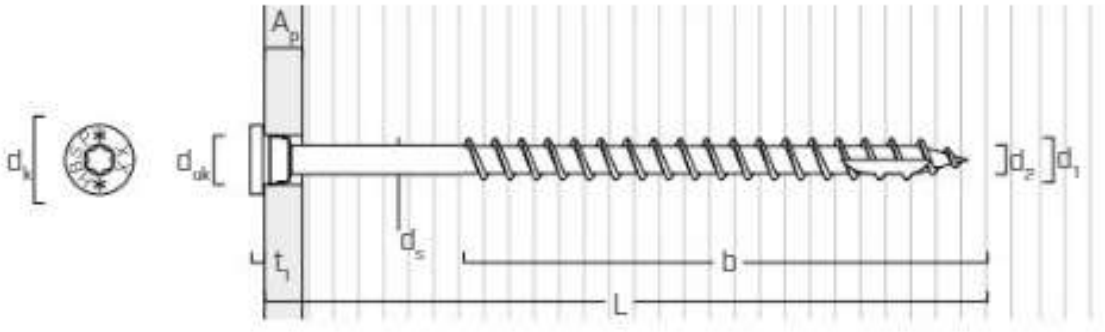

$n := 30$ "Number of screws"

$M_{y.k} := 20057\ N\ mm$ "Charicaristic yield moment"

$f_{ax.k} := 11.7\ \frac{N}{mm^2}$ "Charicaristic withdrawal resistance"

$\rho_a := 350\ \frac{N}{mm^2}$ "referance density for withdrawal resistance"

$f_{head} := 10.5\ \frac{N}{mm^2}$ "Characteristic head-pull through resistance"

$f_{tens.k} := 20.1\ kN$ "Characteristic tensile strenght"

$\alpha := 90\ deg$ "Angel of screws according to the grain"

$k_{ax} := 1$ "For angle 90 deg"

$K_\beta := 1$ "For timber"

$F_{ax.Rk.screw} := 3.954\ kN$ "Axial withdrawal capacity per bolt"

$F_{vD.Rk} := 5.9537\ kN$ “Characteristic shear resistance per screw”

Friction bolts

$\mu_p := 0.3$ "Friction between plate and bolt"

$n_C := 2$ "Number of friction bolts"

$n_{fb} := 2$ "Number of friction surfaces per bolt"

Distances between supports and support criteria:

"All the distances to the centers of the connections were calculated according to the opper middle edge of conncetion D"

Reactions	Supports			
	A	B	C	D
Δx	Free	Free	Free	Fixed
Δy	Free	Free	Fixed	Free
Δz	Free	Free	Fixed	Free
ϕx	Fixed	Free	Fixed	Fixed
ϕy	Fixed	Free	Fixed	Fixed
ϕz	Fixed	Free	Fixed	Fixed

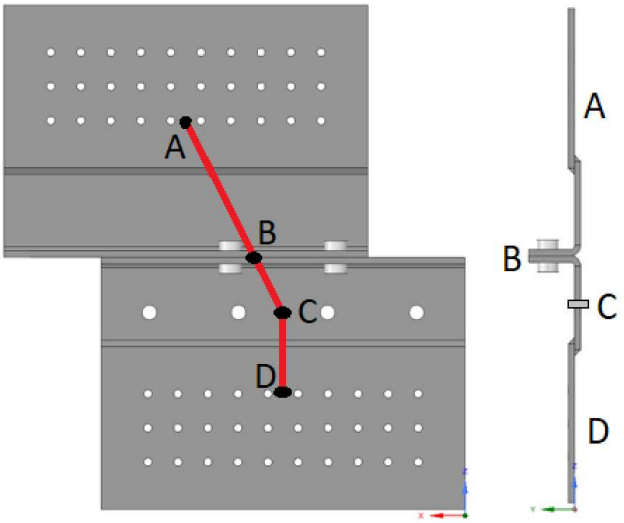

"Global distances for tension profile"

$d_{yAB} := 27.5\ \text{mm}$

$d_{zAB} := -178\ \text{mm}$

$d_{yBC} := -\left(d_{yAB} + 2 \cdot t_p\right) = -0.0435\ \text{m}$ "midd point between bolts"

$d_{zBC} := -60\ \text{mm}$

$d_{yCD} := -d_{yBC} - d_{yAB} = 16\ \text{mm}$

$d_{zCD} := -123\ \text{mm}$

$d_{xAB} := -120\ \text{mm}$

"Ajusted distances with regards to the behaviour of support C for compressed profile"

$d_{xAB.c} := \left(\frac{d_{zAB}}{d_{zAB} + d_{zBC}}\right) \cdot d_{xAB} = -89.7479\ \text{mm}$ "Center of compression force acting on fricition connectort"

$d_{xBC.c} := d_{xAB.c} - d_{xAB} = 30.2521\ \text{mm}$ "Resulting distance to support D"

External forces acting on system:

Forces acting on compression profile:

Following the approach of external force application of profiles, an itnitial critical horizontal force is assumed:

$P_x := 30000\ \text{N}$ "Total external horizontal force acting on compression profile"

For n.floors it is assumed that the mass distribution an floor height is constant equal to height of CLT element:

$n_{floors} := 4$ "Number of floors in building"

$z := Height_i\left(n_{floors}, H_{CLT}\right) = [\,3\ \ 6\ \ 9\ \ 12\,]\ \text{m}$ "Floor height"

$P_{xB} := P_x \cdot \frac{1}{\sum_{z} z} = 3000\ \text{N}$ "Horizontal force in support B for profile in tension"

$P_{xA} := P_x - P_{xB} = 27000\ \text{N}$ "Horizontal force in support A for compressed profile"

The average total force acting on the two profiles and on support A of the two profiles are approximated:

$\lambda := 0.585$ "Reduction factor for maximum vertical load in tension profile"

$P_{x.avg} := \frac{(1+\lambda)\cdot P_x}{2} = 23775\ \text{N}$ "Total force on two profiles"

$P_{xA.avg} := \frac{(1+\lambda)\cdot P_{xA}}{2} = 21397.5\ \text{N}$ "Total vertical force in connection A of the profiles"

Force from weight of a complete CLT element with four profile halfs:

$P_{element} := (-g)\cdot\left(m_{CLT} + m_{8\_2B}\cdot 4\right) = -4964\ \text{N}$ "Equivalent system weight per profile"

Equivalent vertical force on tension and compression profiles:

$P_{zD} := \left(-P_{x.avg}\right)\cdot\left(\frac{H_{CLT}}{B_{CLT}-B}\right) + \frac{P_{element}}{4} = -21333\ \text{N}$ "Vertical force in compression support D accounting for system weight"

$P_{zD.t} := P_{x.avg}\cdot\left(\frac{H_{CLT}}{B_{CLT}-B}\right) + \frac{P_{element}}{4} = 18851\ \text{N}$ "Vertical force in tension support D"

The vertical force of the system above is then approximated from P.xA.avg:

$$P_{zA} := \left(-P_{xA.avg}\right) \cdot \left(\frac{H_{CLT}}{B_{CLT} - B}\right) + \frac{P_{element}}{4} = -19323\ \text{N}$$ "Vertical force in compression support A"

$$P_{zA.t} := P_{xA.avg} \cdot \left(\frac{H_{CLT}}{B_{CLT} - B}\right) + \frac{P_{element}}{4} = 16841\ \text{N}$$ "Vertical force in tension support A"

Pretension of friction connection (second from bottom):

The pretension requrires for the compressed profile is calculated for the two bolts:

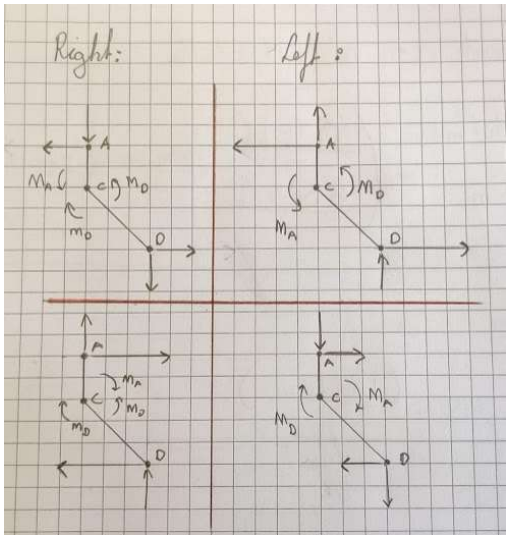

$$k_s := 0.93$$ "EC3 table 3.6 to conservative"

$$F_{p.C.compression} := \frac{\left(P_{xA} - \left|P_{zA}\right| \cdot \mu_p\right)}{k_s \cdot n_{fb} \cdot n_C \cdot \mu_p}$$

$$F_{p.C.compression} = 18.9991\ \text{kN}$$ "Maximum pretension"

The friction force resulting from the bolt pretension is calculated for the tension connection:

$$F_{s.Rk.tension} := k_s \cdot n_{fb} \cdot \mu_p \cdot \left(n_C \cdot F_{p.C.compression} + \frac{P_{zA}}{n_{fb}}\right)$$

$$F_{s.Rk.tension} = 15.8118\ \text{kN}$$ "Resulting friction capactiy for profile in tension"

The total friction force of the system is calculated as the sum of the forur friction bolts:

$$F_{s.Rk.tot} := F_{s.Rk.tension} + P_{xA}$$

$$F_{s.Rk.tot} = 42.8118\ \text{kN} \quad = \quad 2 \cdot P_{xA.avg} = 42.795\ \text{kN}$$

Finally λ is adjusted until the average vertical force equals the friction force.

The horizontal force distribution for the tension profile is approximated:

$$P_{xA.t} := \left(-P_{xA}\right) \cdot \lambda = -15795\ \text{N}$$ "Horizontal force in support A for compressed profile"

$$P_{xB.t} := \left(-P_{xB}\right) \cdot \lambda = -1755\ \text{N}$$ "Horizontal force in support B for profile in tension"

$$P_{x.t} := P_{xA.t} + P_{xB.t} = -17550\ \text{N}$$ "Roughly equivalent to tension friction force"

Compression profile- connection A:

Reaction forces and moments:

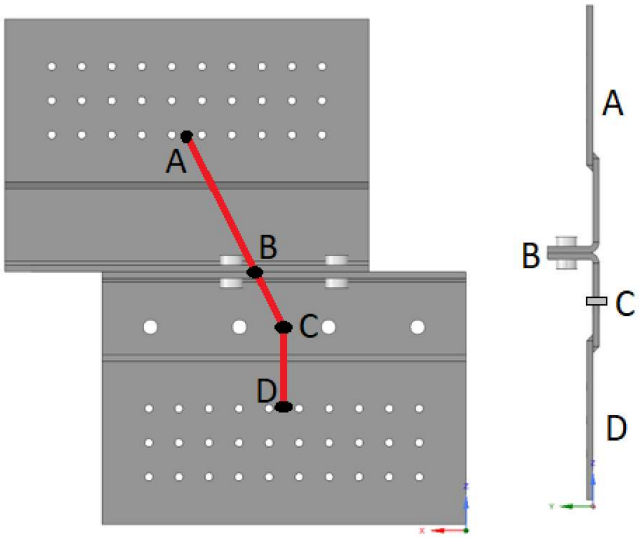

Shear reaction from applied shear force:

"Shear reaction in screws acting opposite of the applied shear force"

$$R_{xA.Ek} := -\frac{P_{xA}}{n_D}$$ "Horizontal shear force per screw"

$$R_{xA.Ek} = -0.9\ \text{kN}$$

Shear reaction from applied normal force:

"Shear reaction acting opposite of applied force"

$$R_{zA.Ek} := \frac{-P_{zA}}{n_D}$$ "Vertical shear force per screw"

$$R_{zA.Ek} = 0.6441\ \text{kN}$$

Moment reactions are calculated calculated for a cantilever with point loads in connection B:

Moment about y-axis:

$$R_{xAB} := P_{xA}$$ "Vertical reaction force acting on system B-A"

$$R_{zBA} := P_{zA}$$ "Horizontal reaction froce in B for system B-A"

$$M_{yA} := R_{xAB} \cdot d_{zAB} + R_{zBA} \cdot \left(-d_{xAB.c}\right)$$

$$M_{yA} = -6.5402\ \text{kN m}$$

Moment about x-axis:

M.x was calculated as a cantilecer with a reactionforce R.zC.

$$R_{zBA} := -P_{zA}$$ "Vertical reaction force in B for system B-A"

$$M_{xA} := R_{zBA} \cdot d_{yAB} = 0.53\ \text{kN m}$$

$$M_{xA} = 0.5314\ \text{kN m}$$

Moment about z-axis:

Reaction moment M.z was calculated as a cantilever with a reaction force R.xC

$$R_{xBA} := -P_{xA}$$

$$M_{zA} := R_{xBA} \cdot \left(-d_{yAB}\right)$$ "The horizontal force is considered to act at the center of the two bolts"

$$M_{zA} = 0.7425\ \text{kN m}$$

Shear forces due to M.y

The shear forces ar calculated according to theory of In plane eccentrically loaded connections:

The distances from geometrical connection center:

$$r_{Az.My} := \begin{bmatrix} p_2 & p_2 & p_2 & p_2 & p_2 & p_2 & p_2 & p_2 & p_2 & p_2 \\ 0 & 0 & 0 & 0 & 0 & 0 & 0 & 0 & 0 & 0 \\ -p_2 & -p_2 & -p_2 & -p_2 & -p_2 & -p_2 & -p_2 & -p_2 & -p_2 & -p_2 \end{bmatrix}$$

$$r_{Ax.My} := \begin{bmatrix} 4.5\cdot p_1 & 3.5\cdot p_1 & 2.5\cdot p_1 & 1.5\cdot p_1 & 0.5\cdot p_1 & -(0.5\cdot p_1) & -(1.5\cdot p_1) & -(2.5\cdot p_1) & -(3.5\cdot p_1) & -(4.5\cdot p_1) \\ 4.5\cdot p_1 & 3.5\cdot p_1 & 2.5\cdot p_1 & 1.5\cdot p_1 & 0.5\cdot p_1 & -(0.5\cdot p_1) & -(1.5\cdot p_1) & -(2.5\cdot p_1) & -(3.5\cdot p_1) & -(4.5\cdot p_1) \\ 4.5\cdot p_1 & 3.5\cdot p_1 & 2.5\cdot p_1 & 1.5\cdot p_1 & 0.5\cdot p_1 & -(0.5\cdot p_1) & -(1.5\cdot p_1) & -(2.5\cdot p_1) & -(3.5\cdot p_1) & -(4.5\cdot p_1) \end{bmatrix}$$

Distance from connection center to screws:

$$r_{A.My} := SRSS_{ij}\left(r_{Az.My}, r_{Ax.My}\right)$$ "Use the sum of square formula for the matrices"

$$r_{A.My} = \begin{bmatrix} 0.1722 & 0.1365 & 0.1018 & 0.0697 & 0.0459 & 0.0459 & 0.0697 & 0.1018 & 0.1365 & 0.1722 \\ 0.167 & 0.1299 & 0.0928 & 0.0557 & 0.0186 & 0.0186 & 0.0557 & 0.0928 & 0.1299 & 0.167 \\ 0.1722 & 0.1365 & 0.1018 & 0.0697 & 0.0459 & 0.0459 & 0.0697 & 0.1018 & 0.1365 & 0.1722 \end{bmatrix} \text{m}$$

The squared value of the distance:

$$r_{A.My.sq} := Prtoduct_{ij}\left(r_{A.My}, r_{A.My}\right)$$ "Use the product formula to calculate squared values"

$$r_{A.My.sq} = \begin{bmatrix} 0.0297 & 0.0186 & 0.0104 & 0.0049 & 0.0021 & 0.0021 & 0.0049 & 0.0104 & 0.0186 & 0.0297 \\ 0.0279 & 0.0169 & 0.0086 & 0.0031 & 0.0003 & 0.0003 & 0.0031 & 0.0086 & 0.0169 & 0.0279 \\ 0.0297 & 0.0186 & 0.0104 & 0.0049 & 0.0021 & 0.0021 & 0.0049 & 0.0104 & 0.0186 & 0.0297 \end{bmatrix} \text{m}^2$$

The torsion formula is the used to calculate the force distribution:

$$F_{Av.My} := \frac{\left(-M_{yA}\right)\cdot r_{A.My}}{\sum r_{A.My.sq}}$$ "Shear distribution"

$$F_{Av.My} = \begin{bmatrix} 2.99 & 2.37 & 1.77 & 1.21 & 0.8 & 0.8 & 1.21 & 1.77 & 2.37 & 2.99 \\ 2.9 & 2.26 & 1.61 & 0.97 & 0.32 & 0.32 & 0.97 & 1.61 & 2.26 & 2.9 \\ 2.99 & 2.37 & 1.77 & 1.21 & 0.8 & 0.8 & 1.21 & 1.77 & 2.37 & 2.99 \end{bmatrix} \text{kN}$$

Equivalent shear components:

$$F_{xA.My} := Division_{ij}\left(Prtoduct_{ij}\left(F_{Av.My}, r_{Az.My}\right), r_{A.My}\right)$$ "Shear component in x-axis"

$$F_{xA.My} = \begin{bmatrix} 0.73 & 0.73 & 0.73 & 0.73 & 0.73 & 0.73 & 0.73 & 0.73 & 0.73 & 0.73 \\ 0 & 0 & 0 & 0 & 0 & 0 & 0 & 0 & 0 & 0 \\ -0.73 & -0.73 & -0.73 & -0.73 & -0.73 & -0.73 & -0.73 & -0.73 & -0.73 & -0.73 \end{bmatrix} \text{kN}$$

$$F_{zA.My} := Division_{ij}\left(Prtoduct_{ij}\left(F_{Av.My}, r_{Ax.My}\right), r_{A.My}\right)$$ "Shear component in z-axis"

$$F_{zA.My} = \begin{bmatrix} 2.9 & 2.26 & 1.61 & 0.97 & 0.32 & -0.32 & -0.97 & -1.61 & -2.26 & -2.9 \\ 2.9 & 2.26 & 1.61 & 0.97 & 0.32 & -0.32 & -0.97 & -1.61 & -2.26 & -2.9 \\ 2.9 & 2.26 & 1.61 & 0.97 & 0.32 & -0.32 & -0.97 & -1.61 & -2.26 & -2.9 \end{bmatrix} \text{kN}$$

screw tension and CLT compression due to M.x:

The method used from out of plane eccentrically loaded bolt connection is ues with maximum elastic strain for screws at characteristical axial screw capactiy equal to maximum elastic strain of CLT at characteristic compression capacity:

The N.A distance percentage factor is calculated:

$\lambda_{CLT.Mx} := 0.549$ "Percentage of connection distance from CLT edge"

$c_{MxA} := \left(H - e_2\right) \cdot \lambda_{CLT.Mx} = 0.07796\ m$ "Edge distance for CLT"

The resulting distance from N.A to screws are calculated from the transposed matrix:

$$r\_initial_{A.Mx} := \begin{bmatrix} e_2 & e_2+p_2 & e_2+2\cdot p_2 \\ e_2 & e_2+p_2 & e_2+2\cdot p_2 \\ e_2 & e_2+p_2 & e_2+2\cdot p_2 \\ e_2 & e_2+p_2 & e_2+2\cdot p_2 \\ e_2 & e_2+p_2 & e_2+2\cdot p_2 \\ e_2 & e_2+p_2 & e_2+2\cdot p_2 \\ e_2 & e_2+p_2 & e_2+2\cdot p_2 \\ e_2 & e_2+p_2 & e_2+2\cdot p_2 \\ e_2 & e_2+p_2 & e_2+2\cdot p_2 \\ e_2 & e_2+p_2 & e_2+2\cdot p_2 \end{bmatrix}^{T} - c_{MxA} = \begin{bmatrix} -0.02 & \cdots \\ 0.022 & \cdots \\ 0.064 & \end{bmatrix} m$$

"Distances from N.A for screws"

The screwes in the compression area are not allowed to contribute to moment resistance and are removed:

$$r_{A.Mx} := Matrix\_remove\_negative_{ij}\left(r\_initial_{A.Mx}\right)$$

$$r_{A.Mx} = \begin{bmatrix} 0 & 0 & 0 & 0 & 0 & 0 & 0 & 0 & 0 & 0 \\ 0.022 & 0.022 & 0.022 & 0.022 & 0.022 & 0.022 & 0.022 & 0.022 & 0.022 & 0.022 \\ 0.064 & 0.064 & 0.064 & 0.064 & 0.064 & 0.064 & 0.064 & 0.064 & 0.064 & 0.064 \end{bmatrix} m$$

The squared distance is calcutated:

$$r_{A.Mx.sq} := Prtoduct_{ij}\left(r_{A.Mx}, r_{A.Mx}\right)$$

Distance to screw force resultant is calculated from the sum of moments about the N.A:

$$T_{A.Mx} := \frac{r_{A.Mx}}{\left(\sum r_{A.Mx.sq}\right)} = \begin{bmatrix} 0 & 0 & 0 & 0 & 0 & 0 & 0 & 0 & 0 & 0 \\ 0.481 & 0.481 & 0.481 & 0.481 & 0.481 & 0.481 & 0.481 & 0.481 & 0.481 & 0.481 \\ 1.396 & 1.396 & 1.396 & 1.396 & 1.396 & 1.396 & 1.396 & 1.396 & 1.396 & 1.396 \end{bmatrix} \frac{1}{m}$$

$$dm_{screw.Mx} := \frac{\sum Prtoduct_{ij}\left(T_{A.Mx}, r_{A.Mx}\right)}{\sum T_{A.Mx}}$$

"Distance from neutral axis to resultant force in Screws"

$$dm_{screw.Mx} = 53.29\ mm$$

The resulting moment arm is calculated from the center of the screw force and the equivalent position of the triangular CLT compression force:

$$z_{A.Mx} := dm_{screw.Mx} + \frac{2}{3} \cdot c_{MxA}$$ "Connection moment arm"

$$z_{A.Mx} = 105.26 \text{ mm}$$

Resulting moments on compression and tension side from the N.A:

$$M_{x.screws} := \left| M_{xA} \right| \cdot \frac{dm_{screw.Mx}}{z_{A.Mx}} = 0.269 \text{ kN m}$$ "Moment acting on screws from N.A"

$$M_{x.CLT} := \left| M_{xA} \right| \cdot \frac{\frac{2}{3} \cdot c_{MxA}}{z_{A.Mx}} = 0.262 \text{ kN m}$$ "Moment acting on CLT from N.A"

Resulting tension forces in screws:

$$F_{Aax.Mx} := \frac{M_{x.screws} \cdot r_{A.Mx}}{\left(\sum r_{A.Mx.sq} \right)}$$ "Force distribution in screws"

$$F_{Aax.Mx} = \begin{bmatrix} 0 & 0 & 0 & 0 & 0 & 0 & 0 & 0 & 0 & 0 \\ 0.1293 & 0.1293 & 0.1293 & 0.1293 & 0.1293 & 0.1293 & 0.1293 & 0.1293 & 0.1293 & 0.1293 \\ 0.3756 & 0.3756 & 0.3756 & 0.3756 & 0.3756 & 0.3756 & 0.3756 & 0.3756 & 0.3756 & 0.3756 \end{bmatrix} \text{ kN}$$

$$\sum F_{Aax.Mx} = 5048.3884 \text{ N}$$ "Sum of tension forces"

Maximum compression stress of CLT:

$$I_{z.CLT} := \frac{B \cdot c_{MxA}^{3}}{3} = 7.1068 \cdot 10^{-5} \text{ m}^4$$ "Moment of inertia of CLT about N.A"

$$\sigma_{max.CLT.Mx} := \frac{M_{x.CLT} \cdot c_{MxA}}{I_{z.CLT}} = 0.2878 \frac{\text{N}}{\text{mm}^2}$$ "Maximum stress acting on CLT"

Force resultant in CLT:

$$\frac{\sigma_{max.CLT.Mx} \cdot c_{MxA}}{2} \cdot B = 5048.3884 \text{ N}$$ "Sum of compression forces"

Maximum screw strain:

The maximum strain of the screws and CLT were both calculated considering the maximum CLT strain perpendicular to the grain, with the maximum strain asumed to act at the characteristic screw tension capacity:

$$\varepsilon_{CLT.Mx} := \frac{\sigma_{max.CLT.Mx}}{f_{c.90.k}} \cdot 0.0083 = 0.001$$ "Maximum strain on CLT"

$$\varepsilon_{screw.Mx} := \frac{\max\left(F_{Aax.Mx} \right)}{F_{ax.Rk.screw}} \cdot 0.0083 = 0.0008$$ Maximum strain in screws"

The strain ratio of change along the connecton is then calculated for the tension and compression part:

$$\varepsilon'_{CLT} := \frac{\varepsilon_{CLT.Mx}}{c_{MxA}} = 0.0123 \cdot \frac{1}{m}$$ "CLT strain/distrance ratio"

$$\varepsilon'_{screw} := \frac{\varepsilon_{screw.Mx}}{e_2 + 2 \cdot p_2 - c_{MxA}} = 0.0123 \cdot \frac{1}{m}$$ "Screw strain/distrance ratio"

The resulting rate of change should be zero when the neurtal axis has been determined correctly trough the ajustment of λ.CLT.Mx:

$$\varepsilon'_{CLT} - \varepsilon'_{screw} = -5.331 \cdot 10^{-5} \cdot \frac{1}{m}$$

screw tension and CLT compression due to M.z:

The same procedure as for M.x is used for the force calculations of M.z

$$\lambda_{CLT.Mz} := 0.248$$

$$c_{MzA} := \left(B - e_1\right) \cdot \lambda_{CLT.Mz} = 0.0972 \text{ m}$$

$$\left(r\_initial_{A.Mz}\right) := \begin{bmatrix} e_1 + 9 \cdot p_1 & e_1 + 9 \cdot p_1 & e_1 + 9 \cdot p_1 \\ e_1 + 8 \cdot p_1 & e_1 + 8 \cdot p_1 & e_1 + 8 \cdot p_1 \\ e_1 + 7 \cdot p_1 & e_1 + 7 \cdot p_1 & e_1 + 7 \cdot p_1 \\ e_1 + 6 \cdot p_1 & e_1 + 6 \cdot p_1 & e_1 + 6 \cdot p_1 \\ e_1 + 5 \cdot p_1 & e_1 + 5 \cdot p_1 & e_1 + 5 \cdot p_1 \\ e_1 + 4 \cdot p_1 & e_1 + 4 \cdot p_1 & e_1 + 4 \cdot p_1 \\ e_1 + 3 \cdot p_1 & e_1 + 3 \cdot p_1 & e_1 + 3 \cdot p_1 \\ e_1 + 2 \cdot p_1 & e_1 + 2 \cdot p_1 & e_1 + 2 \cdot p_1 \\ e_1 + p_1 & e_1 + p_1 & e_1 + p_1 \\ e_1 & e_1 & e_1 \end{bmatrix}^T - c_{MzA}$$

$$r\_initial_{A.Mz} = \begin{bmatrix} 294.8 & 257.7 & 220.6 & 183.4 & 146.3 & 109.2 & 72.1 & 35 & -2.1 & -39.2 \\ 294.8 & 257.7 & 220.6 & 183.4 & 146.3 & 109.2 & 72.1 & 35 & -2.1 & -39.2 \\ 294.8 & 257.7 & 220.6 & 183.4 & 146.3 & 109.2 & 72.1 & 35 & -2.1 & -39.2 \end{bmatrix} \text{mm}$$

$$r_{A.Mz} := Matrix\_remove\_negative_{ij}\left(r\_initial_{A.Mz}\right)$$

$$r_{A.Mz.sq} := Prtoduct_{ij}\left(r_{A.Mz}, r_{A.Mz}\right)$$

$$F_{Aax.Mz} := \frac{M_{zA} \cdot r_{A.Mz}}{\sum r_{A.Mz.sq}}$$

$$F_{Aax.Mz} = \begin{bmatrix} 0.265 & 0.2316 & 0.1982 & 0.1649 & 0.1315 & 0.0982 & 0.0648 & 0.0315 & 0 & 0 \\ 0.265 & 0.2316 & 0.1982 & 0.1649 & 0.1315 & 0.0982 & 0.0648 & 0.0315 & 0 & 0 \\ 0.265 & 0.2316 & 0.1982 & 0.1649 & 0.1315 & 0.0982 & 0.0648 & 0.0315 & 0 & 0 \end{bmatrix} \text{kN}$$

Distance to screw force resultant:

$$T_{A.Mz} := \frac{r_{A.Mz}}{\left(\sum r_{A.Mz.sq}\right)} = \begin{bmatrix} 0.357 & 0.312 & 0.267 & 0.222 & 0.177 & 0.132 & 0.087 & 0.042 & 0 & 0 \\ 0.357 & 0.312 & 0.267 & 0.222 & 0.177 & 0.132 & 0.087 & 0.042 & 0 & 0 \\ 0.357 & 0.312 & 0.267 & 0.222 & 0.177 & 0.132 & 0.087 & 0.042 & 0 & 0 \end{bmatrix} \frac{1}{\text{m}}$$

$$dm_{screw.Mz} := \frac{\sum Prtoduct_{ij}\left(T_{A.Mz}, r_{A.Mz}\right)}{\sum T_{A.Mz}}$$

"Distance from neutral axis to resultant force in Screws"

$$dm_{screw.Mz} = 208.74 \text{ mm}$$

Resulting moment arm:

$$z_{A.Mz} := dm_{screw.Mz} + \frac{2}{3} \cdot c_{MzA}$$

"Connection moment arm"

$$z_{A.Mz} = 273.55 \text{ mm}$$

Resulting moments on compression and tension side:

$$M_{z.screws} := \left|M_{zA}\right| \cdot \frac{dm_{screw.Mz}}{z_{A.Mz}} = 0.567 \text{ kN m}$$

"Moment acting on screws from N.A"

$$M_{z.CLT} := \left|M_{zA}\right| \cdot \frac{\frac{2}{3} \cdot c_{MzA}}{z_{A.Mz}} = 0.176 \text{ kN m}$$

"Moment acting on CLT from N.A"

Resulting tension forces in screws:

$$F_{Aax.Mz} := \frac{M_{z.screws} \cdot r_{A.Mz}}{\left(\sum r_{A.Mz.sq}\right)}$$

"Force distribution in screws"

$$F_{Aax.Mz} = \begin{bmatrix} 0.2022 & 0.1767 & 0.1513 & 0.1258 & 0.1004 & 0.0749 & 0.0495 & 0.024 & 0 & 0 \\ 0.2022 & 0.1767 & 0.1513 & 0.1258 & 0.1004 & 0.0749 & 0.0495 & 0.024 & 0 & 0 \\ 0.2022 & 0.1767 & 0.1513 & 0.1258 & 0.1004 & 0.0749 & 0.0495 & 0.024 & 0 & 0 \end{bmatrix} \text{kN}$$

$$\sum F_{Aax.Mz} = 2714 \text{ N}$$

"Sum of tension forces"

Maximum compression stress of CLT:

$$I_{x.CLT} := \frac{H \cdot c_{MzA}^{3}}{3} = 6.1252 \cdot 10^{7} \text{ mm}^{4}$$

"Moment of inertia of CLT about N.A"

$$\sigma_{max.CLT.Mz} := \frac{M_{z.CLT} \cdot c_{MzA}}{I_{x.CLT}} = 0.2792 \frac{\text{N}}{\text{mm}^{2}}$$

"Maximum stress acting on CLT"

Force resultant in CLT:

$$\frac{\sigma_{max.CLT.Mz} \cdot c_{MzA}}{2} \cdot H = 2714 \text{ N}$$

"Sum of compression forces"

Maximum screw strain:

$$\varepsilon_{CLT.Mz} := \frac{\sigma_{max.CLT.Mz}}{f_{c.90.k}} \cdot 0.0083 = 0.0009$$ "Maximum strain on CLT"

$$\varepsilon_{screw.Mz} := \frac{\max\left(F_{Aax.Mz}\right)}{F_{ax.Rk.screw}} \cdot 0.0083 = 0.0004$$ Maximum strain in screws"

Strain ratio:

$$\varepsilon'_{CLT.Mz} := \frac{\varepsilon_{CLT.Mz}}{c_{MzA}} = 0.0095 \cdot \frac{1}{m}$$ "CLT strain/distrance ratio"

$$\varepsilon'_{screw.Mz} := \frac{\varepsilon_{screw.Mz}}{\left|e_2 + 2 \cdot p_2 - c_{MzA}\right|} = 0.0095 \cdot \frac{1}{m}$$ "Screw strain/distrance ratio"

$$\varepsilon'_{CLT.Mz} - \varepsilon'_{screw.Mz} = 5.8175 \cdot 10^{-5} \cdot \frac{1}{m}$$

Tension profile:
Reaction forces and moments in

Shear reaction from applied shear force:

Shear reaction in screws acting opposite of the applied shear force:

$$R_{xA.t} := -\frac{P_{xA.t}}{n_D}$$ "Horizontal shear force per screw"

$$R_{xA.t} = 0.5265\ kN$$

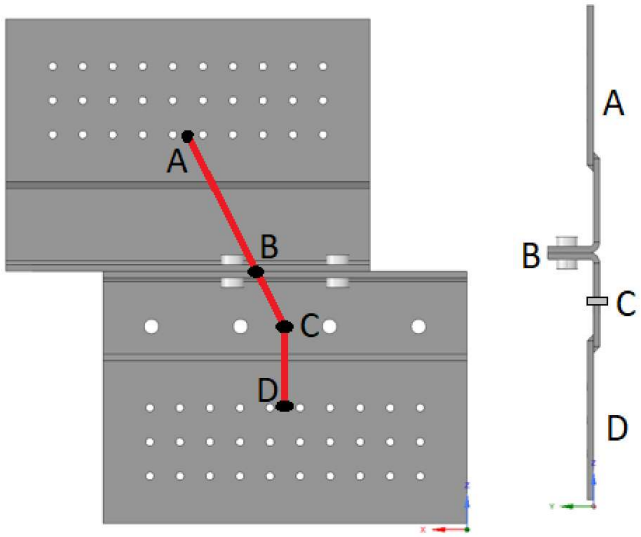

Shear reaction from applied normal force:

Shear reaction acting opposite of applied force

$$R_{zA.t} := -\frac{P_{zA.t}}{n_D}$$ "Vertical shear force per screw"

$$R_{zA.t} = -0.5614\ kN$$

Moment about y-axis:

Because of the assumed moment resistance of connection C, the Moment M.yD was calculated as a fixed-fixed system from support B - D, free to deflect in x direction in support B. The resulting global moment reaction was:

$$R_{xBA.t} := -P_{xA.t}$$ "Vertical reaction force acting on system B-D"

$$R_{zBA.t} := -P_{zA.t}$$ "Horizontal reaction froce in B for system B-D"

$$M_{yA.t} := R_{xBA.t} \cdot d_{zAB} + R_{zBA.t} \cdot \left(-d_{xAB}\right)$$

$$M_{yA.t} = -4.8325\ kN\ m$$

Moment about x-axis:

M.x was calculated as a cantilecer with a reactionforce R.zC.

$R_{zBA.t} := -P_{zA.t}$ "Vertical reaction force in C for system C-D"

$M_{xA.t} := R_{zBA.t} \cdot \left(-d_{yAB}\right)$

$M_{xA.t} = 0.4631\ \text{kN m}$

Moment about z-axis:

Reaction moment M.z was calculated as a cantilever with a reaction force R.xC

$R_{xBA.t} := -P_{xA.t}$ "Horizontal reaction force in C for system C-D"

$M_{zA.t} := R_{xBA.t} \cdot \left(-d_{yAB}\right)$

$M_{zA.t} = -0.4344\ \text{kN m}$

Shear forces due to M.y

The placement of the critical screws for the different forces were ignored, since it was observed that the critical forces would always act at the same screw in one of the outer corners. The same distance matrix is used as for the compression profile:

$$F_{Av.t.My} := \frac{\left(-M_{yA.t}\right) \cdot r_{A.My}}{\sum r_{A.My.sq}}$$ "Shear forces distribution"

$$F_{Av.t.My} = \begin{bmatrix} 2.21 & 1.75 & 1.31 & 0.9 & 0.59 & 0.59 & 0.9 & 1.31 & 1.75 & 2.21 \\ 2.15 & 1.67 & 1.19 & 0.72 & 0.24 & 0.24 & 0.72 & 1.19 & 1.67 & 2.15 \\ 2.21 & 1.75 & 1.31 & 0.9 & 0.59 & 0.59 & 0.9 & 1.31 & 1.75 & 2.21 \end{bmatrix} \text{kN}$$

The shear components are calculated:

$F_{xA.t.My} := Division_{ij}\left(Prtoduct_{ij}\left(F_{Av.t.My}, r_{Az.My}\right), r_{A.My}\right)$

$$F_{xA.t.My} = \begin{bmatrix} 0.54 & 0.54 & 0.54 & 0.54 & 0.54 & 0.54 & 0.54 & 0.54 & 0.54 & 0.54 \\ 0 & 0 & 0 & 0 & 0 & 0 & 0 & 0 & 0 & 0 \\ -0.54 & -0.54 & -0.54 & -0.54 & -0.54 & -0.54 & -0.54 & -0.54 & -0.54 & -0.54 \end{bmatrix} \text{kN}$$

$F_{zA.t.My} := Division_{ij}\left(Prtoduct_{ij}\left(F_{Av.t.My}, r_{Ax.My}\right), r_{A.My}\right)$

$$F_{zA.t.My} = \begin{bmatrix} 2.15 & 1.67 & 1.19 & 0.72 & 0.24 & -0.24 & -0.72 & -1.19 & -1.67 & -2.15 \\ 2.15 & 1.67 & 1.19 & 0.72 & 0.24 & -0.24 & -0.72 & -1.19 & -1.67 & -2.15 \\ 2.15 & 1.67 & 1.19 & 0.72 & 0.24 & -0.24 & -0.72 & -1.19 & -1.67 & -2.15 \end{bmatrix} \text{kN}$$

Screw tension and CLT compression due to M.x.t:

Resulting moments on compression and tension side:

$$M_{x.screws.t} := \left|M_{xA.t}\right| \cdot \frac{dm_{screw.Mx}}{z_{A.Mx}} = 0.234\ \text{kN m}$$ "Moment acting on screws from N.A"

$$M_{x.CLT.t} := \left|M_{xA.t}\right| \cdot \frac{\frac{2}{3} \cdot c_{MxA}}{z_{A.Mx}} = 0.229\ \text{kN m}$$ "Moment acting on CLT from N.A"

Resulting tension forces in screws:

$$F_{Aax.Mx.t} := \frac{M_{x.screws.t} \cdot r_{A.Mx}}{\left(\sum r_{A.Mx.sq}\right)}$$ "Force distribution in screws"

$$F_{Aax.Mx.t} = \begin{bmatrix} 0 & 0 & 0 & 0 & 0 & 0 & 0 & 0 & 0 & 0 \\ 0.1127 & 0.1127 & 0.1127 & 0.1127 & 0.1127 & 0.1127 & 0.1127 & 0.1127 & 0.1127 & 0.1127 \\ 0.3273 & 0.3273 & 0.3273 & 0.3273 & 0.3273 & 0.3273 & 0.3273 & 0.3273 & 0.3273 & 0.3273 \end{bmatrix} \text{kN}$$

$$\sum F_{Aax.Mx.t} = 4399.9635\ \text{N}$$ "Sum of tension forces"

Maximum compression stress of CLT:

$$I_{z.CLT.t} := \frac{B \cdot c_{MxA}^{3}}{3} = 7.1068 \cdot 10^{-5}\ \text{m}^4$$ "Moment of inertia of CLT about N.A"

$$\sigma_{max.CLT.Mx.t} := \frac{M_{x.CLT.t} \cdot c_{MxA}}{I_{z.CLT}} = 0.2508\ \frac{\text{N}}{\text{mm}^2}$$ "Maximum stress acting on CLT"

Force resultant in CLT:

$$\frac{\sigma_{max.CLT.Mx.t} \cdot c_{MxA}}{2} \cdot B = 4399.9635\ \text{N}$$ "Sum of compression forces"

Maximum screw strain:

The maximum strain of the bolts and CLT were both calculated considering the maximum compression perpendicular to the grain.

$$\varepsilon_{CLT.Mx.t} := \frac{\sigma_{max.CLT.Mx.t}}{f_{c.90.k}} \cdot 0.0083 = 0.0008$$ "Maximum strain on CLT"

$$\varepsilon_{screw.Mx.t} := \frac{\max\left(F_{Aax.Mx.t}\right)}{F_{ax.Rk.screw}} \cdot 0.0083 = 0.0007$$ "Maximum strain in screws"

Strain ratio:

$$\varepsilon'_{CLT.t} := \frac{\varepsilon_{CLT.Mx.t}}{c_{MxA}} = 0.0107 \cdot \frac{1}{m}$$ "CLT strain/distrance ratio"

$$\varepsilon'_{screw.t} := \frac{\varepsilon_{screw.Mx.t}}{e_2 + 2 \cdot p_2 - c_{MxA}} = 0.0107 \cdot \frac{1}{m}$$ "Screw strain/distrance ratio"

$$\varepsilon'_{CLT.t} - \varepsilon'_{screw.t} = -4.6463 \cdot 10^{-5} \cdot \frac{1}{m}$$

Screw tension and CLT compression due to M.z.t:

Resulting moments on compression and tension side:

$$M_{z.screws.t} := \left|M_{zA.t}\right| \cdot \frac{dm_{screw.Mz}}{z_{A.Mz}} = 0.331 \text{ kN m}$$ "Moment acting on screws from N.A"

$$M_{z.CLT.t} := \left|M_{zA.t}\right| \cdot \frac{\frac{2}{3} \cdot c_{MzA}}{z_{A.Mz}} = 0.103 \text{ kN m}$$ "Moment acting on CLT from N.A"

Resulting tension forces in screws:

$$F_{Aax.Mz.t} := \frac{M_{z.screws.t} \cdot r_{A.Mz}}{\left(\sum r_{A.Mz.sq}\right)}$$ "Force distribution in screws"

$$F_{Aax.Mz.t} = \begin{bmatrix} 0.1183 & 0.1034 & 0.0885 & 0.0736 & 0.0587 & 0.0438 & 0.0289 & 0.014 & 0 & 0 \\ 0.1183 & 0.1034 & 0.0885 & 0.0736 & 0.0587 & 0.0438 & 0.0289 & 0.014 & 0 & 0 \\ 0.1183 & 0.1034 & 0.0885 & 0.0736 & 0.0587 & 0.0438 & 0.0289 & 0.014 & 0 & 0 \end{bmatrix} \text{kN}$$

Maximum compression stress of CLT:

$$I_{x.CLT} := \frac{H \cdot c_{MzA}^{3}}{3} = 6.1252 \cdot 10^{-5} \text{ m}^4$$ "Moment of inertia of CLT about N.A"

$$\sigma_{max.CLT.Mz.t} := \frac{M_{z.CLT.t} \cdot c_{MzA}}{I_{x.CLT}} = 0.1633 \frac{\text{N}}{\text{mm}^2}$$ "Maximum stress acting on CLT"

Capacity control:

The axial forces acting on the system are a result Mx and Mz:

Resulting axial forces acting on screws:

"M.x and M.z are the only contributers to the axial forces of the system:

$$F_{Aax.tot} := F_{Aax.Mx} + F_{Aax.Mz} = \begin{bmatrix} 0.202 & 0.177 & 0.151 & 0.126 & 0.1 & 0.075 & 0.049 & 0.024 & 0 & 0 \\ 0.331 & 0.306 & 0.281 & 0.255 & 0.23 & 0.204 & 0.179 & 0.153 & 0.129 & 0.129 \\ 0.578 & 0.552 & 0.527 & 0.501 & 0.476 & 0.45 & 0.425 & 0.4 & 0.376 & 0.376 \end{bmatrix} \text{kN}$$

$$F_{Aax.Ek} := \max\left(F_{Aax.tot}\right) = 0.5778 \text{ kN}$$ "Axial force on screws in compression system"

$$F_{Aax.tot.t} := F_{Aax.Mx.t} + F_{Aax.Mz.t} = \begin{bmatrix} 0.118 & 0.103 & 0.088 & 0.074 & 0.059 & 0.044 & 0.029 & 0.014 & 0 & 0 \\ 0.231 & 0.216 & 0.201 & 0.186 & 0.171 & 0.156 & 0.142 & 0.127 & 0.113 & 0.113 \\ 0.446 & 0.431 & 0.416 & 0.401 & 0.386 & 0.371 & 0.356 & 0.341 & 0.327 & 0.327 \end{bmatrix} \text{kN}$$

$$F_{Aax.Ek.t} := \max\left(F_{Aax.tot.t}\right) = 0.4456 \text{ kN}$$ "Axial force on screws in tension system"

Resulting maximum CLT compression:

"Maximum compressive stress for CLT is considderd to act at the top right corner of the connection resulitng in the maximum compression being the sum of critical compression from M.z and M.y:"

$$\sigma_{clt.Ek} := \sigma_{max.CLT.Mx} + \sigma_{max.CLT.Mz}$$

$$\sigma_{clt.Ek} = 0.567 \frac{\text{N}}{\text{mm}^2}$$

$$\boxed{\frac{\sigma_{clt.Ek}}{f_{c.90.k}} = 0.227}$$

$$\sigma_{clt.Ek.t} := \sigma_{max.CLT.Mx.t} + \sigma_{max.CLT.Mz.t}$$

$$\sigma_{clt.Ek.t} = 0.4142 \frac{\text{N}}{\text{mm}^2}$$

$$\boxed{\frac{\sigma_{clt.Ek.t}}{f_{c.90.k}} = 0.166}$$

Resulting maximum shear force acting on screws:

"The maximum shear from moments M.x and M.z and forces R.px are summed for respective axes."

$$F_{xA.tot} := R_{xA.Ek} + F_{xA.My}$$

$$F_{xA.tot} = \begin{bmatrix} -0.17 & -0.17 & -0.17 & -0.17 & -0.17 & -0.17 & -0.17 & -0.17 & -0.17 & -0.17 \\ -0.9 & -0.9 & -0.9 & -0.9 & -0.9 & -0.9 & -0.9 & -0.9 & -0.9 & -0.9 \\ -1.63 & -1.63 & -1.63 & -1.63 & -1.63 & -1.63 & -1.63 & -1.63 & -1.63 & -1.63 \end{bmatrix} \text{kN}$$

$$F_{zA.tot} := R_{zA.Ek} + F_{zA.My}$$

$$F_{zA.tot} = \begin{bmatrix} 3.548 & 2.903 & 2.257 & 1.612 & 0.967 & 0.321 & -0.324 & -0.969 & -1.614 & -2.26 \\ 3.548 & 2.903 & 2.257 & 1.612 & 0.967 & 0.321 & -0.324 & -0.969 & -1.614 & -2.26 \\ 3.548 & 2.903 & 2.257 & 1.612 & 0.967 & 0.321 & -0.324 & -0.969 & -1.614 & -2.26 \end{bmatrix} \text{kN}$$

"As a result of the even distribution of shear forces from external forces and the maximum shear force from moments acting in corner scres, it is determined that the maximum shear wil act in one of the four corners resulting in the SRSS of the maximum shear force in x and z direction."

$$F_{vA.Ek} := \sqrt{\left(\text{Max}\left(\left|\text{mat2sys}\left(F_{xA.tot}\right)\right|\right)\right)^2 + \left(\text{Max}\left(\left|\text{mat2sys}\left(F_{zA.tot}\right)\right|\right)\right)^2}$$

$F_{vA.Ek} = 3904.5468\ \text{N}$ "Critical shear force force of compression profile"

"The maximum shear from moments M.x.t and M.z.t and forces R.px are summed for their respective axes."

$$F_{xA.tot.t} := R_{xA.t} + F_{xA.t.My}$$

$$F_{xA.tot.t} = \begin{bmatrix} 1.066 & 1.066 & 1.066 & 1.066 & 1.066 & 1.066 & 1.066 & 1.066 & 1.066 & 1.066 \\ 0.526 & 0.526 & 0.526 & 0.526 & 0.526 & 0.526 & 0.526 & 0.526 & 0.526 & 0.526 \\ -0.013 & -0.013 & -0.013 & -0.013 & -0.013 & -0.013 & -0.013 & -0.013 & -0.013 & -0.013 \end{bmatrix} \text{kN}$$

$$F_{zA.tot.t} := R_{zA.t} + F_{zA.t.My}$$

$$F_{zA.tot.t} = \begin{bmatrix} 1.584 & 1.107 & 0.631 & 0.154 & -0.323 & -0.8 & -1.277 & -1.753 & -2.23 & -2.707 \\ 1.584 & 1.107 & 0.631 & 0.154 & -0.323 & -0.8 & -1.277 & -1.753 & -2.23 & -2.707 \\ 1.584 & 1.107 & 0.631 & 0.154 & -0.323 & -0.8 & -1.277 & -1.753 & -2.23 & -2.707 \end{bmatrix} \text{kN}$$

$$F_{vA.Ek.t} := \sqrt{\left(\text{Max}\left(\left|\text{mat2sys}\left(F_{xA.tot.t}\right)\right|\right)\right)^2 + \left(\text{Max}\left(\left|\text{mat2sys}\left(F_{zA.tot.t}\right)\right|\right)\right)^2}$$

$F_{vA.Ek.t} = 2909.3223\ \text{N}$ "Critical shear force of tension profile"

"EN 1995 1-1:2008 does not give an expression for the combined characteristic capacity of screws. As a result eq. (8.28) is adapted for characteristic values by exchanging the design values for characteristic values:"

$$\left(\frac{F_{Aax.Ek}}{F_{ax.Rk.screw}}\right)^2 + \left(\frac{F_{vA.Ek}}{F_{vD.Rk}}\right)^2 = 0.4514$$

"Characteristic utilization for profile in compression: $P_x = 30\ \text{kN}$

$$\left(\frac{F_{Aax.Ek.t}}{F_{ax.Rk.screw}}\right)^2 + \left(\frac{F_{vA.Ek.t}}{F_{vD.Rk}}\right)^2 = 0.2515$$

"Characteristic utilization for profile in tension: $P_{x.t} = -17.55\ \text{kN}$

"Calculating for a γ factor of 1.25 the design utilization yields the following design utilization for a load P.x:

$$F_{vD.Rd} := \frac{F_{vD.Rk}}{1.25} \qquad F_{ax.Rd} := \frac{F_{ax.Rk.screw}}{1.25}$$

$$\left(\frac{F_{Aax.Ek}}{F_{ax.Rd}}\right)^2 + \left(\frac{F_{vA.Ek}}{F_{vD.Rd}}\right)^2 = 0.705$$

"Design utilization for profile in compression"

$$\left(\frac{F_{Aax.Ek.t}}{F_{ax.Rd}}\right)^2 + \left(\frac{F_{vA.Ek.t}}{F_{vD.Rd}}\right)^2 = 0.3929$$

Desing utilization for profile in tension"

Concrete connection calculations

Forces acting on system

Reaction forces in connection C in regards to system BC:

$R_{xC} := -P_{xB} = -3000\ N$ "horizontal reaction force in connecton B"

$R_{zC} := P_{zD} + P_{zA} = -40655.8737\ N$ "Vertical reaction force in connection B"

$R_{xD} := R_{xC}$

The M.y in support B was calculated as the sum of the moments in B from a fixed-fixed moment system A-B and a fixed-fixed system B-D. This was done because support B prohibited any rotation in the support, thus prohibiting the transfer of moments. Point C was also considered moment resisting for moments about the y-axis.

$M_{yC.BC} := \left(P_{xA} + P_{xB}\right) \cdot d_{zBC} + P_{zA} \cdot d_{xBC.c} = -2.3846\ kN\ m$ "M.y from horizontal force in support A"

$M_{yC.DC} := (-0.5) \cdot \left(P_{xA} + P_{xB}\right) \cdot \left(-d_{zCD}\right) = -1.845\ kN\ m$ "M.y from horizontal force in support D"

$M_{yC} := M_{yC.BC} + M_{yC.DC}$ "Sum of M.y resisted by support B"

$M_{yC} = -4.2296\ kN\ m$

M.x is calculated as the sum of the momet created from the vertical force acting in connection A and C:

$M_{xC.BC} := P_{zA} \cdot d_{yBC} = 0.8406\ kN\ m$

$M_{xC.DC} := 0.5 \cdot P_{zD} \cdot \left(-d_{yCD}\right) = 0.1707\ kN\ m$

$M_{xC} := \left(M_{xC.BC} + M_{xC.DC}\right)$ "Resultant moment"

$M_{xC} = 1.0112\ kN\ m$

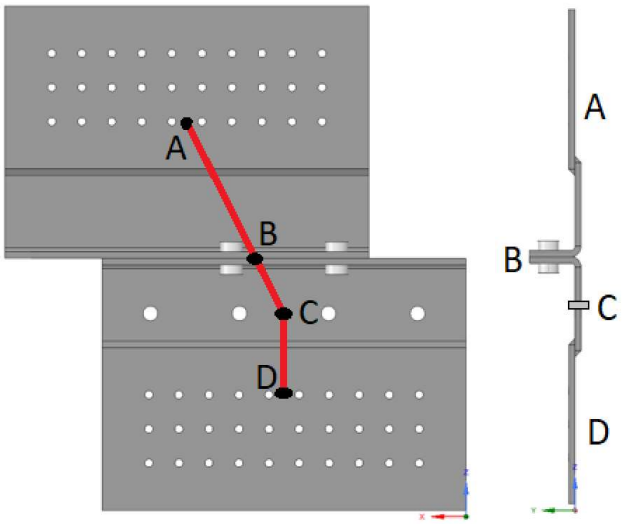

M.y is calculated as a sum of the force acting on

$M_{zC.BC} := \left(P_{xA}\right) \cdot d_{yBC} = -1.1745\ kN\ m$

$M_{zC.DC} := 0.5 \cdot \left(-\left(P_{xA} + P_{xB}\right)\right) \cdot \left(-d_{yCD}\right) = 0.24\ kN\ m$

$M_{zC} := \left(M_{zC.BC} + M_{zC.DC}\right)$

$M_{zC} = -0.9345\ kN\ m$

Reaction forces in concrete anchors due to M.y:

The calculation is done using the same principle as connection D for M.y with the center determined by symetri:

$$r_{C.My} := \left[1.5 \cdot d_{x.anchor} \;\; 0.5 \cdot d_{x.anchor} \;\; (-0.5) \cdot d_{x.anchor} \;\; (-1.5) \cdot d_{x.anchor} \right]$$

$$r_{C.My} = \left[0.165 \;\; 0.055 \;\; -0.055 \;\; -0.165 \right] \text{m}$$

$$r_{C.My.sq} := Prtoduct_{ij}\left(r_{C.My}, r_{C.My}\right)$$

$$r_{C.My.sq} = \left[0.0272 \;\; 0.003 \;\; 0.003 \;\; 0.0272 \right] \text{m}^2$$

The moment calculated was already the reaction of the screws resulting in the use of the moment exiting the connection being -M.yB:

$$F_{zC.My} := -\frac{M_{yC} \cdot r_{C.My}}{\sum r_{C.My.sq}}$$

$$F_{zC.My} = \left[11.54 \;\; 3.85 \;\; -3.85 \;\; -11.54 \right] \text{kN}$$

Reaction forces in concrete anchors due to M.z:

The same procedure as for M.x is used for the force calculations of M.z

$n_{t.anchors} := 4$ "Number of anchors"

$\lambda_{Concrete.Mz} := 0.251$ "Connection percentage distance from concrete edge"

$c_{MzC} := \left(\left(n_{t.anchors} - 1\right) \cdot d_{x.anchor} + e_{x.anchor}\right) \cdot \lambda_{Concrete.Mz} = 0.0979 \text{ m}$ "Concrete edge distance to neutral axis"

$$r\_initial_{C.Mz} := \begin{bmatrix} e_{x.anchor} + 3 \cdot d_{x.anchor} \\ e_{x.anchor} + 2 \cdot d_{x.anchor} \\ e_{x.anchor} + d_{x.anchor} \\ e_{x.anchor} \end{bmatrix}^{T} - c_{MzC}$$

$$r\_initial_{C.Mz} = \left[292.1 \;\; 182.1 \;\; 72.1 \;\; -37.9 \right] \text{mm}$$

$r_{C.Mz} := Matrix\_remove\_negative_{ij}\left(r\_initial_{C.Mz}\right)$ "Compression screws are removed"

$r_{C.Mz.sq} := Prtoduct_{ij}\left(r_{C.Mz}, r_{C.Mz}\right)$ "Squared distances"

Distance to screw force resultant:

$$T_{C.Mz} := \frac{r_{C.Mz}}{\left(\sum r_{C.Mz.sq}\right)} = \left[\begin{array}{cccc} 2.362 & 1.472 & 0.583 & 0 \end{array}\right] \frac{1}{m}$$

$$dm_{anchor.Mz} := \frac{\sum Prtoduct_{ij}\left(T_{C.Mz}, r_{C.Mz}\right)}{\sum T_{C.Mz}}$$

"Distance from neutral axis to resultant force in anchors"

$$dm_{anchor.Mz} = 226.41 \text{ mm}$$

Resulting moment arm:

$$z_{C.Mz} := dm_{anchor.Mz} + \frac{2}{3} \cdot c_{MzC}$$

"Connection moment arm"

$$z_{C.Mz} = 291.67 \text{ mm}$$

Resulting moments on compression and tension side:

$$M_{z.anchor} := \left|M_{zC}\right| \cdot \frac{dm_{anchor.Mz}}{z_{C.Mz}} = 0.725 \text{ kN m}$$

"Moment acting on anchors from N.A"

$$M_{z.Concrete} := \left|M_{zC}\right| \cdot \frac{\frac{2}{3} \cdot c_{MzC}}{z_{C.Mz}} = 0.209 \text{ kN m}$$

"Moment acting on concrete from N.A"

Resulting tension forces in screws:

$$F_{Cax.Mz} := \frac{M_{z.anchor} \cdot r_{C.Mz}}{\left(\sum r_{C.Mz.sq}\right)}$$

"Force distribution in anchors"

$$F_{Cax.Mz} = \left[\begin{array}{cccc} 1.7131 & 1.068 & 0.4229 & 0 \end{array}\right] \text{kN}$$

$$\sum F_{Cax.Mz} = 3204 \text{ N}$$

"Sum of tension forces"

Maximum compression stress of CLT:

$$I_{x.Concrete} := \frac{2 \cdot d_{z.anchor} \cdot c_{MzC}^{3}}{3} = 3.7521 \cdot 10^{-5} \text{ m}^4$$

"Moment of inertia of concrete about N.A"

$$\sigma_{max.Concrete.Mz} := \frac{M_{z.Concrete} \cdot c_{MzC}}{I_{x.Concrete}} = 0.5455 \frac{\text{N}}{\text{mm}^2}$$

"Maximum stress acting on concrete"

Force resultant in CLT:

$$\frac{\sigma_{max.Concrete.Mz} \cdot c_{MzC}}{2} \cdot 2 \cdot d_{z.anchor} = 3204 \text{ N}$$

"Sum of compression forces"

Maximum screw strain:

$$\varepsilon_{Concrete.Mz} := \frac{\sigma_{max.Concrete.Mz}}{E_{cm}} = 1.8207 \cdot 10^{-5}$$

"Maximum strain on concrete"

$$A_{anchor} := 157 \text{ mm}^2$$

$$\varepsilon_{anchor.Mz} := \frac{\max\left(F_{Cax.Mz}\right)}{A_{anchor} \cdot E_s} = 5.4558 \cdot 10^{-5}$$ Maximum strain in anchors"

Strain ratio:

$$\varepsilon'_{Concrete.Mz} := \frac{\varepsilon_{Concrete.Mz}}{c_{MzC}} = 0.186 \ \frac{1}{km}$$ "concrete strain/distrance ratio"

$$\varepsilon'_{anchor.Mz} := \frac{\varepsilon_{anchor.Mz}}{\left|r\_initial_{C.Mz\ 1}\right|} = 0.1868 \ \frac{1}{km}$$ "anchors strain/distrance ratio"

$$\varepsilon'_{Concrete.Mz} - \varepsilon'_{anchor.Mz} = -7.785 \cdot 10^{-7} \cdot \frac{1}{m}$$

Reaction forces in anchors due to M.xB

$n_{anchors} := 4$ "Number of anchors"

$H_C := d_{z.anchor} = 0.06 \ m$ "Height of connection"

$\lambda_{Concrete.Mx} := 0.423$

$c_{MxC} := \left(H_C\right) \cdot \lambda_{Concrete.Mx} = 0.02538 \ m$

Since the system only consists of one row of screws, the resultant tension force acts in the middle of the row.

$$dm_{anchor.Mx} := H_C - c_{MxC}$$

Resulting moment arm:

"When the system is linearly elastic the stress distribution of CLT is triangular, resulting in the resultant force acting 2/3 of the distance from the neutral axis.

$$z_{C.Mx} := dm_{anchor.Mx} + \frac{2}{3} \cdot c_{MxC}$$ "Connection moment arm"

$z_{C.Mx} = 51.54 \ mm$

Resulting moments on compression and tension side:

$$M_{x.anchor} := \left|M_{xC}\right| \cdot \frac{dm_{anchor.Mx}}{z_{C.Mx}} = 0.679 \ kN\ m$$ "Moment acting on screws from N.A"

$$M_{x.concrete} := \left|M_{xC}\right| \cdot \frac{\frac{2}{3} \cdot c_{MxC}}{z_{C.Mx}} = 0.332 \ kN\ m$$ "Moment acting on CLT from N.A"

Resulting tension forces in screws:

$$F_{Cax.Mx.tot} := \frac{M_{x.anchor} \cdot dm_{anchor.Mx}}{dm_{anchor.Mx}^2}$$ "Force distribution in screws"

$$F_{Cax.Mx} := \frac{F_{Cax.Mx.tot}}{n_{anchors}} = 4.9051 \ kN$$

Maximum compression stress of concrete:

$$I_{z.concrete} := \frac{B \cdot c_{MxC}^{3}}{3} = 2.4523 \cdot 10^{-6}\ m^4$$ "Moment of inertia of CLT about N.A"

$$\sigma_{max.concrete.Mx} := \frac{M_{x.concrete} \cdot c_{MxC}}{I_{z.concrete}} = 3.4358\ \frac{N}{mm^2}$$ "Maximum stress acting on CLT"

Assuming full adhesion between concrete and anchor allows for the use of strain of steel.

The maximum strain of the bolts and CLT were both calculated considering the maximum compression perpendicular to the grain.

$$\varepsilon_{concrete.Mx} := \frac{\sigma_{max.concrete.Mx}}{E_{cm}} = 0.0001$$ "Maximum strain on CLT"

$$\varepsilon_{anchor.Mx} := \frac{F_{Cax.Mx}}{A_{anchor} \cdot E_s} = 0.0002$$ Maximum strain in screws"

Strain ratio:

For plates to remain plane, the rate of change in strain have to be equal for the tension and compression part of the connection.

$$\varepsilon'_{concrete} := \frac{\varepsilon_{concrete.Mx}}{c_{MxC}} = 4.5182\ \frac{1}{km}$$ "CLT strain/distrance ratio"

Strain ratio changed. Needs to be checked!

$$\varepsilon'_{screw} := \frac{\varepsilon_{anchor.Mx}}{dm_{anchor.Mx}} = 4.5122\ \frac{1}{km}$$ "Screw strain/distrance ratio"

Shear stress due to axial forces:

The shear forces due to axial forces were calculated as evenly distributed because the connection only consisted of one row of edge bolts. (Not two rows whtere the shear forces would be taken by the inner bolts to increase concrete tear out strength.)

Vertical force

$$R_{zC} = -40.6559\ kN$$

$$F_{zC.Rz} := \frac{R_{zC}}{n_{Bx}} = -10.164\ kN$$ "Vertical resistance per anchor"

Horizontal force

$$R_{xC} := -P_{xB} = -3000\ N$$

$$F_{xC.Rx} := \frac{R_{xC}}{n_{Bx}} = -0.75\ kN$$ "horizontal resistance per anchor"

Resulting forces in anchors due to applied forces:

Resulting vertical shear forces

$$F_{zC.Ek} := F_{zC.My} + F_{zC.Rz}$$

$$F_{zC.Ek} = \begin{bmatrix} 1.37 & -6.32 & -14.01 & -21.7 \end{bmatrix} kN$$

Resulting horizontal shear forces

$$F_{xC.Ek} := F_{xC.Rx} \cdot [1\ 1\ 1\ 1]$$

$$F_{xC.Ek} = [-0.75\ -0.75\ -0.75\ -0.75]\ \text{kN}$$

Resulting axial forces

$$F_{axC.Ek} := F_{Cax.Mx} \cdot [1\ 1\ 1\ 1] + F_{Cax.Mz}$$

$$F_{axC.Ek} = [6.618\ 5.973\ 5.328\ 4.905]\ \text{kN}$$

From the results it was determined that the worst anchor was the right anchor because of the largest resulting vertical shear force.

Resulting reaction forces of worst anchor:

$$F_{zC.Ek.crit} := \text{Max}\left(\left|\text{mat2sys}\left(F_{zC.Ek}\right)\right|\right)$$

$$\boxed{F_{zC.Ek.crit} = 21.699\ \text{kN}}$$

$$F_{xC.Ek.crit} := \text{Max}\left(\left|\text{mat2sys}\left(F_{xC.Ek}\right)\right|\right)$$

$$\boxed{F_{xC.Ek.crit} = 0.75\ \text{kN}}$$

$$F_{axC.Ek.crit} := \text{Max}\left(F_{axC.Ek}\right)$$

$$\boxed{F_{axC.Ek.crit} = 6.6182\ \text{kN}}$$

Anchor capactiy control:

Can not find anchors of size M14: As a substitute, Hitist HIT-HY 200 M12 anchors are utilized. The calculations have been done for cracked concrete: No units are assigned, as the calculations are empirical:

$n_{t.anchors} := 4$ "Number of anchors"

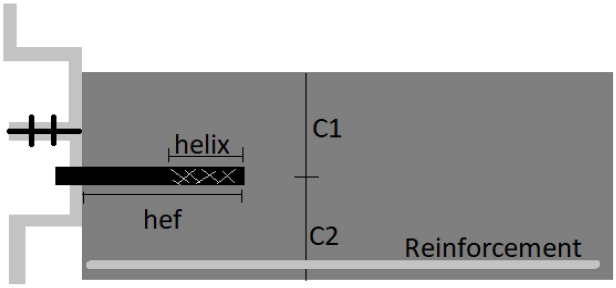

Concrete:

$H_{concrete} := 350\ mm$ "Height of concrette beam"

$H_{concrete.depth} := 300\ mm$ "Concrete depth"

$c_{1.cap} := \frac{H_{concrete}}{2}$ "Upper edge distance"

$c_{2.cap} := c_{1.cap}$ "Lower edge distance" "Assumed to be fixed in the middle"

$s_{1.cap} := 110\ mm$ "Anchor spacing"

$f_{ck.cube.cap} := 25\ \frac{N}{mm^2}$ "Characteristic cubed concrete capacity"

ETA-12/0028: HILTI HIT-HY 200R with HIT-Z: (Table values)

$d_{anchor.cap} := 16\ mm$ "Anchor diameter"

$h_{nom} := 160\ mm$ "Anchor depth"

$h_{ef} := h_{nom}\ mm$ "Effective anchor depth"

$A_{s.anchor} := 157\ mm$ "Area of steel cross section"

$h_{helix} := 95\ mm$ "Length of helix part of anchor"

$C_{cr.sp} := 1.5 \cdot h_{ef} = 240\ mm$

$S_{cr.sp} := 2 \cdot C_{cr.sp} = 480\ mm$

"Pull out area distances valid for : H.concrete.depth / h.nom > 2.3"

$\tau_{rk.ucr} := 22\ \frac{N}{mm^2}$ "Anchor bond resistance"

$f_{uk} := 610\ \frac{N}{mm^2}$ "Characteristic capactiy of anchor"

$f_{yk.anchor} := 490\ \frac{N}{mm^2}$ "Yield strength of anchor"

$S_{cr.Np} := \mathrm{Min}\left(20 \cdot d_{anchor.cap}, 3 \cdot h_{helix}\right)$

$C_{cr.Np} := 0.5 \cdot S_{cr.Np} = 142.5$

"Group pull-out distances"

$k_{\psi 0.g.Np} := 2.3$ "Concrete factor according to ETA-12/0028"

$gamma := 1.5$ "Anchor safety factor"

$c_{min} := 80$

$s_{min} := 80$

"Minimum and maximum anchor distances for M12"

$h_{nom.max} := 192$

"From catalog, of M12 not ETA"

$h_{c.d.min} := h_{nom} + 60 = 220$

Distances and factors determined by ETAG 001:

"Pry out distances"

$S_{cr.N} := 3 \cdot h_{ef} = 480$

$C_{cr.N} := 0.5 \cdot S_{cr.N} = 240$

$\psi_{re.V} := 1.2$ "Anchorage with straight reinforcement"

1.4 "straight reinforcement as well as stir ups closer than 100 m,"

Concrete factors for cracked concrete ETAG 001:

$k_{N0.Rk.c} := 7.2$

$k_{V.Rk.cp} := 2$

$k_{V0.Rk.c} := 1.7$

Tension capactiy

Steel failure:

$N_{Rk.s} := n_{t.anchors} \cdot A_{s.anchor} \cdot f_{uk} = 3.8308 \cdot 10^{5}$ N "Steel capacity"

$\frac{\sum F_{axC.Ek}}{N_{Rk.s}} = 0.0596$ N "Steel utilization for tension"

Eccentricity of resulting axial forces on anchors is determined:

$F_{axC.Ek} = [\, 6.6182 \;\; 5.9731 \;\; 5.328 \;\; 4.9051 \,]$ kN "Resultant tension forces on anchors"

$r_{nB} := [\, 1.5 \cdot s_{1.cap} \;\; 0.5 \cdot s_{1.cap} \;\; (-0.5) \cdot s_{1.cap} \;\; (-1.5) \cdot s_{1.cap} \,]$ "Distance from geometrical connector center"

$r_{nB} = [\, 165 \;\; 55 \;\; -55 \;\; -165 \,]$

$e_n := \frac{\sum Prtoduct_{ij}(r_{nB}, F_{axC.Ek})}{\sum F_{axC.Ek}} = 13.9389$ mm "Eccentricity"

Group pull-out failure:

Next the different group pull out factors are calulated:

$\psi_{re.Np} := \mathrm{Min}\left(0.5 + \frac{h_{ef}}{200}, 1\right) = 1$ "Spalling factor"

$\psi_{ec.Np} := \mathrm{Min}\left(\frac{1}{1 + 2 \cdot \frac{e_n}{S_{cr.Np}}}, 1\right) = 0.9109$ "Eccentricity factor"

$\psi 0_{g.Np} := \mathrm{Max}\left(\left(\sqrt{n_{t.anchors}} - \left(\sqrt{n_{t.anchors}} - 1\right) \cdot \frac{d_{anchor.cap} \cdot \tau_{rk.ucr}}{k_{\psi 0.g.Np} \cdot \sqrt{h_{ef} \cdot f_{ck.cube.cap}}}\right), 1\right) = 1$

$\psi_{g.Np} := \mathrm{Max}\left(\psi 0_{g.Np} - \left(\frac{s}{S_{cr.Np}}\right)^{0.5} \cdot \left(\psi 0_{g.Np} - 1\right)\right) = 1$ "Surface factor"

$\psi_{s.Np} := 0.7 + 0.3 \cdot \frac{c_{1.cap}}{C_{cr.Np}} = 1.0684$ "Edge distance factor"

$A0_{p.N} := S_{cr.Np}{}^{2} = 81225$ "Ideal pull out area"

$A_{p.N} := 2 \cdot \mathrm{Min}\left(c_{1.cap}, C_{cr.Np}\right) \cdot \left(2 \cdot C_{cr.Np} + \left(n_{t.anchors} - 1\right) \cdot s_{1.cap}\right) = 1.7528 \cdot 10^{5}$ "Group pull out area"

$N0_{Rk.p} := \pi \cdot d_{anchor.cap} \cdot h_{helix} \cdot \tau_{rk.ucr} = 1.0505 \cdot 10^{5}$ "Ideal anchor pull out capacity"

$N_{Rk.p} := N0_{Rk.p} \cdot \frac{A_{p.N}}{A0_{p.N}} \cdot \psi_{s.Np} \cdot \psi_{g.Np} \cdot \psi_{ec.Np} \cdot \psi_{re.Np} = 2.2063 \cdot 10^{5}$ "Group pull out capacity"

$\frac{\sum F_{axC.Ek}}{N_{Rk.p}}\,\mathrm{N} = 0.1035$ "Characteristic pull out utilization"

Concrete cone failure:

$\psi_{ec.N} := \mathrm{Min}\left(\frac{1}{1 + 2 \cdot \frac{e_n}{S_{cr.N}}}, 1\right) = 0.9451$ "Eccentricity factor"

$\psi_{re.N} := \mathrm{Min}\left(0.5 + \frac{h_{ef}}{200}, 1\right) = 1$ "Spalling factor"

$\psi_{s.N} := \mathrm{Min}\left(0.7 + 0.3 \cdot \frac{c_{1.cap}}{C_{cr.N}}, 1\right) = 0.9188$ "Edge distance factor"

$A0_{c.N} := S_{cr.N}{}^{2} = 2.304 \cdot 10^{5}$ "Ideal cone area"

$A_{c.N} := 2 \cdot \mathrm{Min}\left(c_{1.cap}, C_{cr.N}\right) \cdot \left(2 \cdot C_{cr.N} + \left(n_{t.anchors} - 1\right) \cdot s_{1.cap}\right) = 2.835 \cdot 10^{5}$ "Group cone area"

$N0_{Rk.c} := k_{N0.Rk.c} \cdot \sqrt{f_{ck.cube.cap}} \cdot h_{ef}{}^{1.5} = 72858.8773$ "Ideal cone capacity"

$N_{Rk.c} := N0_{Rk.c} \cdot \frac{A_{c.N}}{A0_{c.N}} \cdot \psi_{s.N} \cdot \psi_{re.N} \cdot \psi_{ec.N} = 77845.3116$ "Cone group capacity"

$\frac{\sum F_{axC.Ek}}{N_{Rk.c}}\,\mathrm{N} = 0.2932$ "Characteristic cone group capcatiy"

Splitting failure:

$\psi_{ec.N.sp} := \mathrm{Min}\left(\frac{1}{1 + 2 \cdot \frac{e_n}{S_{cr.N}}}, 1\right) = 0.9451$ "Eccentricity factor"

$\psi_{re.N.sp} := \mathrm{Min}\left(0.5 + \frac{h_{ef}}{200}, 1\right) = 1$ "Spalling factor"

$\psi_{s.N.sp} := \mathrm{Min}\left(0.7 + 0.3 \cdot \frac{c_{1.cap}}{C_{cr.sp}}, 1\right) = 0.9188$ "Edge distance factor"

$$\psi_{h.sp} := \mathrm{Min}\left(\frac{H_{concrete.depth}}{\mathrm{Min}\left(C_{cr.sp}, c_{1.cap}\right) + \mathrm{Min}\left(C_{cr.sp}, c_{2.cap}\right)}, 1.5\right) = 0.8571$$ "concrete depth factor"

"ideal anchor splitting area"

$$A0_{c.N.sp} := S_{cr.sp}{}^{2} = 2.304 \cdot 10^{5}$$

$$A_{c.N.sp} := 2 \cdot \mathrm{Min}\left(c_{1.cap}, C_{cr.sp}\right) \cdot \left(2 \cdot C_{cr.sp} + \left(n_{t.anchors} - 1\right) \cdot s_{1.cap}\right) = 2.835 \cdot 10^{5}$$ "Group splitting area"

$$N0_{Rk.c.sp} := k_{N0.Rk.c} \cdot \sqrt{f_{ck.cube.cap}} \cdot h_{ef}{}^{1.5} = 72858.8773$$ "Ideal anchor splitting capacity"

$$N_{Rk.c.sp} := N0_{Rk.c.sp} \cdot \frac{A_{c.N.sp}}{A0_{c.N.sp}} \cdot \psi_{s.N.sp} \cdot \psi_{re.N.sp} \cdot \psi_{ec.N.sp} \cdot \psi_{h.sp} = 66724.5528$$ "Group splitting capacity"

$$\frac{\sum F_{axC.Ek}}{N_{Rk.c.sp}}_{\mathrm{N}} = 0.3421$$ "Characteristic splitting utilization"

Shear capacity:

Eccentricity and equivalent critical size and dirrection of shear force:

$$F_{zC.Ek} = \left[\begin{array}{cccc} 1.37 & -6.32 & -14.01 & -21.7 \end{array}\right] \mathrm{kN}$$ "Resulting vertical force"

$$Forces_{V.C} := Matrix\_remove\_positive_{ij}\left(F_{zC.Ek}\right)$$ "Resulting negative values"

$$Forces_{V.C} = \left[\begin{array}{cccc} 0 & -6.3189 & -14.009 & -21.6992 \end{array}\right] \mathrm{kN}$$

$$F_{xC.Ek} = \left[\begin{array}{cccc} -0.75 & -0.75 & -0.75 & -0.75 \end{array}\right] \mathrm{kN}$$ "Horizontal shear forces"

$$r_{vertical} := \left[\begin{array}{cccc} 1.5 \cdot s_{1.cap} & 0.5 \cdot s_{1.cap} & (-0.5) \cdot s_{1.cap} & (-1.5) \cdot s_{1.cap} \end{array}\right]$$ "Placement of anchors from center of anchors"

$$e_{v.x} := \frac{\sum Prtoduct_{ij}\left(r_{vertical}, Forces_{V.C}\right)}{\sum Forces_{V.C}} = -95.2557$$ "Vertical eccentricity of shear force"

$$Force_{\alpha} := \mathrm{atan}\left(\frac{\sum F_{xC.Ek}}{\sum Forces_{V.C}}\right)$$ "Angle of resulting shear force

$$Force_{\alpha} = 0.0713 \quad rad$$

$$e_{v} := \cos\left(Force_{\alpha}\right) \cdot e_{v.x}$$ "equivalent anchor group eccentricity"

$$e_{v} = -95 \quad mm$$

$$F_{shear.concrete.tot} := \sqrt{\left(\sum Forces_{V.C}\right)^{2} + \left(\sum F_{xC.Ek}\right)^{2}}$$

$$F_{shear.concrete.tot} = 42134.0399 \ \mathrm{N}$$ "Equivalent anchor shear force"

Steel failure:

"Characteristic steel capacity"

$$V_{Rk.s} := n_{t.anchors} \cdot 0.5 \cdot A_{s.anchor} \cdot f_{uk} = 1.9154 \cdot 10^{5}$$

"Characteristic steel utilization"

$$\frac{F_{shear.concrete.tot}}{N_{Rk.s}} = 0.11 \quad \text{N}$$

Pry-out failure:

Because the anchor group is affected by a torsion moment, the critical pry-out capactiy is calculated for the critical bolt:

$\psi_{ec.N.crit} := 1$ "No eccentricity for a singular bolt" "Eccentricity factor"

$$\psi_{re.N} := \text{Min}\left(0.5 + \frac{h_{ef}}{200}, 1\right) = 1$$ "Spalling factor"

$$\psi_{s.N} := \text{Min}\left(0.7 + 0.3 \cdot \frac{c_{1.cap}}{C_{cr.N}}, 1\right) = 0.9188$$ "Edge distance factor"

$$A0_{c.N} := S_{cr.N}^{2} = 2.304 \cdot 10^{5}$$ "Ideal tension pry out area"

$$A_{c.N.crit} := 2 \cdot \text{Min}\left(c_{1.cap}, C_{cr.N}\right) \cdot \left(C_{cr.N} + \frac{s_{1.cap}}{2}\right) = 1.0325 \cdot 10^{5}$$ "Tension pry-out area for critical anchor"

$$N0_{Rk.c.crit} := k_{N0.Rk.c} \cdot \sqrt{f_{ck.cube.cap}} \cdot h_{ef}^{1.5} = 72858.8773$$ "Characteristic tension pry-out capactiy"

$$N_{Rk.c.crit} := N0_{Rk.c} \cdot \frac{A_{c.N.crit}}{A0_{c.N}} \cdot \psi_{s.N} \cdot \psi_{re.N} \cdot \psi_{ec.N} = 28351.0703$$ "Concrete tension cone failure of critical shear anchor"

Using the tension capactiy of the critical anchor, the pry-out failure for the critical anchor is calculated as:

$$V_{Rk.cp} := k_{V.Rk.cp} \cdot N_{Rk.c.crit} = 56702.1405$$ "Pry out faillure capacity"

$$V_{Ek.crit.anchor} := \sqrt{F_{zC.Ek.crit}^{2} + F_{xC.Ek.crit}^{2}} = 21712.1228 \quad \text{N}$$ "Characteristic load acting on critical shear anchor"

$$\frac{V_{Ek.crit.anchor}}{V_{Rk.cp}} = 0.3829 \quad \text{N}$$ "Characteristic pry out utilization"

Concrete edge failure:

"Using the eccentriceties and force angel the factors are calculated"

$$\psi_{ec.V} := \text{Min}\left(\sqrt{\frac{1}{1 + \frac{2 \cdot e_{v}}{3 \cdot c_{1.cap}}}}, 1\right) = 1$$

$c_{1.cap} = 175$

$$\psi_{\alpha.V} := \mathrm{Max}\left(\sqrt{\frac{1}{\left(\cos\left(Force_{\alpha}\right)\right)^2 + \left(\frac{\sin\left(Force_{\alpha}\right)}{2.5}\right)^2}}, 1\right) = 1.0021$$ "Resultant force angel factor"

$$\psi_{h.V} := \mathrm{Max}\left(\left(\frac{1.5 \cdot c_{1.cap}}{\mathrm{Min}\left(H_{concrete.depth}, 1.5 \cdot c_{1.cap}\right)}\right)^{\frac{1}{2}}, 1\right) = 1$$ "Concrete depth factor"

$$A0_{c.V} := 4.5 \cdot c_{1.cap}{}^2 = 1.3781 \cdot 10^5$$ "Ideal anchor edge area"

$$A_{c.V} := 1.5 \cdot c_{1.cap} \cdot \left(2 \cdot 1.5 \cdot c_{1.cap} + 3 \cdot s_{1.cap}\right) = 2.2444 \cdot 10^5$$ "Anhor group edge area"

$$\alpha_{V0.Rk.c} := 0.1 \cdot \left(\frac{h_{ef}}{c_{1.cap}}\right)^{\frac{1}{2}} = 0.0956$$

$$\beta_{V0.Rk.c} := 0.1 \cdot \left(\frac{d_{anchor.cap}}{c_{1.cap}}\right)^{0.2} = 0.062$$

$$V0_{Rk.c} := k_{V0.Rk.c} \cdot d_{anchor.cap}{}^{\alpha_{V0.Rk.c}} \cdot h_{ef}{}^{\beta_{V0.Rk.c}} \cdot \sqrt{f_{ck.cube.cap}} \cdot c_{1.cap}{}^{1.5} = 35132.7528$$

$$V_{Rk.c} := V0_{Rk.c} \cdot \frac{A_{c.V}}{A0_{c.V}} \cdot \psi_{h.V} \cdot \psi_{\alpha.V} \cdot \psi_{ec.V} \cdot \psi_{re.V} = 68806.0983\ N$$ "Concrete edge shear capacity"

$$\frac{F_{shear.concrete.tot}}{V_{Rk.c}\ \mathrm{N}} = 0.6124$$ "Characteristic edge capactiy utilization"

Combined shear and tension:

The critical capactiy ration is calculated from the critical uti8lization of tension and shear":

$$\left(\frac{F_{shear.concrete.tot}}{V_{Rk.c}\ \mathrm{N}}\right)^2 + \left(\frac{\sum F_{axC.Ek}}{N_{Rk.c}\ \mathrm{N}}\right)^2 = 0.4609$$ "Characteristic anchor utilization"

The characteristic capactiy for the anchor group is far exceeded...

Design utilization of characteristic load:

$$\left(\frac{1.5 \cdot F_{shear.concrete.tot}}{V_{Rk.c}\ \mathrm{N}}\right)^2 + \left(\frac{1.5 \cdot \left(\sum F_{axC.Ek}\right)}{N_{Rk.c}\ \mathrm{N}}\right)^2 = 1.0371$$ "Design anchor utilization"

APPENDIX D:

Lateral force method calculations

Lateral force method calculations:

$g := 9.81 \frac{N}{kg}$

$q := 1$ "Seismic structure damping factor: considdering viscous damping of 5%"

Type 2 elastic response spectra for ground type C:

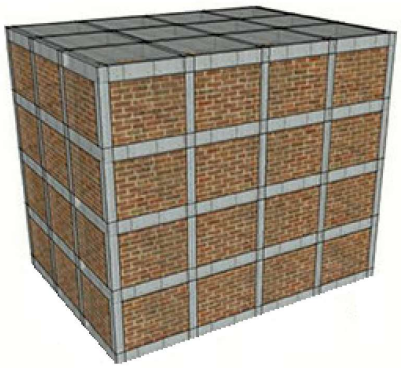

$S := 1.5$

$T_B := 0.1\ s$

$T_C := 0.25\ s$

$T_D := 1.2\ s$

PGA's tested:

$a_{g1} := 0.1 \cdot g$ "PGA for low seismic area"

$a_{g2} := 0.35 \cdot g$ "PGA for high seismic area"

Structure dimensions:

$n_f := 4$ "Number of floors"

$H := 12\ m$ $\boxed{H_1 := \frac{H}{m}}$ "Structurer height"

$A_{floor} := 18 \cdot 26\ m^2$ "Area per floor"

$c_t := 0.3\ m$ "Height of RC beam cross-section"

Seismic gravity loading

$\psi_{2i.imposed\_load} := 0.3$ "According to EN 1990 Table A1.1. ψ2 is equal to zero for snow and wind loads, outside of scandinavia, and is therefore ignored for this example"

$\varphi_{story} := 0.8$ "According to EN 1998-1 table 4.2 for storys withcorrelated occupncies"

$\psi_{Ei} := \varphi_{story} \cdot \psi_{2i.imposed\_load}$ "Roof is considderd a story for this example, as it makes little difference"

"The self weight is simplified by only considering the weight of each floor consisting of 300 mm concrete floors."

$\rho_c := \frac{25}{g} \frac{kN}{m^3}$ "Normal weight concrete with consideration of reinforcement, according to EN 1990-1-1 Table A.1"

$m_s := A_{floor} \cdot c_t \cdot n_f \cdot \rho_c$ "Simplified structure self weight"

$m_s = 1578\ ton$

$Q_I := 2.0 \frac{kN}{m^2}$ "Imposed load"

Inertial effect load combination according to EN 1998-1 equation 3.17:

$m := m_s + \frac{\psi_{Ei} \cdot Q_I \cdot A_{floor} \cdot n_f}{g} = 1679\ ton$

Latteral force method:

Fundamental period acording to 4.3.3.2.2(3) for moment resistant concrete space frame.

$C_t := 0.075\ \mathrm{s\ m}^{-\frac{3}{4}}$ "Units of factor adjusted for the empirical formula"

$T_1 := C_t \cdot H^{\frac{3}{4}}$ "Natural period of undamped structure"

$T_1 = 0.48\ \mathrm{s}$

Design spectrum for elastic analysis acording to 3.2.2.5

$\beta := 0.2$ "Recomended value of lower bound factor"

Tc≤T1≤Td: "Period criteria"

$S_{d1} := \mathrm{Max}\left(a_{g1} \cdot S \cdot \frac{2.5}{q} \cdot \left(\frac{T_C}{T_1}\right), \beta \cdot a_{g1}\right) = 1.9019\ \frac{\mathrm{m}}{\mathrm{s}^2}$ "Design spectrum value of low PGA"

$S_{d2} := \mathrm{Max}\left(a_{g2} \cdot S \cdot \frac{2.5}{q} \cdot \left(\frac{T_C}{T_1}\right), \beta \cdot a_{g2}\right) = 6.6567\ \frac{\mathrm{m}}{\mathrm{s}^2}$ "Design spectrum value of high PGA"

Correlation factor on account of reduced effective modal mass:

$2 \cdot T_C = 0.5\ \mathrm{s} > T_1 = 0.4836\ \mathrm{s}$ "Criteria for use of correlation factor"

$\lambda := 0.85$ "Correlation factor for modal mass"

Base shear:

$F_{b1} := S_{d1} \cdot m \cdot \lambda = 2461.7942\ \mathrm{kN}$ "Lower seismic"

$F_{b2} := S_{d2} \cdot m \cdot \lambda = 8616.2796\ \mathrm{kN}$ "Higher seismic"

Required system slip force:

$\rho_s := 0.2$ "Optimal percentage of total load"

$F_{s1} := \rho_s \cdot F_{b1} = 492.3588\ \mathrm{kN}$ "Lower seismic"

$F_{s2} := \rho_s \cdot F_{b2} = 1723.2559\ \mathrm{kN}$ "Higher seismic"

Total slip force of a single friction system cloumn utilizing even force distribution:

$F_{s.col} := 48.22\ \mathrm{kN}$ "Friciton column slip capacity"

Number required system columns:

$n_{fc1} := \frac{F_{s1}}{n_f \cdot F_{s.col}} = 2.5527$ "Low PGA"

$n_{fs2} := \frac{F_{s2}}{n_f \cdot F_{s.col}} = 8.9343$ "High PGA"

Norges miljø- og biovitenskapelige universitet
Noregs miljø- og biovitskapelege universitet
Norwegian University of Life Sciences

Postboks 5003
NO-1432 Ås
Norway